

**Transport of reactive contaminants
in heterogeneous soil systems**

Promotor: dr ir F.A.M. de Haan
hoogleraar in de bodemhygiëne en de
bodemverontreiniging

Co-promotor: dr W.H. van Riemsdijk
universitair hoofddocent in de bodemhygiëne en de
bodemverontreiniging

2

**BIBLIOTHEEK
STARINGGEBOUW**

**S.E.A.T.M. van der Zee
TRANSPORT OF REACTIVE CONTAMINANTS
IN HETEROGENEOUS SOIL SYSTEMS**

Proefschrift
ter verkrijging van de graad van
doctor in de landbouwwetenschappen,
op gezag van de rector magnificus,
dr C.C. Oosterlee,
in het openbaar te verdedigen
op vrijdag 29 april 1988
des namiddags te vier uur in de aula
van de Landbouwuniversiteit te Wageningen



15n 268155*

4 AUG. 1988

Aan mijn moeder

ABSTRACT

Van der Zee, S.E.A.T.M., 1988, Transport of reactive contaminants in heterogeneous soil systems. Doctoral thesis, Agricultural University, Wageningen, The Netherlands 283 pages, four appendices.

Transport of reactive contaminants was studied in soil systems that exhibit pronounced variability with respect to the flow and sorption parameters and the solute feed function at the inlet boundary. Emphasis was given to the sorption and transport of orthophosphate (P) in soil. An approximate P sorption kinetics model was derived, that is based on a mechanistic description of reaction processes at the microscopic scale. The approximate model, that involves a reversible adsorption according to Langmuir kinetics, and an irreversible diffusion-precipitation reaction, as a function of a concentration scaled time variable, described experimental sorption and desorption data well. Validation by predicting P-transport using independently assessed sorption parameter values, showed a reasonable agreement between experimental and numerical results. With the distributions of sorption model parameters and soil variables found for a field and a watershed, transport was simulated for homogeneous and heterogeneous soil systems at conditions resembling those of the field. It appeared that only a smaller part of sorbed P is subject to desorption, and that transport in many cases conforms to shock front displacement. Transport at field conditions, furthermore, appeared to be largely controlled by P-sorption and to a lesser extent by flow.

Assuming soil in the field may be described as a number of parallel, non-interacting columns, and assuming piston type displacement, P-transport was described if the sorption capacity and P-input differ for each column, using stochastic theory. The main trends for P-displacement in such a heterogeneous field were in agreement with experimental data, and showed large differences with the solutions of the convection-dispersion equation for average parameter values. An analytical solution for a more specific case supported these findings, for heavy metal transport, and showed faster breakthrough in the small concentration range than expected using average parameter values. The effect of transversal interaction between two layers with different properties showed that the loss of solute from the layer with the largest transport velocity may be significant, when at the sharp interface, in the direction of flow, soil properties vary much.

Additional Index Words: distribution, unreacted shrinking core, scaling, reversibility, Monte Carlo simulations, groundwater, surface water eutrophication, copper, cadmium, phosphate.

BIBLIOTHEEK STARINGGEBOUW

Stellingen:

1. Bij vertikaal transport in de bodem van reaktieve verbindingen, wordt het moment waarop doorbraak begint bij een horizontaal referentievlak, in sterkere mate bepaald door de variabiliteit in het horizontale vlak van bodemeigenschappen en van transportrandvoorwaarden, dan door hydrodynamische microdispersie.

dit proefschrift.

2. De veronderstelling van perfecte transversale menging in de zandlaag bij de beschrijving van transport evenwijdig aan de gelaagdheid voor de proefopzet van Starr et al., leidt slechts tot accurate resultaten bij geringe dikte van de zandlaag.

Starr, R.C., R.W. Gillham, and E.A. Sudicky, Experimental investigation of solute transport in stratified porous media, 2. The reactive case, Water Resour. Res. 21(7), 1043-1050, 1985.
dit proefschrift.

3. Het "Transfer Function Model" van Jury, leidt alleen tot verbeterde inzichten en voorspellingen, indien de functies van dit model mechanistisch ingevuld worden.

Jury, W.A., Simulation of solute transport using a transfer function model, Water Resour. Res., 18(2) 363-368, 1982.

4. Dat bij de binding van fosfaat aan goethiet naast adsorptie een tweede proces van vastlegging optreedt, is in de argumentatie van Barrow et al. een veronderstelling en niet een conclusie, zoals zij suggereren.

Barrow, N.J., L. Madrid, and A.M. Posner, A partial model for the rate of adsorption and desorption of phosphate by goethite, J. Soil Sci., 32, 399-407, 1981.

5. Het modelleren van fosfaattransport waarbij chemisch evenwicht wordt verondersteld, leidt tot irreële resultaten.

6. Het gebruik van niet-probabilistische modellen suggereert een overschatting van het inzicht.

7. Het volgens de BET-methode vastgestelde specifiek oppervlak, zegt alleen dan iets over het adsorptie-oppervlak als de adsorberende stof gelijke dimensies heeft als het stikstofmolecuul of indien het oppervlak niet poreus is.

8. Het landelijk meetnet bodemkwaliteit is ongeschikt voor het op korte termijn vaststellen van veranderingen in de totaalgehalten van elementen in de bodem.

9. Omdat de huidige gemiddelde diffuse belasting van landbouwgronden met cadmium en lood groter is dan de aanvaardbare afvoer in gewassen en grondwatervoeding, moet de belasting met deze elementen gereduceerd worden.

Ferdinandus, Gon, Beperking van de aanvoer is de enige echte oplossing, Problemen met zware metalen in de landbouw, doktoraal verslag, Bodemkunde en Plantevoeding, Landbouwuniversiteit Wageningen, 1987.

10. Indien de functies die het semi-variogram en een aanwezige trend beschrijven niet a priori bekend zijn, leidt dit tot de introductie van subjectiviteit bij het toepassen van "universal kriging".

Royle, A.G., F.L. Clausen, and P. Frederiksen, Practical universal kriging and automatic contouring, Geo-Processing, 1, 377-394, 1981.

11. Milieu-confrontatie werkt milieu-bewustzijn beter in de hand dan milieu-educatie.
12. Ook voor de landbouwuniversiteit is het van belang om milieutechnisch onderzoek althans gedeeltelijk te combineren met onderzoek naar de maatschappelijke aspecten van de milieuproblematiek.
13. Het met terugwerkende kracht in werking laten treden van de Harmonisatie Wet ("zesjarenmaatregel"), is een schending van het opgewekt vertrouwen en getuigt daardoor niet van behoorlijk bestuur.
14. Problemen zijn er niet om te worden opgelost; zij zijn slechts de polen waartussen de voor het leven noodzakelijke spanning wordt opgewekt.

Hermann Hesse, Een golfje op de stroom, uitspraken en aforismen uit boeken en brieven, derde druk, De Arbeiderspers, Amsterdam, 1977.

15. Het is logischer om te spreken van een verhoging dan van een verdieping van een gebouw.
16. Er lopen kletsnatte clowns in de optocht
maar de mensen langs de kant
dragen veel betere maskers
tegen weer en wind bestand

Herman van Veen, En nooit weerom, 1974

Stellingen bij het proefschrift van
S.E.A.T.M. van der Zee
Transport of reactive contaminants in heterogeneous soil systems
Wageningen, 29 april 1988

WOORD VOORAF

De afgelopen jaren heb ik veel tijd en energie gestoken in het bewerken van dit proefschrift. Zonder de hulp van velen zou het echter niet mogelijk geweest zijn om dit proefschrift in haar huidige vorm te presenteren.

Van de betrokkenen ben ik in eerste instantie mijn ouders dankbaar, wier warme belangstelling en steun me altijd heeft geholpen.

Verder gaat mijn dank uit naar mijn promotor Frans de Haan en mijn co-promotor Willem van Riemsdijk. Beiden hebben me alle vrijheid gegeven in de invulling van mijn onderzoek. Onder meer door het reeds verrichte voor-onderzoek, de vele discussies en infrastructurele zaken hebben Frans en Willem het kader geschapen voor een goede en zeker ook prettige voortgang van dit onderzoek.

Een van de hoofdstukken van dit proefschrift (hoofdstuk 11) vloeit voort uit werk dat ik heb uitgevoerd met Hans van Duljn (Vakgroep Wiskunde en Informatica, Technische Universiteit Delft). Ik heb de samenwerking met Hans als zeer motiverend ervaren en de prettige manier waarop hij me de mogelijkheden van de wiskunde voor mijn vakgebied toonde vindt duidelijk zijn weerslag in de rest van dit proefschrift.

Voor het grote aantal zorgvuldig uitgevoerde analyses en voor hun hulp bij de begeleiding van de vele studenten bedank ik Betsie van Loenen en Egbert Nab.

Een deel van de experimenten is uitgevoerd met de mooie kolommetjes gemaakt door Simon Maasland, terwijl voor andere metingen de ondersteuning door leden van de sectie grond- en gewasanalyse en het service-lab onontbeerlijk waren. Deze en andere inbreng van de vakgroep Bodemkunde en Plantevoeding, waar dit onderzoek is uitgevoerd, waardeer ik zeer.

Speciale dank gaat uit naar Karin Sijmans, Inge Stakman, Herma Roseboom, Anja de Weerd en Ria Slootman, die ik de afgelopen vier jaren een flinke portie werk heb bezorgd. De vaak snelle en prettige samenwerking, onder andere bij het typen van de manuscripten die niet altijd echt eenvoudig waren, stel ik zeer op prijs.

Veel studenten hebben, vaak zelfstandig en op een enthousiaste wijze, een bijdrage geleverd aan mijn onderzoek. Graag bedank ik met name Henri Spanjers, Ronald Hopman, Nelleke Kleijn, Hettie de Jong, Bertram Lammers, Maarten Nederlof, Aukje Gjaltema, Bert Caris, Maarten Saaltink, Joost Martens, Giel Custers, Onno de Ruiter en Jaap Mus, wier inbreng herkenbaar in dit proefschrift is terug te vinden.

De prettige en ongedwongen sfeer op de vakgroep hebben er zeker toe bijgedragen, dat ik met plezier op de afgelopen jaren terugkijk. In nog sterkere mate geldt dit voor de morele steun thuis, van Gon. Met haar expertise in balansen, heeft zij mijn persoonlijke balans in evenwicht weten te brengen.

Sjoerd van der Zee,
maart 1988

CONTENTS

1.	GENERAL INTRODUCTION	1
1.1	Contamination of agricultural soils	1
1.2	Excessive manure disposal in intensive animal husbandry	2
1.3	Phosphate saturated soils	4
1.4	Transport of reactive contaminants	5
1.5	References	9
2.	A NEW TECHNIQUE FOR ASSESSMENT OF REVERSIBLY ADSORBED PHOSPHATE	13
2.1	Introduction	13
2.2	Theory	15
2.3	Materials and methods	18
2.4	Results	19
2.5	Discussion	21
2.6	Conclusions	28
2.7	Appendix 1: Mathematical description of dilution experiments	29
2.8	Notation	30
2.9	References	31
3.	MODEL FOR THE REACTION KINETICS OF PHOSPHATE WITH OXIDES AND SOIL	35
3.1	Introduction	36
3.2	Theory	39
3.2.1	The surface reacton	39
3.2.2	The diffusion/precipitation reaction	40
3.2.2.1	<i>Unreacted shrinking core model for single particle size</i>	41
3.2.2.2	<i>Correspondence to other models</i>	46
3.2.2.3	<i>Unreacted shrinking core model for particle size distribution</i>	48
3.2.2.4	<i>The diffusion/precipitation model for pure oxides and soils</i>	55
3.3	Conclusion	58
3.4	Notation	59
3.5	References	61
4.	EXTRAPOLATION AND INTERPOLATION BY TIME-SCALING IN SYSTEMS WITH DIFFUSION CONTROLLED KINETICS AND FIRST ORDER REACTION RATES	65
4.1	Introduction	65
4.2	Background of scaling	66
4.3	Applications of time scaling	71
4.4	Conclusions	77
4.5	References	77
5.	PHOSPHATE SORPTION KINETICS AND TRANSPORT IN SMALL COLUMNS	81
5.1	Introduction	81
5.2	Mathematical formulation	82
5.3	Materials and methods	85
5.4	Parameter assessment and data analysis	86

5.5	Results and discussion	87
5.6	Conclusions	97
5.7	Appendix 1: Isotherm construction	98
5.8	Appendix 2: Values used to simulate transport	99
5.9	Notation	100
5.10	References	101
6.	MODEL FOR LONG TERM PHOSPHATE REACTION KINETICS IN SOIL	105
6.1	Introduction	105
6.2	Theoretical background	107
6.3	Materials and methods	110
6.4	Results and discussion	111
6.5	Conclusions	121
6.6	Notation	121
6.7	References	122
7.	SPATIAL VARIABILITY OF PHOSPHATE ADSORPTION PARAMETERS AND EFFECT ON LONG TERM LEACHING	127
7.1	Introduction	127
7.2	Theory	129
7.3	Materials and methods	133
7.4	Results and discussions	134
7.5	Conclusions	144
7.6	Notation	145
7.7	References	146
8.	TRANSPORT OF PHOSPHATE IN A HETEROGENEOUS FIELD	149
8.1	Introduction	149
8.2	Transport at the column scale	152
8.3	Transport at field scale	156
8.4	Materials and methods	158
8.5	Calculations	159
8.6	Results	160
8.7	Parameter analysis	164
8.8	Profile development in time	165
8.9	Discussion	168
8.10	Conclusions	171
8.11	Notation	172
8.12	References	173
9.	TRANSPORT OF REACTIVE SOLUTE IN SPATIALLY VARIABLE SOIL SYSTEMS	177
9.1	Introduction	178
9.2	Theory	180
9.2.1	Column scale transport	180
9.2.2	Field scale transport	184
9.3	Discussion	187
9.3.1	Column scale profile	187

9.3.2	Statistics of In Y	190
9.3.2.1	<i>Time dependence for discontinuous input</i>	190
9.3.2.2	<i>Limiting case of continuous input</i>	192
9.3.2.3	<i>Unsaturated flow</i>	193
9.3.2.4	<i>Distribution of the retardation factor</i>	194
9.3.2.5	<i>Correlated velocity and retardation factor</i>	197
9.3.3	Profile of sorbed solute	198
9.4	Conclusions	203
9.5	Notation	205
9.6	References	206
10.	ANALYSIS OF PHOSPHATE LEACHING FROM A HETEROGENEOUS FIELD	211
10.1	Introduction	211
10.2	Theory	214
10.3	Results and discussion	219
10.3.1	Effect of adsorption constant (K)	219
10.3.2	Effect of P-saturated layer thickness (L_s)	222
10.3.3	Effect of adsorption maximum (Q_m)	223
10.3.4	Spatial variability of Q_m and L_s	227
10.5	Environmental implications	231
10.6	Conclusions	235
10.7	Appendix 1: Parameter values used in the simulations	236
10.8	Notation	237
10.9	References	238
11.	SOLUTE TRANSPORT PARALLEL TO AN INTERFACE SEPARATING TWO DIFFERENT POROUS MATERIALS	239
11.1	Introduction	239
11.2	Mathematical formulation	243
11.3	Analytical approximation	244
11.3.1	Approximate interface concentration	249
11.3.2	Loss of solute from the permeable zone	251
11.4	Numerical approximation	254
11.5	Results and discussion	258
11.6	Discussion	261
11.6.1	Limiting case I: $R_2 \rightarrow \infty$	262
11.6.2	Limiting case II: $D_{12} \rightarrow \infty$	265
11.7	Summary and conclusions	267
11.8	References	269
12.	GENERAL CONCLUSION	273
	SUMMARY	275
	SAMENVATTING	279

APPENDICES

- | | |
|---|------------|
| APPENDIX A: A TRAVELLING WAVE SOLUTION FOR TRANSPORT OF A SOLUTE REACTING ACCORDING TO THE LANGMUIR ISOTHERM | A-1 |
| APPENDIX B: VALIDITY OF THE SHOCK FRONT ASSUMPTION FOR PHOSPHATE TRANSPORT AT FIELD CONDITIONS | B-1 |
| APPENDIX C: SOME PROPERTIES OF THE NORMAL AND LOGNORMAL DISTRIBUTIONS | C-1 |
| APPENDIX D: PROTOCOL PHOSPHATE SATURATED SOILS | D-1 |

PUBLICATIONS

The chapters 2-11 were, or will be, published as separate papers with minor modifications. Only, in some cases, sections duplicating results given elsewhere were excluded or modified significantly (chapters 3,5). References are given below.

- Chapter 2: 'A new technique for assessment of reversibly adsorbed phosphate', S.E.A.T.M. van der Zee, L.G.J. Fokkink, and W.H. van Riemsdijk, *Soil Sci. Soc. Am. J.* 51, 599-604, 1987
- Chapter 3: 'Model for the reaction kinetics of phosphate with oxides and soil', S.E.A.T.M. van der Zee and W.H. van Riemsdijk, *Proc. Conf. 'Interactions at the soil colloid-soil solution interface'*, August 24-29 1986, Ghent, Belgium, (in press)
- Chapter 5: 'Sorption kinetics and transport of phosphate in sandy soil', S.E.A.T.M. van der Zee and W.H. van Riemsdijk, *Geoderma*, 38, 293-309, 1986
- Chapter 6: 'Model for long term phosphate reaction kinetics in soils', S.E.A.T.M. van der Zee and W.H. van Riemsdijk, *J. Environ. Qual.*, 1988 (In press)
- Chapter 8: 'Transport of phosphate in a heterogeneous field', S.E.A.T.M. van der Zee and W.H. van Riemsdijk, *Transport Porous Media*, 1, 339-359, 1986
- Chapter 9: 'Transport of reactive solute in spatially variable soil systems', S.E.A.T.M. van der Zee and W.H. van Riemsdijk, *Water Resour. Res.*, 23, 2059-2069, 1987
- Chapter 11: 'Solute transport parallel to an interface separating two different porous materials', C.J. van Duijn and S.E.A.T.M. van der Zee, *Water Resour. Res.*, 22, 1779-1789, 1986

Submitted were:

- Chapter 7: *J. Environ. Qual.*
- Chapter 10: *Water Resour. Res.*

1. GENERAL INTRODUCTION

1.1 Contamination of agricultural soils

One of the incentives for soil research is to obtain understanding that may be useful for improving agricultural production, both quantitatively and qualitatively. Because productivity of soil as well as e.g. ground water quality may be affected adversely by soil contamination, understanding of the effects of soil contamination has become another major motive for soil research. The nature of the contaminants, the pathways by which they enter and leave the soil system, and the soil functions that are primarily in hazard, may be very diverse. To focus the discussion I therefore consider only a factor many soils have in common: diffuse source contamination. This type of contamination may be characterized by a source that is not well defined with respect to its place, and that has therefore no well defined trends, at the scale of interest.

In The Netherlands several diffuse source contaminations affect most soils in agricultural use, though with a varying intensity. Examples are the atmospheric deposition of e.g. NO_x , NH_3 , and SO_x , that may result in enhanced soil acidification [Van Grinsven et al., 1986, Ulrich and Matzner, 1983], the atmospheric deposition of heavy metals [Thornton, 1986, Van De Meent et al., 1984, Ferdinandus, 1987], and the disposal of animal manure containing large amounts of phosphorus, nitrogen, potassium, and heavy metals [Lexmond et al., 1982, Henkens, 1983, Ferdinandus, 1987]. The high deposition rates of such compounds may lead to a number of problems, such as crop-yield reduction, too high contents of certain elements in consumable products, that cause a hazard to human or animal health, and a deterioration of the quality of ground and surface water [Lexmond, 1980, MacNicol and Becket, 1985, Denneman et al., 1985, Hirst et al., 1961, Ma, 1983, Van Riemsdijk et al., 1987, Van Der Zee et al., 1987]. Because the environmental problem, caused by high application rates of phosphorus present in animal manure, is given emphasis in this thesis, this aspect is considered next in a little more detail.

1.2 Excessive manure disposal in intensive animal husbandry

Since 1950 agricultural practice in The Netherlands has changed as a result of economical, sociological, and technical developments. Because of the increasing demand for dairy products and meat, and the necessity of improved labour productivity as labour costs rose, the agricultural production process needed to be intensified. Improved animal disease control and manure storage facilities, and economical use of food concentrates enabled high livestock densities, that could become independent of the agricultural land area at disposition of the farmer [Van Daalen, 1985, Wadman et al., 1987]. The intensive animal husbandry is characterized by a large net import of e.g. nutrient elements, and the production of large quantities of animal manure that contain the main fraction of the imported nutrient elements. Despite animal manure transport to other locations, most of it is disposed of in the production area. Thus quantities of elements far exceeding the crop's requirements are applied to soils in agricultural use. Because maize responds favourably to excessive disposal rates of animal manure, fields receiving large amounts of manure are often cropped with maize [Wadman et al., 1987]. The amounts not used by the crops may accumulate in the soil, or, if the accumulation rate is smaller than the difference in the rates of application and of uptake, leave the soil compartment.

One of the pathways with which compounds applied in manure may leave the soil system, is by leaching in the percolating soil water to ground water. Problems may arise if water quality becomes less than acceptable in view of quality standards set by the government for groundwater recharge [VTCB, 1986, VROM, 1986] and for drinking water. For instance, excessive manure disposal caused nitrate concentrations higher than the acceptable value of $50 \text{ mg NO}_3^- \text{ l}^{-1}$ in groundwater in some Dutch regions [Appelo et al., 1982, Bleuten and Cerutti, 1984, Steenvoorden et al., 1986].

Another compound that may lead to environmental problems is phosphate. Because in many situations in areas with intensive animal husbandry the application rates exceed the phosphorus crop uptake rates, accumulation and leaching of phosphorus may occur [Lexmond et al., 1982, 1985, Van Riemsdijk et al., 1985a, b, Breeuwsma and

Schouwman, 1986]. Phosphorus may reach the surface water both by transport through ground water and by surface runoff. When in surface water phosphate concentrations occur that exceed 0.15 g P m^{-3} (or 0.005 mol m^{-3}) [IMP 1985-1989], excessive algae growth may occur in Dutch surface water. This eutrophic state of the surface water is undesirable because of induced fish mortality due to low oxygen concentrations in the water, the adverse effects on the possibilities for recreation in this water, and problems with preparation of drinking water.

Besides the agricultural contribution to the P-load of Dutch surface water other contributions are e.g. P imported by the large rivers entering The Netherlands, and P originating from domestic or waste water discharge [Beek, 1979]. To protect surface water quality and to improve the current situation government regulations are in preparation or already issued, to decrease the discharge of phosphorus in surface water. Among others because it is unacceptable that the agricultural contribution would increase where other contributions should decrease, as well as to ascertain effectivity of regulations, also regulations to limit the agricultural contribution are well under way now. In the context of the Soil Protection Act, a General Governmental Measure (A.M.v.B) was issued on the use of animal manure, which became effective on April 1, 1987 [VTCB, 1986]. In several phases the annual excess of manure disposed (excess with respect to P-uptake by crops) is constrained to decreasing limits, and in the last phase, starting in the year 2000, excessive disposal is prohibited. To avoid environmental problems for the intermediate period, due to deterioration caused by a limited number of fields with large P-emissions (currently or in near future) to groundwater, an exception clause to these regulations was made for so called P-saturated soils. Because part of the work in this thesis emanated from a project for the ministry VROM (Ministry of Housing, Physical Planning and Environment), that concerned P-saturated soils [Van Der Zee et al. 1988] some backgrounds are given of this regulation and the problems addressed in the context of this project.

1.3 Phosphate saturated soils

Annual uptake rates of phosphate by crops are of the order of magnitude of $70 \text{ kg P}_2\text{O}_5 \text{ ha}^{-1} \text{ y}^{-1}$ or $972 \text{ mol P ha}^{-1} \text{ y}^{-1}$. This number may be compared to applications of 270 to $500 \text{ kg P}_2\text{O}_5 \text{ ha}^{-1} \text{ y}^{-1}$ occurring at average in the communities of St. Oedenrode and Son and Breugel, respectively. At the community-scale of observation extreme situations are averaged out that may occur at the field scale. Thus one field is known to have received a quantity of manure equivalent to approximately $5000 \text{ kg P}_2\text{O}_5 \text{ ha}^{-1}$ in half a year. Such extreme manure disposal rates may lead to unwanted environmental consequences very fast (apart from organo-leptic shock). An exception clause for P-saturated soils in the A.M.v.B. on the use of animal manure, aims at preventing adverse effects caused by disposal of large quantities of manure. Thus, no manure disposal is allowed on phosphate saturated soils, i.e., the total amount of phosphate applied to such soils should not exceed phosphorus uptake by crops.

In the advice given by the VTCB [1986] no definition was formulated of a phosphate saturated soil. The ministry VROM contracted the Department of Soil Science and Plant Nutrition (Agricultural University, Wageningen) to provide an appropriate definition and to give a description how such soils should be experimentally indentified. This is done in the Protocol Phosphate Saturated Soils [Van Der Zee et al., 1988]. At the same time the Soil Survey Institute [Stiboka] was asked to identify those regions suspected of harbouring many (having a high density of) phosphate saturated soils. Several problems obstructed the solution of the questions asked. Whereas a start had been made to describe phosphate transport in fields, as well as with quantifying desorption, the combination was not yet attempted. Moreover it became necessary to describe these processes such that not only the intellectual problem was solved, but that also the assessment of P-saturated soils was based on an environmentally justified criterion, was accurate, can be duplicated, and is simply and in a routine fashion executable, for different Dutch soils.

In view of these (partly self-posed) constraints, simplifications were inevitable. A number of these simplifications that underlay much of this thesis, but were not subject of investigation, are given in

this section. First of all, only the behaviour and transport of the ortho-phosphate ion is considered as most phosphorus in animal manure is in this form, either in solution or as solid phosphates that are well soluble at acid pH-values (pH<6) [Fordham and Schwertmann, 1977, Gerritse, 1976, Gerritse and Eksteen, 1978]. Displacement of organic phosphorus compounds (a minor fraction in animal manure, and subject to transformation to ortho-phosphate) supposedly does not constitute a major hazard with respect to eutrophication problems [Gerritse, 1976, Lexmond et al., 1982]. For the concentration range occurring in soils receiving large amounts of manure, several suggestions were made. While Lexmond et al., [1982] assume concentrations up to a maximum of 5 mol P m^{-3} , De Haan and Van Riemsdijk [1986] observed that in an almost P-saturated topsoil-liquid pigs manure mixture in the field, the P-concentration was buffered at the value of 3 mol P m^{-3} .

For these reasons, only the reaction and displacement of ortho-phosphate (henceforth denoted by P, for brevity) was considered, with the concentration range bounded by 3 mol m^{-3} at the maximum. It may be noteworthy that transport in groundwater is not considered in the protocol. As was shown by Van Der Zee et al., [1987] residence times for P in groundwater are hard to quantify for Dutch conditions in general, due to the diverse geohydrological conditions and uncertainty in P-sorption in groundwater systems. Hence, the ground water system is a safety margin (of unknown magnitude).

1.4 Transport of reactive contaminants

The central problem considered in this thesis, is the transport of phosphate through soil to groundwater.

Whereas emphasis was given to phosphate transport in this thesis, the main point holds also for other contaminants that react with soil. For the cases studied, where the contaminant is sorbed with a high affinity, and the distribution ratio (equal to the amount sorbed relative to the amount dissolved) is large, the simplifications made are usually more appropriate though, than in case of weak, almost linear sorption. The main problems encountered in developing an appropriate description of transport under field conditions, may be summarized by two terms: reactivity and heterogeneity.

The reactivity problem is discussed mainly for phosphate. Due to the high P-sorption rates in soils containing little P initially, transport is often so slow, that evaluation of transport under field conditions (and the sorption rate at large reaction times) is difficult. Therefore another approach is necessary to quantify P transport in the field. The approach followed consisted of 1. developing a sorption model that may be evaluated with short term laboratory experiments, 2. validation of this model with independent transport experiments at high flow velocities in small soil columns, 3. extension of the model such that it is consistent to long term sorption experiments, 4. numerical simulation of the main trends of transport in hypothetical soil columns at field conditions (e.g. small flow velocity, layering etc.). This approach was also followed by Van Riemsdijk [1979] and Beek [1979], and in this thesis many of their results, and extensions by Lexmond et al. [1982] and Van Riemsdijk et al. [1984], are used. However, when transport can be simulated with a validated sorption model, for soil columns as these may occur in the field, the transport problem in the field is not yet resolved. This is due to the heterogeneity of soil systems and of boundary conditions in the field. This heterogeneity accounts for different vertical transport velocities of the contaminant at different places in the field. Different (water) flow velocities were shown to occur at different places in the field by Biggar and Nielsen [1976] and Nielsen et al. [1973]. The large effects this may have on solute transport was shown by Bresler and Dagan [1979], Dagan and Bresler [1979], and Jury [1982]. More recent implications of spatial variability for non-reacting solutes were provided by Jury et al. [1986], White et al. [1986], and Van Ommen et al. [1988a, 1988b]. For reactive solute, spatial variability of flow velocities as well as sorption parameters may have an equally profound effect on field averaged displacement. However, due to the slow transport velocities in the field these effects are hard to quantify for reacting solutes. Beek [1979] observed that with realistic parameters for flow and dispersion coefficients under field conditions and with validated sorption parameters, no good description of the observed field averaged P-front could be obtained. A possible reason for this lack of agreement was among others the spatial variability of P-sorption. The approach to

quantify the effect of spatial variability on transport is discussed in this thesis. The basic idea was presented by De Haan et al. [1986] and Van Der Zee et al. [1987]. Further illustrations were given recently by De Haan et al. [1987] and Van Der Zee et al. [1988].

The articles underlying the different chapters of this thesis are not given in a chronological sequence, but have been presented such that it allows more systematic reading. First a phosphate sorption model is described and validated, and parameter assessment for the field studies is discussed. This is followed by the chapters dealing with transport in spatially variable fields.

Thus in Chapter 2 a new desorption technique for soil-phosphate is described, that is used in several later chapters. In Chapter 3 an approximate P sorption kinetics model is developed, that is based on a mechanistic description of reaction processes occurring at the microscopic scale. Part of this model, concerning the diffusion-precipitation process, leads to a promising scaling technique. This technique, its limitations, and some illustrative examples are considered in Chapter 4.

Parameters assessment for the P-sorption kinetics model is described in Chapter 5. In this chapter also the validation of the model is done by numerically predicting breakthrough of P for small columns and comparison of these results with independent experimental data.

A simplified version of the sorption kinetics model is given in Chapter 6. With this model, sorption is described for large numbers of samples, and large sorption times. For application in a routine fashion, it is shown how the over all sorption rate constant may be assessed from short term sorption experiments, and how differences in soil reactivity may be accounted for simply. Illustrative examples show how the over all pseudo sorption maximum is related to soil properties, and that these variables are spatial variates.

When it is of interest to consider P-desorption for large numbers of soil samples, as for spatially variable soil systems, a routine fashion is required to evaluate which part of overall sorption is reversibly sorbed, and with what affinity. This problem is considered in Chapter 7. Special attention is given to the spatial variability of parameters and variables, and some consequences for criteria of P-

saturated soils in the context of the Protocol Phosphate Saturated Soils (Appendix D).

To describe transport in spatially variable fields, use is made of stochastic theory. In Chapter 8 a first approach, based on normally distributed P-input and pseudo sorption maximum for P is given. Results were obtained with Monte Carlo simulations. An analytical solution for a similar problem concerning heavy metal transport is given in Chapter 9, assuming lognormal distributions of the input, the flow velocity, and the retardation factor. When, e.g. in the context of the Protocol Phosphate Saturated Soils, disposal of animal manure and phosphate is stopped, phosphate will be redistributed in the soil profile. This situation is studied in Chapter 10 for columns as well as for the field studied also in Chapter 8, that exhibits pronounced spatial variability. In this first approach considering P-redistribution in a spatially variable field, only the reversible P-adsorption was taken into account.

In Chapter 11 transport is described for a different heterogeneous flow domain than in Chapters 8-10. The flow domain consists of two layers with different porosities, flow velocities and retardation factors, that are separated by a sharp interface parallel to the direction of flow. In view of the small P-concentrations allowed to pass the phreatic ground water level, the assumption of linear sorption may be acceptable in groundwater. The problem studied in Chapter 11 then may serve as an analogon for P transport in groundwater, even though this paper was originally focussed on more general aspects of contaminant transport.

In Chapter 12 the main conclusion is given. Inevitably, with the limited time at my disposition, some important topics had to be given a lower priority. For a better balance some topics, not taken into account in the main text, were added in the appendices. These often preliminary results as well as some background information were supplied mainly to justify assumptions made in the main text, or for easy reference. Most of the work presented in this thesis was, or will be, published in refereed international journals. Details on references are provided after the contents-section.

1.5 References

- Appelo, C.A.J., G.J.W. Krajenbrink, C.C.D.F. van Ree, and L. Vasák, Beïnvloeding van de grondwaterkwaliteit in het infiltratiegebied van de Noordwestelijke Veluwe, Inst. Earth Sciences, Free Univ. Amsterdam 140 pp, 1982
- Beek, J., Phosphate retention by soil in relation to waste disposal, Ph.D thesis, Agricultural Univ., Wageningen, 1979
- Biggar, J.W., and D.R. Nielsen, Spatial variability of leaching characteristics of a field soil, Water Resour. Res., 12, 78-84, 1976
- Bleuten, W., and M. Cerutti, De huidige en toekomstige nitraat-en sulfaatbelasting van grond- en drinkwater van de Nederlandse pleistocene randgebieden, H₂O, 17, 208-212, 1984
- Breeuwsma, A., en O.F. Schoumans, Fosfaat ophoping en -uitspoeling in de bodem van mestoverschot gebieden. Report 1866, Dutch Soil Survey Inst., 1986
- Bresler, E., and G. Dagan, Solute dispersion in unsaturated heterogeneous soil at field scale, II, applications, Soil Sci.Soc.Am.J. 43, 467-472, 1979
- Dagan, G., and E. Bresler, Solute dispersion in unsaturated heterogenous soil at field scale, I, Theory, Soil Sci.Soc.Am.J. 43, 461-467, 1979
- De Haan, F.A.M., and W.H. van Riemsdijk, Behaviour of inorganic contaminanants in soil, In: J.W. Assink and W.J. van den Brink, (eds), Contaminated Soil, 19-32, Martinus Nijhoff, Dordrecht, 1986
- De Haan, F.A.M., M.G. Keizer, Th.M. Lexmond, W.H. van Riemsdijk, and S.E.A.T.M. van der Zee, Some recent developments and approaches in soil protection research, Neth.J.Agr.Sci., 34, 361-370, 1986
- De Haan, F.A.M., S.E.A.T.M. van der Zee, and W.H. van Riemsdijk, The role of soil chemistry and soil physics in protecting soil quality; variability of sorption and transport of Cd as an example, Neth.J.Agric.Sci., 35, 347-359, 1987
- Denneman, W.D., H.E. van Capelleveen, and N.M. van Straalen, Bijdrage aan de ecologische normstelling van bodembescherming opgesteld t.b.v. Voorlopige Technische Commissie Bodembescherming, Free

- Univ. Amsterdam, In: Bijlagen behorende bij het advies Bodemkwaliteit, (VTCB) Leidschendam, 1986
- Ferdinandus, H.H.M., Beperking van de aanvoer is de enige echte oplossing, problemen met zware metalen in de landbouw, Ir.thesis, Agric.Univ. Wageningen, 1987
- Fordham, A.W., and U. Schertmann, Composition and reactions of liquid manure (Gülle) with particular reference to phosphate II Solid phase components, J. Environ.Qual., 6, 136-140, 1977
- Gerritse, R.G., Phosphorus compounds in pig slurry and their retention in the soil, In: J.H. Voorburg (ed.) Utilization of manure by land spreading (EUR 5672e) pp 257-277, Luxembourg, 1976
- Gerritse, R.G., and R. Eksteen, Dissolved organic and inorganic phosphorus compounds in pig slurry, J.Agric.Sci. (Cambridge), 90, 39-45, 1978
- Henkens, Ch.H., Beleid ten aanzien van cadmium aanvoer in de akkerbouw, De Buffer, 29, 1-48, 1983
- Hirst, J.M., H.H. le Riche, and C.L. Bascomb, Copper accumulation in the soil of apple orchards near Wisbech, Plant Pathology 10, 105-108. 1961
- Indicatief Meerjaren programma Milieubeheer, 1986-1990, Ministries of VROM, L.&V. and V.&W., 's Gravenhage, 1985
- Jury, W.A., Simulation of solute transport using a transfer function model, Water Resour. Res., 18, 363-368, 1982
- Jury, W.A., G. Sposito, and R.E. White, A transfer function model of solute transport through soil, 1, Fundamental concepts, Water Resour. Res. 22, 243-247, 1986
- Lexmond, Th.M., The effect of soil pH on copper toxicity to forage maize grown under field conditions, Neth.J.Agric.Sci., 28, 164-183, 1980
- Lexmond, Th.M., W.H. van Riemsdijk, and F.A.M. de Haan, Onderzoek naar fosfaat en koper in de bodem in het bijzonder in gebieden met intensieve veehouderij, Agric.Univ.Wageningen, 1982
- Lexmond, Th.M., W.H. van Riemsdijk, and F.A.M. de Haan, Variatie in het fosfaatbindend vermogen, geïllustreerd met waarnemingen in de provincie Gelderland, Bedrijfsontwikkeling, 16, 180-184, 1985
- Ma, W., Regenwormen als bio-indicators van bodemverontreiniging. Reeks Bodembescherming 15, 's-Gravenhage, Staatsuitgeverij, 1983

- MacNicol, R.D., and P.H.T. Becket, Critical tissue concentrations of potentially toxic elements, *Plant and Soil*, 85, 107-129, 1985
- Nielsen, D.R., J.W. Biggar, and K.T. Erh, Spatial variability of field measured soil-water properties, *Hilgardia*, 42, 215-221, 1973
- Steenvoorden, J.H.A.M., H. Fonck, and H.P. Oosterom, Losses of nitrogen from intensive grassland systems by leaching and runoff, In: H.G. van der Meer, J.C. Rijden, and G.C. Ennik (eds.), *Nitrogen fluxes in intensive grassland systems*, *Developm. Plant Soil Sci.*, 23, 85-97, Martinus Nijhoff Publ., 1986
- Thornton, J., Metal contamination of soils in U.K. urban gardens: implications to health, In: J.W. Assink, and W.J. van den Brink (eds.), *Contaminated Soil* Martinus Nijhoff Publ., Dordrecht, 203-209, 1986
- Ulrich, B., and E. Matzner, Abiotische Folgewirkungen der weiträumige Ausbreitung von Luftverunreinigungen, *Luftreinhaltung Forschungsbericht* 104 02 615
- Van Daalen, M., De ontwikkeling van de intensieve veehouderij, *Cahiers Bio-wetenschappen en Maatschappij* 10, 14-23, 1985
- Van de Meent, D., J. van Oosterwijk, and T. Aldenberg, RID-VEWIN meetnet regenwater 1978-1982, Deel I: Samenvatting en statistische bewerking van de meetresultaten, Deel Ia: De meetnet gegevens, Bilthoven, RIVM, 1984
- Van Der Zee, S.E.A.T.M., W.H. van Riemsdijk, H.N.M. Ferdinandus, and F.A.M. de Haan, Fosfaat uitspoeling bij overmatige drijfmestdosering, *Meststoffen*, 14-18, 1987
- Van Der Zee, S.E.A.T.M., W.H. van Riemsdijk, and F.A.M. de Haan, Transport of heavy metals and phosphate in heterogeneous soils, In: *Proc. 2nd Int'l TNO-Conf. Contaminated Soil*, Hamburg, April, 1988
- Van Der Zee, S.E.A.T.M., W.H. van Riemsdijk, Th.M. Lexmond, and F.A.M. de Haan, Vulnerability in relation to physico-chemical compound behaviour, and spatially variable soil properties, *Proc. Int'l Conf. Vulnerability of Soil and Groundwater to pollutants*, TNO-CHO publ. no. 38, 515-525, 1987
- Van Der Zee, S.E.A.T.M., W.H. van Riemsdijk, and F.A.M. de Haan, Toelichting op het protocol fosfaat verzadigde gronden, *Agric.Univ.Wageningen*, (in preparation), 1988

- Van Grinsven, J.J.M., F.A.M. de Haan, and W.H. van Riemsdijk, Effects of acid deposition on soil and groundwater, in: T. Schneider (ed.) Acidification and its Policy Implications, Elsevier, Amsterdam, pp. 65-75, 1986
- Van Ommen, H.C., M.Th. van Genuchten, W.H. van der Molen, R. Dijkma, and J. Hulshof, Experimental and theoretical analysis of transport from a diffuse source of contamination, submitted J. Hydrol., 1988a
- Van Ommen, H.C., J.W. Hopmans, and S.E.A.T.M. van der Zee, Prediction of solute breakthrough from scaled soil physical properties, submitted J. Hydrol., 1988b
- Van Riemsdijk, W.H., Reaction mechanisms of phosphate with $Al(OH)_3$ and sandy soil, PhD thesis, Agric.Univ.Wageningen, 1979
- Van Riemsdijk, W.H., L.J.M. Boumans, and F.A.M. de Haan, Phosphate sorption by soils, I. A diffusion-precipitation model for the reaction of phosphates with metal oxides in soil, Soil Sci.Soc.Am.J. 48, 537-540, 1984
- Van Riemsdijk, W.H., S.E.A.T.M. van der Zee, Th.M. Lexmond, and F.A.M. de Haan., Fosfaatbelasting van de bodem in het Dommeldal, Bedrijfsontwikkeling 16, 175-179, 1985a
- Van Riemsdijk, W.H. et al., Nutrienten belasting in het Dommeldal, Agric.Univ., Wageningen, 1985b
- Van Riemsdijk, W.H., Th.M. Lexmond, C.G. Enfield, and S.E.A.T.M. van der Zee, Phosphorus and heavy metals: accumulation and consequences, In: Animal manure on Grassland and Fodder Crops, Fertilizer or Waste?, H.G. van der Meer et al (eds.), Martinus Nijhoff Publ., Dordrecht, 213-228, 1987
- VROM, Discussie notitie Bodemkwaliteit, In: Bijlagen behorende bij het advies Bodemkwaliteit., Ministry VROM, Leidschendam (VTCB), 1986
- VTCB, Advies besluit dierlijke meststoffen, Leidschendam, 1986
- Wadman, W.P., C.M.J. Sluijsmans, and L.C.N. de la Lande Cremer, Value of animal manure: changes in perception, In: Animal manure on Grassland and Fodder Crops, Fertilizer or Waste? H.G. van der Meer et al (eds.) Martinus Nijhoff Publ., Dordrecht, 1-16, 1987

2. A NEW TECHNIQUE FOR ASSESSMENT OF REVERSIBLY ADSORBED PHOSPHATE

Abstract

A new desorption technique for soil-phosphate is described, in which iron oxide coated filterpaper is used as an "infinite" sink for P. This technique is applied to study desorption kinetics for nine sandy soils. The desorption can be explained with a simple Langmuir kinetics model. The mean value of the desorption rate constants found is $k_d = 0.2 \pm 0.08 \text{ hours}^{-1}$. The estimated errors that are due to re-equilibration during the experiments are less than experimental error. The amounts of P desorbed with the new technique, P_i , are compared to the amounts that desorb if a conventional dilution technique, P_w , is used. The new technique desorbs more P than the conventional method ($P_i > P_w$). By comparing P_i with oxalate-extractable P (P_{ox}) it is evident that reversibly adsorbed P rarely exceeds one third of P_{ox} . Differences between the soils can be explained in terms of the oxalate extractable amounts of Fe and Al.

2.1 Introduction

The reaction of phosphate (denoted P) with soil minerals has been studied from the scope of soil fertility, theoretical soil chemistry and environmental concerns. In non-calcareous soils P reacts mainly with clay minerals and with the oxides of aluminum (Al) and iron (Fe). It has been established, that the over-all reaction often does not reach equilibrium at practical laboratory time scales and that it is only partially reversible [Barrow, 1979; Beek, 1979; Van Riemsdijk and De Haan, 1980; Enfield et al., 1981]. The reversibility of the reaction and the desorption kinetics are of major concern for fertilizer application efficiency and mobility of soil-P. For the reaction, several processes have been proposed that may occur simultaneously.

It has been established that the surfaces of (hydr)oxides of Al and Fe have a high affinity for P. The adsorption reaction onto the

surface of these hydroxides has fast kinetics (for a review see Beek and Van Riemsdijk, 1982). The effects of the solution concentration of P and the pH on the adsorption reaction are important. Besides rapid adsorption a long term reaction with slower kinetics may occur. This reaction was described by Novak and Petschauer [1975], Enfield et al. [1981], Barrow [1983] and Van Riemsdijk et al. [1984a] as a diffusion controlled process. The various descriptions of the slower reaction are conceptually different but all assumed a reaction of P with the bulk of the reactive solid phase, occurring concurrently with the rapid adsorption. The slow reaction was considered responsible for P-fixation, i.e., sorption-desorption hysteresis reported in literature [Kuo and Lotse, 1974; McLaughlin et al., 1977; Beek, 1979]. It is assumed here, that P-fixation is caused by a conversion of metal oxides into a metal-phosphate phase [Van Riemsdijk et al., 1984a], having slow dissolution kinetics. In that case mobilization of solid phase P is dominated by desorption of P, which was adsorbed onto the surface of the reactive solid phase. However, the experimental study of desorption may then still be complicated by the slow sorption process. Apparent readsorption as observed by Muns and Fox [1976] and Barrow [1979] was attributed to the progress of the slow reaction, because the concentration of P was not negligible during their desorption experiments. Even if a significant bulk reaction does not occur, re-equilibration prohibits the estimation of the amount of reversibly sorbed P if only one solid-solution ratio is used.

To overcome this problem, a series of measurements may be performed as a basis for extrapolation to "infinite" large dilution [Barrow, 1979]. Another feasible approach is to measure desorption as a function of time and to fit the observations to model equations [Barrow et al., 1981; Sharpley, 1983]. At large dilutions, or at low initial P contents of the soil, analytical inaccuracy may cause poor reproducibility of the results. Therefore a modification using anion resins was developed by Amer et al. [1955] to avoid these problems. The resin served as a competitor with soil for dissolved P, thus maintaining a low P concentration in solution. The amounts of desorbed P found using resins correlated well with plant P uptake [Cook and Hislop, 1963; Walmsley and Cornforth, 1973; Elrashidi et al., 1975]. However, separation of the resin from the soil may cause substantial

problems and competition of other anions for the resin may be pronounced as the resins are not very specific for P. Sibbesen [1978] concluded that the rate of P desorption from soil controlled the rate of transfer of P from soil to resin. However, Vaidyanathan and Talibudeen [1970] suggested, that diffusion of P into the resin may be rate limiting, which would complicate the assessment of the desorption kinetics parameters. Barrow and Shaw [1977b] concluded that no experimental conditions can be created to assure that the resin acts as an "infinite sink" for P by keeping the solution P concentration insignificant.

In this study the desorption kinetics of P are studied using a new experimental technique. In contrast to most anion resins the sink employed shows a preference for P over other anions common in soil and may be retrieved easily from soil suspensions. The errors involved due to build-up of a small concentration of P during the desorption experiments are discussed. The new technique is used in a routine procedure to assess the reversibly sorbed P in 24 sandy and clayey soils. The relations between reversibly sorbed P and some soil parameters are discussed.

2.2 Theory

The assessment of the amount of reversibly sorbed P, Q_0 , is done by perturbing the equilibrium in a soil solution. Upon dilution with electrolyte or addition of a sink, P will desorb until a new equilibrium is reached. To describe the equilibrium of P with soils or oxides, several multicomponent, electrostatic models were proposed [Barrow et al., 1981; Sigg and Stumm, 1981; Goldberg and Sposito, 1984] which incorporate the effects of pH and P concentration. Only the model by Barrow et al. [1981] has been extended to describe the kinetics of adsorption and desorption. For the rate of desorption they used:

$$\frac{dQ}{dt} = -k_d Q \quad (1)$$

where Q is the adsorbed amount of P, k_d is the desorption rate constant, t is the time.

Equation (1) is used here to assess the amount of P adsorbed and the value of k_d for the soils. This procedure is justified if an "infinite sink" is present that keeps the P concentration in solution, c , negligibly low.

To understand the errors involved if c is small but not negligible, equation (1) is extended to the combined kinetics equation:

$$\frac{dQ}{dt} = k_a c (Q_m - Q) - k_d Q \quad (2)$$

where k_a = adsorption rate constant

Q_m = adsorption maximum

At equilibrium ($\frac{dQ}{dt} = 0$) equation (2) reduces to the Langmuir equation:

$$Q = \frac{K Q_m c}{1 + K c} \quad (3)$$

where $K = k_a/k_d$. For the soils considered here the adsorption data at constant pH could be described very well [Van der Zee et al., 1986; Van der Zee and Van Riemsdijk, 1986]. We do not intend to describe desorption over a wide range of pH, and thus equation (2) is preferred over more general electrostatic models.

If desorption occurs in the presence of an "infinite sink", which has a sufficiently high capacity and affinity to ensure a negligible concentration, c , and complete desorption at infinite time, the following conditions may be formulated:

$$t = 0, \quad Q = Q_0, \quad c = c_0 \quad (4)$$

$$t > 0, \quad Q = Q(t), \quad c = 0 \quad (5)$$

Then equation (1) can be integrated to yield

$$Q(t) = Q_0 \exp(-k_d t) \quad (6)$$

The values of Q_0 and k_d obtained from desorption experiments using an "infinite sink" may be combined with other sorption parameters, determined from sorption data, for a complete description of

sorption/desorption behaviour. This description may be used to describe P displacement in columns [Van der Zee and Van Riemsdijk, 1986]. In the case of animal manure disposal that concerns quantities far exceeding the crop's demands for P, near saturation of the soil with P becomes feasible. The total inorganic P content of P saturated soils (\equiv total sorption maximum, F_m) is the sum of the adsorption maximum (Q_m) and the maximal sorption due to the slow reaction (S_m). It was shown by Beek [1979], Beek et al. [1980] and recently by Van der Zee and Van Riemsdijk [1987] that F_m (mmol.kg^{-1}) may be related to the oxalate extractable fractions of Fe and Al (mmol.kg^{-1}) by

$$F_m = \alpha_m (Fe + Al)_{ox} \quad (7)$$

If soil is not P saturated the total sorption, F , is smaller than F_m and a ratio smaller than α_m is found, i.e., $\alpha = F/(Fe + Al)_{ox}$. The oxalate extractable part of Fe and Al represents mainly the Fe and Al present in the soil as reactive, amorphous (hydr)oxides [Beek, 1979]. That inorganic P is predominantly associated with this fraction was shown for a large number of different soils by Lexmond et al. [1982], who found that oxalate extractable P, P_{ox} , equals 0.92 F (Chapter 6). Henceforth we approximate F by P_{ox} . This knowledge and relation (7) are used by Van der Zee and Van Riemsdijk [1986] to model the vertical P displacement in a field that is heterogeneous with respect to the Fe and the Al contents. For soils that vary in the content of reactive material the adsorption maximum will also vary. In analogy with eq. (7) the adsorption maximum is expressed as a function of $(Fe + Al)_{ox}$:

$$Q_m = \beta_m (Fe + Al)_{ox} \quad (8)$$

As generally $Q_0 < Q_m$, also the proportionality parameter $\beta (= Q_0/(Fe+Al)_{ox})$ will be less than or equal to β_m . Note that the ratio β/α , approximately equal to Q_0/P_{ox} , represents the fraction of P adsorbed reversibly with respect to the total (inorganic) P content.

2.3 Materials and methods

Subsamples of the air dried and sieved soils were extracted with acid ammonium-oxalate according to Schwertmann [1964]. Fe, Al and P were measured in the extract. The pH was measured in the supernatant after shaking 20 g air-dried soil overnight in 0.05 L 0.01 M CaCl_2 . Organic carbon was oxidized with dichromate according to [Mebius, 1960]. The green color due to Cr^{3+} formed was quantitated at wavelength of 585 nm [Metson, 1960]. To relate the color intensity to organic carbon content $(\text{COONa})_2$ was used as a reference. The amount of desorbed P was measured with the procedure of Sissingh [1971] and is denoted by P_w . This quantity gives water desorbable P on the basis of a volume of soil instead of soil mass. Routinely the P_w -value is given in mg P_2O_5 per liter soil.

The "infinite sink" consists of iron-oxide impregnated filter paper (Schleicher & Schuell, 602 h, ϕ 150 mm), cut into 2 x 10 cm strips, prepared by saturation in 0.4 M FeCl_3 solution and subsequent gentle pulling through a 2.7 M NH_4OH solution. The impregnated paper was dried after washing with distilled water. Such a filter paper strip contains approximately 120 μmol Fe and has a BET-specific surface area of 1.5 m^2 (paper and oxide) as determined by N_2 -gas adsorption (Carlo Erba Strumentazione Sorptomatic 1800). Desorption experiments were carried out in 100 ml screw-capped glass jars (Schott Duran) equipped with a perspex paper holder.

To determine desorbable P, 1 g of soil was suspended in 40 cm^3 of electrolyte solution (always 5×10^{-4} M KCl and 5×10^{-3} M CaCl_2). Each jar equipped with the chosen number of strips was rotated end-over-end at 30 rpm for the designated period of time (up to 66 hours). Afterwards the strips were removed, washed in demineralized water and air dried (room temperature). Both Fe and P associated with the filter paper were extracted in 0.04 L of 0.2 M H_2SO_4 during 4 h of end-over-end shaking at 30 rpm in polyethylene bottles. This caused a complete dissolution of the iron oxide associated with the paper. The same procedure was used to determine adsorption of P from a standard solution onto the filter paper. However, in that case concentrations in solution were also measured. All measurements of P were made colorimetrically [Murphy and Riley, 1962].

2.4 Results

The adsorption of P from a standard solution onto the Fe oxide coated paper as a function of contact time is given in Fig. 1a. For the conditions imposed, a maximum is reached after approximately 15 h. The adsorption isotherm for the contact time of 20 h, presented in Fig. 1 indicates that the sorption is indeed of the high affinity type, as one strip of paper is able to adsorb about 18 μmol of P under these conditions without leaving measurable amounts in solution. The effect of the amount of sink used is shown in Fig. 2 for two contact times for the soils denoted as LOT 1 (moderate content of native P) and as BAEX 1 (extremely high content of native P). If more than three strips of paper are used for each g of soil the desorbed amount becomes nearly independent of the amount of sink employed. This suggests that the concentration build-up is insignificant in that case.

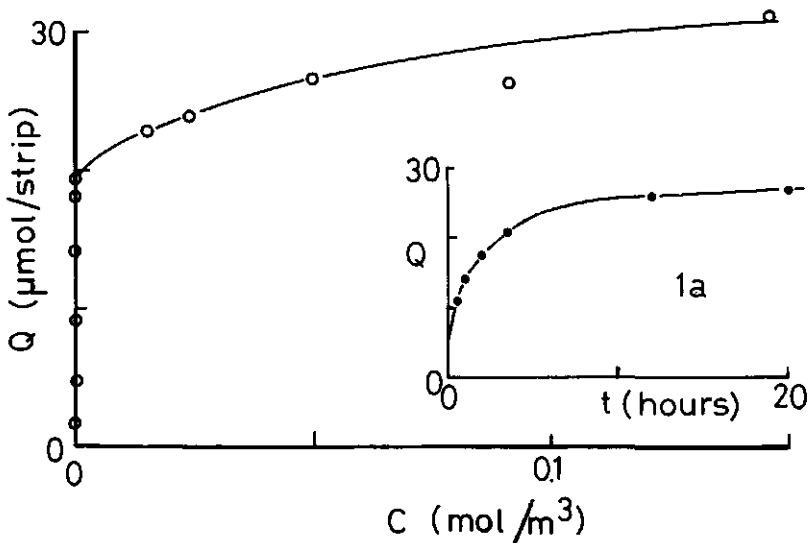


Figure 1: Adsorption of phosphate onto one strip (2 x 10 cm) of iron oxide paper. Q as a function of c for contact time of 20 h. Inset figure 1a: Q as a function of time.

Thus the desorption rate controls the transfer of P from soil to sink, and the desorption kinetics may be studied by applying equation (6), provided 4 paper strips/g soil are used. This type of study was carried out for nine sandy soils. Although at long desorption times, Q will become low enough to facilitate equilibration, see equation (2), all desorption times (up to 66 h) were used for estimating the model parameters using non-linear optimization techniques. The resulting parameter values are compiled in Table 1. The data exhibit a large variation in Q_0 found for different soils by fitting eq. (6). The resulting value of k_d is $0.2 \pm 0.08 \text{ h}^{-1}$.

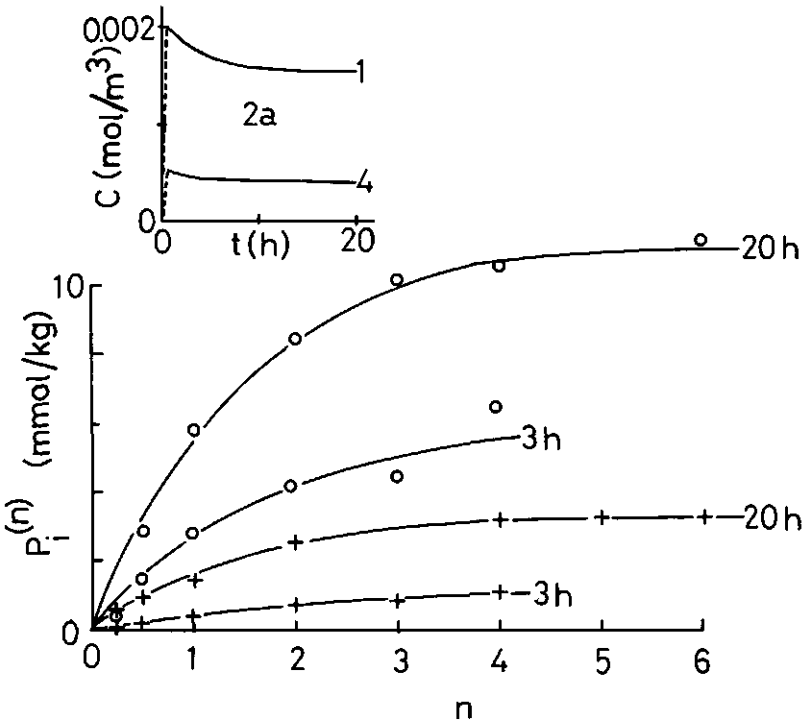


Figure 2: The amount desorbed, P_i , as a function of the number of iron oxide coated paper strips per gram soil, n , for two soils. + : LOT 1 and o : BAEX 1. Desorption time as indicated in figure. Inset figure 2a: calculated concentration c as a function of time t . Numbers indicate the number of paper strips used, n .

Taking for k_d the mean value plus one standard deviation (0.28 h^{-1}) or minus one standard deviation (0.12 h^{-1}) the amount of desorbed P after 20 h desorption time equals (eq. 6) 99.7% and 89% of Q_0 , respectively. Therefore a desorption time of 20 h is reasonable to assess the amount of reversibly adsorbed P.

Table 2 lists the amounts of P desorbed when the iron oxide coated paper is applied in standard fashion ($P_i^{(1)}$, $P_i^{(4)}$), using 1 and 4 strips, respectively and a desorption time of 20 h). The results of a dilution method (P_w), the oxalate extractable amounts of P, Fe and Al, as well as the organic carbon content and pH are also listed in Table 2. Fig. 3 shows that $P_i^{(1)}$ and $P_i^{(4)}$ are correlated well with P_w , and Fig. 4 shows that $P_i^{(4)}$ is weakly correlated with P_{Ox} .

Table 1: Values of the amount of phosphate initially adsorbed reversibly, Q_0 , and the desorption rate constant, k_d , for 9 Dutch soils, as obtained by curve-fitting of equation (6).

Soil	$Q_0 \text{ mmol kg}^{-1}$	$k_d \text{ h}^{-1}$
SIM R	0.63	0.216
YSS 5	3.16	0.079
BAR 6	4.48	0.137
HAR 4	4.47	0.194
MIL 1	4.56	0.218
BAEX 3	6.03	0.246
MER 1	6.97	0.185
HAR 6	8.78	0.214
BAEX 1	12.51	0.353

2.5 Discussion

The desorption kinetics have been studied for nine closely related, non-calcareous, sandy soils. As the differences in the reactive solid phase surfaces for these soils are expected to be minor, and as k_d for a given adsorbate (P) is a constant characterizing the reactive surface, a narrow range in k_d values may be expected. The average k_d -

value (0.2 h^{-1}) corresponds well with the value calculated by Barrow et al. [1981] for the goethite surface : 0.15 h^{-1} .

The values of k_d are obtained by means of equation (6). However, as re-equilibration is bound to occur, the estimates of Q_0 and k_d are biased. Since the concentrations of P in solution after long equilibration times are generally too small to be measured (less than $5 \times 10^{-4} \text{ mol m}^{-3}$), the errors in Q_0 and k_d must be evaluated indirectly.

Assuming equilibrium at long equilibration times and a final concentration of $c_f = 5 \times 10^{-4} \text{ mol m}^{-3}$ the error in Q_0 is obtained from the Langmuir isotherm, by inserting c_f . Using values of K and Q_m of the order as reported for similar soils by Van der Zee and Van Riemsdijk [1986], ($K \approx 10\text{-}50 \text{ m}^3 \text{ mol}^{-1}$ and $Q_m \approx 10 \text{ mmol kg}^{-1}$), yields an error in Q_0 of less than 2.5% of Q_m . This is within experimental error.

For an estimation of the error in k_d resulting from the build-up in P concentration, equation (2) is integrated for the artificial condition of a small and constant $c=c_f$. This yields:

$$Q(t) = \frac{K Q_m c_f}{1 + K c_f} \{ 1 - \exp[-(k_a c_f + k_d)t] \} + Q_0 \exp[-(k_a c_f + k_d)t] \quad (9)$$

Setting $Q_f = K Q_m c_f / (1 + K c_f)$, eq. (9) is rewritten:

$$\frac{Q(t) - Q_f}{Q_0 - Q_f} = \exp[-(k_a c_f + k_d)t] \quad (10)$$

By the analogy of equation (10) with equation (6) it is apparent that the error in k_d may be approximated by the term $k_a c_f$. For a value of $k_a = 10$ to $50 \text{ m}^3 \text{ mol}^{-1} \text{ h}^{-1}$ [Van der Zee and Van Riemsdijk, 1986] the error in k_d will be approximately 0.005 h^{-1} , which is within experimental error.

Thus at first glance the errors in Q_0 and k_d , resulting from a finite solution concentration of P, are insignificant. However, the concentration of P is not constant. Notably in the beginning when the desorption rate of soil P is highest, the solution concentration of P may be larger than at later times and at equilibrium. To calculate the P solution concentration over time, the desorption process is simulated for the BAEX 1 soil in the presence of one and four paperstrips per gram soil. Equation (2) is solved numerically for the

Table 2. Selected properties of 24 Dutch soils.

Soil	no.	C _{org} wgt. %	pH	P _{ox} ⁻¹ mmol kg ⁻¹	Fe _{ox} ⁻¹ mmol kg ⁻¹	Al _{ox} ⁻¹ mmol kg ⁻¹
AST 1	1	1.2	6.0	16.1	3.1	25.2
AST 3	2	2.3	5.8	24.0	71.7	34.5
BAEX 1	3	1.7	5.4	35.7	35.5	22.3
BAEX 3	4	1.2	4.8	16.6	20.9	15.2
BAR 1	5	1.9	5.0	27.9	95.5	28.7
BAR 6	6	2.1	5.5	17.6	39.5	63.3
EIB 4	7	2.5	5.4	15.1	35.7	41.9
EIB 5	8	2.5	5.5	17.4	13.0	38.6
GEN 2	9	2.6	5.8	16.2	120.4	57.4
GEN 3	10	1.3	5.3	40.0	49.3	41.4
HAR 4	11	1.9	5.3	18.3	14.5	50.4
HAR 5	12	2.1	5.5	18.0	14.2	49.9
HAR 6	13	2.2	5.4	23.8	13.8	44.7
LOT 1	14	2.0	5.1	15.2	9.8	64.3
MER 1	15	2.0	5.2	23.8	25.0	25.5
MER 4	16	4.0	5.9	24.5	45.5	33.3
MER 5	17	11.3	5.3	31.5	295.8	37.4
MER 6	18	10.1	5.4	19.0	171.4	27.9
MIL 1	19	1.9	5.6	13.8	17.2	19.6
MIL 2	20	2.3	5.6	24.3	19.1	20.9
SIM R	21	2.5	5.3	5.3	53.7	36.0
VRE 1	22	4.2	5.3	11.0	7.6	76.4
VRE 2	23	3.4	5.4	10.6	7.1	75.0
YSS 5	24	3.2	5.5	10.3	27.4	35.9

	α	P _w mg P ₂ O ₅ L ⁻¹	P _i ⁽¹⁾ mmol kg ⁻¹	P _i ⁽⁴⁾ mmol kg ⁻¹	β	material
1	0.569	218	3.80	8.66	0.306	s
2	0.226	36	5.10	3.36	0.032	s
3	0.618	300	1.12	11.49	0.199	s
4	0.460	140	2.65	5.19	0.144	s
5	0.224	54	1.36	2.79	0.022	s
6	0.171	50	1.36	4.53	0.044	s
7	0.195	42	0.92	2.66	0.034	s
8	0.337	145	2.84	5.88	0.114	s
9	0.091	53	1.68	3.31	0.019	cl
10	0.441	178	3.48	8.52	0.094	sl
11	0.282	65	1.85	4.42	0.068	s
12	0.201	85	2.40	3.39	0.053	s
13	0.407	173	3.66	7.24	0.124	s
14	0.205	42	1.07	4.46	0.060	s
15	0.471	134	3.13	5.39	0.107	s
16	0.311	67	1.91	5.26	0.067	s
17	0.095	19	1.02	2.74	0.008	ps
18	0.095	13	0.51	1.49	0.007	ps
19	0.375	93	2.16	4.46	0.121	s
20	0.608	217	4.15	9.24	0.231	s
21	0.059	13	0.31	0.73	0.008	si
22	0.131	54	1.94	3.45	0.041	s
23	0.129	49	1.54	3.27	0.040	s
24	0.163	36	0.80	2.33	0.037	s

C_{org}: organic carbon

s: sandy soil; cl: clay loam, sl: sandy loam;

ps: peaty sand; si: silt loam (Soil Survey Staff, 1960).

soil and for the sink, respectively, taking into account the correct mass balances with the solution. The parameters used in this simulation were estimated from Fig. 1 for the sink, and taken from Table 2 for the soil. The adsorption rate constant for the soil was set at $25 \text{ m}^3 \text{ mol}^{-1} \cdot \text{h}^{-1}$. The inset of Fig. 2 shows the result of the simulation. A fast initial increase in c is followed by a slow decrease for $t > 0.5 \text{ h}$, and for times larger than 0.5 h is approximately constant. Moreover, if four paperstrips per g of soil are employed, c remains below the detection limit even for the soil with the high content of desorbable P. In conjunction with the results of Fig. 2 (given in the previous section) the result of this calculation supports the validity of the assumption that the sink (4 strips per g soil) causes a virtually complete desorption of adsorbed P and that the desorption rate of soil P is rate controlling. The sink may thus be called an "infinite sink".

The prominent effect of the sink may be illustrated by comparing the amounts desorbed with this sink (P_i) with the amounts desorbed using a conventional dilution technique. For the conventional method the procedure of Sissingh [1971], used widely in the Netherlands for fertilization recommendations, is used and the amounts desorbed are denoted by P_w . For 24 soils and 20 h desorption time the measured values of P_i (using one and four paperstrips) are given as a function of P_w in Fig. 3. The correlation is good with $\rho(P_i^{(1)}, P_w) = 0.976$ and $\rho(P_i^{(4)}, P_w) = 0.957$ (both 1% significance) as expected when two similar techniques are compared. Assuming a bulk density of 1250 kg m^{-3} the unit of P_w (expressed in $\text{mg P}_2\text{O}_5 \text{ L}^{-1}$) may be converted into mmol kg^{-1} by multiplication with 1.125×10^{-2} . Doing so we find that $P_i^{(4)} > P_i^{(1)} > P_w$. This may be of interest to soil fertility studies as apparently P_i may still be successfully correlated to P uptake by plants when P_w fails due to analytical inaccuracy for soils low in P [Sissingh, personal communication]. The new technique is not equivalent to an "infinite dilution" technique. In the latter case the concentration will rise for all times. This was shown not to be the case for the new technique. However, near equilibrium the partitioning of P between soil, solution and sink for the new method is similar to that between soil and solution for a dilution technique. Hence, the sink added may at equilibrium be

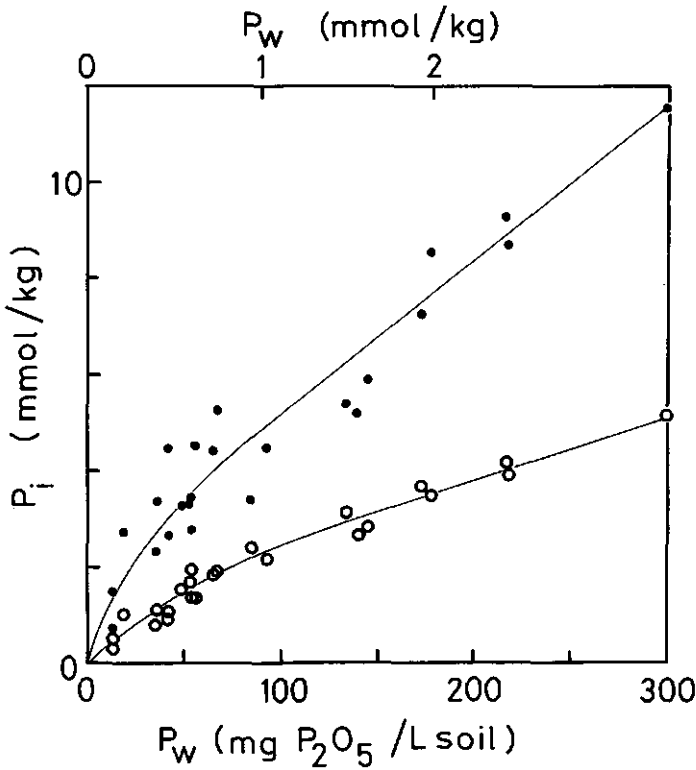


Figure 3: Amounts desorbed $P_i^{(1)}$ (o) and $P_i^{(4)}$ (●) as a function of P_w . Desorption time for P_i of 20 hours.

expressed in terms of a dilution ratio R (weight soil per volume electrolyte). This may be done numerically (iterative procedures) or analytically (Appendix 1). If the final concentration of P is $5 \times 10^{-4} \text{ mol m}^{-3}$ and the parameter values given earlier [Van der Zee and Van Riemsdijk, 1986] are used, the calculated value of R (which is the solid:solution ratio in $\text{kg} \cdot \text{m}^{-3}$) is found to be approximately 0.1 kg m^{-3} . Thus use of four paper strips corresponds approximately to 0.1 g of soil in one L electrolyte, whereas the method of Sissingh [1971] corresponds approximately to 30 g L^{-1} . The effect of the desorbable P present initially, ($Q_{\text{des}} = Q_0 - Q_f$) on the amount desorbed is shown for some values of R in Fig. 5. The computed values of Q_{des} indicate that desorption for $R = 0.1 \text{ kg m}^{-3}$ is practically complete whereas it is incomplete for R values of $100, 10,$ and 1 kg m^{-3} .

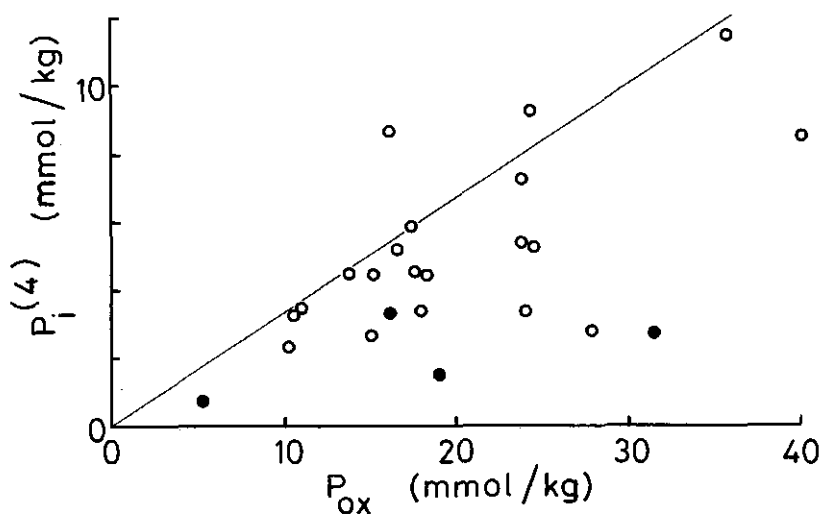


Figure 4: Amount desorbed, $P_i^{(4)}$ as a function of P_{ox} . Sandy soils (o) and other soils (●) and the line $P_i^{(4)} = P_{ox}/3$. Desorption time is 20 h.

The relation between P_i ($R \approx 0.1 \text{ kg m}^{-3}$ for $P_i^{(4)}$) and P_w (with $R \approx 30 \text{ kg m}^{-3}$) shown in Fig. 3 is curvilinear. Such curvilinear relationships are often encountered if fractionation techniques are compared and may be attributed to the effect of the non-linear isotherm. Calculating the amounts desorbed, Q_{des} , with the expressions in the appendix (for the same parameter values as used to construct Fig. 5) for dilution ratios $R = 0.1, 1, \text{ and } 10 \text{ kg m}^{-3}$ we can construct a figure similar to Fig. 3. Thus on the vertical axis we give the amount desorbed for the three values of R and on the horizontal axis Q_{des} for $R = 10 \text{ kg m}^{-3}$. By varying Q_0 in the range of 0 to 10 mmol kg^{-1} the three lines of Fig. 6 result. Indeed the curvilinear trend is found except for the lowest (1:1) line. The scatter in Fig. 3 may result among others from differences in Q_m and K between soils and analytical error, apart from the applicability of the simplified model.

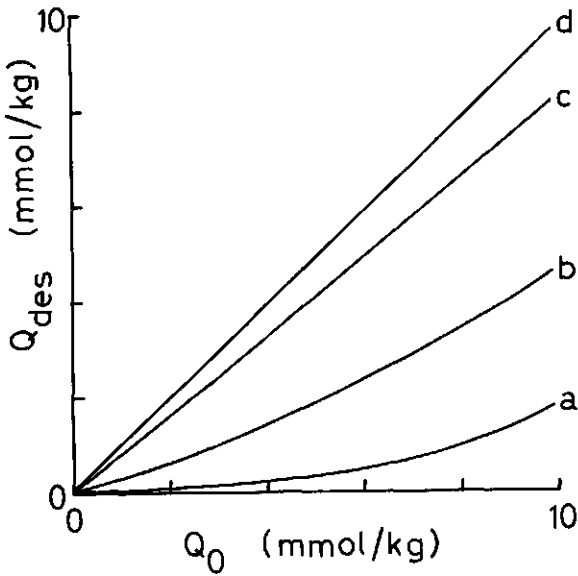


Figure 5: Desorbed amount as a function of desorbable P initially present. $R = 100$ (a); 10 (b); 1 (c); and 0.01 (d), respectively. ($Q_m = 10 \text{ mmol kg}^{-1}$ and $K = 50 \text{ m}^3 \text{ mmol}^{-1}$).

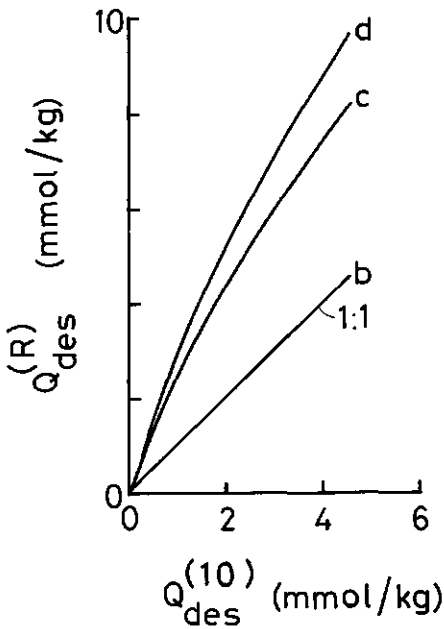


Figure 6: Desorbed amount for three R values as a function of desorbed amount for $R = 10 \text{ kg m}^{-3}$. b: $R = 10$; c: $R = 1$ and d: $R = 0.1$. The parameter values and range in Q_0 as in figure 5.

The quantities P_i and P_w provide an indication of reversibly adsorbed P (Q) whereas P_{ox} is approximately equal to total inorganic P, F. Since in the field adsorption and desorption stages alternate the temporal variations of Q will be larger than of F. The poor correlation ($\rho = 0.58$, significance 1%) between $P_i^{(4)}$ and P_{ox} may be in part attributed to the differences in sensitivity of Q and F to desorption. Where clearly F_m is larger than Q_m the data in Fig. 4 also show that F is much larger than the reversibly adsorbed P at the moment of sampling (Q_0). Regression analysis of Q_0 and F yields information for the situation at the moment of sampling but this is not of prime interest. Instead we are interested in the relation between Q_m and F_m . It is possible to get an impression of this relation as four soils are practically P-saturated, i.e., AST 1, MIL 2, BAEX 1 and BAEX 3 [Lexmond et al., 1982]. For these soils ($Q=F_m$, $F=F_m$) the relationship is approximately $Q_m = F_m/3$. The line giving $Q = F/3$ is shown Fig. 4. Since $\alpha_m \approx 0.6$ it follows from the above and eqs. (7) and (8) that $\beta_m \approx 0.2$.

2.6 Conclusions

1. Iron oxide coated filter paper may be used to approximate an "infinite" sink for P.
2. Using the new technique the desorption rate constant, k_d , may be assessed. The value obtained for nine sandy soils ($0.2 \pm 0.08 \text{ h}^{-1}$) is very close to the value of the k_d reported by Barrow [1981] for goethite.
3. With the new technique also P adsorbed, Q_0 , may be assessed.
4. The errors expected in k_d and Q_0 estimated with the new technique are dominated by experimental error and not by the fact that the sink is only an approximation of an infinite sink.
5. P desorbable in 20 hrs is found to be much lower than total inorganic P.
6. The adsorption maximum, Q_m , is approximately one third of maximum inorganic P content or one fifth of oxalate extractable (Fe + Al).
7. Iron oxide coated filter paper may be used on a routine basis to compare P contents of different soils and is an alternative to conventional dilution methods at low native P contents. For

14204

comparative purposes the sink is useful for different soils (sandy and clayey soils and peaty sands with very different contents of $(\text{Fe} + \text{Al})_{\text{OX}}$).

ACKNOWLEDGEMENT

The idea to use iron oxide coated filter paper originated from Dr. H.A. Sissingh, Institute of Soil Fertility in Haren, The Netherlands.

2.7 Appendix 1: Mathematical description of dilution experiments

An equation for the conservation of mass links the solid-liquid interphase to the liquid phase. If the solid-liquid ratio (weight soil/volume water) is denoted by R then $(R^* = 0.001 R, \text{ because } c \text{ is expressed on a molar and } Q \text{ on a mmolar - basis})$

$$\frac{dc}{dt} = - R \frac{dQ}{dt} \quad (1.1)$$

or

$$- c(t) = R^* [Q(t) - Q_0] \quad (1.2)$$

Introduction of (1.2) into equation (2) and integration yields:

$$c(t) = \frac{c_1 - c_2 \left\{ \frac{c_1}{c_2} \exp [-k_a(c_1 - c_2)t] \right\}}{1 - \left\{ \frac{c_1}{c_2} \exp [-k_a(c_1 - c_2)t] \right\}} \quad (1.3)$$

where c_1 and c_2 in equation (1.3) are given by ($j = 1, 2$):

$$c_j = \frac{1}{2} \left\{ (c_3 - 1/K) + (-1)^j [c_3^2 + (1/K)^2 + 2(c_3 + 2Q_m^*)/K]^{1/2} \right\} \quad (1.4)$$

and $c_3 = (Q_0 - Q_m) R^*$.

An expression in terms of $Q(t)$ is equally feasible, although $Q(t)$ follows also from combination of (1.2) and (1.3). At equilibrium, i.e., $t \rightarrow \infty$, the desorbed amount is thus given by

$$Q_{des}^{(R)} = c_2 (R^*, Q_0) / R^* \quad (1.5)$$

If Q_m and K are kept fixed then $c_2 = c_2(R^*, Q_0)$ depends only on Q_0 and R . Figs. 5 and 6 are constructed using equation (1.5) for several values of R , and values of Q_0 from 0 to $0.99 \times Q_m$.

2.8 Notation

c	concentration ($\text{mol} \cdot \text{m}^{-3}$)
c_0	concentration at $t = 0$ ($\text{mol} \cdot \text{m}^{-3}$)
c_f	final concentration at $t \rightarrow \infty$ ($\text{mol} \cdot \text{m}^{-3}$)
F	total sorbed amount ($\text{mmol} \cdot \text{kg}^{-1}$)
F_m	total sorption maximum ($\text{mmol} \cdot \text{kg}^{-1}$)
k_a	adsorption rate constant ($\text{m}^3 \cdot \text{mol}^{-1} \cdot \text{kg}^{-1}$)
k_d	desorption rate constant (h^{-1})
K	adsorption constant ($\text{m}^3 \cdot \text{mol}^{-1}$)
P_i	amount desorbed with the iron oxide paper ($\text{mmol} \cdot \text{kg}^{-1}$)
P_{ox}	oxalate extractable P ($\text{mmol} \cdot \text{kg}^{-1}$)
P_w	water desorbable P ($\text{mg P}_2\text{O}_5 \cdot \text{L}^{-1}$)
Q	reversibly adsorbed amount ($\text{mmol} \cdot \text{kg}^{-1}$)
Q_{des}	desorbed amount ($\text{mmol} \cdot \text{kg}^{-1}$)
Q_f	adsorbed amount at $c = c_f$ ($\text{mmol} \cdot \text{kg}^{-1}$)
Q_m	adsorption maximum ($\text{mmol} \cdot \text{kg}^{-1}$)
Q_0	adsorbed amount at $t = 0$, $c = c_0$ ($\text{mmol} \cdot \text{kg}^{-1}$)
R	solid:solution ratio ($\text{kg} \cdot \text{m}^{-3}$)
t	time (h)
$\alpha; \alpha_m$	saturation factor and maximal saturation factor for total sorption
$\beta; \beta_m$	saturation factor and maximal saturation factor for reversible adsorption

2.9 References

- Amer, F., D.R. Bouldin, C.A. Black and F.R. Duke, Characterization of soil phosphorus by anion exchange resin and ^{32}P equilibration. *Plant and Soil* 6: 391-408, 1955.
- Barrow, N.J., The description of desorption of phosphate from soil. *J. Soil Sci.* 30: 259-270, 1979.
- Barrow, N.J., A mechanistic model for describing the sorption and desorption of phosphate by soil. *J. Soil Sci.* 34: 733-750, 1983.
- Barrow, N.J., L. Madrid and A.M. Posner, A partial model for the rate of adsorption and desorption of phosphate by Goethite. *J. Soil Sci.* 32: 399-407, 1981.
- Barrow, N.J. and T.C. Shaw, Factors affecting the amount of phosphate extracted from soil by anion exchange resin. *Geoderma* 18: 309-323, 1977.
- Beek, J., Phosphate retention by soil in relation to waste disposal. PhD thesis, Agricultural University, Wageningen, 1979.
- Beek, J., W.H. van Riemsdijk, and K. Koenders, Aluminum and iron fractions affecting phosphate bonding in a sandy soil treated with sewage water. *Proc. Symp. Agr. Chemicals in soils.* Jerusalem, 1976: pp 369-379, 1980.
- Beek, J., and W.H. van Riemsdijk, Interaction of orthophosphate ions with soil. In: *Soil Chemistry, B. Physico-chemical models.* G.H. Bolt (Ed.), Elsevier Sci. Publ. BV, Amsterdam, pp 259-284, 1982.
- Cooke, I.J., and J. Hislop, Use of anion-exchange resin for the assessment of available soil phosphate. *Soil Sci.* 96: 308-312, 1963.
- Elrashidi, M.A., A. van Diest, and A.H. El-Damaty, Phosphorus determination in highly calcareous soils by the use of an anion exchange resin. *Plant and Soil* 42: 273-286, 1975.
- Enfield, C.G., T. Phau, D.M. Walters and R. Ellis Jr, Kinetic model for phosphate transport and transformation in calcareous soils, I. *Soil Sci. Soc. Amer. J.* 45: 1059-1064, 1981.
- Goldberg, S. and G. Sposito. A chemical model of phosphate adsorption by soils: I. Reference oxide minerals. *Soil Sci. Soc. Amer. J.* 48: 772-778, 1984.

- Kuo, S. and E.G. Lotse, Kinetics of phosphate adsorption and desorption by Hematite and Gibbsite. *Soil Sci.* 116: 400-406, 1974.
- Lexmond, Th.M., W.H. van Riemsdijk and F.A.M. de Haan, Onderzoek naar fosfaat en koper in de bodem in het bijzonder in gebieden met intensieve veehouderij. Staatsuitgeverij, Den Haag, 1982.
- McLaughlin, J.R., J.C. Ryden and J.K. Syers, Development and evaluation of a kinetic model to describe phosphate sorption by hydrous ferric oxide gel. *Geoderma* 18: 295-307, 1977.
- Mebius, L.J, A rapid method for the determination of organic carbon in soil. *Anal. Chim. Acta* 22: 120-124, 1960.
- Metson, A.J, Methods of chemical analysis for soil survey samples. New Zealand Department of Science and Industrial Resources. Soil Bureau Bulletin no. 12, 1956.
- Munns, D.N. and R.L. Fox, The slow reaction which continues after phosphate adsorption: kinetics and equilibrium in some tropical soils. *Soil Sci. Soc. Amer. Proc.* 40: 46-51, 1976.
- Murphy, J. and J.P. Riley, A modified single solution method for the determination of phosphate in natural waters. *Anal. Chim. Acta* 27: 31-36, 1962.
- Novak, L.T., and F.J. Petschauer, Kinetics of the reaction between orthophosphate ions and Muskegon dune sand. *J. Environ. Qual.* 8: 312-318, 1975.
- Rahman, Z.B.A, The fate of phosphate fertilizer in Malaysian soils and its effect on plant uptake. Ph.D. thesis, Gent, Belgium pp. 25-78, 1982.
- Schwertmann, U. Differenzierung der Eisenoxiden des Bodens durch Extraktion mit Ammoniumoxalaat Lösung. *Z. Pflanzenernährung, Düngung und Bodenkunde*, 105: 194-202, 1964.
- Sharpley, A.N, Effect of soil properties on phosphorus desorption. *Soil Sci. Soc. Amer. J.* 47: 462-467, 1983.
- Sibbesen, E. An investigation of the anion-exchange resin method for soil phosphate extraction. *Plant and Soil* 50: 305-321, 1978.
- Sigg, L., and W. Stumm, The interaction of anions and weak acids with the hydrous goethite (α - FeOOH) surface. *Colloids Surfaces* 2: 101-117, 1981.

- Sissingh, H.A., Analytical procedure of the P_w method, used for the assessment of the phosphate status of arable soils in the Netherlands. *Plant and Soil*, 34: 483-486, 1971.
- Soil Survey Staff, Soil classification, A comprehensive system. Soil Conservation service, USDA, p 254, 1960.
- Vaidyanathan, L.V., and O. Talibudeen, Rate processing in the desorption of phosphate from soils by ion-exchange resins. *J. Soil Sci.* 21: 173-183, 1970.
- Van der Zee, S.E.A.T.M. and W.H. van Riemsdijk, Sorption kinetics and transport of phosphate in sandy soil. *Geoderma* 38: 293-309, 1986.
- Van der Zee, S.E.A.T.M. and W.H. van Riemsdijk, Transport of phosphate in a heterogeneous field. *Transport in Porous media*, 2: 339-359 1987.
- Van der Zee, S.E.A.T.M., W.H. van Riemsdijk, and F.A.M. de Haan, Reaction kinetics and transport of phosphate: parameter assessment and modelling. In: *Contaminated Soil*, J.W. Assink and W.J. van den Brink (Eds.). Martinus Nijhoff Publ., Dordrecht, pp 157-160, 1986.
- Van Riemsdijk, W.H., L.J.M. Boumans and F.A.M. de Haan, Phosphate sorption by soils. I. A diffusion precipitation model for the reaction of phosphate with metaloxides in soil. *Soil Sci. Soc. Amer. J.* 48: 537-541, 1984.
- Van Riemsdijk, W.H. and J. Lyklema, Reaction of phosphate with gibbsite ($Al(OH)_3$) beyond the adsorption maximum. *J. Colloid Interface Sci.* 76: 55-66, 1980.
- Van Riemsdijk, W.H. and F.A.M. de Haan, Reaction of orthophosphate with a sandy soil at constant supersaturation. *Soil Sci. Soc. Amer. J.* 45: 261-266, 1981.
- Walmsley, D., and I.S. Cornforth, Methods of measuring available nutrients in West Indian soils II. Phosphorus. *Plant and Soil* 39: 93-101, 1973.

3. MODEL FOR THE REACTION KINETICS OF PHOSPHATE WITH OXIDES AND SOIL

Abstract

The reaction of P with oxides and with soil is assumed to consist of two simultaneously occurring processes: adsorption onto the reactive surfaces and diffusion into the solid bulk phase where precipitation occurs. The relatively fast adsorption reaction is described with the Langmuir kinetics equation. The diffusion/precipitation process is described with the Unreacted Shrinking Core (USC) model. For a spherical geometry (single size) the pseudo-steady state approximations are given that relate the fractional conversion of the reactive solid phase to the reaction time and the time required for the complete conversion. These solutions are given for three limiting cases, i.e., where the rate of mass transfer through a stagnant fluid film, the diffusion rate through the converted zone, and the reaction rate at the sharp interface between the converted and the non-converted zones, respectively, are controlling the overall reaction rate. The conversion may be given as a function of the product of bulk solution concentration and reaction time. Using probability theory the mean conversion of an ensemble of particles with different sizes is related to the product of bulk solution concentration and time. An analytical solution is given for an exponential size probability density function if the interface reaction rate is controlling the overall reaction rate. With this solution the pronounced non-linear conversion and sorption behaviour caused by the size distribution is illustrated. Since the soil system is usually very complex and heterogeneous the analytical solutions obtained are of very limited practical use. A simplified diffusion/precipitation model is derived from the analytical solutions that relates sorption, S , to the exposure integral, I . This functional relation $S(I)$ has to be assessed experimentally for soil.

3.1 Introduction

The reaction of P with soil and soil minerals has been given much attention in soil science and in aquatic chemistry literature. In non-calcareous soils the reaction is predominantly with solid phase constituents of Al and Fe [Beek, 1979]. This reaction was found to approach equilibrium very slowly, with a reaction rate that becomes relatively small for large reaction times, t [Beek and Van Riemsdijk, 1982; Barrow and Shaw, 1975a; Van Riemsdijk and De Haan, 1981]. It was observed frequently that the reaction is only partially reversible and that the reversibility decreases if the reaction time increases [Barrow and Shaw, 1975b; Beek, 1979]. The amount desorbed also depends on the soil weight: solution volume ratio [Van Der Zee et al., 1987a] and initial desorption may be followed by renewed retention after some time [Munns and Fox, 1976]. Van Riemsdijk and Lyklema [1981] showed that for gibbsite the reaction may continue in excess of monolayer P-coverage. In recent studies concerning soils that received large amounts of animal manure slurries, large ratios $\alpha = 0.5 - 0.6$ ($\alpha = P_{ox}/(Fe+Al)_{ox}$) of the oxalate extractable fractions were found [Van Der Zee and Van Riemsdijk, 1987a, Van Der Zee et al., 1987]. Such findings suggest that besides an adsorption reaction of P with the surface of reactive solid phases, other reaction processes also occur. Often it was found that a single mathematical expression could not describe the kinetics of the reaction for a large range of t or concentration c . The reaction of P with soil and soil minerals was described by more than one equation by Mansell et al. [1977 a,b], Beek [1979], Van Riemsdijk [1979]. Enfield et al. [1981a,b] considered a fast adsorption onto the surface of reactive minerals as well as a slower precipitation reaction with Fe, Al, and Ca. Barrow [1983] developed an involved model where adsorption is the precursor reaction of a solid state diffusion of P into the bulk of reactive minerals. The adsorption was described by a simplified version of the model developed earlier by Bowden [1973] and Bowden et al. [1980]. The adsorption equation used (Table 1) was a Langmuir equation adapted to take the surface charge of the solid phase into account. The slower diffusion process was the result of the gradient in Q caused by the adsorption and it was modelled by means of the parabolic diffusion

law. By assuming linear superposition of solutions of the amounts diffused the changes in Q in the course of time were taken into account (eq. 1.3). Based on findings by Bowden et al. [1980] the almost linear dependency of the surface potential on the amount adsorbed was taken into consideration. A similar relation was assumed for the penetrated amount and surface potential (eq. 1.4). Since adsorbing surfaces of minerals such as oxides may be heterogeneous, the equations were solved for a normally distributed surface potential (eq. 1.1). This was done after discretizing this frequency distribution.

Table 1: Equations for the model of Barrow [1983]

probability density function for initial potential (no P-sorption), Ψ_0 :

$$f_{\Psi_0}(i) = \frac{1}{s_{\Psi_0} \sqrt{2\pi}} \exp \left[-\left(\frac{\Psi_0(i) - m_{\Psi_0}}{s_{\Psi_0}} \right)^2 \right] \quad (1.1)$$

adsorption equation

$$Q/A_{sp} = \frac{(Q_{max}/A_{sp}) \alpha \gamma Kc \exp \left[-\frac{zF\Psi}{RT} \right]}{1 + \alpha \gamma Kc \exp \left[-\frac{zF\Psi}{RT} \right]} \quad (1.2)$$

diffused amount:

$$S/A_{sp} = \frac{2}{\sqrt{\pi}} \left\{ \left[\frac{Q_0}{A_{sp}} \right] \sqrt{(\tilde{D}_s f t / \omega^2)} + \sum_j \left[\frac{Q(t_j) - Q(t_{j-1})}{A_{sp}} \right] \sqrt{(\tilde{D}_s f t_j (t - t_j) / \omega^2)} \right\} \quad (1.3)$$

correction for potential:

$$\Psi(i) = \Psi_0(i) - m_1 \left[\frac{Q(t)}{Q_m} \right](i) - m_2 \left[\frac{S(t)}{Q_m} \right](i) \quad (1.4)$$

The model of Barrow [1983] was used for oxides by Bolan and Barrow [1984]. With the model summarized in Table 1 a good fit was obtained of P-sorption data for oxide and soil for a wide range of concentrations and time and many experimentally observed effects were reproduced well for a variety of conditions. However, the model is

quite complicated with as many as 8 fitting parameters. Barrow [1983] remarked that the solutions of fitting procedures were non-unique, i.e. several combinations of parameter values yielded approximately the same fitting accuracy. This limits the confidence in the physical relevance of the parameter values found and in the accuracy of extrapolation to other conditions or reaction times.

It was observed recently in soil treated with large amounts of P from animal manure slurries that due to reaction of P with Fe and Al oxides a high degree of conversion of the metal oxides into metal phosphate may occur (assuming 1:1 stoichiometry) [Van Der Zee et al., 1987a; Van Der Zee and Van Riemsdijk, 1986; 1987]. It is worthwhile to remark that high conversions are not predicted by Barrow's model since the diffusion process is modelled for the semi-infinite diffusion domain. Thus, even for high c and large t the decreasing potential will lead to small values of Q or the fractional surface saturation θ [Barrow, 1983], and to a small concentration in the solid phase (conversion). This artefact may be solved by assuming m_2 to be nonlinear at large values of S in which case another fitting parameter is required. Although Barrow did not report the subdivision of total sorption, F , into adsorption, Q , and diffusion, S , the conversion of the reactive phase was probably predicted to be low due to the rapidly decreasing solution concentration [Barrow, 1983; Bolan and Barrow, 1984].

It may be noted from eq. 1.3 that if the surface coverage is high (by keeping the concentration high and fixed) the diffused amount increases excessively. This is caused by the large values of the thermodynamic factor $f (= 1/(1-\theta))$ which become infinitely large for $\theta \rightarrow 1$. When the model was fitted, a small surface coverage, θ was generally found [Barrow, 1983]. In our opinion the model proposed by Barrow is sophisticated but should not be applied to soils. To attribute all heterogeneity to the distribution of Ψ_0 in a system containing many minerals, many of which may be non-pure mixtures of several elements (Al, Fe, Si, etc.), with many different geometries, particle sizes, and which mutually interact seems questionable. Since the model of Barrow has no sound theoretical foundation, the parameter values obtained with this model will have a limited physical relevance.

In this contribution P-sorption is described mathematically for an ensemble of spherical oxide particles with a distributed particle size in order to show the effect of this size distribution. Then, using relationships resulting from this analysis we give a simplified sorption kinetics model for P-sorption to soil which is of use even if the nature, geometries, and dimensions of the reactive phase minerals are unknown.

3.2 Theory

3.2.1 The surface reaction

The removal of P from a solution in contact with soil or oxides (of Al, Fe) is initially fast and decreases rapidly with increasing contact time. The fast reaction is generally assumed to be an adsorption process [Van Riemsdijk, 1979; Enfield et al., 1981 a,b; Barrow et al., 1981; Barrow, 1983; Van der Zee and Van Riemsdijk, 1986]. The adsorption was described with sophisticated models by Bowden [1973], Sigg and Stumm [1981], and Goldberg and Sposito [1984]. Here we intend to describe only the effects of concentration and time for which such sophistication is not necessary.

The adsorption process is assumed to be reversible with the net rate given by (for symbols see the Notation)

$$\frac{dQ}{dt} = k_a c (Q_m - Q) - k_d Q \quad (1)$$

At equilibrium the rates of the forward and of the backward reactions are equal ($\frac{dQ}{dt} = 0$), yielding the Langmuir equation

$$Q = \frac{K Q_m c}{1 + K c} \quad (2)$$

In order to determine the desorption rate constant (k_d) we cause desorption in the presence of a high affinity - high capacity sink for P as described by Van Der Zee et al. [1987]. Due to the presence of the sink the adsorption part in eq. (1) is negligible compared to the desorption part and eq. (1) becomes

$$\frac{dQ}{dt} = -k_d Q \quad (3)$$

The amount desorbed (Q^*) follows from the amount initially adsorbed (Q_{in}) and $Q(t)$:

$$Q^* = Q_{in} - Q(t) \quad (4)$$

Integration of (3) and combination with (4) yields

$$Q^*(t) = Q_{in} \{1 - \exp(-k_d t)\} \quad (5)$$

By performing desorption for different desorption times and fitting the data to eq (5) Q_{in} and k_d can be assessed.

3.2.2 The diffusion/precipitation reaction

The long term removal of solution-P caused by the reaction with soil or oxides was described by Van Riemsdijk et al. [1984] as a diffusion of P into the solid phase and the conversion of this phase into a phosphate precipitate. The backward reaction is controlled by dissolution kinetics or some sort of diffusion process. Due to the low solubility and slow dissolution this process (henceforth referred to as sorption, S) is assumed to be irreversible on a practical timescale for experiments. The sorption, S, is described with the Unreacted Shrinking Core model (USC) known from the chemical engineering literature [Wen, 1968]. The mathematical equations of the USC-model will be given for a single spherical particle of metal oxide. Using probability theory this description is extended to an ensemble of spherical particles that is characterized by a probability density function (frequency function) of particle radii. This mathematical analysis is used to illustrate the effect of size heterogeneity on overall sorption as well as to give the foundation for the scaling of reaction time. This leads to a unique relation that gives sorption as a function of an exposure variable proposed by Van Riemsdijk et al. [1984], and Van Der Zee et al. [1988].

3.2.2.1 *Unreacted shrinking core model for single particle size*

When soil or oxides are brought into contact with a solution containing P, a concentration gradient is created, that will give rise to a diffusive flux towards the interior of the solid phase. This gradient may be interpreted twofold, i.e. as a gradient of P in the solid state due to adsorption [Barrow, 1983], or as a gradient in the micro pores of the solid. Since solid state diffusion processes generally are extremely slow, we assume that the transport of P occurs through the micropores of the solid. Upon the contact of P with the metal in the oxide structure it is assumed that a reaction occurs by which the metal oxide is converted into a metal phosphate. Thus a product layer (Me-phosphate) develops which will gradually become thicker at the expense of the Me-oxide in the particle interior. This process may be modelled by means of the Unreacted Shrinking Core model [Wen, 1968].

The Unreacted Shrinking Core model describes a heterogeneous surface reaction in which either the pores of the unreacted solid are practically impervious to the reactant (P) or the reaction rate is so much larger than the diffusion rate that the reaction zone that separates the region of product (Me-phosphate) from the region with unreacted solid (Me-oxide) is very thin. If the reactant has access to the whole particle (including the unconverted part), then one speaks of a homogeneous surface reaction. Most natural situations are intermediate relative to these two limiting cases. We will assume that the unreacted core of Me-oxide is inaccessible to P and discuss the constraints this imposes later in this study.

For a single (spherical) particle, or single particle size, the mass balance equations may be given assuming that the overall conversion due to the slow process is the result of:

1. The rate of mass transfer of P through a fluid film surrounding a particle.
2. The rate of P diffusion through the Me-phosphate product layer.
3. The reaction rate at the interface of the product layer and the unreacted solid core of Me-oxide.

In this contribution the rate of transport of reaction product out of the sphere is not taken into account. Due to these three resistances

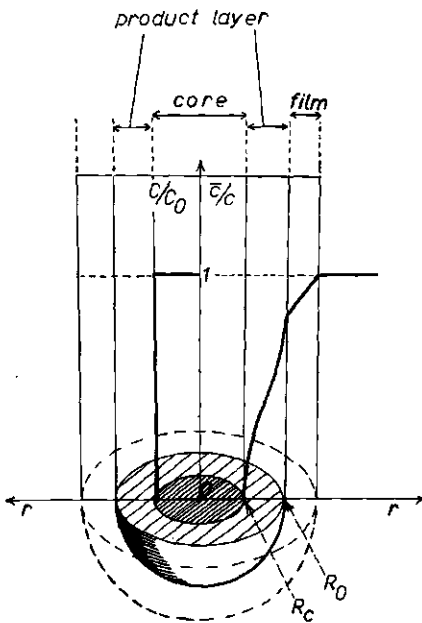


Figure 1:
Schematization of the Unreacted
Shrinking Core model

the P-concentration decreases in the direction perpendicular to the particle surface going from the bulk solution towards the core interior, as shown in Figure 1. The transport equation for this system is given for spherical geometry by

$$\epsilon \frac{\partial \bar{c}}{\partial t} = D_s \left[\frac{\partial^2 \bar{c}}{\partial r^2} + \frac{2}{r} \frac{\partial \bar{c}}{\partial r} \right] \quad R_0 > r > R_c \quad (6)$$

The transport equation must be solved for the conditions:

$$D_s \left. \frac{\partial \bar{c}}{\partial r} \right|_{R_0} = k_f (c - \bar{c}_s) \quad r = R_0 \quad (7)$$

(i.e. diffusive flux rate at $r = R_0$ is given by mass transfer)

$$D_s \left. \frac{\partial \bar{c}}{\partial r} \right|_{R_c} = m k_s C_0 \bar{c}_c \quad r = R_c \quad (8)$$

(i.e. diffusion flux rate at core surface equals the reaction rate)

$$D_s \left. \frac{\partial \bar{c}}{\partial r} \right|_{R_c} = -m C_0 \frac{\partial R_c}{\partial t} \quad (9)$$

(i.e. displacement interface is proportional to diffusion flux rate at interface). In eq. (8) we have assumed that the reaction is first order with respect to the solute. A higher order would complicate the mathematical analysis considerably and we have no evidence that a higher order would be more appropriate.

The process described by eqs. (6)-(9) is frequently encountered in chemical engineering, mining, and applied mathematics literature [Lu, 1966; Wen, 1968; Ockendon and Hodgkins, 1975; Wilson et al, 1978; Davis and Hill, 1982]. Examples where a porous product or leached layer develops are the reduction of iron ore in blast furnaces [Evans and Koo 1979], the leaching of primary sulfide ores (pyrite: FeS_2 ; chalcopyrite: CuFeS_2) [Braun et al, 1974; Bartlett, 1974; Brent Hiskey and Wadsworth, 1974] and oil shale gasification [Wen, 1968]. The opposite situation where a non-porous protective oxide coating is formed is the oxidation of elemental aluminum.

Mathematically the USC model is a moving boundary or Stefan problem. The difficulty in solving such moving boundary problems is usually to find a suitable transformation of variables. Approximate analytical solutions for the time of complete conversion where the concentration c (in the bulk of the solution) is much less than the density of the solid, C_0 , were obtained by Stewartson and Waechter [1976], Soward [1980] and Davis and Hill [1982]. The solution of the USC model is much simplified if the time derivative in eq (6) is set equal to zero, in which case the pseudo-steady state solution can be found.

The validity of the assumption of pseudo-steady state was discussed by Bischoff [1963], Bowen [1965], Bischoff [1965], Davis and Hill [1982] and Hill [1984]. The pseudo steady state solution appears applicable if c/C_0 is of the order of 10^{-3} according to Bischoff [1963] whereas Davis and Hill [1982] noted, that when this ratio is 10^{-2} , a good agreement between the pseudo steady state solution and their other approximations is found. Physically, the pseudo-steady state assumption represents a slowly moving interface with a rapid establishment of the equilibrium concentration distribution. Then the amount of solute required to advance the interface a small distance, is controlled by the amount necessary to convert the unreacted solid in this shell.

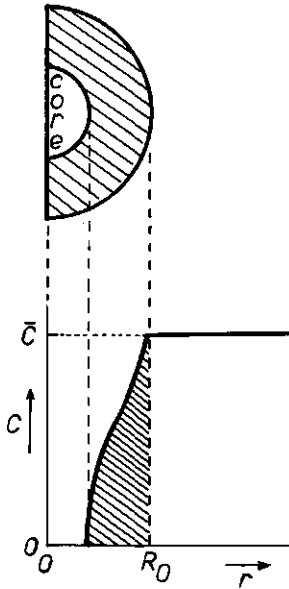


Figure 2:
Illustration of the Pseudo Steady State assumption where solute storage in the pore volume (hatched) is neglected with respect to total diffusion in $\Delta t = t_2 - t_1$ through the particle surface (arbitrary units).

The storage of dissolved solute in the product layer pores is negligible. In Fig. 2 this condition is illustrated. The pseudo-steady state approximation is valid if the storage in the pores indicated by the hatched area is small with respect to the amount diffused between t_1 and t_2 . It is to be expected that this is the case for P reacting with Me-oxides and therefore we will give the solutions for the case of pseudo-steady state [Wen, 1968; Braun et al, 1974].

Of prime interest for the present discussion is the rate of reaction as a function of time. It is therefore convenient to give the time needed to reduce the radius of the unreacted core from R_0 to R_c :

$$\begin{aligned}
 t = & \frac{mR_0 C_0}{c} \left\{ \frac{1}{3} \left[k_f^{-1} - \frac{R_0}{D_s} \right] \left[1 - (R_c/R_0)^3 \right] + \right. \\
 & \left. + \frac{1}{m k_s C_0} \left(1 - \frac{R_c}{R_0} \right) + \frac{R_0}{2D_s} \left[1 - (R_c/R_0)^2 \right] \right\} \quad (10)
 \end{aligned}$$

By insertion of $R_c = 0$ for the time of completed reaction of the sphere, $t = \tau$, into eq. (10) we find

$$\tau = \frac{m R_0 C_0}{c} \left[\frac{1}{3k_f} + \frac{R_0}{6D_s} + \frac{1}{m k_s C_0} \right] \quad (11)$$

where we recognize the three rate coefficients of mass transfer, interface reaction rate and product layer diffusion in the right hand side of eq. (11). Now, it is convenient to express the reaction time in terms of the degree of conversion, X. The conversion is the fraction (volumetric or by mass, assuming C_0 constant in the core) of the sphere that has reacted:

$$X = 1 - R_c^3 / R_0^3 \quad (12)$$

Three limiting cases are of particular interest. The conversion - time relation for a single sphere are given if one of the resistances in eqs. (10) and (11) is controlling the overall reaction rate. It may be noted that mixed controll was studied by Lu [1963] and Spitzer et al. [1966], and Van Der Zee et al. [1988].

Limiting case I: Fluid film mass transfer is rate controlling.

Then we find ($k_f \ll k_s; D_s$) that

$$t/\tau_I = X \quad (13)$$

and

$$\tau_I = \frac{m R_0 C_0}{3k_f c} \quad (14)$$

Limiting case II: Diffusion through Me-phosphate product layer is rate controlling.

Then ($D_s \ll k_f; k_s$) eqs. (10) and (12) lead to

$$t/\tau_{II} = 1 - 3(1-X)^{2/3} + 2(1-X) \quad (15)$$

where

$$\tau_{II} = \frac{m R_0^2 C_0}{6 D_s c} \quad (16)$$

Limiting case III: Reaction rate at the interface is rate controlling leading to ($k_s \ll k_f; D_s$)

$$t/\tau_{III} = 1 - (1-X)^{1/3} \quad (17)$$

with

$$\tau_{III} = \frac{R_0}{k_s c} \quad (18)$$

3.2.2.2 Correspondence to other models

The expressions given above were found for the case of a core that is not penetrable for the solute (P). However, it may be possible for some or all reactive oxides that such penetration occurs. In that case, instead of a heterogeneous surface reaction, we have a homogeneous surface reaction that occurs in the whole volume of the sphere, though not necessarily at the same rate everywhere. In reality, most conversion problems should probably be considered intermediate to the simplified homogeneous and heterogeneous cases. It may be shown [Wen, 1968] that the homogeneous model (D_s constant in $r \in (0, R_0)$) and the heterogeneous model correspond limiting case II in which case a distinction is difficult between the two models. When the reaction at the interface is rate limiting (while k_f large) the solution of the homogeneous model is mathematically different from the solution given by eqs. (17) and (18). However, even in this case the differences in the conversion-time relationships are not very large and the distinction between the homogeneous and heterogeneous models on an experimental basis is difficult [Wen, 1968].

If the order of the reaction, the order of magnitude of the rate constants (k_f, k_s, D_s) and the variation of the rate constants with e.g. temperature, concentration, porosity (differing for product layer and core) or other variables are unknown, we should be very reluctant to ascribe physical relevance to parameter values obtained by fitting one of the models to experimental results. Deviations from model assumptions (e.g. influence of counter diffusion of reaction products, non-spherical geometry, electrostatic effects, particle size

distributions) will even further complicate the problems of parameter assessment. This is also the case for other complex models (e.g. Barrow, 1983) and the uniqueness, physical relevance and extrapolation possibilities of parameter sets obtained by fitting are also questionable.

We finish this section with some remarks on the observations by Van Riemsdijk [1979] who found that the reactive edges of gibbsite became rough after reaction with P. Moreover the total surface area increased during the reaction, which proceeded far enough to exceed monolayer coverage. These findings suggest that Al-phosphate may have a larger specific volume than the original Al-oxide. Thus it is possible that the porosity (as well as D_g) in the product layer is in fact larger than for the original oxide. This supports the use of the USC model provided \tilde{D}_g in the oxide core is sufficiently less than D_g in the product layer. Another case is where the reaction product ablates, caused for example by mechanical abrasion in batch experiments. Assuming that k_f is proportional to R_c^{-1} found in case where no product layer develops (the second resistance associated with D_g is neglected), we have if fluid film mass transfer is rate controlling that

$$t/\tau_I' = 1 - (1-X)^{2/3} \quad (19)$$

where

$$\tau_I' = \frac{m R_O^2 C_O}{2 D_{mol} c} \quad (20)$$

and D_{mol} is the molecular diffusion coefficient in a free solution [Wen, 1968]. If the rate is controlled by the reaction rate at the interface which seems more realistic for the reaction of P with oxides, eqs. (17) and (18) still hold.

3.2.2.3 Unreacted shrinking core model for particle size distribution

In this section we consider the mean conversion of an ensemble of particles with different radii, using probability density functions to describe the fractions of particles within a specified range of the radius. First the time-conversion relationships found are inverted. For the ensemble the mean conversion as a function of reaction time may be calculated using probability theory. This leads to some general observations discussed in the next section. The procedure as proposed here was used by Braun et al. [1974] to describe the conversion of sulfide ores. The particle size distribution was taken into consideration by numerical integration of the amount reacted for the discretized distribution function. Bartlett [1973], with a similar approach numerically evaluated a lognormal size distribution and showed the effect of the mean size on the conversion-time behaviour.

The time-conversion relationships of the previous section may be written as

$$t/\tau = 1 - g(1-X) \quad (21)$$

and inverted this yields

$$X = 1 - g^{-1}(1-t/\tau) \quad (22)$$

For an ensemble of particles that has a radius probability density function (PDF) given by f_{R_0} the mean conversion, \bar{X} , may be calculated with the first moment [Papoulis, 1965]:

$$\bar{X} = \int_{-\infty}^{\infty} X(R_0) f_{R_0} dR_0 \quad (23)$$

The first moment is equivalent to the expectation value.

It is easy to see that if mass transfer is rate controlling this leads to

$$\bar{X} = 1 - \int_{-\infty}^{\infty} (1-t/\tau) f_{R_0} dR_0 \quad (24)$$

and if the reaction rate is rate-controlling, to

$$\bar{X} = 1 - \int_{-\infty}^{\infty} (1-t/\tau)^3 f_{R_0} dR_0 \quad (25)$$

Furthermore, as f_{R_0} is a PDF we have

$$\int_{-\infty}^{\infty} f_{R_0} dR_0 = 1 \quad (26)$$

The case where diffusion through the product layer is rate controlling may be worked out similarly, but the inversion (22) is difficult to obtain. Approximating (15) by an expression that is simple to invert, a similar result to (25) and (26) could be obtained. Such an approach is omitted here as it does not affect the main line of thought.

In eqs. (24) and (25) the time of complete conversion, τ , depends on the initial radius, R_0 . Therefore it is convenient to relate particles of different sizes by transformation to dimensionless quantities. Here we have chosen to express all radii and conversion-times in terms of the radius (R_s) and conversion-time (τ_s) of the smallest particle. Then

$$T = t/\tau_s \quad (27)$$

$$R = R_0/R_s \quad (28)$$

It can be shown that the radii and conversion times of two particles, each with the same conversion, X , are given by

$$\frac{\tau_1}{\tau_2} = \left(\frac{R_{0,1}}{R_{0,2}} \right)^v \quad (29)$$

where $v = 1.5 - 2$ if fluid film mass transfer is rate controlling; $v = 2$ for diffusion through the product layer rate controlling; and $v = 1$ if the reaction rate at the interface is rate controlling [Wen, 1968]. With (27) - (29) the term t/τ in (24) and (25) is expressed in terms of τ_s and R_s . Thus

$$\tau = \tau_s \left(\frac{R_0}{R_s}\right)^v \quad (30)$$

leads to

$$t/\tau = (t/\tau_s) (R_s/R_0)^v \quad (31a)$$

or

$$t/\tau = T R^{-v} \quad (31b)$$

Equation (23) may now be solved if an appropriate PDF is chosen. For illustrative purposes we do so for $v = 1$ and for the Exponential PDF. The Exponential PDF with a smallest size equal to R_s is defined as

$$f_{R_0} = s \exp [s(R_s - R_0)] \quad R_0 > R_s \quad (32a)$$

$$f_{R_0} = 0 \quad R_0 < R_s \quad (32b)$$

The expectation value (mean radius) is given by the first moment

$$\text{EXP} \{R_0\} = \int_{-\infty}^{\infty} R_0 f_{R_0} dR_0 \quad (33)$$

where the bar denotes the random nature of the variable. Integration yields for the Exponential PDF

$$\text{EXP} \{R_0\} = R_s + 1/s \quad (34)$$

Similarly the variance equals the second central moment [Skopp, 1984]:

$$\text{VAR} \{R_0\} = \int_{-\infty}^{\infty} [R_0 - \text{EXP} \{R_0\}]^2 f_{R_0} dR_0 \quad (35)$$

which yields after integration for the Exponential PDF

$$\text{VAR} \{R_0\} = s^{-2} \quad (36)$$

If one wishes to have an indication of the relative (with respect to the mean) degree of variation the coefficient of variation, CV, is

usually given:

$$CV \{R_0\} = [\text{VAR} \{R_0\}]^{1/2} / \text{EXP} \{R_0\} \quad (37)$$

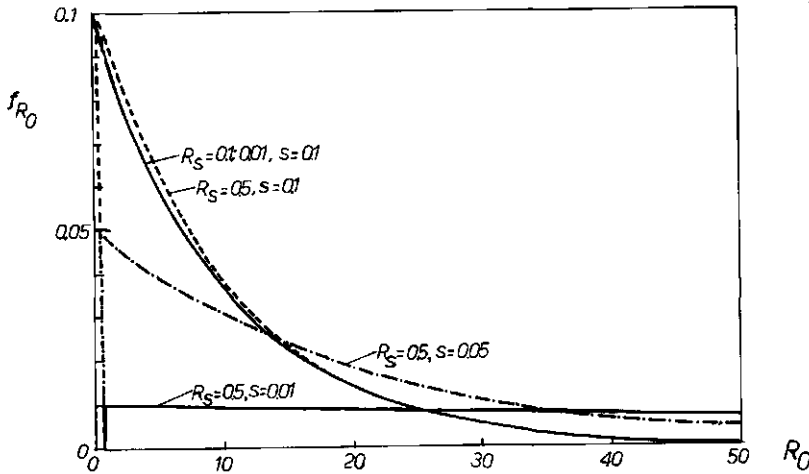


Figure 3: Illustration of the Exponential PDF.

Hence for the Exponential PDF ($R_s > 0$)

$$CV \{R_0\} = [sR_s + 1]^{-1} \quad (38)$$

As $CV \{R_0\}$ increases, the ensemble heterogeneity with respect to particle size also increases. The shape of the exponential PDF is given for reference in Fig. 3.

Combination of eqs. (23), (24) or (25), (27), (28), (31) and (32) leads to the integral

$$\bar{X} = 1 - \int (1 - TR^{-v})^q s \exp [sR_s (1-R)] R_s dR \quad (39)$$

where v and q depend on the rate controlling step and q follows from the function g (eq. 21). Equation (39) may be integrated if the integration boundaries are known. The upper boundary for the Exponential PDF is ∞ as the probability to find particles with a radius exceeding any positive value is finite (though small as this value becomes large). The lower boundary poses a problem. As soon as the reaction time is larger than τ_s the particles with the smallest

radii will have reacted completely. It can be seen from eqs. (13), (15) and (17) that if $t > \tau$ the conversion of particles for which the complete conversion time is exceeded would become larger than unity. As \bar{X} is a fraction this is unrealistic. In eq. (39) this artefact would lead to a negative contribution to \bar{X} of those particles already converted. This artefact is avoided by integrating only over the range of R_0 for which complete conversion is not yet established. Thus we find two integrals, i.e.,

$$T < 1 \quad \bar{X} = 1 - \int_1^{\infty} (1 - TR^{-p})^q s \exp [sR_s(1-R)] R_s dR \quad (40a)$$

$$T > 1 \quad \bar{X} = 1 - \int_T^{\infty} (1 - TR^{-p})^q s \exp [sR_s(1-R)] R_s dR \quad (40b)$$

The solution of eq. (40) if the reaction rate at the interface is rate controlling is ($v = 1$; $q = 3$):

$$T < 1 \quad \bar{X} = -3T^2 sR_s + T^3 sR_s/2 - T^3 (sR_s)^2/2 + E_1(sR_s) \exp (sR_s) \{3TsR_s + 3(TsR_s)^2 + (TsR_s)^3/2\} \quad (41a)$$

$$T > 1 \quad \bar{X} = 1 - \exp [sR_s(1-T)] \{1 + 5 (TsR_s)/2 + \frac{1}{2} (TsR_s)^2\} + E_1(TsR_s) \exp (sR_s) \{3TsR_s + 3(TsR_s)^2 + (TsR_s)^3/2\} \quad (41b)$$

In eq. (41) $E_1(y)$ is the exponential integral [Abramowitz and Stegun, 1964, p. 228]:

$$E_1(y) = \int_y^{\infty} u^{-1} \exp (-u) du \quad u \in \langle 0, \infty \rangle \quad (42)$$

This integral $E(y)$ diverges for $y \rightarrow 0$, hence R_s must be larger than zero. In Fig. (4) the effect of s on $\bar{X}(T)$ and in Fig (5) the effect of R_s on $\bar{X}(T)$ is shown. When s decreases and R_s is constant, or if R_s decreases and s is constant the coefficient of variation increases. Hence, for the Exponential PDF the dimensionless time, T , required to

obtain an almost complete conversion of the ensemble increases as a larger heterogeneity with respect to particle sizes is considered. This finding is in agreement to what is expected intuitively. Note that the horizontal axes (T) for Figs. (4) and (5) are the same. The real time axes (t) belonging to the three curves in Fig. (4) are also the same. This is not the case for the three curves in Fig. (5) as $t = T \tau_s$ and τ_s depends on R_g ! Figures (4) and (5) illustrate the effect of a size distribution instead of one fixed, mean size, as for $T = 1$ the particles with size R_g are completely converted. Hence, if this were the only size present \bar{X} would have been unity. That this is not the case is due to the range of the radius, R_0 . For comparison with Chapters 4 and 5 also the curves as a function of $\ln(T)$, instead of T, are shown in Figure 6.

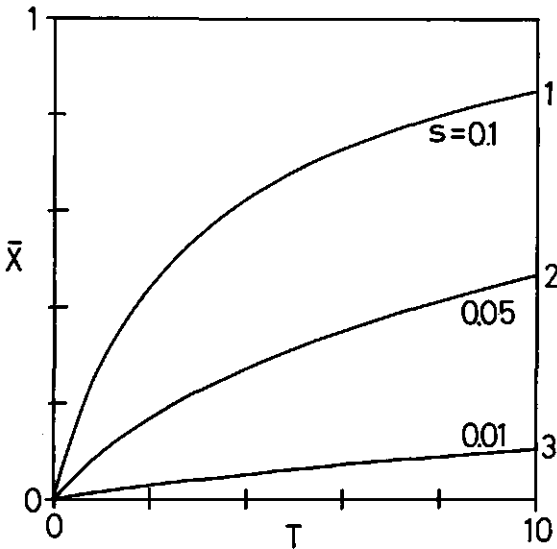


Figure 4: Mean conversion as a function of dimensionless time: effect of s.

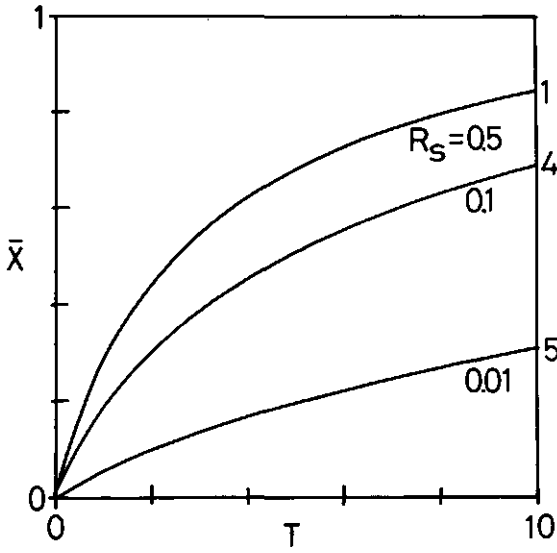


Figure 5: Mean conversion as a function of dimensionless time: effect of R_S .

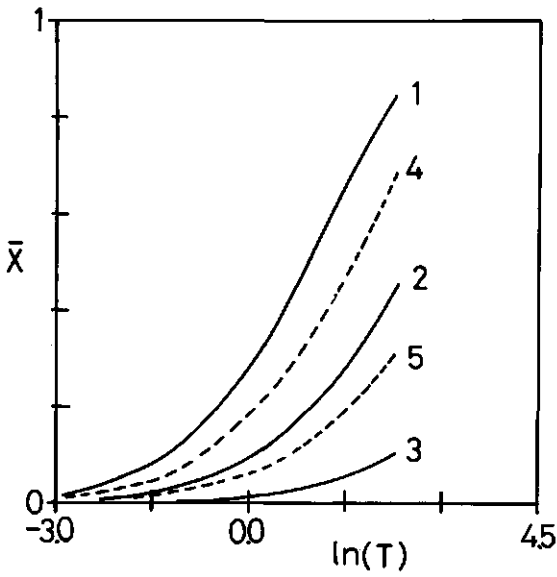


Figure 6: Mean conversion as a function of $\ln(T)$.

3.2.2.4 *The diffusion/precipitation model for pure oxides and soils*

In the previous sections we derived expressions that relate the conversion of a single spherical (oxide) particle and the mean conversion for an ensemble of such particles with differing radii, to the reaction time. The applicability of this model to pure oxides is limited by e.g.

- (i) the number of model parameters and constants
- (ii) deviations from spherical geometry
- (iii) uncertainty with respect to the variables occurring in the PDF of R_0 , as well as the shape (exponential, rectangular, ...) of this PDF.

In one of the earlier sections it was already mentioned that it may be difficult to distinguish experimentally between quite different diffusion - precipitation models (homogeneous, heterogeneous) for the relatively simple system of a single particle size, especially if resistances are of comparable order. Thus, the USC-model itself may not be applicable and instead an intermediate of the homogeneous and heterogeneous surface models should be considered. Even in the case of a pure homo-disperse oxide sol one may therefore expect that due to the scatter of experimental data uncertainty persists concerning 1) the most accurate mathematical formulation, 2) the uniqueness and physico-chemical relevance of the parameter values found by fitting models such as discussed here. This uncertainty is enhanced by the non-ideal geometry one may expect with respect to the particle shape, as generally a geometry factor correcting for non-ideal behaviour may be necessary. Related to this is the geometric instability due to surface imperfections which may be either smoothed out or amplified in the course of the conversion [Braun et al., 1974]. The nature of the PDF of R_0 will also introduce new parameters that will obscure the understanding of the system if the PDF is not characterized accurately and independently from the conversion (sorption) studies.

The above indicates the high demands posed with respect to knowledge of a pure oxide sol and the nature of the reaction of P with the oxide prior to the fitting of models to experimental data. It also shows the limitations of deterministic modelling for such systems.

For soils such deterministic modelling, that is already difficult for well defined oxide systems, must be discarded completely. While this is partly due to the unknown variation in particle shapes and geometries, it is also caused by the occurrence of several reactive solid phases (several oxides of non-pure nature, clay mineral edges etc.), interactions among soil colloids, and other complications. Therefore it is necessary to simplify the diffusion precipitation model to the extent that knowledge of the soil system becomes compatible with the input of the reduced model.

The simplification is done in the following way. First, observe that the time required for complete conversion, τ , is inversely proportional to the concentration in the bulk of the solution, c (eqs. 14, 16, 18, 20). This holds for spherical as well as for other geometries (see e.g. Davis and Hill, 1982, Van Der Zee et al., 1988). Furthermore, it was found that the mean conversion for an ensemble of particles, \bar{X} , is a function of dimensionless time for spherical particles (eq.41). This is also the case for other geometries (Chapter 4). Hence, we may write

$$\bar{X} = G(c t) \quad (43)$$

where G represents a function of T ($\sim c t$). Thus the mean conversion is given by a unique function of the product of concentration and time, for a certain soil or ensemble of particles. However, as the function G is a combination of many relations which are valid for specific geometries and size distributions, the form of G it is not known a priori. If the USC-model applies for all soil minerals the same conversion occurs for a long reaction time at low c or short reaction time at high c . This result was also found by Van Riemsdijk et al. [1984a] and is in fact a basis to scale reaction time. Such scaling is of great importance as it is clearly undesirable to be forced to do very long term sorption experiments in order to find the constants in the conversion (i.e, sorption)-time relationships [Van Der Zee and Van Riemsdijk, 1988].

It was assumed that c is constant in the analyses given so far. Now we assume that the solutions for c changing over the course of the

reaction (batch experiments) are additive. This is a tolerable approximation if the pseudo steady state assumption is acceptable. Then it can be shown that product ct must be replaced an exposure integral, I , which is a concentration - weighted dimensionless of reaction time

$$I = (c_r t_r)^{-1} \int_0^t c dt \quad (44)$$

where c_r and t_r are equal to unity in the units employed. A particular value of the dimensionless quantity I may be obtained by many different concentration-time combinations. Two special cases are given of eq. (44). In the first case a concentration, c_e , exists below which, under the prevailing conditions, no reaction occurs as the solubility product of the Me-phosphate is not exceeded. Then eq. (44) becomes

$$I = (c_r t_r)^{-1} \int_0^t (c - c_e) dt \quad (44a)$$

In the second case the concentration is kept constant and if $c_e \ll c$ [Van Riemsdijk, 1979; Van Riemsdijk et al., 1984a; Van Der Zee and Van Riemsdijk, 1986] then eq. (44) becomes simply

$$I = \frac{c t}{c_r t_r} \quad (44b)$$

With eqs. (43) and (44) a unique relationship between \bar{X} and I is given. Since the amount S that has diffused into the solid phase equals

$$S = mw C_0 \bar{X} / \rho_s \quad (45)$$

the nature of the function $S(I)$ may be established experimentally. The nature of the mathematical function for $S(I)$ is unknown but any relationship that fits the data can be chosen. Thus a polynomial of I such as (N smaller than the number of measurement points)

$$S = \sum_{i=0}^N a_i (I)^{1/i} \quad (46a)$$

may be considered as well as a polynomial as used by Van Der Zee and Van Riemsdijk [1986]:

$$S = \sum_{i=0}^N a_i \{\ln(I)\}^i \quad (46b)$$

As the polynomial in eq. (46) must be assessed experimentally its use implies long term sorption experiments if high concentrations are of interest. If, however, relatively low or intermediate concentrations, for which the same reaction product is formed (m is a fixed constant), are studied then the reaction times may be scaled down by measuring at high values of c . A third alternative for equation (46) is given in Appendix B.

3.3 Conclusion

In this paper a physico-chemical description of the reaction of phosphate with soil and the corresponding mathematical formulation of this process were addressed. Due to agreement in the literature about the description of the adsorption process [Van Riemsdijk, 1979; Barrow et al., 1981; Enfield et al., 1981a,b; Barrow, 1983; Van Der Zee and Van Riemsdijk, 1986] emphasis was given to the long term sorption reaction. This relatively slow process exhibits quite different kinetics than the adsorption reaction and is assumed to involve the bulk of the reactive solid phase.

The bulk process was described with the Unreacted Shrinking Core (USC) model known from chemical engineering literature. In this model the reactant (P) diffuses into the solid phase where a reaction (precipitation) occurs. Conditions are such that the unreacted solid phase is virtually inaccessible to the reactant and therefore two solid phases are found: the unreacted solid phase (in this case consisting of metal oxides) and the reaction product (consisting of metal phosphate). The mathematical equations describing the USC-model may be solved easily if the assumption of steady state is made. The pseudo steady state solutions in terms of conversion-time relations are given for spherical geometry and for three limiting cases. These cases refer to the resistances against the transport of P to the sharp

interface where the reaction occurs and the rate of reaction at this interface. Using stochastic theory the solutions may be used to describe the relationship between the mean conversion of an ensemble of particles with different radii and the time. For simple cases this may be done analytically, as is illustrated for an Exponential PDF with the reaction rate at the interface controlling the rate. With this analysis for a very idealized system it was possible to show the very pronounced effect of particle size heterogeneity on the relation between mean conversion and time.

However, in many cases non-ideal behaviour of the system as well as experimental inaccuracy prohibit the distinction between the different conversion-time relationships as well as the assessment of whether the USC-model (or similarly involved models) is applicable at all. The theory presented, though, resulted in the important conclusion that the mean conversion, which is related to the amount of P precipitated, is a unique function of the product of concentration in the bulk of the solution and the reaction time. This fact was subsequently used to give a relationship between sorption, (S) due to the diffusion/precipitation process and an exposure integral (I), for the cases that the concentration varies in time. Since the relationship S(I) is not known a priori it should be evaluated experimentally. The elegance is in the nature of the exposure integral, I, which may be used to scale the reaction time. Thus, by determination of S(I) at a large concentration and a short time, the long term sorption behaviour at low concentration may also be found, since one function applies to a range of different concentrations.

3.4 Notation

A_{sp}	specific surface area, [$m^2 \cdot kg^{-1}$]
C_o	concentration of the oxide, [$mol \cdot m^{-3}$]
CV	coefficient of variation
D_{mol}	coefficient of molecular diffusion, [$m^2 \cdot h^{-1}$]
D_s	coefficient of diffusion in product (Me-phosphate) layer, [$m^2 \cdot h^{-1}$]
\tilde{D}_s	coefficient of diffusion in oxide [$m^2 \cdot h^{-1}$]

$E_1(y)$	exponential integral
EXP	expectation value
F	1. Faraday (Table 1) 2. Total amount sorbed/reacted [mmol.kg ⁻¹]
G	functional relationship
I	exposure integral
K	Langmuir constant, [m ³ .mol ⁻¹]
N	polynomial order
Q	amount adsorbed, [mmol.kg ⁻¹]
Q _m	adsorption maximum, [mmol.kg ⁻¹]
Q*	amount desorbed, [mmol.kg ⁻¹]
R	1. gas constant (Table I) 2. dimensionless radius oxide particle
R _c	radius of the unreacted core, [m]
R _s	initial radius of the smallest oxide particle, [m]
R ₀	initial radius of the oxide particle, [m]
S	amount precipitated, [mmol.kg ⁻¹] or diffused (eqn. I.3)
T	dimensionless time
VAR	variance
X	conversion
\bar{X}	mean conversion of an ensemble of particles
a _i , a _j	constants
c	concentration [mol.m ⁻³]
\bar{c}_c, \bar{c}_s, c	concentration [mol.m ⁻³] at unreacted core surface, at particle surface, and in the bulk of the solution, respectively
c _r	reference concentration [mol.m ⁻³]
\bar{c}	concentration in particle [mol.m ⁻³]
c _e	equilibrium concentration, solubility, [mol.m ⁻³]
f	thermodynamic factor
f _{R₀} , f _{ψ₀}	probability density function of R ₀ and of ψ ₀ , resp.
g	functional relationship
k _s	reaction rate constant at interface, [m ⁴ . mol ⁻¹ . h ⁻¹]
k _f	mass transfer coefficient, [m.h ⁻¹]
k _a	adsorption rate constant, [m ³ . mol ⁻¹ . h ⁻¹]
k _d	desorption rate constant, [h ⁻¹]
m	stoichiometric coefficient
m _{ψ₀}	average value of ψ ₀ , [V]

m_1, m_2	parameters
q	parameter
r	radial distance from centre of sphere, [m]
s	constant, [m ⁻¹]
s_{Ψ}^0	standard deviation of Ψ_0 , [V]
t	time [h]
v	parameter
w	conversion factor mol \rightarrow mmol, $w = 1000$
y	lower integration boundary in Exponential intergral
z	valency (Table I)
Ψ	electrostatic potential in the plane of adsorption, [V]
α	1. ratio of oxalate extractable fractions 2. proportion of P present as HPO_4^{2-} (Table 1)
γ	activity coefficient in solution
ϵ	porosity of the oxide
θ	relative surface coverage by adsorption
ρ_s	bulk density of oxide [kg.m ⁻³]
τ	time to complete conversion particle [h]
τ_s	time to complete conversion smallest particle [h]
ω	thickness adsorbed layer, [m]
in	initial condition (subscript)
ox	oxalate extractable quantity (subscript)

3.5 References

- Barrow, N.J., A mechanistic model for describing the sorption of phosphate by soil. J. Soil Sci. 34: 733-750, 1983.
- Barrow, N.J., L. Madrid and A.M. Posner, A partial model of adsorption and desorption of phosphate by goethite. J. Soil Sci. 32: 399-407, 1981.
- Barrow, N.J. and T.C. Shaw, The slow reactions between soil and anions. 2. Effect of time and temperature on the decrease in phosphate concentration in the soil solution. Soil Sci. 119: 167-177, 1975a.
- Barrow, N.J. and T.C. Shaw, The slow reactions between soil and anions. 5. Effects of period of prior contact on the desorption of phosphate from soils. Soil Sci. 119: 311-320, 1975b.
- Bartlett, R.W., A combined pore diffusion and chalcopyrite dissolution

- kinetics model for in situ leaching of a fragmented copper porphyry. International Symposium on Hydrometallurgy, D.J.I. Evans and R.S. Schoemaker (eds.). A.I.M.E. New York, pp. 331-374, 1972.
- Beek, J., Phosphate retention by soil in relation to waste disposal. PhD thesis, Agricultural University Wageningen, 1979.
- Beek, J. and W.H. van Riemsdijk, Interactions of orthophosphate ion with soil. In: G.H. Bolt (ed.), Soil Chemistry B. Physico-Chemical Models. Elsevier, Amsterdam: 259-284, 1982.
- Bischoff, K.B., Accuracy of the pseudo steady state approximation for moving boundary diffusion problems. Chem. Eng. Sci. 18: 711-713, 1963.
- Bischoff, K.B., Further comments on the pseudo steady state approximation for moving boundary diffusion problems. Chem. Eng. Sci. 20: 783-784, 1965.
- Bolan, N.S., N.J. Barrow, and A.M. Posner, Describing the effect of time on sorption of phosphate by iron and aluminum hydroxides. J. Soil Science 36: 187-197, 1985.
- Bowden, J.W., Models for ion adsorption on mineral surfaces. PhD thesis University Western Australia, 1973.
- Bowden, J.W., S. Nagarajah, N.J. Barron, A.M. Posner, and J.P. Quirk, Describing the adsorption of phosphate, citrate, and selenite on a variable charge mineral surface. Austr. J. Soil Res. 18: 49-60, 1980.
- Bowen, J.R., Comments on the pseudo steady state approximation for moving boundary problems. Chem. Eng. Sci. 20: 712-713, 1965.
- Braun, R.L., A.E. Lewis, and M.E. Wadsworth, In-Place leaching of primary sulfide ores: Laboratory leaching data and kinetics model. Metallurgical Transactions 5: 1717-1726, 1974.
- Brent Hiskey, J., and M.E. Wadsworth, Galvanic conversion of chalcopyrite. In: F.F. Aplan, W.A. McKinney, and A.D. Pernicelli (eds.), Solution Mining Symposium, AIME, New York: 422-445, 1974.
- Davis, G.B., and J.M. Hill, A moving boundary problem for the sphere. IMA J. Applied Math. 29: 99-111, 1982.
- Enfield, C.G., T. Phan, D.M. Walters, and R. Ellis Jr., Kinetic model for phosphate transport and transformation in calcareous soils I. Soil Sci. Soc. Am. J. 45: 1059-1064, 1981a.
- Enfield, C.G., T. Phan, D.M. Walters, and R. Ellis Jr., Kinetic model

- for phosphate transport and transformation in calcareous soils II. Soil Sci. Soc. Am. J. 45: 1064-1070, 1981b.
- Goldberg, S., and G. Sposito, A chemical model of phosphate adsorption by soils: I. Reference oxide minerals. Soil Sci. Soc. Am. J. 48: 772-778, 1984.
- Hill, J.M., On the pseudo steady state approximation for moving boundary diffusion problems. Chem. Eng. Sci. 39: 187-190, 1984.
- Lu, W.K., The general rate equation for gas-solid reactions in metallurgical processes. Trans. Metall. Soc. AIME 227: 203-206, 1963.
- Mansell, R.S., H.M. Selim, and J.G.A. Fiskell, Simulated transformations and transport of phosphorus in soil. Soil Sci. 124: 102-109, 1977a.
- Mansell, R.S., H.M. Selim, P. Kanchanasut, J.M. Davidson, and J.G.A. Fiskell, Experimental and simulated transport of phosphorus through sandy soils. Water Resour. Res. 13: 189-194, 1977b.
- Munns, D.N., and R.L. Fox, The slow reaction which continues after phosphate adsorption: kinetics and equilibrium in some tropical soils. Soil Sci. Soc. Am. J. 40: 46-51, 1976.
- Ockendon, J.R., and W.R. Hodgkins (eds.), Moving boundary problems in heat flow and diffusion. Oxford, Clarendon Press, 1975.
- Papoulis, A., Probability, random variables, and stochastic processes. McGraw-Hill, Tokyo, 1965.
- Sigg, L., and W. Stumm, The interaction of anions and weak acids with the hydrous goethite (α -FeOOH) surface. Colloids Surfaces 2: 101-117, 1981.
- Skopp, J., Analysis of solute movement in structured soils. In: J. Bouma and P.A.C. Raats (eds.), Water and solute movement in heavy clay soils, ILRI, Wageningen: 220-228, 1984.
- Soward, A.M., A unified approach to Stefan's problems for spheres and cylinders. Proc. R. Soc. London, A, 373: 131-147, 1980.
- Spitzer, R.H., F.S. Manning, and W.D. Philbrook, Mixed control reaction kinetics in the gaseous reduction of hematite. Trans. Metall. Soc. AIME 236: 293-301, 1966.
- Stewartson, K., and R.T. Waechter, On Stefan's problem for spheres. Proc. R. Soc. London, A, 348: 415-426, 1976.
- Van der Zee, S.E.A.T.M. and W.H. van Riemsdijk, Sorption kinetics and transport of phosphate in sandy soil. Geoderma 38: 293-309, 1986.

- Van der Zee, S.E.A.T.M., and W.H. van Riemsdijk, Transport of phosphate in a heterogeneous field. *Transport Porous Media* 1: 339-359, 1986.
- Van der Zee, S.E.A.T.M., L.G.J. Fokkink, and W.H. van Riemsdijk, A new technique for assessment of reversibly adsorbed phosphate. *Soil Sci. Soc. Am. J.* 51: 599-604, 1987.
- Van der Zee, S.E.A.T.M., and W.H. van Riemsdijk, Model for long term phosphate reaction kinetics in soil. *J. Env. Qual.* (in press), 1988.
- Van der Zee, S.E.A.T.M., W.H. van Riemsdijk, and J.J.M. van Grinsven, Extrapolation and interpolation by time-scaling in systems with diffusion controlled kinetics and first order reaction rates, Chapter 4, this thesis, 1988.
- Van Riemsdijk, W.H., and J. Lyklema, Reaction of phosphate with gibbsite, $Al(OH)_3$, beyond the adsorption maximum. *J. Colloid Interface Sci.* 76: 55-66, 1980.
- Van Riemsdijk, W.H., and F.A.M. de Haan, Sorption kinetics of phosphates with an acid sandy soil, using the phosphatostat method. *Soil Sci. Soc. Am. J.* 45: 261-266, 1981.
- Van Riemsdijk, W.H., L.J.M. Boumans, and F.A.M. de Haan, Phosphate sorption by soils. I. A diffusion-precipitation model for the reaction of phosphate with metal oxides in soil. *Soil Sci. Soc. Am. J.* 48: 537-540, 1984.
- Van Riemsdijk, W.H., Reaction mechanisms of phosphate with $Al(OH)_3$ and a sandy soil. PhD thesis, Agricultural University Wageningen.
- Wen, C.Y., 1968. Noncatalytic heterogeneous solid fluid reaction models. *Ind. Eng. Chem.* 60 (9): 34-54, 1979.
- Wilson, D.G., A.D. Solomon, and P.T. Boggs (eds.), *Moving boundary problems*. New York, Academic Press, 1978.

4. **EXTRAPOLATION AND INTERPOLATION BY TIME-SCALING IN SYSTEMS WITH DIFFUSION CONTROLLED KINETICS AND FIRST ORDER REACTION RATES**

Abstract

The interpolation or extrapolation in time of physico-chemical processes from experimental data is often difficult. A theoretically derived time scaling procedure using an exposure variable of the concentration integrated in time, with at most one adjustable parameter was applied successfully to three systems taken from metallurgical, agricultural and environmental engineering. This scaling rule is potentially useful as a research or management tool, for systems that are too complex for mechanistic modelling.

4.1 Introduction

In chemical, metallurgical, and mining engineering as well as the earth sciences, kinetic processes are often of considerable importance. Kinetics play a role e.g. in ore processing, fuel combustion and oil shale or coal gasification, catalyst regeneration, mineral weathering, and fertilizer nutrient immobilization. Different rate determining steps may be involved in such reactions. These steps can be caused by diffusion, heat transfer, or reaction kinetics. Because the degree of conversion is a function of time the dimension of the system of interest must often be optimized to achieve a certain effectivity. Thus in chemical reactor plants, the fluid velocity must be regulated for optimal results and for optimal fertilization the moment and method of fertilizer application are under constraints. Reaction kinetics may depend on a large number of parameters and variables. Therefore system optimization usually requires the evaluation of the effects of important variables on the reaction kinetics and performance of the system. Even if such an assessment is done only over a limited range of values of the dominant variables the effort may be large. To cut down on this effort the system is often described mathematically. The mathematical expressions are used to fit

the data, and for interpolation and extrapolation to conditions not evaluated experimentally. Using for this purpose empirical models may cause large uncertainties. The problem is simpler if the processes involved are understood physically. Then the mathematical formulation may be based on a realistic physico-chemical model. A particularly usefull approach is to use non-dimensional mathematical equations, or dimensionless numbers such as the Reynolds and Schmidt numbers [Levenspiel, 1972]. The use of such dimensionless quantities is based on scaling rules and was discussed extensively by Bird et al., [1960].

In this paper we present a time-scaling method. The theoretical background is well documented in chemical engineering literature of solid-fluid and solid-gas interactions for relatively simple systems. Processes in such systems are dominated by diffusional transfer or first order reaction kinetics. We show that such time scaling may be feasible, even if the mechanisms are incompletely understood, for complicated reactions systems. The method is illustrated with examples from different fields of interest.

4.2 Background of scaling

The overall kinetics of conversion of a solid phase may be controlled by e.g. the diffusion rate of one of the reactants, the heat transfer rate if heat is produced or consumed, and the concentration. Other factors that may be of importance are e.g. solid characteristics such as specific surface area, solid phase purity, etc. In the case of an isothermal, non-catalytic reaction the conversion rate, (the rate of change of the reacted amount of solid phase relative to the total amount present initially), may be fitted to mathematical functions with at least one constant. Often several empirically fitted rate equations may seem equally appropriate. Moreover, equations with more than one constant may yield similar results for different values of the constants. Therefore, little physical relevance can be attributed to apparent rate constants obtained in this way. For example the general features of the square root of time behaviour of unsteady linear diffusion can be described equally well with an empirical expression for the reaction rate

[Skopp, 1986]. Experimental errors and the similarities in the description of different physico-chemical processes complicate the discrimination between different mathematical descriptions. However, such similarities may be of use if mechanistic understanding of the overall conversion process is small. This is illustrated by considering the conversion of solid phase particles. The conversion rate is controlled by three resistances, acting in series.

The mechanisms causing these resistances are 1) diffusive mass transfer through a stagnant fluid film surrounding a particle, 2) intraparticle diffusion through a layer of converted solid, and 3) first order chemical reaction rate. A model taking these three mechanisms into account is the unreacted shrinking core (USC) model [Levenspiel, 1972, Wen, 1968]. In the USC model the unconverted solid cannot be penetrated by the gaseous or liquid reactant. By reaction at the surface of the unconverted solid, a reaction product layer forms that grows at the expense of the unreacted, and shrinking core. In the different homogeneous conversion model (HC), reactant diffuses into the unreacted solid and the reaction occurs the entire particle. In general the USC model is physically most realistic [Levenspiel, 1972, Wen, 1968]. Because the discrimination of the two models is seldomly possible on the basis of data [Wen, 1968] and the main point of this analysis holds for both models, the approach is illustrated with the USC model.

The exact solution of the mathematical equations describing the USC-model has received much attention in applied mathematics literature. Usually the problem to solve the moving boundary problem of the USC model is to find a suitable transformation of variables [Ockendon and Hodgkins, 1975, Davis and Hill, 1982]. The mathematics are considerably simpler if we assume that the pseudo-steady state assumption is applicable. This assumption was challenged [Davis and Hill, 1982, Bischoff, 1963] but is acceptable for gas-solid reactions or the reactions between dilute electrolytes and a solid [Wen, 1968]. Early solutions of the USC model assumed that the overall conversion rate is controlled by one of the resistances [Yagi and Kunii, 1954]. Later extensions included mixed control [Lu, 1963], a reversible reaction [Lu and Bitsianes, 1966], and swelling or shrinking of the particle [Shen and Smith, 1965]. A pseudo steady state solution is

commonly presented, by considering the fractional conversion (X), as a function of dimensionless time. Dimensionless time is obtained by division of real time with the time (τ) required for complete conversion. The solution for an ensemble of equally sized and shaped particles, and for mixed rate control is given by

$t = \sum_i \tau_i P_i(X)$ [Bartlett, 1971, Braun et al., 1974, Szekely and Propster, 1975], where $P_i(X)$ is a function of X and the resistances are indexed by i (i = 1, 2, or 3).

Table 1: Relationships $P_i(X)$ between fractional conversion (X) and dimensionless time t/τ_i , with i the rate controlling step.

geometry	i=1 Film diffusion	i=2 Product layer diffusion	i= 3 Reaction rate
plate	$P_1=X$	$P_2=X^2$	$P_3=X$
cylinder	$P_1=X$	$P_2=X+(1-X)\ln(1-X)$	$P_3=1-(1-X)^{1/2}$
Sphere	$P_1=X$	$P_2=1-3(1-X)^{2/3}+2(1-X)$	$P_3=1-(1-X)^{1/3}$

Summing the solutions when one of the resistances (i) is rate controlling is allowed because they act in series. In Table 1 the function $P_i(X)$ is given for three particle shapes, and different rate controlling steps (i). Note that for a plate-geometry a linear relation $X(t)$ is found for film diffusion (i=1) as well as for chemical reaction rate (i=3) control. This shows that experimental data conforming to such a relation may be described by both mechanisms as well as by linear combination of i = 1 and i = 3, even though the physico-chemical nature of these rate limiting steps is completely different. The time for complete conversion (τ_i) in Table 1 is invariably inversely proportional to the concentration c in the bulk of the gas or liquid phase. Therefore the conversion-time relation can be expressed as an explicit function of ct, i.e. $ct = F(X)$ where F(X) is a function of X. This is the basis of our scaling rule. By inversion we find that $X = F^{-1}(ct)$. In words this may be formulated as: 'there is a unique (though not necessarily known) functional relationship between the fractional conversion of an ensemble of

particles with the same size and shape and the product of concentration and time'. Moreover, because τ_1 is inversely proportional to c for all situations referred to in Table 1, such a unique relationship is found also for an ensemble with differently shaped but equal sized particles. That a unique relationship between X and ct can also be expected for ensembles with particle size distributions was shown numerically [Bartlett, 1971, Braun et al., 1974, Szekely and Propster, 1975] and analytically (Chapter 3). So far the analysis leading to the concentration-scaled conversion time expression was based on the assumption of a constant bulk concentration in the gas or liquid phase. However, if this bulk concentration varies slowly in time and if the pseudo steady state approximation is valid, scaling of time is still possible. In that case an integral of c over t should be used instead of the variable ct . This integral, that resembles the exposure variable I commonly used in toxicology [Brunekreeff, 1985], may be defined as

$I = \gamma \int (c - c_e) dt$, where γ is a parameter that may be taken equal to unity and that is used to make I non-dimensional. Instead of concentration we use the concentration difference $(c - c_e)$, because in many cases it is realistic to identify a lower (no-effect) level of c , $(c - c_e)$, below which a reaction does not occur. Such a lower bound might be governed by e.g. solubility of the reaction product. For first order chemical reaction rate control the scaling holds also for fast variations in time of c .

With the extended USC model presented so far the process of conversion is described well for an ensemble of well-defined particle shapes and sizes, if a large number of model constants such as reaction stoichiometry, diffusion coefficients and chemical rate constants are known. If, however, these constants are not well-known or if solid phase impurity, solid phase mixtures, etc. complicate the system, then the USC model as such is of limited use. In that case deterministic modelling becomes practically impossible due to the large number of parameters, that may differ for different solid phase constituents, and that are hard to assess experimentally. Unfortunately many natural systems studied in e.g. the earth and environmental sciences are usually very complex. In such systems where

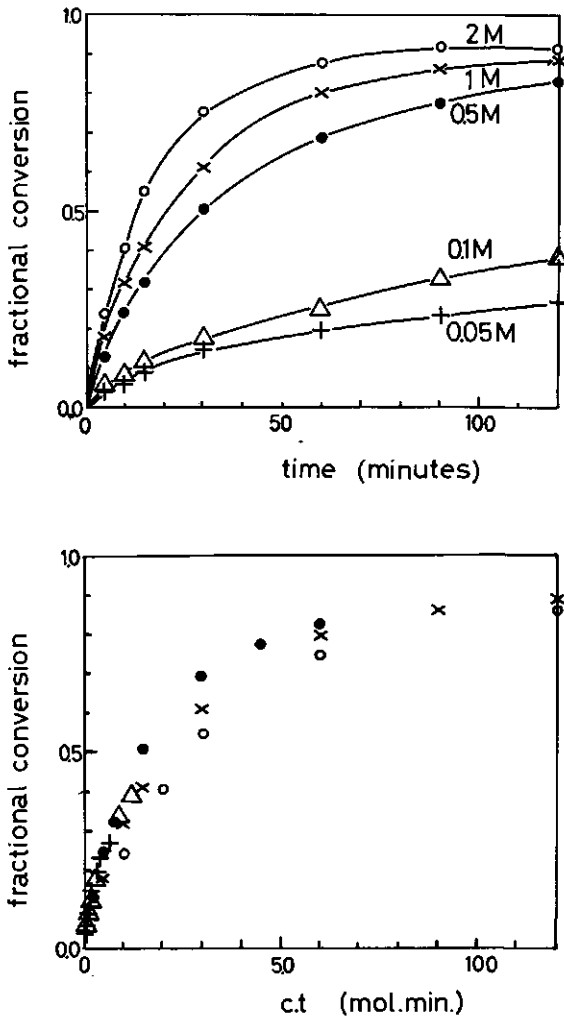


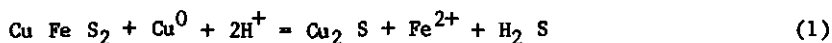
Figure 1: Fractional conversion of chalcopyrite (CuFeS_2) as a function of time (1a: after ref. (18)), and as a function of exposure $I=ct$ (1b). Concentration (c) of H_2SO_4 as indicated in Figure 1a.

mechanistic kinetic models are not applicable, the time scaling method using the exposure integral may still yield good results because the unique relation between X and I is still valid. So, even for systems that are incompletely understood, interpolation in the exposure domain

covered experimentally is still possible. An important consequence of the use of the exposure variable is that a long reaction at a small concentration is equivalent to a short reaction at a large concentration, if I is the same for both cases. Thus extrapolation to long reaction times (and small concentrations) may be done by assessing X(I) for short duration experiments at high concentrations.

4.3 Applications of time scaling

In this section we show three applications of the scaling method which differ in the degree in which the reaction mechanisms are known in detail. The first example is the galvanic conversion of chalcopyrite (CuFeS_2) by metallic copper. This metallurgical process, was described by the USC model [Bartlett, 1971, 1973]. The over-all reaction is given by



The over all reaction rate depends on the rate of proton diffusion to the unconverted chalcopyrite surface and the proton consumption rate at this surface. For relatively narrow ranges of the particle sizes of chalcopyrite and metallic copper the conversion was studied experimentally (at 90 °) [Hiskey and Wadsworth, 1974]. The protons were supplied by adding H_2SO_4 at different concentrations. In Figure 1a some results are given for different, constant concentrations. In accordance with our scaling method a single line (Fig. 1b) is found when the fractional conversion is given as a function of ct .

The next example is the reaction of orthophosphate with soil, which is of interest from the scope of P fertilizer efficiency and for environmental reasons. Due to the reaction in soils containing little phosphorus, fertilizer-P becomes less available as the time after the moment of fertilizer application increases [Rahman, 1982, Van der Zee and Van Riemsdijk, 1988]. Hence the application effectivity decreases also. In soil receiving large quantities of P, leaching of P may eventually cause surface water eutrophication [Beek, 1979, Enfield et al., 1981]. In non-calcareous soil, phosphate reacts predominantly with iron and aluminum oxides [Beek, 1979].

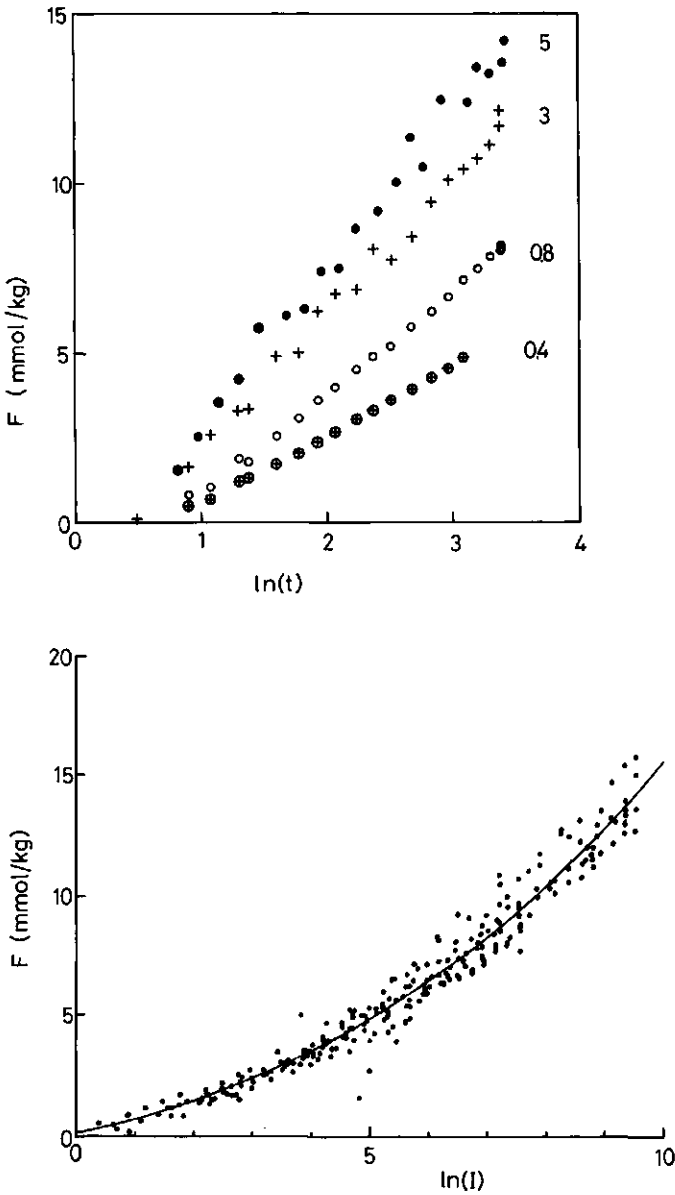


Figure 2: Amount of phosphate that has reacted with soil as a function of the natural logarithm of time (Figure 2a). The concentrations are indicated in $\text{mol}\cdot\text{m}^{-3}$ in the figure. Same amount as a function of the natural logarithm of exposure ($\ln I$) for phosphate concentrations in the range $0.05\text{--}6 \text{ mol}\cdot\text{m}^{-3}$ (Figure 2b). Solid curve is the best fitting third degree polynomial, $c_e = 0.1 \text{ mol}\cdot\text{m}^{-3}$.

The overall reaction that consists of adsorption in combination to a diffusion type process [Barrow, 1983, Van Riemsdijk et al., 1984] can be described as a function of exposure (I) and measured according to Van Riemsdijk and Van der Linden [1984]. In Figure 2a the amount of phosphate reacted as a function of $\ln(t)$ is shown for four different constant concentrations. The logarithmic time scale was taken for convenience to compress the horizontal axis as measurement time varied from 1 minute to 40 hours. A total of ten different concentrations were considered experimentally but only four are shown in Figure 2a. In Figure 2b we show the scaled data for all ten concentrations. Also shown is a best fitting third order polynomial of $\ln(I)$. Considering the complexity of phosphate-soil interaction the scaling result can be considered excellent.

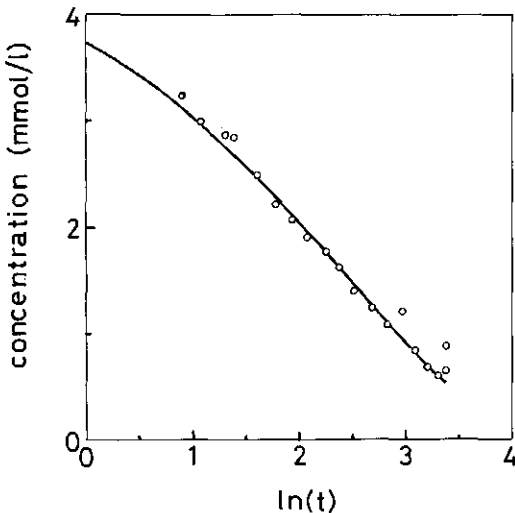


Figure 3: Phosphate concentration in solution (c) as a function of time (t). Experimental points and curve as calculated with the empirical polynomial of Figure 2.

In the same way we could describe the reaction of phosphate with soil for times of approximately one year [Van der Zee and Van Riemsdijk, 1988], so that the results could be used to dimension waste disposal

sites. The use of this approach to evaluate laboratory experiments is illustrated in Figure 3. Using the same experimental set up [Van Riemsdijk and Van der Linden, 1984] a phosphate containing solution was percolated through a column containing the same soil as used in Figure 2. The concentration was not kept constant and therefore decreases by the reaction. The change in concentration as a function of time was predicted using the polynomial function of Figure 2b, and proven to be in excellent agreement with the measured concentrations. These results illustrate the applicability of the scaling procedure at variable concentrations.

A third example is taken from in the field of soil acidification. Atmospheric deposition of SO_x , NO_x and NH_3 on the soil causes soil acidification which affects the ecological functioning of the soil. Infiltration of atmospheric pollutants causes a complex chain of exchange and mineral weathering reactions in the soil. On the long-term mineral weathering controls the soil pH and nutrient status of unfertilized soils. Mineral weathering is still a poorly understood process [Helgeson et al., 1984]. Most research concerning mineral weathering dealt with pure minerals such as feldspar [Helgeson et al., 1984, Chou and Wollast, 1984]. Mainly two mechanisms of weathering have been proposed. The first type conforms to the USC model, either with a product layer that continually increases in thickness [Wollast, 1967, Helgeson, 1971, 1972] or with a constant thickness caused by dissolution of the product layer at the particle surface [Correns, 1963, Paces, 1973]. In an alternative description feldspar dissolution is assumed to be controlled by a surface reaction and incongruent dissolution is attributed to precipitation of aluminum hydroxides or aluminium silicates [Busenberg, 1978, Holdren and Adams, 1982, Helgeson et al., 1984]. In models of the second type, the commonly observed parabolic type kinetics are attributed to e.g. exchange reactions, etch pit formation, mineral impurity, or particle size heterogeneity. Little consensus exists on the microscopic mechanisms that cause the overall kinetics of feldspar weathering, so a mechanistic description of the rate of proton consumption in the more complex soil system is still remote. Nevertheless, a description of the proton consumption rate is desirable to estimate long term effects of atmospheric pollutant deposition. Currently, predictions of such long term effect are usually based on the extrapolation of empirical rate equations [Cosby, 1986].

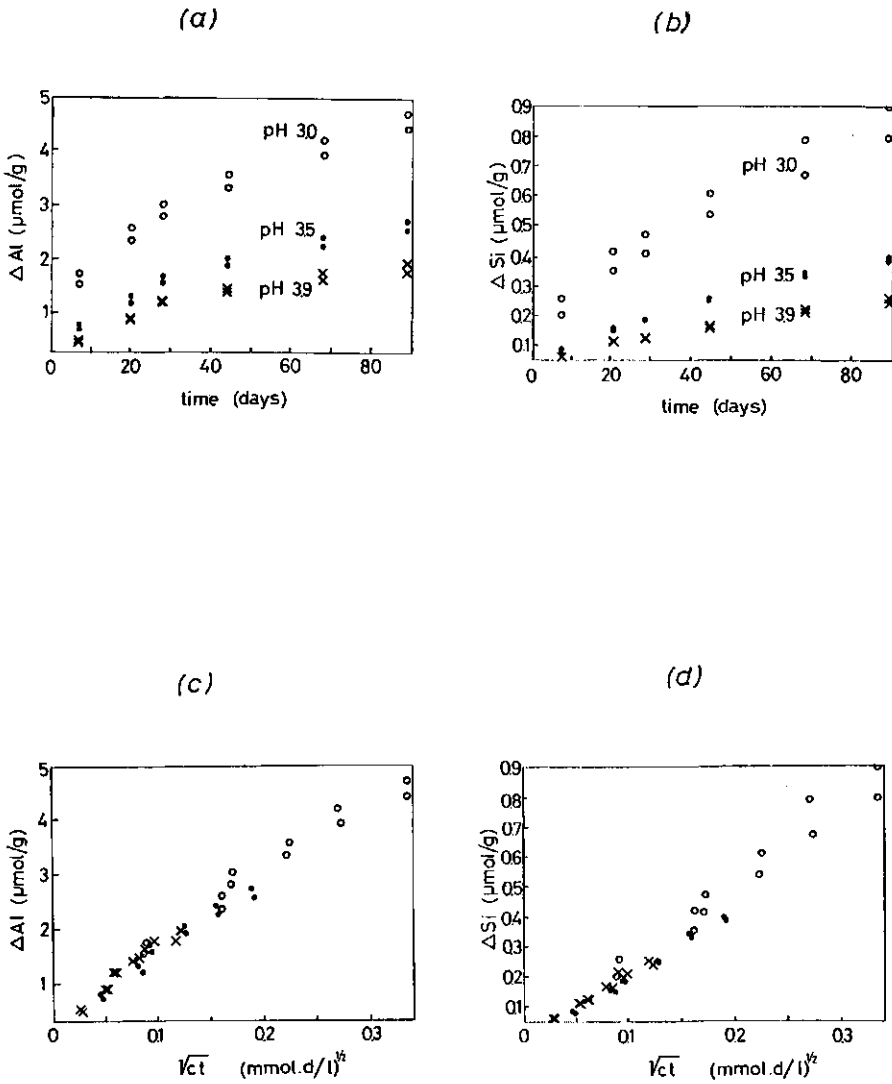


Figure 4: Cumulative amounts of released aluminum (4a,c) and silicium (4b,d), as a function of time (t) and of the square root of exposure (\sqrt{I}). The value of pH as shown in Figure 4a.

To investigate whether the time scaling proposed here may yield an additional instrument for predictions of soil acidification soil columns were leached with solutions with a particular constant, low pH at relatively high flow rates, varied to maintain a constant pH in the soil columns [Van Grinsven, in preparation]. This was done for sandy subsoil samples (70-80 cm depth) [Van Grinsven et al., 1987]. In this soil proton consumption is predominantly caused by the reaction with various silicates and aluminum (hydr)oxides present, resulting in the release of aluminum, calcium and silicon and small amounts of potassium, magnesium, and sodium. When the reaction rates had slowed down considerably after a number of days the experiments were continued in batch for a period of 90 days. The reaction vessels were not shaken and the pH was kept constant by regularly replacing the supernatant solution (every one to three weeks). In the batch experiments Al and Si were the main compounds that were released. The column and batch experiments were done at constant pH values of 3, 3.5 and 3.9. The widely divergent curves showing the amount of a compound released as a function of time for the different solution pH-values, scale very well for the main compounds in both the batch experiments (Figure 4) and the column experiments (not shown). The reproducibility appears to be too good as is seen from the duplicated experimental data in Figure 4. With these results the question to which mechanism or combination of mechanisms causes the observed weathering rates is not answered. In fact, regardless of the mechanisms of the feldspar weathering discussed in the literature the experimental results may be scaled with the exposure variable, I , provided the reaction rate is assumed to be first order with respect to the proton concentration, and rate controlling.

For the assessment of long-term effects of soil acidification, the scaling procedure may yield more reliable results than purely empirical descriptions [Cosby, 1986].

4.4 Conclusions

In this paper we discussed the scaling of time in the case of reactions whose rates are controlled by reactant diffusion, a first order chemical reaction or a combination of these processes. The scaling procedure proposed that has at most one adjustable parameter (c_e) is derived from the unreacted shrinking core (USC) model. A unique relation is found between the amount of reactant or solid phase that has reacted and an exposure variable, which is a function of concentration and time. Moreover, the scaling rule is also valid for other diffusion controlled processes e.g., when abrasion of the product layer occurs, in case of irregular solid phase geometry, when various particle sizes occur or when the composition of the solid phase and the reaction stoichiometry vary as in soil. These and other complications do not affect the possibility to apply our scaling procedure. The scaling procedure may be useful in a semi-empirical basis for interpolation and extrapolation in time for complex real world reaction systems that are not (yet) amenable to a mechanistic description. Once the relationship between conversion and exposure has been established experimentally the conversion as a function of time and concentration may be calculated. Hence, the scaling rule may be a useful tool for the simulation of certain real world problems, either in scientific research or for management purposes.

ACKNOWLEDGEMENT: Permission to use the data of example 3 was given by J.J.M. van Grinsven, which I appreciated very much.

4.5 References

- Barrow, N.J., A mechanistic model for describing the sorption of phosphate by soil. *J. Soil Sci.* 34:733-750, 1983.
- Bartlett, R.W., Conversion and extraction efficiencies for ground particles in heterogeneous process reactors. *Metall. Trans.* Vol 2:2999-3006, 1971.
- Bartlett, R.W., A combined pore diffusion and chalcopyrite dissolution kinetics model for in site leaching of a fragmented copper porphyry. In: *Proc.Int'l Symp. Hydrometall.* AIME New York, 1973.

- Beek, J., Phosphate retention by soil in relations to waste disposal. PhD thesis, Agricultural University Wageningen, The Netherlands, 1979.
- Bird, R.B, W.E. Stewart, and E.N. Lightfoot, Transport phenomena, John Wiley and Sons, Inc. New York, 1960.
- Bischoff, K.B., Accuracy of the pseudo steady state approximation for moving boundary diffusion problems. Chem. Eng. Sci. 18:711-713, 1963.
- Braun, R.L., A.E. Lewis, and M.E. Wadsworth, In-place leaching of primary sulfide ores: Laboratory leaching data and kinetics model. Metall. Trans. Vol 5:1717-1726, 1964.
- Brunekreeft, B., The relationship between environmental lead and blood lead in children: a study in environmental epidemiology. Ph.D. thesis, Agric. University Wageningen, The Netherlands, 1985.
- Busenberg, E., The products of the interaction of feldspars with aqueous solutions at 25°C. Geochim. et Cosmochim. Acta. Vol. 42:1679-1686, 1978.
- Chou, L., and R. Wollast, Study of the weathering of albite at room temperature and pressure with a fluidized bed reactor. Geochim. et Cosmochim. Acta. Vol. 48:2205-2217, 1984
- Correns, C.W., Experiments on the decomposition of silicates and discussion of chemical weathering. Clays and Clay Mineral. Vol. 10:443-459, 1963.
- Cosby, B.J., et al., Estimating catchment water quality response to acid deposition using mathematical models of soil ion exchange processes. Geoderma 38:77-95, 1986
- Davis, G.B., and J.M. Hill, A moving boundary problem for the sphere I.M.A. J. Appl. Math. 29:99-111, 1982
- Enfield, C.G., T. Phan, D.M. Wolters and R. Ellis, Jr., Kinetic model for phosphate transport and transformation in calcareous soils, I & II. Soil Sci. Soc. Am. J. 45: 1059-1064;1064-1070, 1981
- Helgeson, H.C., Kinetics of mass transfer among silicates and aqueous solutions. Geochim. et Cosmochim. Acta Vol. 35: 421-469, 1971.
- Helgeson, H.C., Kinetics of mass transfer among silicates and aqueous solutions: correction and clarification. Geochim. et Cosmochim. Acta, Vol. 36:1067-1070, 1972.

- Helgeson, H.C., W.M. Murphy, and P. Aagaard, Thermodynamic and kinetic constraints on reaction rate among minerals and aqueous solutions.II. Rate constants, effective surface area and the hydrolysis of feldspar. *Geochim. et Cosmochim. Acta* Vol.48:2405-2432, 1984.
- Hiskey, J.B., and M.E. Wadsworth, Galvanic conversion of chalcopyrite, In: F.F. Aplan, W.A. McKinney, and A.D. Pernicelle (eds.) *Solution Mining Symposium*, AIME New York:422-445, 1974
- Holdren, G.R., Jr., and J.E. Adams, Parabolic dissolutions kinetics of silicate minerals: an artifact of non equilibrium precipitation processes? *Geology*, Vol.10:186-190, 1982.
- Levenspiel O., *Chemical reaction engineering*. Chapter 12, 2nd. edition John Wiley and Sons, Inc., Canada 1972.
- Lu, W.K., The general rate equation for gas-solid reactions in metallurgical process. *Trans. Metall. Soc. AIME*. Vol. 227:203-206, 1963.
- Lu, W.K., and G. Bitsianes, The general rate equation for gas-solid reactions in metallurgical processes. II-with restrictions of reversibility of chemical reaction and gaseous equimolar counter diffusion. *Trans. Metall. Soc. AIME*. Vol 236: 531-535, 1966.
- Ockendon, J.R., and W.R. Hodgkins (eds.), *Moving boundary problems in heat flow and diffusion*. Oxford, Clarendon Press, 1965.
- Paces, T., Steady state kinetics and equilibrium between groundwater and granitic rock. *Geochim. et Cosmochim. Acta*. Vol 37:2641-2663, 1973..
- Rahman, Z.B.A., The fate of phosphate fertilizer in Malaysian soils and its effect on plant uptake. PhD thesis, Univ. of Ghent, Belgium, 1982.
- Shen, J., and J.M. Smith, Diffusional effects in gas-solid reactions. *Ind. Eng. Chem. Fundam*, Vol. 4 no 3:293-301, 1965.
- Skopp, J., Analysis of time-dependent chemical processes in soils. *J. Environm. Qual*, Vol. 15, no 3: 205-213, 1986.
- Szekely, J., and M. Propster, A structural model for gas solid reactions with a moving boundary-VI. The effect of grain size distribution on the conversion of porous solids. *Chem. Eng. Sci.* Vol 30:1049-1055, 1975.
- Van Grinsven, J.J.M. A new method to measure mineral dissolution rates in soil samples. (In preparation).

- Van Grinsven, J.J.M., N. van Breemen, and J. Mulder, Impact of acid atmospheric deposition on woodland soils in The Netherlands: I, Calculation of hydrologic and chemical budgets. In press: Soil Sci.Soc.Am. J., 1987.
- Van Der Zee S.E.A.T.M. and W.H. van Riemsdijk, The reaction of phosphate described with adsorption in combination with the unreacted shrinking cure model. Conference 'Interactions at the soil-colloid soil-solution interface. Ghent, Belgium, August 24-29, 1986, - and - , 1986. Sorption kinetics and transport of phosphate in sandy soil. Geoderma, 38: 293-309, 1986.
- Van Der Zee, S.E.A.T.M., and W.H. van Riemsdijk, Model for long term phosphate reaction kinetics in soil. J. Environm. Qual., 1988.
- van Riemsdijk, W.H., L.J.M. Boumans, and F.A.M. de Haan, Phosphate sorption by soils. I.A diffusion-precipitation model for the reaction of phosphate with metal oxides in soil. Soil Sci.Soc.Am.J. 48:537-541. Van Riemsdijk, W.H. and A.M.A. van der Linden, II, Sorption measurement technique, Soil Sci. Soc. Am. J. 48: 541-544, 1984a.
- Wen, C.Y., Non catalytic heterogenous solid fluid reaction models. Ind. Eng. Chem. Vol. 60 no 9: 34-54, 1968.
- Wollast, R., Kinetics of the alteration of K-feldspar in buffered solutions at low temperature. Geochim. et Cosmochim. Acta.Vol.31:635-648, 1967.
- Yagi, S., and D. Kunii, Combustion of carbon particles in flames and fluidized beds. Symp. on Combustion Proc: 231-244. Pittsburgh, 1984.

5. PHOSPHATE SORPTION KINETICS AND TRANSPORT IN SMALL COLUMNS

Abstract

The reaction of ortho-phosphate (P) with sandy soil is described by two processes: a fast and reversible adsorption according to Langmuir kinetics, combined with a non-equilibrium, irreversible, precipitation like process. The precipitation reaction involves the bulk of oxides and is described with a model derived from the unreacted shrinking core model. Model parameters are assessed by performing sorption and desorption experiments. With the parameter values obtained, the transport of P in packed columns is simulated. Good agreement between measured and calculated breakthrough curves is found for the transport of high feed concentration of P and for the leaching of a column presaturated with P. Transport experiments appear to produce additional information that is necessary for the assessment of model parameters.

5.1 Introduction

The reaction of P with soil and its kinetics have been studied intensively [Beek and Van Riemsdijk 1982]. In the non-calcareous, sandy soils the reaction of P is predominantly with oxides of Al and Fe, [Beek, 1979]. Generally the rate of this non-equilibrium process depends amongst others on the P-concentration in solution [Barrow, 1983; 1981; Beek and Van Riemsdijk, 1983]. Measurements indicated that only part of the sorbed P will desorb within a practical time-scale [Barrow, 1983; Beek, 1979]. For Gibbsite it has been shown that sorption in excess of monolayer coverage may occur [Van Riemsdijk and Lyklema, 1980].

The reaction of P with soil was described mathematically with a variety of expressions including the Langmuir and the Freundlich isotherms and rate equations [Sibbesen, 1981; Enfield et al., 1976; Enfield and Shaw, 1975; Shah et al., 1975]. The complexity of the sorption phenomena is indicated by the use of several equations by

e.g. Barrow [1983], Enfield et al., [1981], Beek [1979] and Mansell et al., [1977 a,b]. Recently the diffusion of P into oxides has been proposed by both Van Riemsdijk et al., [1984a] and Barrow [1983]. Their models, however, are conceptually different. Whereas Barrow considered a diffusion process according to penetration theory, Van Riemsdijk et al., assumed a reaction with the bulk of the oxides with diffusion towards the reaction zone as rate-limiting. In the reaction zone, which was assumed infinitely thin, metaloxide is converted to a metal-phosphate by a precipitation like reaction. This model is known in the chemical engineering literature as a shrinking core model. The reaction rate, if the solubility product is exceeded ($c > c_e$), was described using a composite concentration-time variable (chapter 3).

The model of Van Riemsdijk et al., [1984] has been extended by Van der Zee and Van Riemsdijk [1986] to include the observed reversibility of part of the reaction and also to account for the reaction observed at concentrations below the equilibrium concentration. In this study the sorption model of Van der Zee and Van Riemsdijk [1986] is briefly outlined. Next the procedures employed for the estimation of model parameters are illustrated. Since these procedures consist also of column-leaching experiments the transport of P has been simulated, and the experimental and numerical results are compared.

5.2 Mathematical formulation

The removal of P from the soil solution due to its reaction with the oxides of Al and Fe is fast initially and slows down considerably with the progress of the reaction(time). The concept of the diffusion of P into the oxides and subsequent conversion of the oxide into a metalphosphate [Van Riemsdijk et al., 1984] yielded good results. However, their convenient semi-empirical expression giving the amount of P sorbed as a function of the concentration-scaled time variable I is usefull only in the [I]-domain covered experimentally. The reaction of P at concentrations below the equilibrium concentration of P, as governed by the metalphosphate solubility, as well as the backward reaction were not included in their model. Moreover, the reaction at higher values of the concentrations and sorption times, than evaluated

experimentally involved extrapolation that may be subject to considerable error.

In order to account for reactions at low concentrations as well as to include the backward reaction, two separate processes of a different nature and kinetics are distinguished. A fast and completely reversible adsorption process of P on the surface of oxides and metalphosphates already present is described by Langmuir kinetics:

$$\frac{dQ}{dt} = k_a c(Q_m - Q) - k_d Q \quad (1)$$

At equilibrium ($\frac{dQ}{dt} = 0$) the Langmuir isotherm is found:

$$Q = \frac{KQ_m c}{1 + Kc} \quad (2)$$

If desorption of soil-P is enticed, in the presence of a high affinity - high capacity sink for P (Chapter 2) then equation (1) reduces to

$$\frac{dQ}{dt} = -k_d Q \quad (3)$$

and integration with the condition

$$\text{I.C.} \quad t = 0 \quad Q = Q_{in} \quad (4)$$

will yield for the desorbed amount:

$$Q^* = Q_{in} - Q(t) \quad (5)$$

$$Q^*(t) = Q_{in} \{1 - \exp(-k_d t)\} \quad (6)$$

A slower immobilization of P assumed irreversible for laboratory time scales, is described by the diffusion/precipitation process given by Van Riemsdijk et al. [1984] and Van der Zee and Van Riemsdijk [1986] (Chapter 3)

$$S = f(I) \quad (7)$$

where

$$I = \gamma \int (c_p - c_e) dt \quad (8)$$

In eq. (8) γ is used to nondimensionalize I . The function $f(I)$ is given by an experimentally evaluated polynomial of the form:

$$f(I) = a_0 + a_1 \ln(I) + a_2 \{\ln(I)\}^2 \quad (9)$$

In principle other polynomials (e.g. by not taking the natural logarithm of I) are equally feasible. Since the constants of equation (9) are found from experiments they are valid irrespective of the amounts of P adsorbed or precipitated e.g. in a coating in the initial situation. However, it is noted that the values of the constants will depend upon the initial situation, and consequently so will the shape of $f(I)$. Whereas equation (9) is assumed to be valid for all possible initial conditions, these conditions will be intrinsic in any specified shape of $f(I)$ and they must be given. If this is done, an arbitrary reference point for equations (7)-(9) may be chosen:

$$t < 0, \quad I = I_0, \quad S = S_0 \quad (10)$$

It is noted that the values of I and I_0 depend on the units of c and t chosen as I and I_0 have a dimension.

The condition (10) is acceptable if S_0 is small and $\frac{df(I)}{dI}$ is positive for all relevant $I > I_0$. For equation (7)-(9) a condition is given so that no dissolution takes place:

$$c < c_e, \quad c_p = c_e \quad (11a)$$

$$c > c_e, \quad c_p = c \quad (11b)$$

The sorption model for P may be combined with a transport model to study column-leaching experiments. For a uniformly packed sand-column with saturated, steady state carrier flow in one direction, z , the transport equation is given by:

$$(1 - \theta) \rho \frac{\partial F}{\partial t} + \theta \frac{\partial c}{\partial t} = \theta D \frac{\partial^2 c}{\partial z^2} - J^v \frac{\partial c}{\partial z} \quad (12)$$

assuming, that concentration induced density effects may be neglected.

In equation (12), F is:

$$F(t) = Q(t) + S(t) \quad (13)$$

The hydrodynamic dispersion coefficient takes into account the effects of molecular diffusion and of mechanical dispersion [Bolt, 1982; Bear 1979]:

$$D = D_{mol} + D_{mech} \quad (14)$$

The coefficient D_{mol} is the tortuosity corrected molecular diffusion coefficient in a free solution and the mechanical dispersion coefficient is given by [Bear, 1979; Pfankuch, 1963]:

$$D_{mech} = \lambda (J^v / \theta) \quad (15)$$

Here λ is called the medium's dispersivity.

The initial and boundary conditions for the transport are:

$$\text{I.C.: } t < 0 \quad c = c_1 \quad 0 < z < z_L \quad (16)$$

$$t > 0 \quad J^v(c_0 - c) = -D \frac{\partial c}{\partial z} \quad z = 0 \quad (17a)$$

$$\text{B.C.: } t > 0 \quad J^v(c_E - c) = -D \frac{\partial c}{\partial z} \quad z = z_L \quad (17b)$$

with no backmixing assumed.

5.3 Materials and methods

The soil NKR-1 was classified as a Spodosol (Table 1). The material used was sampled at the depth of 20-40 cm from a field in pasture, in a cover sand area. The soil HAR-4 was sampled at the depth of 0-20 cm from a field that annually received 160 ton/ha of liquid manure. It is a Spodosol in coversand.

Chemicals used were of pro analyse quality. Background electrolyte contained $1.5 \cdot 10^{-3}$ M CaCl_2 and a potassium concentration of $5 \cdot 10^{-3}$

M by addition of KCl in conjunction to K added as KH_2PO_4 . In some cases the electrolyte differed, however, with negligible effects upon (de)sorption as compared to experimental error.

The desorption kinetics experiments employ Fe-oxide coated paper with a high affinity for P as the extractant to ensure insignificant P-concentrations in solution (Chapter 2). Column-leaching desorption experiments consist of a pre-adsorption stage (7 days percolation with $5 \cdot 10^{-3}$ M KH_2PO_4) followed by a desorption stage with a solution without P. Effluent was collected continuously using a fraction collector. Afterwards the residual P adsorbed was desorbed using Fe-oxide coated paper. Column-leaching adsorption experiments by introducing a P-containing solution without prior adsorption followed the same procedure (see table 2). Total sorption was measured according to Van Riemsdijk and Van der Linden [1984] for concentrations in the range of $5 \cdot 10^{-5}$ - $5 \cdot 10^{-3}$ M KH_2PO_4 . In all experiments the concentration of P was measured with the Molybdenum-Blue method (Murphy and Riley, 1962]. Optimizing procedures were done by non-linear curve fitting according to the Simplex method. The sum of squares (SS) of deviations between experimental (Y_{mi}) and model (\hat{Y}_i) values of the dependent variable was minimized:

$$SS = \sum_{i=1}^N (Y_i - Y_{mi})^2 \quad (23)$$

with

$$\sigma = \{SS/(N-M-1)\}^{\frac{1}{2}} \quad (24)$$

to indicate the goodness of fit.

5.4 Parameter assessment and data analysis

If in reaction experiments the sorption is calculated by determination of the amount of P removed from the solution, then it is not known what part has adsorbed on the surface (Q) and what part has precipitated (S). Thus a way to separate the fractions Q and S of F (eq. 13) must be found. The backward reaction for the diffusion precipitation process may be expected to be controlled by the

solubility of the metal phosphates formed. For such phosphates the equilibrium concentration (c_e) is usually small. For many practical situations we may thus assume S to be irreversible. Then by desorbing soil-P in the presence of an infinite sink we may assess Q_{in} and k_d .

Next a soil column presaturated by P may be leached with feed solution containing no P . In that case the precipitation rate will have become negligible, and Q will be practically at its maximum. At the column outlet the concentration in solution is measured and the corresponding amounts desorbed are calculated as in Appendix 1. This leads to the values of K and Q_m . Now we may calculate for any sorption experiment the adsorbed amount if $c(t)$ is known, by numerically integrating eq.(1). This leads to $S(t)$ if calculated adsorption as a function of time is subtracted from measured total sorption, $F(t)$ (eq. 13). By optimization of S as a function of I for different sorption experiments done at different c , we obtain the polynomial constants of eq.(9).

5.5 Results and discussion

The information compiled in table 1 indicates, that the two soils have rather different contents of P organic matter, Fe and Al . Using $\frac{1}{2}(Fe+Al)$ mmol/kg (oxalate extractable) as a rough estimate for the sorption capacity of such soils for P [Lexmond et al, 1982], then it is clear that the HAR-4 soil is relatively more saturated with P than the NKR-1 soil. This is also clearly reflected in the behaviour of both soils.

For HAR-4 the desorption kinetics experiment yields values of $k_d=0.2 \text{ h}^{-1}$ and $Q_{in}=4.5 \text{ mmol/kg}$. For 8 soils an average value of $\bar{k}_d=0.2 \pm 0.03 \text{ h}^{-1}$ (for desorption times up to 66 h is found). The results for HAR-4 are illustrated in Figure 1. From the scatter of the observations it may be concluded that in fact quite some uncertainty concerning the value of k_d persists. Because P_{ox} is $18.3 \text{ mmol kg}^{-1}$ (Table 1) it appears that merely 25% of the P appears to be sorbed reversibly.

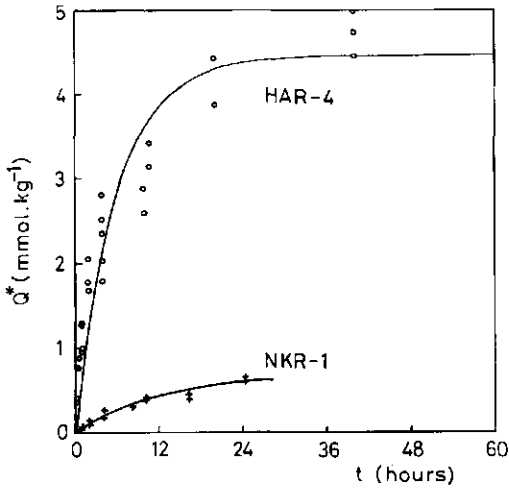


Figure 1. Desorbed amount (Q^*) as a function of time for HAR-4 (o) and NKR-1 (+)

Table 1: Data of the HAR-4 and the NKR-1 soils

Name	HAR-4 ²⁾	NKR-1 ³⁾
Landuse	Arable land	Grassland
Parent material	Coversand	Coversand
Classification ¹⁾	Aquod (Spodosol)	Aquod (Spodosol)
Depth [m]	0-0.2	0.2-0.4
Horizon	Ap	B2
Loam [%]	10	25
Median Grain Size [μm]	150	150
Organic Matter [% wgt]	1.9	5
Oxalate extract. P[mmol/kg]	18.3	3.9
Oxalate extract. Fe[mmol/kg]	14.5	4.1
Oxalate extract. Al[mmol/kg]	50.4	91.0

1) De Bakker [1979], 2) HAR-4: Lexmond et al [1983], 3) NKR-1: Dekkers [1983]

The other values of the adsorption parameters may be obtained considering the P-stat data at low c (supposedly below c_e). For two concentrations, i.e. 0.055 and 0.075 mmol/L, respectively, the adsorption kinetics have been optimized with respect to equation (1).

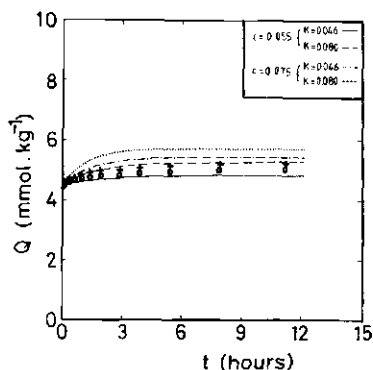


Figure 2: Adsorbed amount (Q) as a function of time for HAR-4.

Observations and simulated curves for two concentrations and two values of K

Table 2. Optimizing results for the sorption parameters.

1. Name	2. Q_{in}	3. Q_m	4. k_a	5. k_d	6. K	7. a_0	8. a_1	9. a_2	10. c_e
HAR-4	4.5	6.8	0.00575	0.125	0.046	0.103	-0.131	0.075	0.2
NKR-1	0.7	16.3	0.005	0.450	0.011	3.05	1.96	0.03	0.04

For polynomial constants t was in minutes; In the Figures t was converted to hours again.

The results are given in Table 2, columns 2-6, and the simulated adsorption as a function of time is shown in Figure 2. The observations are covered well by the optimized curves, although it should be kept in mind that only two concentrations have been considered. That this is possibly a shallow basis for the estimation of the adsorption parameters is reflected by the simulated breakthrough of the column leaching experiment: Figure 3. For this simulation the values of the parameters are taken from Table 2 and Appendix 2. Although the observations are well predicted for the first pore volumes the deviations between observation and the simulated curves become significant after approximately 5 pore volumes.

Nevertheless, recognizing that the constants used for the adsorption-desorption process have been assessed independently the results are considered acceptable. Another approach is given in Appendix 1.

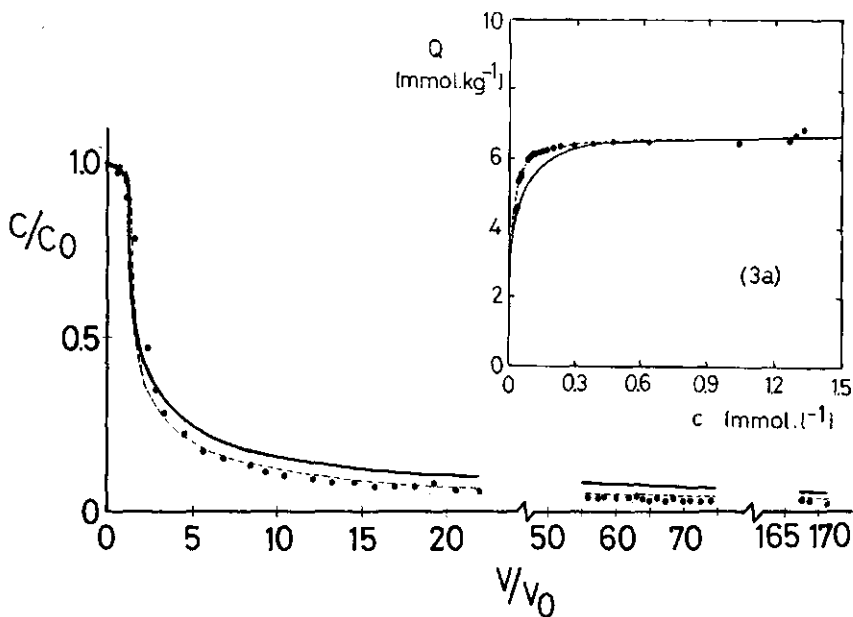


Figure 3: Breakthrough curve for HAR-4. Measured (●) and simulated curves for $K = 0.046 \text{ m}^3/\text{mmol}$ (line) and $K = 0.080 \text{ m}^3/\text{mmol}$ (dashed line). Inset 3a: Adsorption isotherms with $K = 0.046 \text{ m}^3/\text{mmol}$ (line) and $K = 0.080 \text{ m}^3/\text{mmol}$ (dashed line).

In Figure 3a the experimental isotherm data points, found according to this appendix the isotherm obtained by optimizing these data with respect to equation (2), resulting in $K=0.080$ and $Q_m=6.85$, and the isotherm according to Table 2 are shown. This preliminary assessment of the isotherm is based upon the assumptions, that (1) local adsorption equilibrium is assured in the column and (2) concentration gradients in the column are negligible. The simulated response of the breakthrough, using the optimized values $K=0.080$ and $Q_m=6.85$, describes the observations excellently, despite the fact, that i.e. the concentration gradients in the column are certainly not negligible

initially (Chapter 10). In Figure 3a this is indicated by the erroneous position of the points at the right side of the plot. The results are quite promising with respect to the applicability of column-experiments in the assessment of P-adsorption parameters.

Besides the two concentrations mentioned also P-stat experiments have been performed at concentrations in the range 0.2-5.0 mmol/L. If the amounts adsorbed for these experiments are subtracted from the total sorption F (equation 13) and the rest (S) is optimized with respect to equations (7)-(9), then the polynomial constants are found. This is done for trial values of c_e . As the optimizing result (σ) is rather insensitive to c_e , a narrow range for this parameter may not be obtained. These estimation of c_e is approximately 0.1-0.2 mmol/l, which is in agreement with values reported by Van Riemsdijk et al., [1984]. Setting $c_e=0.2$ mmol/l implies that the experiments with higher c may not be used in the adsorption parameter assessment discussed earlier (reversible kinetics). The polynomial constants which are reported in Table 2, complete the description of the sorption kinetics for HAR-4 (Figure 4).

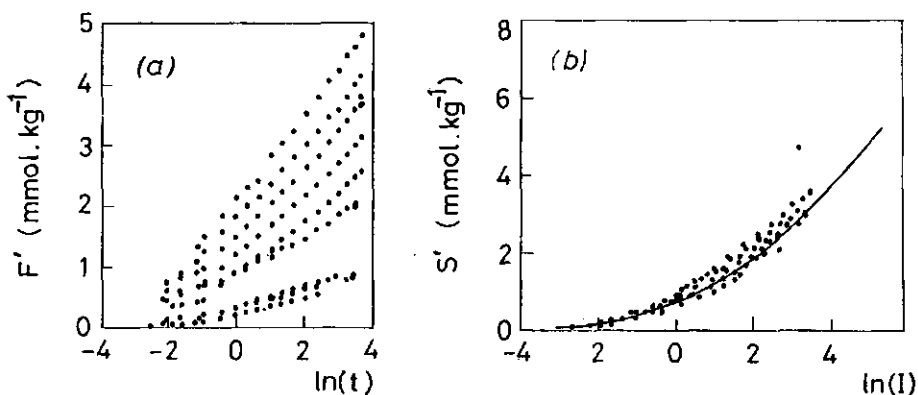


Figure 4: Total measured sorption, F' , as a function of $\ln(t)$ (Figure 4a), and measured precipitation, S' , as a function of $\ln(I)$.

As can be seen the scaling of time by concentration, by using exposure (I) as variable leads to a relatively narrow band of the data points. For comparison it may be noted that the shape of the scaled curve for different concentrations is similar to the conversion-(dimensionless)

time curves given in Chapter 3. It should be noted also that although the polynomial constants were obtained for time in minutes, the time in Figure 4 is in hours. Furthermore, what is shown is actually not F and S , but the total measured sorption and measured precipitation, i.e., excluding already sorbed P at the beginning of the experiments. Using the observations of the P-stat experiments (i.e.: F, c, t) both the adsorption and the precipitation may be simulated. In Figure 5 the subdivision of the measured F in S and Q , respectively, is shown. The agreement of the observations and the simulated F is considered fairly good as use has been made for the diffusion-precipitation process of only one adjustable parameter: c_e . For the HAR-4 soil the processes may be described rather satisfactory for the conditions considered.

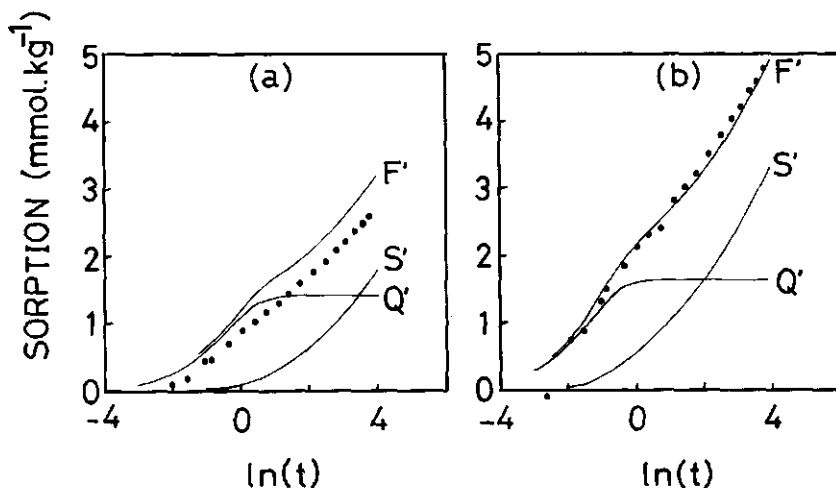


Figure 5: Total sorption (F'), adsorption (Q') and precipitation (S') simulated with the data of Table 2, and measured F' at a) $c = 0.24$ mmol/l and B) $c = 0.67$ mmol/l (HAR-4). Primes denote that initial contents were disregarded.

In the analysis of the NKR-1 soil a different behaviour is observed with respect to the sorption and desorption processes. The desorption kinetics experiment for the NKR-1 (see Figure 1) reveals the small content of initially desorbable P : i.e. $Q_m = 0.7$ mmol/kg. This value is quite small compared to the estimated total

sorption capacity, and about a fourth of the total P extractable by oxalate. The k_d -value of 0.45 h^{-1} is of the order of magnitude of k_d values mentioned earlier.

Unlike in the case of the HAR-4 soil, the other adsorption parameters may not be estimated directly from the P-stat sorption measurements, using the experimental data for low concentrations of P. The reason that this can not be done, is, that the result from a column experiment for NKR-1 suggests a rather low value of c_e which means, that at low c precipitation may already occur. Thus, the isotherm has been directly estimated from the concentrations in the effluent of a column-leaching experiment, and Q, according to Appendix 1. In Figure 6 the experimental isotherm data points are given.

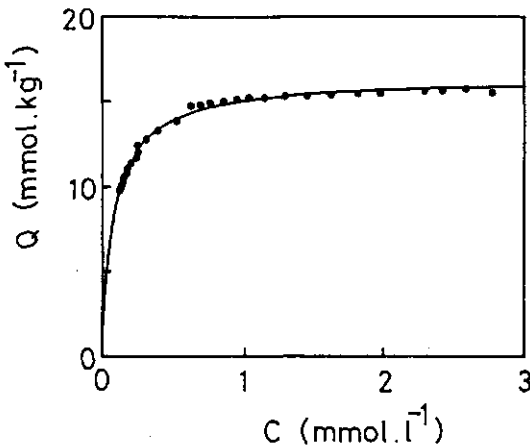
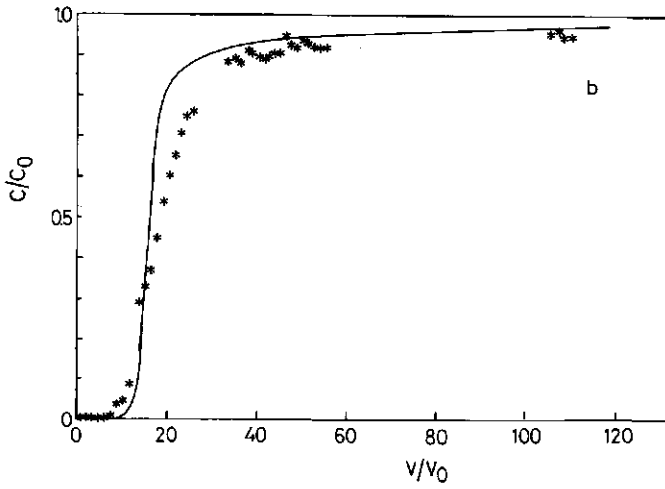
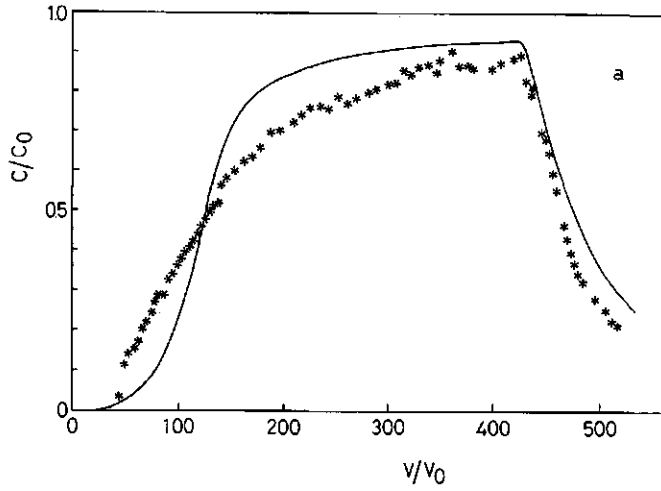


Figure 6:
Adsorption isotherm
for NKR-1 (Table 2).

For these results the parameters are given in Table 2. The estimated adsorption maximum (reversible) is large as would be expected from the aluminium and iron content of the soil. The isotherm is considerably less steep than the HAR-4 isotherm. This causes the increased buffering at higher concentrations during the desorption phase of the column experiment (Figure 7). The polynomial constants were found for a value of $c_e = 0.04 \text{ mmol.l}^{-1}$. These values for the parameters of the NKR-1 soil are subsequently used for the simulation of the transport of P in order to get an impression of the



6

Figure 7: Breakthrough curves for NKR-1. Observations (*) and simulated curves with the parameter values of Table 2 and Appendix 2.

compatibility of the sorption kinetics model with the behaviour of P in this soil. The observations and the simulated breakthrough curve are shown in Figure 7a. The feed solution in this experiment contained 0.2 mmol P/l. It is concluded that the overall sorption kinetics in this case of transport of P is not described well by the parameters of table 2. In Figure 7b similar results for a feed solution concentration of 3 mmol P/l are shown, that are predicted better by simulation of the transport process. As in Figure 7a, first breakthrough is predicted a little too late, and the tailing appears to be somewhat less pronounced in the simulated curves as compared to the observations. Better agreement was found for the experiments of Figure 8. The variation in the flow velocity occurring for the experiment with $c_0=0.2$ mmol/l was taken into account in the simulations (Appendix 2).

The assumption, that the value of c_e for the NKR-1 soil is less than approximately 0.2 mmol/l. It is based upon the shape of the experimental breakthrough curve of P for this soil. In the case that c_0 is less than or equal to c_e , the solute is only subject to adsorption according to Langmuir kinetics. If adsorption may be described by the Langmuir isotherm (local equilibrium) then P will be displaced according to a travelling wave (steady state front: Appendix A). The "breakthrough curve" of such a travelling wave is quite different from the curve presented in Figure 7. In the case, that local adsorption equilibrium is not attained the transport processes will still be very similar to the phenomenon of the travelling wave and the breakthrough curve will bear much resemblance to the one found for a travelling wave. Therefore c_e is estimated to be significantly less than 0.2 mmol/l.

A case of interest is the perturbation of the transport phenomena discussed above by the sorption according to the diffusion precipitation process. The deformation of the breakthrough curve will be similar to effects that occur, if immobile water or a heterogeneous flow domain is considered (see e.g. De Smedt et al., 1981; Raats, 1981; Bolt, 1982). An analysis that bears some physical resemblance to the processes discussed here, is given by Rasmuson [1981].

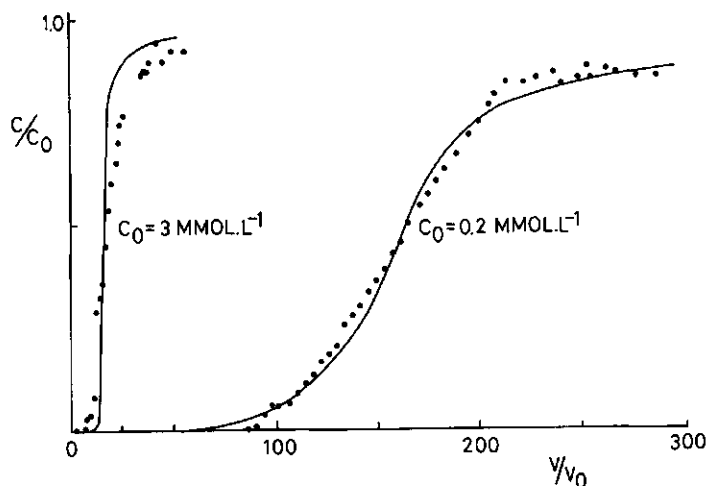


Figure 8: Breakthrough curves for the NKR-1 Soil. Parameter values given in Table 2 and Appendix 2.

To demonstrate the perturbation of the breakthrough curve several values of c_e were chosen, keeping the polynomial fixed (see Table 2: NKR-1 soil). If the value of c_e is taken equal to the concentration in the feed solution, then the solute adsorbs according to Langmuir kinetics. If lower values are taken, the perturbation of the breakthrough curve will be larger if c_e is smaller: Figure 9. For illustrative purposes this perturbation is shown with the same polynomial in all cases. As the polynomial obtained by optimizing the P-stat experiments depends on the c_e chosen, also simulations have been performed where for a given value of c_e the appropriate polynomial constants are used. However, due to the relatively small importance of the precipitation process the effects are negligible. The effect of the slow process appears to be a decrease in the travel velocities of the concentrations exceeding c_e . However, also for smaller concentrations the travel velocity is slightly affected. This is an illustration of the fact that in the case of non-linear, favourable isotherm the travel velocities of the higher concentrations affect the velocity for the lower concentration range.

Finally, as the choice of the order of the polynomial is somewhat

arbitrary, the order was varied for the NKR-1 soil from 1 to 3. It was noted, that the effects were small. It should be realized that if the transport problem is such, that the value of I exceeds the experimentally evaluated domain of I , the choice of the polynomial (order) affects the nature of the extrapolation procedure (Appendix B). In that case, at least, the choice of the degree should be made with care.

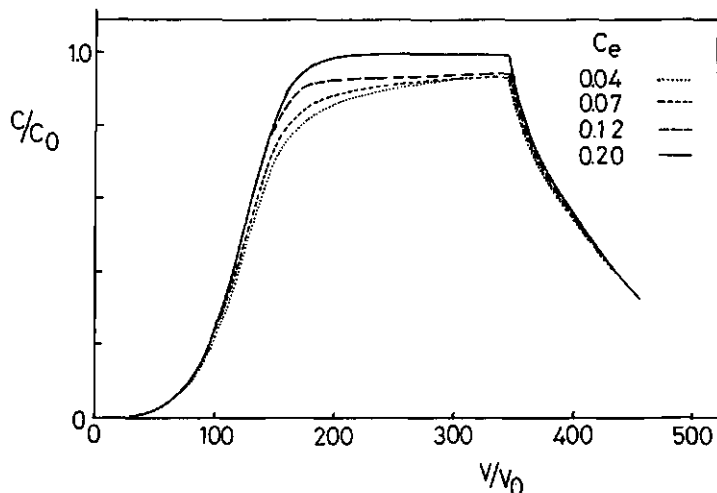


Figure 9. Breakthrough curves for the indicated values of c_e parameter values as in Figure 7a.

5.6 Conclusions

The results presented for the HAR-4 soil indicate, that the desorption of the sorption kinetics of P according to the two processes proposed, i.e., a reversible adsorption described by Langmuir kinetics and a precipitation of P with diffusion of P into oxides as rate limiting, is promising for the description of the experimental results. The prediction of an independent column leaching experiment is satisfactory. Results concerning another soil (NKR-1) show that it behaves quite different from the HAR-4 soil: the adsorption isotherm seems to be significantly less steep for the NKR-1 soil and the precipitation process seems to occur at lower concentrations of P. The precipitation process is less important than in the case of HAR-4. The

results of the column experiment of the HAR-4 soil considered indicate, that this technique may present additional information, that is not easily obtained otherwise. Examples are e.g. the parameters K and Q_m for the adsorption process if the diffusion precipitation process prohibits the direct assessment from P-stat experiments. The value of c_e that is only inaccurately estimated from data obtained with the P-stat technique may possibly be estimated by studying the breakthrough curve of P. However, then there must be certainty, that the breakthrough curve is not significantly affected by other processes with similar effects (e.g. immobile water).

5.7 Appendix 1: Isotherm construction

From the breakthrough curve of a column that is P-saturated (i.e., $Q = Q_m$ at $t = 0$) and which is leached with a solution containing no P, the isotherm may be constructed.

Neglecting concentration gradients in the column and assuming adsorption equilibrium, the desorbed amount after n_1 effluent solution samples are taken, equals

$$Q_{n_1}^* = \sum_{j=1}^{n_1} \{V_j c_j - V_0(c_{j-1} - c_j)\} \quad (1-1)$$

where $Q_{n_1}^*$ is the desorbed amount, on average for the whole column, V_j is the sample volume of the jth sample and c_j is the P-concentration in this sample, V_0 is one pore volume of the column. Q^* is thus calculated for all (n) samples. After the last sample the column soil material is analysed and this yields the residual amount of P still adsorbed (Q_R). Thus the total amount of P adsorbed reversibly after the nth sample equals

$$Q_n = Q_R \quad (1-2)$$

The total amount adsorbed at the moment that leaching starts equals

$$Q(t=0) = Q_n^* + Q_R \quad (1-3)$$

and for any sample j the amount still adsorbed and in equilibrium with c_j measured in this samples is

$$Q_j(c_j) = Q_n^* - Q_j^* + Q_R \quad (1-4)$$

Because for all sample we know both Q_j and c_j ($j = 0, \dots, n$), we can fit equation (2) to these data to obtain K ($=k_a/k_d$) and Q_m .

5.8 Appendix 2: Values used to simulate transport

	HAR-4	NKR-1 (Fig.7a)	NKR-1 (Fig.7b)
θ	0.40	0.65	0.40
ρ	1780.0	1035.0	1600.0
J^v	0.080	0.059	0.050
D_{mol}	$9 \cdot 10^{-7}$	$9 \cdot 10^{-7}$	$9 \cdot 10^{-7}$
l	0.0005	0.0005	0.002
z_L	0.04	0.04	0.10
c_0	0.2	0.2	3.0

	NKR-1 (Fig. 8)	NKR-1 (Fig. 8)
θ	0.50	0.505
ρ	1011.0	1087.0
J^v	$t < 44h: 0.094; t > 44h: 0.048$	0.0556
D_{mol}	$9 \cdot 10^{-7}$	$9 \cdot 10^{-7}$
l	0.002	0.002
z_L	0.04	0.04
c_0	0.2	3.0

ACKNOWLEDGEMENTS: The curve fitting programs were made by H. de Jong and H.L.M. Spanjers and data acquisition as well as data analysis were done mainly by R. Hopman and C.E. Kleijn. For their able assistance I am very gratefull.

5.9 Notation

Q	adsorbed phosphate (reversible)	mmol/kg
S	precipitated phosphate (irreversible)	mmol/kg
F	sorbed phosphate (sum of Q and S)	mmol/kg
I	concentration-time integral	mmol.min/m ³
J ^V	carrier specific discharge	m ³ /m ² .h
D	diffusion-dispersin coefficient	m ² /h
N	number of samples	
M	number of optimized parameters	
K	adsorption constant	m ³ /mmol
V	volume	m ³
t	time	h
z	distance	m
c	concentration of P	mmol/m ³
k _a	adsorption rate constant	m ³ /mmol.h
k _d	desorption rate constant	1/h
a ₀ , a ₁ , a ₂ , a ₃	polynomial constants	
λ	dispersivity	m
m	exponent	
θ	volumetric water content	
ρ	bulk density solid phase	kg/m ³
σ	standard deviation of fit	

subscripts:

e	with c: equilibrium
E	with c: effluent
i	with c: initial concentration
O	with c: feed solution c in column experiments
	with V: soil column pore volume
in	with Q: initially adsorbed
m	with Q: adsorption maximum
L	with z: column length

5.10 References

- Barrow, N.J., L. Madrid and A.M. Posner. A partial model of adsorption and desorption of phosphate by Goethite. *J. Soil Sci.* 32: 399-407, 1981.
- Barrow, N.J. A mechanistic model for describing the sorption and desorption of phosphate by soil. *J. Soil Sci.* 34: 733-750, 1983.
- Bear, J. *Hydraulics of groundwater*. McGraw-Hill Inc., New York, 1979.
- Beek, J. Phosphate retention by soil in relation to waste disposal. PhD thesis, Agricultural University, Wageningen, 1979.
- Beek, J. and W.H. van Riemsdijk. Interactions of orthophosphate ions with soil. In: *Soil Chemistry B, Physico-Chemical Models* (ed. G.H. Bolt). Elsevier Sci. Publ. Co., Amsterdam, 1982.
- Bolt, G.H. Movement of solutes in soil: Principles of Adsorption/Exchange Chromatography. In: *Soil Chemistry B, Physico-Chemical Models* (ed. G.H. Bolt). Elsevier Sci. Publ. Co. Amsterdam, 1982.
- De Bakker, H. Major soils and soil regions in the Netherlands. Dr. W. Junk B.V. Publ. The Hague, 1979.
- Dekkers, J.M.J. De bodemgesteldheid van 15 percelen i.v.m. fosfaat onderzoek. Stiboka Report 1742. (Dutch), 1983.
- De Smedt, F., P.J. Wierenga and A. van der Beken. Theoretical and Experimental Study of solute movement through porous media with mobile and immobile water. *Vrije Universiteit Brussel* (6), 1981.
- Enfield, C.G., C.C. Harlin and B.E. Bledsoe. Comparison of five kinetic models for orthophosphate reactions in mineral soils. *Soil Sci. Soc. Am. Proc.* 40: 243-249, 1976.
- Enfield, C.G. and D.C. Shaw. Comparison of two predictive nonequilibrium one-dimensional models for phosphorus sorption and movement through homogeneous soils. *J. Environ. Qual.* 4: 198-202, 1975.
- Enfield, C.G., T. Phan, D.M. Walters and R. Ellis Jr. Kinetic model for phosphate transport and transformation in calcareous soils, I and II. *Soil Sci. Soc. Am. J.* 45: 1059-1064 and 1064-1070, 1981.
- Lexmond, Th.M., W.H. van Riemsdijk en F.A.M. de Haan. Onderzoek naar fosfaat en koper in de bodem in het bijzonder in gebieden met

- intensieve veehouderij. Staatsuitgeverij, Den Haag. Serie Bodembescherming nr. B0-9, 1982.
- Mansell, R.S., H.M. Selim and J.G.A. Fiskell. Simulated transformations and transport of phosphorus in soil. *Soil Sci.* 124(2): 102-109, 1977a.
- Mansell, R.S., H.M. Selim, P. Kanchanasut, J.M. Davidson and J.G.A. Fiskell. Experimental and simulated transport of phosphorus through sandy soils. *Water Resources Research* 13: 189-194, 1977b.
- Murphy, J. and J.P. Riley. A modified single solution method for the determination of phosphate in natural waters. *Anal. Chim. Acta* 27: 31-36, 1962.
- Pfannkuch, H.O. Contribution à l'étude des déplacements de fluides miscibles dans un milieu poreux. *Rev. Inst. Fr. Pét.* 18: 215-270, 1963.
- Raats, P.A.C. Transport in structured porous media. In: *Proc. Euromech. 143, Delft, 2-4 sept. 1981, pp. 221-226. (F.B.J. Barends, A. Verruijt, Eds.), 1981.*
- Rasmuson, A. Diffusion and sorption in particles and two dimensional dispersion in a porous medium. *Water Resources Research* 17(2): 321-328, 1981.
- Shah, D.B., G.A. Coulman, L.T. Novak and B.G. Ellis. A mathematical model for phosphorus movement in soils. *J. Environ. Qual.* 4: 87-92, 1975.
- Sibbesen. Some new equations to describe phosphate sorption by soils. *J. Soil Sci.* 32: 67-74, 1981.
- Van Riemsdijk, W.H. and Lyklema, J. Reaction of phosphate with gibbsite, $Al(OH)_3$, beyond the adsorption maximum. *J. Colloid Interface Sci.* 76: 55-66, 1980.
- Van Riemsdijk, W.H., L.J.M. Boumans and F.A.M. de Haan. Phosphate sorption by soils. I. A diffusion precipitation model for the reaction of phosphate with metal oxides in soil. *Soil Sci. Soc. Am. J.* 48: 397-541, 1984a.
- Van Riemsdijk, W.H. and A.M.A. van der Linden. Phosphate sorption by soils. II. Sorption measurement technique. *Soil Sci. Soc. Am. J.* 48: 541-544, 1984.
- Van Riemsdijk, W.H., A.M.A. van der Linden and L.J.M. Boumans. Phosphate sorption by soils. III. The P diffusion precipitation

model tested for three acid sandy soils. Soil Sci. Soc. Am. J. 48: 545-548, 1984b.

Van der Zee, S.E.A.T.M. and W.H. van Riemsdijk. Model for the reaction kinetics of phosphate with oxides and soil. Conf. 'Interactions at the soil-colloid soil-solution interface, August 24-29, 1986, Ghent, Belgium, 1986.

6. MODEL FOR LONG TERM PHOSPHATE REACTION KINETICS IN SOIL

Abstract

A simplified reaction kinetics model for long term P-sorption in soils receiving large quantities of P-rich animal manure is presented. Results from soil analyses for samples taken in 84 fields in nine different soil types indicate that the oxalate extractable P provides a good estimation of total P. Sorption experimental data for reaction periods up to 249 days show that measured sorption is proportional to $\ln(t)$. Total sorption, F , (at long reaction periods) that includes P already present (P_{OX}) appears to be proportional to the sum, M , of oxalate extractable Fe and Al. These results are described with a model where soil reactivity is related linearly to M , and the reaction kinetics are expressed in terms of a composite concentration time variable, I . This leads to the relationship $F = kM \ln(I)$ where k is a characteristic of the soil. Comparison with results in literature indicate that the concentration dependence of the reaction is accurately described by using I instead of time as a variable. Differences in reactivity (k) for different soil horizons or soil types are apparent from the different k -values for topsoils and subsoils. Sorption measured during 40 hours (F_r) may be extrapolated to long term (1-2 years) sorption (F_m) for each soil separately without correction of the value of I for the reaction period in the field by simply setting $F_m = P_{OX} + 1.8 F_r$. For a P-concentration of 5 mmol L^{-1} this leads to a value of $\alpha_m = F_m/M = 0.63 \pm 0.14$ for topsoils. Extrapolation using the average k -value found for short term sorption experiments results in the same value of α_m .

6.1 Introduction

The behaviour of P in soil has received much attention in soil science literature. Because of the often limited P availability for plants the emphasis has been given to P fertilization requirements for optimal plant growth. During the past decades, disposal of waste water

and animal manure slurries have caused P-saturation of soils and a surface water eutrophication hazard after leaching of P [Ryden et al., 1973; Beek, 1979; Gerritse, 1980; Enfield et al., 1981]. This is caused by the application of P in this kind of waste, that far exceeds the plant uptake of phosphorus. Many studies have focussed on the nature and the rate of the reaction of P with soil [Van Riemsdijk and De Haan, 1981, Beek, 1979]. The reaction has been shown to be non-equilibrium and only partially reversible with a concentration dependent reaction rate [Beek and Van Riemsdijk, 1982, further reference given there]. The over all reaction may continue for very long times [Barrow and Shaw, 1975; Munns and Fox, 1976; Van Riemsdijk and De Haan, 1981]. The reaction has been described by Van Riemsdijk [1979], Enfield et al. [1981], Barrow [1983], Van Riemsdijk et al. [1984a], and Van Der Zee et al. [1986] with P-adsorption in combination to P diffusion into the bulk of the solid phase.

One of the main problems caused by disposal of P-rich waste is the eutrophication that results after leaching of P into surface waters. Transport of P has been studied by Logan and McLean [1973], Mansell et al [1977a,b], Beek [1979], Enfield et al. [1981], De Willigen et al. [1982], Raats et al. [1982], Mansell et al. [1985], Van Der Zee et al. [1986] and Van Der Zee and Van Riemsdijk [1986a]. These studies indicated that the description of short term laboratory transport experiments may be done satisfactorily. However, the applicability of reaction models and of parameter values found for laboratory circumstances to transport in the field remains questionable.

An important parameter is the constant describing the kinetics of the reaction of P, e.g., a characteristic reaction time [Beek, 1979, De Willigen et al., 1982, Raats et al., 1982]. This parameter controls the fraction of potential sorption that occurs in the field at a particular flow velocity and P concentration. The mobilization of the sorption capacity over the years in actual field conditions is hard to assess experimentally. Therefore, there is a need for methods that can be used to extrapolate short term sorption measurements to long term sorption occurring in years.

The scope of this contribution is to present a model that can be used to estimate long term P sorption from short term sorption measurements performed in a routine fashion in the laboratory. The

proposed model is based on a mechanistic viewpoint of the sorption processes involved and is compatible with descriptions given in the literature. The input data are easily measurable since the model is intended for use in practical (field) situations such as P leaching due to high applications of sewage water or animal manure slurries. The model described is relatively simple as both the assessment of large and diverse data sets and the simulation of field situations with deterministic models is considered to be impractical or even impossible. This is due in part to the spatial variability of natural systems, i.e., a field or watershed, with respect to important variables such as the contents of the dominating reactive solid phase constituents. In order to deterministically describe such a heterogeneous system, the spatial distribution of important variables needs to be known. However, in most cases prime interest concerns the system-averaged behaviour [Dagan and Bresler, 1979, Elabd et al., 1986, Van Der Zee and Van Riemsdijk, 1986b]. This is possible with stochastic models that take soil heterogeneity into account. In such models the input variables usually are characterized by a distribution instead of a fixed (average) value. The model described in this paper was used to estimate long term sorption from the distribution of a soil reactivity variable found by short term sorption measurements for an ensemble of 84 rather different soils. This work shows that the estimated sorption for the ensemble of soil agrees well with the measured sorption and that extrapolation may be done using statistics of the ensemble instead of extrapolation for each individual soil.

6.2 Theoretical background

Dissolved and solid orthophosphates predominate in animal manure slurries whereas organic phosphorus compounds constitute a minor fraction of total P [Gerritse, 1977, 1980]. Since organic compounds generally will be converted into inorganic constituents [Castro and Rolston, 1977] we consider only orthophosphate (P) assuming that the soil is in a steady state with respect to organic P content.

The reaction rate of P is a function of concentration and of time (amount of reaction product) and is described with different

mathematical expressions by Mansell et al. [1977a,b], Van Riemsdijk and De Haan [1981], Enfield et al. [1981], Barrow [1983], Van Riemsdijk et al. [1984] and Van Der Zee and Van Riemsdijk, [1986a]. We assume that the over all reaction (F) is the result of two processes, i.e., a relatively fast, reversible adsorption (Q) and a practically irreversible, diffusion/precipitation (S). Furthermore, it is not unreasonable to expect that for a soil already containing P the adsorption rate is sufficiently high to reach virtual equilibrium within a short time such as a day [Van Der Zee and Van Riemsdijk, 1986a]. Therefore, the reaction rate for longer times will be approximately equal to the slow sorption rate, i.e., $dF/dt \approx dS/dt$. For the sorption rate, we use the expression also used by Van Riemsdijk and De Haan [1981]:

$$\frac{dS}{dt} = a_1 \exp(-a_2 S) \quad (1)$$

where a_1 and a_2 are constants, assuming that the adsorption rate $(\frac{dQ}{dt})$ is small for times longer than a day. Integration for $t_a = (a_1 a_2)^{-1}$ and $S(t_a) = 0$, where t_a is negligibly small, yields

$$S = a_2^{-1} \ln[a_1 a_2 t] \quad (2)$$

Van Riemsdijk and De Haan [1981] found for short term reaction times that a_1 was proportional to c . No clear relationship between a_2 and c was found. In an alternative description of the slow sorption process by Van Riemsdijk et al. [1984a], it was assumed that P diffusion was rate limiting with respect to the precipitation like process. For such cases Van Riemsdijk et al. [1984] showed that then the sorption can be expressed as a function of a new composite variable I given by

$$I = \int (c - c_e) dt / (c_r t_r) \quad (3)$$

where c_e is the equilibrium concentration for the metalphosphate under the prevailing conditions and $c_r t_r$ equals one in the units used. Van Der Zee and Van Riemsdijk [1986a] used a second degree polynomial of $\ln(I)$ to describe sorption (excluding adsorption) measured for a reaction time of one week. However, their data can also be described

well by a linear function of $\ln(I)$. Setting in eq. (2) $a^*c = a_1a_2$ and measuring S at constant c as done by Van Riemsdijk and Van Der Linden [1984] and Van Der Zee and Van Riemsdijk [1986a] also leads to such a linear relationship of S and $\ln(I)$:

$$S = a_2^{-1} \ln(a^*ct) = a_2^{-1} \ln(I) + \text{constant} \quad (4)$$

It may be noted that with the new variable, I , the same sorption may be obtained different combinations of c and t . It is most practical to perform measurements at one concentration which is relevant to concentrations occurring in field situations. Thus for the animal manure slurry polluted soils of interest here, concentrations in the order of 1-3 mmol P L⁻¹ are realistic [De Haan and Van Riemsdijk, 1986]. For sewage water disposal, the relevant concentration is a factor ten smaller [Beek, 1979].

If it is assumed that the adsorption capacity is almost reached or that the adsorption (Q) may also be described with eq. (4) then we can replace S by $F (=Q+S)$ in eqs. (1), (2) and (4). For soils differing with respect to P reactivity, the constants a_2 and a^* will differ. The reactivity appears to depend on the content of amorphous oxides of Fe and Al. Beek [1979] showed that P was predominantly associated to the oxalate extractable metal content, $M (= Fe_{ox} + Al_{ox})$. The oxalate extractable P, P_{ox} , is approximately equal to (Fe+Al)-associated P according to Kurmies fractionation method [Kurmies, 1972]. Therefore, it seems reasonable to assume that the reaction capacity, F_m , is proportional to M , i.e., $F_m = \alpha M$. By defining a saturation factor $\alpha = F/M$ we may then compare soils with different contents of P and oxalate extractable Fe and Al. If we choose the units of c and t such that the constant in eq. (4) may be neglected we find:

$$\alpha = k \ln(I) \quad (5)$$

where $k = [a_2M]^{-1}$. Also we find

$$\alpha = \frac{P_{ox} + F_r}{M} \quad (6)$$

where F_r is the amount that is sorbed in laboratory experiments in

addition to P already present, P_{ox} . The factor α is a better variable to compare different soils with respect to P-saturation than is e.g. $P_{ox}+F_r$, because if α is used the results are normalised with respect to the reactive soil constituents.

6.3 Materials and methods

Soil was sampled in 84 fields situated in the Netherlands. Topsoil (0-0.2 m) and subsoil samples with 0.1 m -depth increments till 1 m depth were taken in fields in agricultural use and in reference locations (virgin soil or soil not recently in agricultural use). Each sample was obtained by mixing 15-20 subsamples per field. Air dried homogenized samples of the layer 0.3-0.4 and 0.4-0.5 m were mixed. On the pulverized ($\phi < 0.05$ mm) soil, oxalate extractable P, Fe, and Al were assessed according to Schwertmann [1964]. Elementary soil composition was determined by X-ray fluorescence analysis.

Prior to initiation of sorption experiments, soil was equilibrated during one week with a 1.5 mmol L^{-1} CaCl_2 solution. Short term sorption (experiment a, 40 hours) was measured according to Van Riemsdijk and Van der Linden [1984]. Long term sorption (experiments b, c, and d) was measured by batch experiments. In the batch experiments, soil/solution ratios were varied to keep c approximately constant (10-20% decrease in c in the first 8 days) while at the same time allowing for a large enough concentration difference in order to determine the calculated sorption with sufficient accuracy.

After 8 days, the P reacted was replenished. Reaction vessels were kept in darkness (temperature 298 K) for the designated reaction periods (experiment b:32d, c: 129d, d: 249 d). At the P concentrations used in the experiments the biological conversion of P may be assumed negligible [White, 1981]. Evaporated solution was regularly replenished and the vessels shaken. In all cases the solution contained $1.5 \text{ mmol CaCl}_2 \text{ L}^{-1}$. The concentration of P added as KH_2PO_4 was 5 mmol L^{-1} for the layer 0-0.2 m and 0.5 mmol L^{-1} for the layer 0.3-0.5 m. For the experiments involving the subsoil samples, $4.5 \text{ mmol KCl L}^{-1}$ was present in the solution in order to avoid effects of different K-concentrations compared to the experiment with the topsoil

samples. Ortho-phosphate was measured according to Murphy and Riley [1962], and is approximately equal to total dissolved P.

6.4 Results and discussion

The oxalate extractable fractions of P, Fe, and Al with respect to total contents shown in Fig. 1 are on average 0.93, 0.37, and 0.11, respectively. The extraction efficiency for sandy soils is higher than for the non-sandy soils. The oxalate extractable amount, P_{ox} , gives a good estimate of total P both for soils heavily polluted with animal manure, and for soils low in P. The total amounts for Fe and Al give no idea of the amounts that are oxalate extractable. Some statistics are given in Table 1 for the oxalate extractable amounts. The large coefficients of variation (standard deviation/mean) indicate the large differences between individual soils.

Table 1: Statistics of some variables assuming normal distribution

variable	topsoil		subsoil	
	mean	st.dev.	mean	st.dev.
Fe_{ox}	42.6	16.3	24.5	23.4
Al_{ox}	35.0	42.3	38.1	13.3
M	77.6	41.8	62.6	27.0
P_{ox}	19.0	9.3	7.7	9.8
α_0	0.27	0.14	0.13	0.14
$\alpha(2)^*$	0.48	0.09	0.27	0.15
$\alpha(32)^*$	0.40	0.15	0.32	0.16
$\alpha(129)^*$	0.55	0.13	0.38	0.18
$\alpha(249)^*$	0.61	0.13	0.39	0.19

* index is sorption time in days.

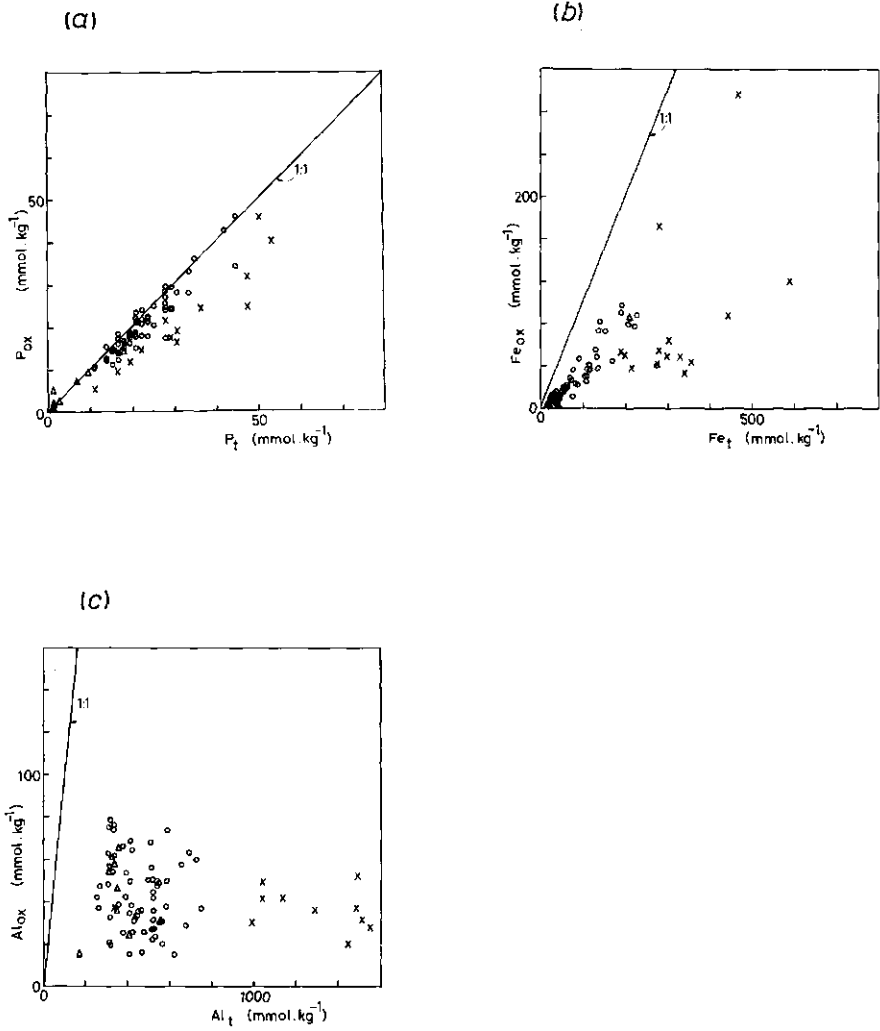


Fig. 1: Oxalate extractable content in topsoil samples as a function of total content for P (a), Fe (b), and Al (c). Reference locations (Δ), sandy agricultural soils (o) and non-sandy agricultural soils (x).

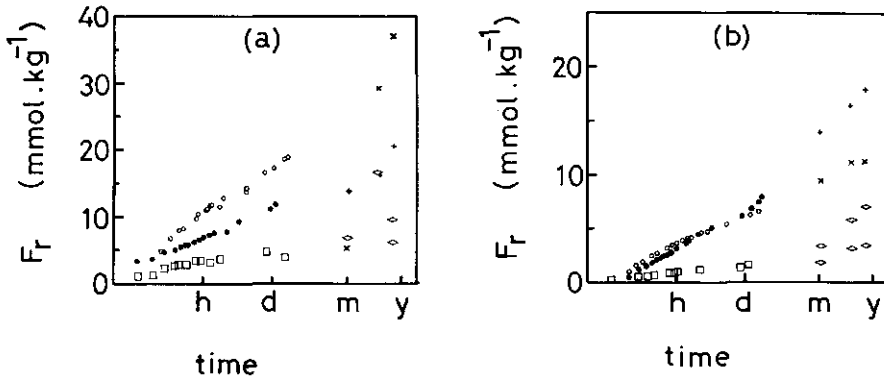


Fig. 2: Measured sorption, F_r , as a function of reaction time (logarithmic scale with h = hour, d = day, m = month, y = year)

Figure → soil			2a:topsoil		2b:subsoil	
	exp.(a)	exps.(b-d)	P_{ox}	α_0	P_{ox}	α_0
AST 9	o	x	12.1	0.145	1.2	0.039
HAR 4	•	+	18.3	0.282	1.3	0.019
BAEX 1	□	◊	35.7	0.618	18.3	0.374

The importance of the amounts Fe_{ox} and Al_{ox} is suggested by eq. (6). The sorption (in excess of P_{ox}) measured in the laboratory, F_r , is shown in Fig. 2 for three soils as a function of reaction time (logarithmic scale). We find that F_r is a linear function of $\ln(t)$. The validity of the hypothesis that the reaction capacity is proportional to M is evaluated using eq. (6) by summing F_r measured after 249 days reaction time and P_{ox} . We assume that for this reaction period the soil becomes practically P-saturated. Consequently we may consider whether F estimated by $P_{ox} + F_r$ is proportional to M . It is shown in Fig. 3 that this is indeed the case for the topsoils. For the smaller reaction periods (experiments a - c) that are not shown, this is also the case; but the variance of α is relatively larger due to the larger effect of the differences in initial conditions (i.e., P_{ox}). The relation of eq. (6) also holds for the subsoils. Due to the

smaller P-concentration, however, the final value of I is smaller; and the effects of differences in P_{OX} is larger. Consequently, the variance in α is relatively larger than for the topsoils. The α values found after a reaction time at $t = 249$ d are $\alpha = 0.61 \pm 0.13$ for the topsoils at $c = 5 \text{ mmol L}^{-1}$ and $\alpha = 0.34 \pm 0.19$ for the subsoils at $c = 0.5 \text{ mmol L}^{-1}$.

We noted that the sorption F_r changes linearly with the logarithm of reaction time for both the topsoils (Fig. 2) and the subsoils. By adding P_{OX} to F_r the total sorption, F, is found. Since the P application history differs, the values of $\alpha_0 (= P_{OX}/M)$ differ also for the different samples. Hence, the true value of the variable I comprises of a term I_0 , related to P_{OX} , and a term I_r , related to F_r :

$$I = I_0 + I_r \quad (7)$$

If we denote α/α_0 by γ and combine eq. (5) with eq. (7) this yields

$$\gamma = \ln(I_0 + I_r) / \ln(I_0) \quad (8)$$

After rearrangement eq. (8) becomes

$$(I_0)^\gamma - I_0 - I_r = 0 \quad (9)$$

In eq. (9) I_0 is the only unknown variable which may be assessed by iterative procedures. By using the values of α and I_r belonging to each of the experiments a-d and thus four I_0 values are found for each soil. As the data of experiment a were most reproducible, those were used to assess I_0 . Summation of I_0 and the I_r -values corresponding to the experiments a to d result in the values of I (eq. 7). Using the I-values, k for each soil may be estimated with eq. (5) for each soil using the data of experiments a to d. For each experiment the statistics of k are given in Table 2 for the topsoils and the subsoils. We find that the mean values of k for the subsoils are smaller than for the topsoils.

Table 2: Statistics of k found for the topsoil and for the subsoil samples at four reaction times. Values of I_0 found in eq. (9) based on short term reaction experiments (experiment a: $t = 40$ hours).

Topsoils

experiment	a	b	c	d
mean	0.045	0.033	0.040	0.043
standard deviation	0.012	0.012	0.010	0.009

Subsoils

experiment	a	b	c	d
mean	0.035	0.032	0.033	0.033
standard deviation	0.021	0.017	0.017	0.016

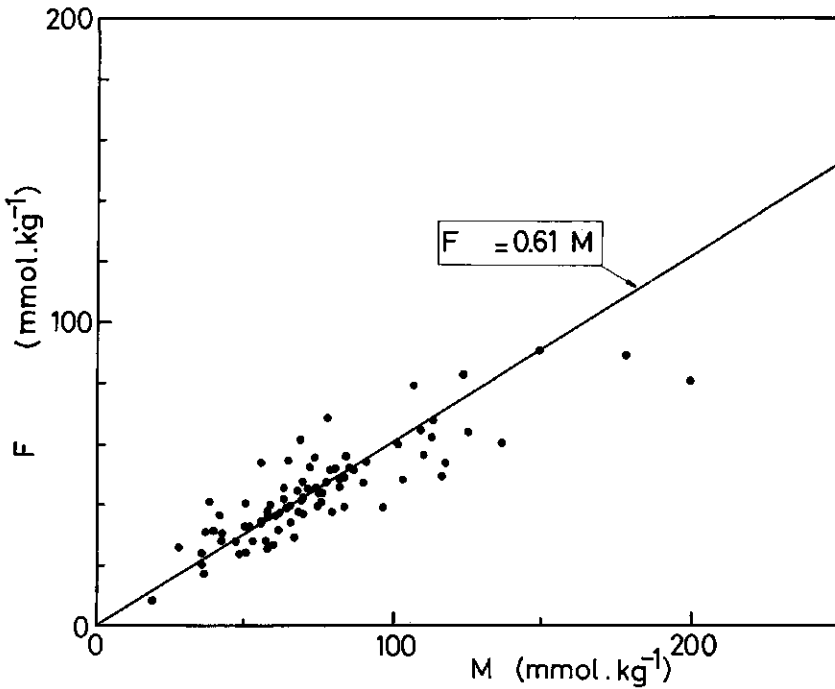


Figure 3: Total sorption, F , for 249 days reaction time as a function of the sum M of oxalate extractable Fe and Al for topsoil samples. Line corresponds to $\alpha = 0.61$.

These differences in k -values are not attributed to the different concentrations used in the sorption experiments for the topsoils and the subsoils. The concentration dependence of k was assumed negligible as it was shown for a number of different soils that sorption for each soil separately may be effectively described by relations such as eq. (4) for a much wider range of concentrations ($0.05 - 5 \text{ mmol L}^{-1}$) [Van Riemsdijk et al., 1984b, Van der Zee et al., 1986, and Van der Zee and Van Riemsdijk 1986a]. It is also worthwhile to observe that Van Riemsdijk et al. [1984b], found different parameter values in their polynomial function relating F to I for two layers ($0-0.2 \text{ m}$ and $0.3-0.5 \text{ m}$ depth) from one profile. Therefore, it is likely that one unique value of k is not realistic. Instead due to differences between soils or horizons in the relative contributions of Fe and Al to M, organic matter content, redox potential etc. the k -value also differs. This assumption is supported by the maximal value α_m estimated by Van Der Zee and Van Riemsdijk [1986b] for the topsoil in a single field: $\alpha_m = 0.53 \pm 0.07$. If this value found for one year reaction time and concentration $c = 3 \text{ mmol L}^{-1}$ is corrected to the I -value corresponding to experiment d, we find that it is within a standard deviation of $\alpha = 0.61 \pm 0.13$. The standard deviation for the closely related samples of Van Der Zee and Van Riemsdijk [1986b] is much smaller than for the heterogeneous population (peaty, sandy and clayey soils) considered here. Hence, we may conclude that their ensemble constitutes a subpopulation of the 84 soils and that their results agree with the results obtained here. A closer inspection of the data showed that no smaller standard deviations result for α or k if different soil types are distinguished. For closely related samples e.g. from the same field, the variation was smaller than for the whole ensemble of 84 soils. The standard deviations of the k -values of the subsoil samples (Table 2) are relatively large. This may be due to the differences in the soil profiles. For some profiles the layer $0.3-0.5 \text{ m}$ exhibits topsoil characteristics (anthropogenic cover), whereas in other cases the material is from the C-horizon.

As the mean values of k are comparable for experiments a and d, the mean predicted long term sorption using the data of experiment a will be good. This is seen in Fig. 4 where for the topsoils α for a reaction time of 249 days at $c = 5 \text{ mmol L}^{-1}$ is predicted and compared

with the measured value of α . The same conclusion holds for the subsoil samples. It is obvious that two-day sorption experiments with an automated set-up [Van Riemsdijk and Van Der Linden, 1984] are preferred over less reproducible, long term batch experiments. Therefore, the applicability of extrapolation of two day sorption experiments to longer times is of interest. In Fig. 5., the measured α -values for experiments a-d are shown for the topsoils as a function of $\ln(I)$ (eq. 7). Also shown is the curve described by eq. (5). Except for experiment b the long term batch experiments are well in agreement with each other. Noteworthy is the negligible part of I_0 in I at the long term (exp. d). A shortcoming of the model (eq. 5) is that α is unbounded as $I \rightarrow \infty$. This is not considered serious

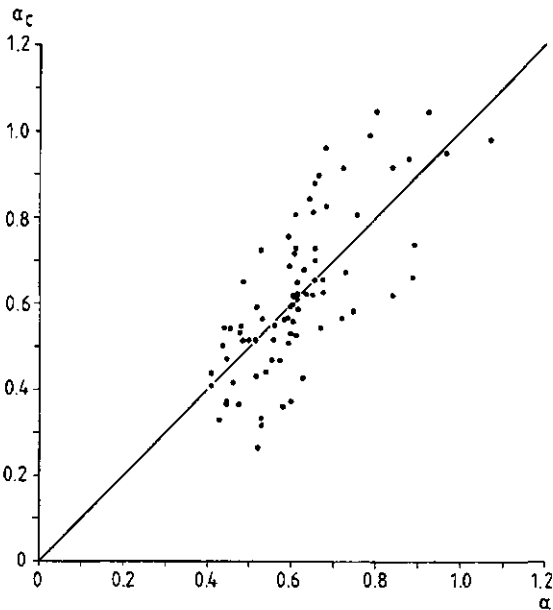


Fig. 4: Calculated α -value, α_c , for topsoil samples as a function of measured α at reaction time of 249 days (exp. d). Values of I_0 and k to calculate α_c found from exp. a and measured α from eq. (6).

due to the extremely small sorption rates at high I . However, it necessitates an operational definition of the sorption maximum, F_m . Thus consider a time t_1 and a time $t_2 = nt_1$ (where $n > 1$). Now we define $\alpha_m = F_m/M = \alpha(t_1)$ such that it satisfies

$$\alpha(t_2) - \alpha(t_1) < f \alpha(t_1) \quad (10)$$

where f is a designated fraction e.g. 0.01 or 0.05.

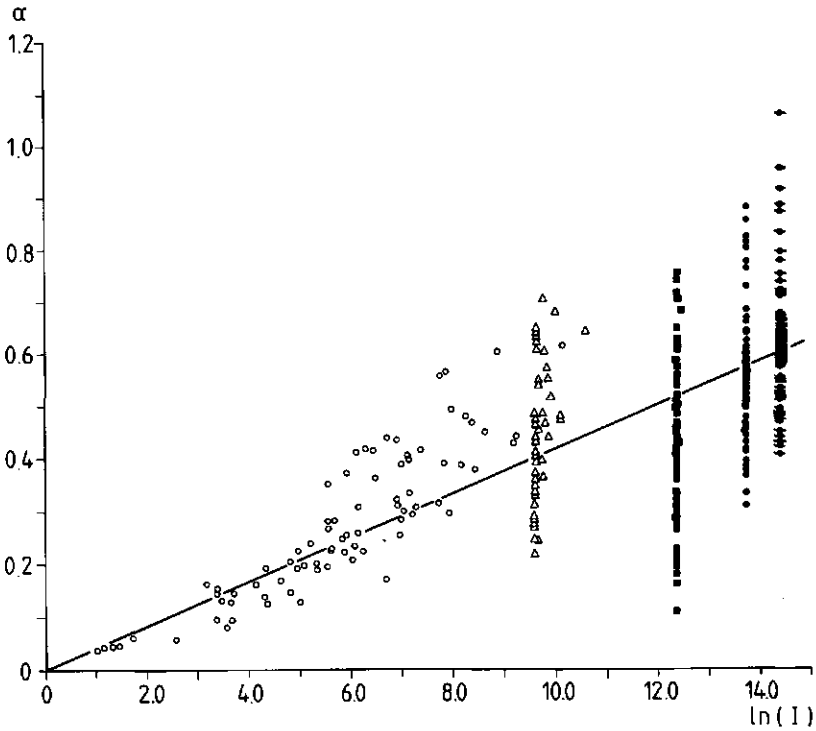


Fig. 5: Measured α (eq. 6) as a function of $\ln(I)$ for topsoils as sampled (α_0 : o) and after laboratory reaction times of 40 hours (Δ), 32 days (\blacksquare), 129 days (\bullet) and 249 days (\blacklozenge). Values of I_0 and k used are based on α found for experiment a.

This may be rewritten using eq. (5) as

$$ct_1 > n^{1/f} \quad (11)$$

where time is in the units for which eqs. (2)-(5) hold (i.e., minutes) and assuming that the reaction occurs at $c = 1-3 \text{ mmol L}^{-1}$ (De Haan and Van Riemsdijk, 1986). Setting $n \approx 2$ which corresponds to doubling the reaction time and $f = 0.05$, then $t_1 \approx 2$ years. On a logarithmic scale this leads to a constant factor of approximately 1.8 to extrapolate α of a 40 hours sorption experiment to α_m at 2 years reaction time. It follows from the negligible contribution of I_0 in I at long reaction times (Fig. 5) that the error by not accounting for I_0 is insignificant if a factor of 1.8 is used (i.e., $F_m = P_{ox} + 1.8 F_r$).

An independent test of the simple model is to compare total sorption (\hat{F}) for a reaction time of 249 days that is calculated using the k -value found for experiment a with measured total sorption $F = P_{ox} + F_r$ of experiment d. This is done in Fig. 6. We see that although individual samples may show significant differences the whole ensemble is predicted very well. This is reflected also by the α -values corresponding to \hat{F} (with $\alpha = 0.64 \pm 0.17$) and F (with $\alpha = 0.61 \pm 0.13$) which are not significantly different at the 5% level. In recent developments to model large scale systems generally the whole ensemble is of interest instead of individual samples [Warrick et al., 1977, Dagan and Bresler, 1979, Elabd et al., 1986, Van der Zee and Van Riemsdijk, 1986b]. In such cases the processes are described using stochastic theory, and the system yields a distributed response instead of one definite (single valued) result. It is essential that frequency distributions are employed instead of deterministic average values for the input of such stochastic models. Thus, both the average and the variance and shape of the distribution are used and reflected in the model output. The use of distributions is preferred especially if a large part of the variances is not due to experimental inaccuracy but should be attributed to heterogeneity. Examples of such heterogeneous variables influencing the system behaviour are the contents of organic carbon, clay minerals and soil moisture regime [De Haan et al., 1987].

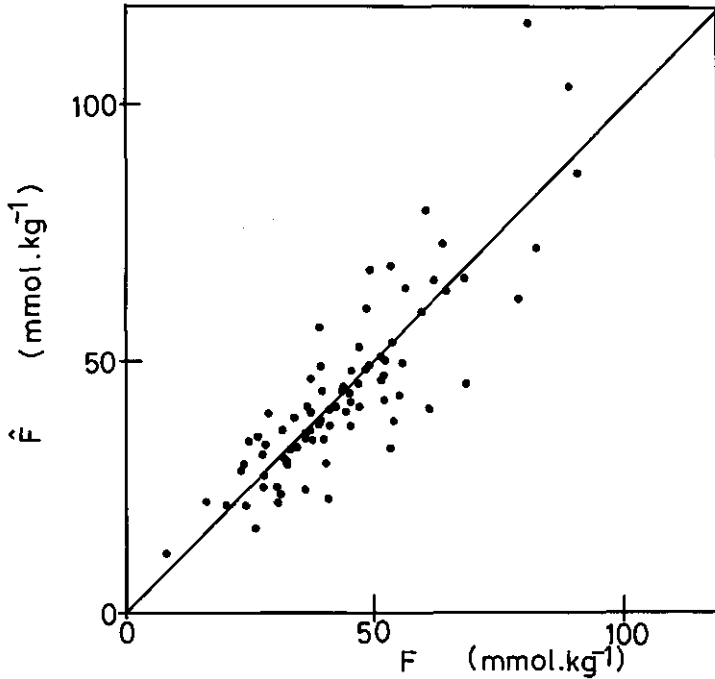


Fig. 6: Total sorption after 249 days laboratory reaction time calculated with average k , \hat{F} , as a function of measured sorption, F , using eq. (12b).

For such an approach, sophisticated microscopic descriptions requiring much input that is difficult to assess are of limited use. In the situation considered here concerning field or regional scale P-accumulation and displacement caused by extreme animal manure applications to soil, the number of samples clearly limits the sophistication of data assessment in the laboratory [Van der Zee and Van Riemsdijk, 1986b]. The proposed model for long term sorption that may be summarized as

$$F = k M \ln (I) \tag{12a}$$

$$F_m = \alpha M_m = (P_{ox} + 1.8 F_r) \tag{12b}$$

where F_r is sorption after 40 hours, combines great simplicity (conceptual and with regard to data assessment) to compatibility with more complex mechanistic models.

6.5 Conclusions

1. For the soils studied P_{OX} is a good approximation of total P.
2. The conclusion by Beek (1979) that P is predominantly associated to oxalate extractable fractions of Fe and Al is valid for the soils studied.
3. Reaction capacity (F_m) is proportional to the sum (M) of oxalate extractable Fe and Al. The proportionality factor (α) is both concentration and time dependent.
4. Extrapolation of sorption measured in 40 hours to 2 year reaction time (same concentration) may be done by multiplication with a factor of 1.8. Adding P_{OX} yields total sorption where a correction for different initial conditions with respect to I is not necessary.
5. Extrapolation of sorption for an ensemble of soils using the relation $F = kM \ln(I)$ with the ensemble averaged k-value found from short term (40 hours) sorption experiments leads to an accurate estimate of long term (249 days) sorption.
6. A maximal value $\alpha_m = 0.63 \pm 0.14$ is obtained, if the sorption measurements are extrapolated for the topsoils to reaction time of 2 years at $c = 3 \text{ mmol L}^{-1}$. $\approx 3 \text{ mol/m}^3$

(249 days)

ACKNOWLEDGEMENT: We thank M.M. Nederlof for assistance with the calculations.

6.6 Notation

a^*	sorption rate constants
a_1, a_2	
c	concentration
c_r	concentration unit reference
f	acceptable fractional change in α

F	total sorption (Q + S)
F_r	total sorption minus initially sorbed P (P_{ox})
\hat{F}	total sorption estimated with ensemble averaged k and eq. (12a)
I	concentration time integral
I_m	maximum of I - domain covered
I_0	I-value corresponding to α_0
I_r	I-value corresponding to F_r/M
k	reactivity constant
M	sum oxalate extractable Fe and Al
n	constant
Q	reversible adsorption
S	irreversible sorption (precipitation)
t	time
t_a	integration constant, time with S = 0
t_r	time unit reference
α	fractional P-saturation constant
α_m	α -value at P-saturation
α_0	P_{ox}/M
γ	α/α_0

6.7 References

- Barrow, N.J., A mechanistic model for describing the sorption and desorption of phosphate by soil. *J. Soil Sci.* 34: 733-750, 1983.
- Barrow, N.J., and I.C. Shaw, The slow reaction between soil and anions: 5. Effects of period of prior contact on the desorption of phosphate from soils. *Soil Science* 119, 311-320, 1975.
- Beek, J., Phosphate retention by soil in relation to waste disposal. PhD thesis, Agricultural University, Wageningen, 1979.
- Beek, J., and W.H. van Riemsdijk, Interactions of orthophosphate ions with soil. In: *Soil Chemistry B, Physico-Chemical Models* (Ed. G.H. Bolt). Elsevier Sci. Publ. Co., Amsterdam, pp. 259-284, 1982.
- Castro, G.L., and D.E. Rolston, Organic Phosphate transport and hydrolysis in soil. Theoretical and experimental evaluation. *Soil Sci. Soc. Am. J.* 41: 1085-1092, 1977.

- Dagan, G., and E. Bresler, Solute dispersion in unsaturated heterogeneous soil at field scale: I Theory. *Soil Sc. Soc. of Am. Journal* 43: 461-467, 1979.
- De Haan, F.A.M. and W.H. van Riemsdijk, Behaviour of inorganic contaminants in Soil. In: *Contaminated Soil* (J.W. Assink and W.J. van den Brink, eds.) Martinus Nijhoff Publ., Dordrecht, pp 19-32, 1986.
- De Haan, F.A.M., S.E.A.T.M. van der Zee, and W.H. van Riemsdijk, The role of soil chemistry and soil physics in protecting soil quality; variability in sorption and transport of Cd as an example. *Netherlands Journal of Agricultural Science* (in press), 1987.
- De Willigen, P., P.A.C. Raats and R.G. Gerritse, Transport and fixation of phosphate in acid, homogeneous soils, II Computer simulation. *Agriculture and Environment* 7: 161-174, 1982.
- Elabd, H., W.A. Jury and M.M. Uliath, Spatial variability of pesticide adsorption parameters. *Environ. Sci. Technol.* 20 (3): 256-260, 1986.
- Enfield, C.G., T. Phan, D.M. Wolters and R. Ellis, Jr., Kinetic model for phosphate transport and transformation in calcareous soils, I and II. *Soil Sci. Soc. Am. Journal* 45: 1059-1064; 1064-1070, 1981.
- Gerritse, R.G., Mobility of phosphorus from pig slurry in soils. In: *Phosphorus in sewage sludge and animal waste slurries*. (Hucker, T.W.G. and G. Catroux, eds.). D. Reidel Publ. Co., Dordrecht, the Netherlands, pp. 347-366, 1980.
- Gerritse, R.G., Phosphorus compounds in pig slurry and their retention in the soil. In: *Utilization of manure by land spreading*. (Voorburg, ed.). CEC publication EUR 5672e: 257-277, 1977.
- Gerritse, R.G., P. de Willigen and P.A.C. Raats, Transport and fixation of phosphate in acid, homogeneous soils, III Experimental case study of acid sandy soil columns heavily treated with pig slurry. *Agric. and Environment* 7: 175-185, 1982.
- Kurmies, B., Zur Fraktionierung der Bodenphosphaten (with English summary). *Die Phosphorsäure*, 29: 118-151, 1972.
- Logan, T.J. and E.O. Mc Lean, Effects of phosphorus application rate, soil properties and leaching mode on ³²P movement in soil columns. *Soil. Sci. Soc. Am. Proc.* 37: 371-374, 1973.

- Mansell, R.A., P.J. McKenna, E. Flaig and M. Hall, Phosphate movement in columns of sandy soil from a wastewater-irrigated site. *Soil Sci.* 140 (1): 59-68, 1985.
- Mansell, R.S., H.M. Selim, and J.G.A. Fiskell, Simulated transformations and transport of phosphorus in soil. *Soil Sci.* 124: 102-109, 1977b.
- Mansell, R.S., H.M. Selim, P. Kanchanasut, J.M. Davidson, and J.G.A. Fiskell, Experimental and simulated transport of phosphorus through sandy soil. *Water Resour. Res.* 13: 189-194, 1977a.
- Munns, D.N. and R.L. Fox, The slow reaction which continues after phosphate adsorption: kinetics and equilibrium in some tropical soils. *Soil Sci. Soc. Am. J.* 40: 46-51, 1976.
- Murphy, J., and J.P. Riley, A modified single solution method for the determination of phosphate in natural waters. *Analytica Chimica Acta*, 27: 31-36, 1962.
- Raats, P.A.C., P. de Willigen, and R.G. Gerritse, Transport and fixation of phosphate in acid, homogeneous soils, I Physico-mathematical model. *Agric. and Environment* 7: 149-160, 1982.
- Ryden, J.C., Syers, J.K. and Harris, R.F., Phosphorus in run off and streams. *Advances in Agronomy*, 25: 1-45, 1973.
- Schwertmann, U., Differenzierung der Eisenoxiden des Bodens durch Extraction mit Ammoniumoxalaat Lösung. *Zeitschrift für Pflanzenernährung, Düngung und Bodenkunde*, 105: 194-202, 1964.
- Van Riemsdijk, W.H., L.J.M. Boumans and F.A.M. de Haan, Phosphate sorption by soils, I A diffusion-precipitation model for the reaction of phosphate with metal oxides in soil. *Soil Sci. Soc. Am. Journal* 48: 537-541, 1984a.
- Van Riemsdijk, W.H., and F.A.M. de Haan, Sorption kinetics of phosphate with an acid sandy soil, using the phosphatostat method. *Soil Sci. Soc. Am. Journal*, 45: 261-266, 1981.
- Van Riemsdijk, W.H., and A.M.A. van der Linden, Phosphate sorption by soils, II Sorption measurement Technique. *Soil Sci. Soc. Am. Journal*, 48: 541-545, 1984.
- Van Riemsdijk, W.H., A.M.A. Van Der Linden, and L.J.M. Boumans, Phosphate sorption by soils, III. The P. diffusion-precipitation model tested for three acid sandy soils. *Soil Sci. Soc. Am. Journal*, 48: 545-548, 1984b.

- Van Der Zee, S.E.A.T.M. and W.H. van Riemsdijk, orption kinetics and transport of phosphate in sandy soil. *Geoderma* 38: 293-309, 1986a.
- Van der Zee, S.E.A.T.M. and W.H. van Riemsdijk, Transport of phosphate in a heterogeneous field. *Transport in Porous Media* 1: 339-359, 1986b.
- Van der Zee, S.E.A.T.M., W.H. van Riemsdijk, and F.A.M. de Haan, Reaction kinetics and transport of phosphate: parameter assessment and modelling. In: *Contaminated Soil* (J.W. Assink and W.J. van den Brink, eds.), Martinus Nijhoff Publ., Dordrecht, pp 157-160, 1986.
- Warrick, A.W., G.J. Mullen, and D.R. Nielsen, Scaling field-measured soil hydraulic properties using a similar media concept. *Water Resour. Res.* 13 (2): 355-362, 1977.
- White, R.E., Pathways of phosphorus in soil. In: *Phosphorus in sewage sludge and animal waste slurries*. (T.W.G. Hucker and G. Catroux, eds.), D. Reidel Publ. Co., Dordrecht, pp. 21-44, 1981.

7. SPATIAL VARIABILITY OF PHOSPHATE ADSORPTION PARAMETERS AND EFFECT ON LONG TERM LEACHING

Abstract

Reversible phosphate (P) adsorption for acid soils with a narrow pH-range is described with the Langmuir kinetics equation. The adsorption equilibrium is given by the Langmuir equation. Using a combination of two experimental desorption techniques, i.e., desorption in water and desorption in the presence of an "infinite" sink for P respectively, the adsorption maximum (Q_m) and the adsorption constant (K) can be assessed for soils (pre-)saturated with P. The adsorption maximum is proportional with the sum of oxalate extractable iron and aluminium (M) i.e., $Q_m \approx 0.135 M$, for topsoil samples from a field as well as for topsoil samples from a watershed. The K-values found for the field and for the watershed samples were in the same order of magnitude ($K = 15-25 \text{ m}^3 \cdot \text{mol}^{-1}$). In view of experimental accuracy it is justified to conclude that the adsorption maximum and the adsorption constant, as well as the amounts of P desorbed with the two techniques, are spatially variable properties. These properties appear to be distributed normally as well as lognormally, using the Kolmogorov-Smirnov test statistic, at the significance level of 1% and 5% (β_m , Q_m , K).

With an analytical approximation, that relates the thickness of the P-saturated topsoil layer with the maximum leached concentration, the effect of spatial variability is shown. With the experimental analysis and data analysis discussed, the variability and uncertainty in the adsorption maximum and adsorption constant can be specified in a routine fashion for large numbers of samples.

7.1 Introduction

In the Netherlands government regulations were issued that prohibit excessive animal manure slurries disposal on soil that is saturated with phosphate (P). This was considered necessary in order

to prevent future surface water eutrophication due to leaching of P present in the animal manure. However, part of the phosphate that has accumulated in soil is adsorbed reversibly and may thus be mobilized after manure disposal (exceeding uptake by plants) is stopped [Beek, 1979; Van Der Zee and Van Riemsdijk, 1986a]. Therefore the assessment of the reversibly sorbed fraction and of the P desorption behaviour are of interest from the scope of environmental concern.

Much work has been done with respect to the reaction of P with soil, its kinetics and the reversibility of this reaction. It was found that the reaction depends among others on the pH, P concentration, and the amount sorbed [Beek and Van Riemsdijk, 1982; Goldberg and Sposito, 1984]. Furthermore sorption-desorption hysteresis was observed, i.e., at time scales comparable with the sorption time only a fraction of previously sorbed P is able to desorb [Beek, 1979; Barrow, 1979]. For gibbsite it was shown by Van Riemsdijk and Lyklema [1980] that sorption in excess of monolayer coverage may occur. Observations, as mentioned here, have caused several researchers to believe that to consistently describe the overall reaction, more than one process has to be distinguished at the macroscopical (soil sample scale) level. It was proposed by Van Riemsdijk [1979], Enfield et al. [1981a,b], Barrow [1983], Van Riemsdijk et al. [1984], and Van Der Zee and Van Riemsdijk [1986a] that the overall reaction consists of a relatively fast, reversible adsorption and a relatively slow, practically irreversible diffusion type process. Where the different models for the diffusion type process are conceptually different, consensus existed that the reversible adsorption equilibrium may be described with the Langmuir equation or with electrostatic models [Van Riemsdijk, 1979; Barrow et al., 1981; Enfield et al., 1981a,b]. However, the assessment of the Langmuir parameters may be complicated by the occurrence of the diffusion type process. To solve this problem Enfield et al. [1981a,b] assumed that adsorption is practically finished before the diffusion process becomes of importance. Barrow [1983] assessed the parameters of both processes by fitting all the model equations simultaneously to the sorption data. Assuming that both processes occur simultaneously and that the diffusion type process is practically irreversible, Van Der Zee and Van Riemsdijk [1986a] estimated the adsorption parameters

by fitting model equations to desorption data. The diffusion type process was considered to be a precipitation of phosphates. Because the solubility of metal phosphate precipitates is usually small and dissolution kinetics are often slow the assumption of irreversibility for the diffusion process was considered acceptable. However, as the precipitation reaction may proceed during desorption experiments [Munns and Fox, 1976; Barrow, 1979], presaturation of soil with P or the application of a high affinity-high capacity sink for soil-P is required [Van Der Zee and Van Riemsdijk, 1986a; Van Der Zee et al., 1987]. Applying such a sink [Van Der Zee et al., 1987a] found that the reversibly adsorbed fraction rarely exceeded one third of total soil-P in soils not previously saturated with P.

In this study we apply two desorption techniques to soil samples with a P content as sampled and to soil samples presaturated with P. These samples were obtained from a single field and from a watershed. By combination of the data acquired the adsorption maximum and the adsorption constant may be estimated. Besides the mean values of these parameters also their variability is of interest due to the intrinsic heterogeneity of soil. In calculations of P-leaching in the field this heterogeneity may be taken into consideration if the probability density functions (PDF) of relevant parameters are known [Van Der Zee and Van Riemsdijk, 1987]. Hence, for the two regions studied the PDF's of the parameters are given.

7.2 Theory

To describe the adsorption of P by soils and soil minerals models differing in complexity and versatility were proposed. Multicomponent electrostatic models were given by Bowden et al. [1977], Barrow et al. [1981], Sigg and Stumm [1981], Bolt and Van Riemsdijk [1982], and Goldberg and Sposito [1984a,b]. Such models incorporate the effects of P-concentration, pH and electrolyte composition on the equilibrium distribution of P over the solution and the solid-solution interface. Barrow et al. [1981] have extended such a model for the description of adsorption-desorption kinetics.

We intend to describe adsorption-desorption in a narrow pH-range

for acid soils in which case P-adsorption is not very dependent on pH [Van Riemsdijk and Van Der Zee, 1986b]. Hence a simpler approach is feasible and the adsorption process is described by:

$$\frac{dQ}{dt} = k_a c(Q_m - Q) - k_d Q \quad (1)$$

At equilibrium, equation (1) may be rearranged into the Langmuir equation:

$$Q = \frac{K Q_m c}{1 + Kc} \quad (2)$$

where $K=k_a/k_d$, is the adsorption constant. To assess the amount reversibly adsorbed (Q) the equilibrium described by equation (2) is perturbed. When the effect of the precipitation is forced to be negligible by pre-saturation of the soil with phosphate then this process does not affect the desorption process. As an "infinite sink" for P is brought into a soil suspension, P will desorb from the soil and adsorb on the sink. With an "infinite sink" we refer to a material that has such an affinity and capacity for P-sorption that the build-up of a P-concentration in the solution is negligible. Van der Zee et al. [1987a] showed that their P-sink consisting of iron oxide coated filterpaper qualifies for the prefix "infinite". In a case of desorption using this sink the conditions apply that

$$t=0 \quad Q=Q_0 \quad c=c_0 \quad (3a)$$

$$t>0 \quad Q=Q(t) \quad c=0 \quad (3b)$$

and equation (1) becomes

$$\frac{dQ}{dt} = -k_d Q \quad (4)$$

Equation (4) is integrated for conditions (3) and setting $Q^*=Q_0-Q(t)$ this yields

$$Q^*(t)=Q_0 \{1-\exp(-k_d t)\} \quad (5)$$

It was shown by Van Der Zee et al. [1987a] that if a sufficient amount

of the sink of oxide paper is applied (4 paperstrips/gram soil) the exponential term in equation (5) has become negligible after 20 h desorption time. Hence in that case $Q^*(t > 20) = Q_0$.

If desorption is enticed by dilution of the soil suspension with water according to the P_w -method of Sissingh [1971] the concentration does not become zero. Instead an equation for the conservation of mass links the concentration change in solution to the amount desorbed. Using the notation of Van Der Zee et al. [1987a] we find

$$\frac{dc}{dt} = -R^* \frac{dQ}{dt} \quad (6)$$

where $R^* = 0.001 R$, and R is the solid/solution ratio in $\text{kg} \cdot \text{m}^{-3}$. The factor 0.001 is due to the units used for c ($\text{mol} \cdot \text{m}^{-3}$) and Q ($\text{mmol} \cdot \text{kg}^{-1}$). Equation (6) may be integrated to

$$-c(t) = R^* [Q(t) - Q_0] \quad (7)$$

Combination of equations (1) and (7) and integration yields an expression for the concentration [Van Der Zee et al., 1987a]. At equilibrium an expression for c is found that may also be obtained directly from the conservation of mass (equation 7) and the Langmuir equation, and is given by

$$c = \frac{1}{2} \{ (c_3 - K^{-1}) + [c_3^2 + K^{-2} + 2(c_3 + 2Q_m R^*) K^{-1}]^{\frac{1}{2}} \} \quad (7a)$$

where c_3 is given by Van der Zee et al. [1987a] as

$$c_3 = (Q_0 - Q_m) R^* \quad (7b)$$

Hence, the desorbed amount equals

$$Q^* = c / R^* \quad (8)$$

Combination of equations (7) and (8) results in

$$Q^* = \frac{1}{2} \{ (c_3 - K^{-1}) + [c_3^2 + K^{-2} + 2(c_3 + 2Q_m R^*) K^{-1}]^{\frac{1}{2}} \} / R^* \quad (9)$$

By simple manipulations with equation (9) we may derive an explicit equation for the adsorption constant, K:

$$K = (Q_0 - Q^*) / \{R^* Q^* [Q_m + Q^* - Q_0]\} \quad (10)$$

With the considerations presented so far the framework to assess the adsorption parameters is given. The parameters of interest are Q_0 , Q_m , and K. Also the amount desorbed for a designated value of R^* , i.e., Q^* , needs to be known to assess K. We assume that the amount desorbed with the "infinite" sink, of samples not presaturated with P, equals Q_0 . For P-presaturated samples the amount desorbed with this method yields $Q=Q_m$. The amount Q^* in equation (10) is assessed by desorption of pre-saturated samples according to the method of Sissingh [1971], where $R=20 \text{ kg.L}^{-1}$, i.e., $R^*=0.02$.

The laboratory procedure to presaturate soil samples with P and desorbing P with the two techniques is time demanding. Therefore it is of interest to use the information obtained to relate the values of Q_m and K to soil properties that may be measured cheaply and in a routine fashion. Such relationships may be used for other regions to estimate potential desorption. Soil properties that may be of use are the oxalate extractable contents of Fe and Al, as it was shown by Beek [1979], Van Der Zee and Van Riemsdijk [1986c, 1988] and Van Der Zee et al. [1987a], that the pseudo sorption maximum (F_m) of the over all reaction is proportional to the sum M of oxalate extractable Fe and Al. Assuming that such a proportionality exists also for the adsorption maximum, Q_m , i.e. the surface-volume ratio of the reactive solid phases for different soils is assumed to be approximately constant, we define

$$\beta_m = Q_m / M \quad (11)$$

For a few practically P-saturated samples Van Der Zee et al. [1987a] found a value of $\beta_m \approx 0.2$.

In an earlier study Van Der Zee and Van Riemsdijk [1986c] observed that M and the amount of P applied to soil in animal manure slurries were spatially variable properties. They showed that it is important to take this heterogeneity into account in calculations of P-

displacement in a field, which may be done using stochastic theory. In their description of P-displacement they considered not only the mean values of relevant properties but the whole PDF, assuming normal distributions. For a normally distributed variable, X, the PDF is given by

$$f_X = \frac{1}{s_X \sqrt{2\pi}} \exp \left[-\left(\frac{X - m_X}{s_X} \right)^2 \right], \quad -\infty < X < \infty \quad (12)$$

Clearly this PDF is not the most logical one, even if it describes the variability well, as the relevant properties (e.g. Q_m, M, K) cannot become negative in reality. Hence it is more realistic to assume a lognormal PDF. For a lognormally distributed variable Y equal to $\exp(X)$ the PDF is given by

$$f_Y = \frac{1}{Y s_X \sqrt{2\pi}} \exp \left[-\left(\frac{\ln Y - m_X}{s_X} \right)^2 \right], \quad 0 < Y < \infty \quad (13)$$

It was shown by Simmons [1981] that if $CV\{Y\}$ equal to s_Y/m_Y is small little differences exist in the shape of a lognormal or the corresponding normal PDF. Hence approximately normally distributed variables may also be assumed lognormally distributed (Appendix C).

7.3 Materials and methods

Soil was sampled in a 6 ha. field and a 800 ha. watershed, encompassing this field, in the vicinity of St. Oedenrode, the Netherlands. At 101 locations on four transects in the field and 51 locations on a regular grid (0.4 x 0.4 km) in the watershed soil samples were taken to 1 m depth or until groundwater was reached. In this study only the topsoil (0-0.2 m) was used. Sampling and pretreatment of the samples were described by Van Der Zee and Van Riemsdijk [1986b]. In the laboratory the oxalate extractable contents of P, Fe and Al were measured [Van Der Zee and Van Riemsdijk, 1988]. Presaturation was done with a solution containing 4 mol $\text{KH}_2\text{PO}_4 \text{ m}^{-3}$, 2 mol $\text{KCl} \text{ m}^{-3}$, and 1.5 mol $\text{CaCl}_2 \text{ m}^{-3}$ during 10 days (in batch). The amount of soil was 7g or 10 g depending on the observed decrease of concentration which was at most 1 mol $\text{P} \cdot \text{m}^{-3}$. Desorption of samples

with P-content as sampled and of presaturated samples was done according to both the P_w -method of Sissingh [1971] and the P_t -method.

The distributions were tested with the Kolmogorov-Smirnov test statistic [Rubinstein, 1981]. Using the values obtained for the mean and standard deviation of X ($=\ln(Y)$) the theoretical value of the cumulative probability of each value X_t ($i=1, \dots, 101$ for the field; $i=1, \dots, 51$ for the region) was calculated with

$$\Pr \{X < X_t\} = \frac{1}{\sqrt{2}\pi} \int_{-\infty}^{(X - m_X)/s_X} \exp(-Z^2/2) dZ \quad (14)$$

Also the observed probability

$$\tilde{\Pr} \{X < X_t\} = i/(N + 1) \quad (15)$$

was calculated for the sorted monotonically increasing data set of variable X. The test statistic KS is given by $KS = |\Pr - \tilde{\Pr}|$. At the significance level 0.01, KS for each realization should be smaller than 0.223 (N=51) and 0.160 (N=101). At the significance level of 0.05 these values are 0.187 (N=51) and 0.134 (N=101) [Owen, 1962].

7.4 Results and discussion

Preliminary experiments indicated that for samples with low P-content analytical reproducibility of the P_w -method (CV= 0.17 for P_w) was predominantly limited by errors in the measured P-concentration (CV=0.14). Differences in soil sample weight (CV=0.012) were usually much smaller for this method based on soil-volume [Sissingh, 1971]. The "infinite sink" method yielded more reproducible results (CV=0.06) due to the higher accuracy at low P-contents. In Table 1 the statistics of some variables are given for the field and for the watershed. These data indicate that on average the P-content (F_0) in the field is larger than in the watershed. It was shown by Van der Zee and Van Riemsdijk [1988] that the degree of saturation of soil with P may be expressed with the ratio $\alpha = F/M$. Here F is the total amount of P sorbed to the soil. It was also shown that this amount F may be assessed with the oxalate extractable amount according to Van der Zee and Van Riemsdijk [1988].

Table 1: Statistics of soil properties and normality of the distributions. *: 0.01 significance, **: 0.05 significance

variable X	mean m_X	standard deviation s_X	variation coefficient CV(X)	normal PDF
field				
M	81.0	12.4	0.15	**
F_0	22.9	6.3	0.28	**
α_0	0.29	0.08	0.28	**
α_{10}	0.44	0.07	0.16	**
watershed				
M	68.6	21.9	0.32	**
F_0	13.9	7.6	0.55	**
α_0	0.20	0.11	0.55	**
α_{10}	0.38	0.09	0.24	*

The degree of P-saturation (α_0) for the field appears to be also higher than for the watershed. Furthermore for all four variables the differences (see CV) in the watershed are larger than for the field.

For the field, where the soil was classified as a spodosol at each sampling location, the variability in M is pronounced [Van Der Zee and Van Riemsdijk, 1986c]. Comparing the statistics (m and s) of M for the field and the watershed we find that we may consider the field to be a subpopulation of the watershed.

Table 2: Statistics of desorption - variables and normality of distributions. *: 0.01 significance; **: 0.05 significance

X	FIELD				WATERSHED			
	m_X	s_X	CV _X	normal	m_X	s_X	CV _X	normal
P_w^u	0.0509	0.249	0.49	**	0.313	0.242	0.77	*
P_w^s	4.613	0.775	0.17	**	3.520	0.976	0.28	**
P_f^u	3.549	1.319	0.37	**	2.186	1.565	0.72	**
P_f^s	10.859	1.495	0.14	**	9.041	2.450	0.27	**
β_m	0.134	0.023	0.25	**	0.135	0.034	0.25	**
K	16.3	8.6	0.53	**	24.8	12.6	0.51	**

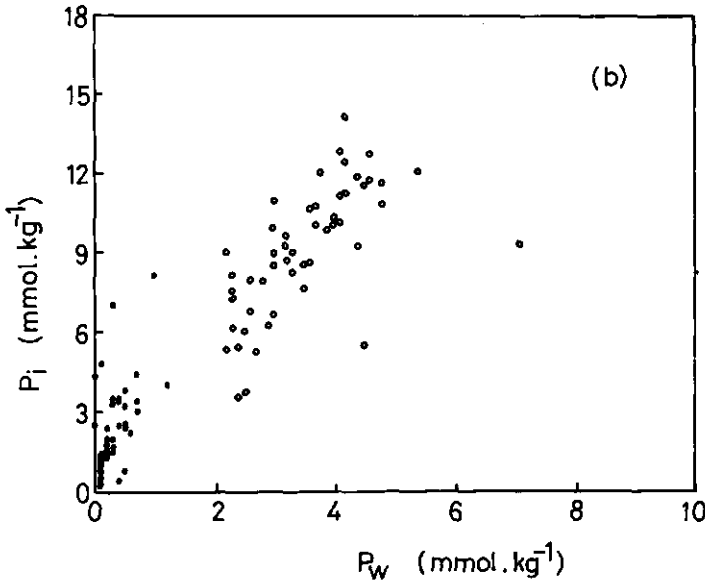
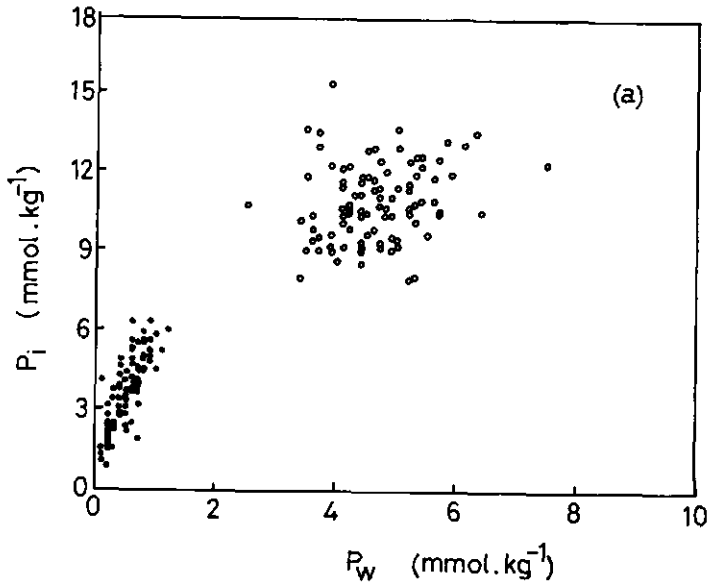


Figure 1 : Desorbed amount using the P_i -method as a function of the desorbed amount using the P_w -method. Presaturated samples (\circ) and samples with phosphate contents as sampled (\bullet).
Fig. 1a: Field; Fig.1b: Watershed.

Although the mean values differ, the PDF(M) for the field falls well within the PDF(M) for the watershed, as the mean plus one standard deviation in both cases are approximately the same. The variability of both F_0 and α_0 is larger for the watershed than for the field. This may be understood qualitatively as different fields, e.g. from different farmers, will have received different quantities of animal manure. Thus in woodland (5 locations) no disposal of slurry occurs and therefore the variation in F_0 and α_0 will be in part due to the low values found for the locations in woodland. In Table 2 the statistics are presented for the desorbed amounts as well as some model parameters. The amount desorbed with the P_i -method is larger than with the P_w -method, which is to be expected [Van Der Zee et al., 1987a]. The desorbed amounts found with the two methods are compared in Figure 1. The correlation between P_i and P_w is considered reasonably good for both the region and the watershed. Also the curvilinear relation between P_i and P_w predicted by Van Der Zee et al [1987a] was found.

Assuming that P_i^S gives a good impression of the adsorption maximum (P-presaturated samples) according to equation (11) a linear relation can be expected between P_i and M. In Figure 2 the P_i^S -values are given as a function of M for both the field and the watershed. In both cases P_i^S is proportional with M. The mean values for the constant β_m are surprisingly close for the two systems studied (Table 2; $\beta_m \approx 0.135$). Apparently significant differences in other variables than M, such as content and nature of organic matter, pH, and soil type hardly affect the relation between P_i^S (i.e., Q_m) and M. By comparison of β_m to α_{10} (which gives the degree of saturation, F/M, after ten days reaction time) we find that one third of solid phase P is adsorbed reversibly. As the value of α will increase somewhat when the presaturation period is longer [Van der Zee and Van Riemsdijk, 1988] the adsorption capacity is actually less than one third of the total sorption capacity.

In Table 2 also the statistics of the adsorption constant, K, are given. The value of K was assessed, assuming desorption equilibrium if use is made of the P_w -method, by means of equation [10].

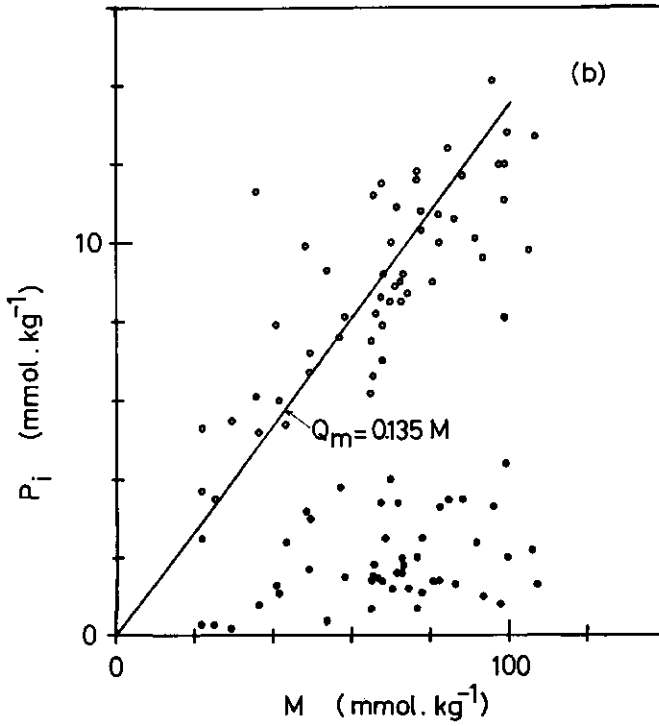
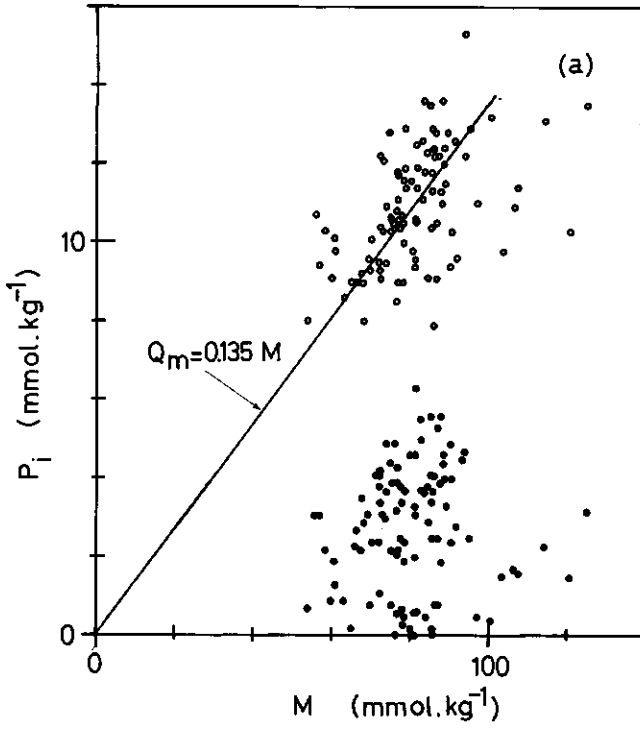


Figure 2:
 P_i as a function
of M . P-presat-
urated samples:
(o) as sampled:
(●). 2a: field,
2b: watershed

Different statistics are found for K for the field and the watershed, although the range found for the field is almost within the range for the watershed. Some differences for K, which is a parameter incorporating e.g. microscopic heterogeneity and pH effects, found for soil samples with different compositions may, however, be expected. A slight correlation between K and M was found (0.025 significance) for the field : $K=0.22M^{-0.41}$ ($r=0.253$). If we compare the K-values with the value obtained for goethite ($K > 200 \text{ m}^3\text{mol}^{-1}$ at pH 6, Van der Zee et al., 1987) we see that it is significantly smaller. Besides differences of the reactive oxide surfaces compared to goethite, this may be caused by competition effects, etc., of e.g. adsorbed silicate [Bolt and Van Riemsdijk, 1982]. The K-values were in the same range as those given by Van der Zee and Van Riemsdijk [1986a].

From the results compiled in Tables 1 and 2 it has become clear that a range of values of the variables is found. In any case the variability in the variables M, F_0 (where F_0 is related to the amount of P applied) and K, is not due only to experimental error but also to spatial variability of soil. Thus, in describing P-displacement and redistribution of P present in soil this variability should be taken into account, e.g. in a way as described by Van Der Zee and Van Riemsdijk [1986c, 1987] and De Haan et al., [1987]. To do so the PDF of important variables should be known and for this reason the distributions of the variables were tested for normality and lognormality. The results of these tests are given in Tables 1-3. It appears that all variables can be described with a normal as well as a lognormal PDF. Some variables appeared to be very well lognormally distributed. For the field the probability plots of M, P_1^S (representing Q_m), β_m , and K are given in Figure 3a-3d. As was mentioned in the theory-section a lognormal PDF is more logical to use than the normal PDF as in that case no negative values are possible. With the proposed methods to assess K and Q_m for a large number of soil samples the distribution of these variables can be determined. This is important because of the significant effect of spatial variability on P-transport and redistribution in the soil profile.

This may be illustrated by considering a homogeneous column with length L and with a sharp P-front at a depth (z_p) of e.g. 0.2 m [Van der Zee and Van Riemsdijk, 1986c]. For depths smaller than $z_p = 0.2 \text{ m}$

the concentration in solution may be as large as 3 mol.m^{-3} . This value is a thousand fold higher than $\tilde{c} = 1-3 \text{ mmol.m}^{-3}$, where \tilde{c} is the lower concentration level above which eutrophication in surface water may occur. When excessive manure disposal is stopped the reversibly adsorbed P in the topsoil ($z < z_p$) may desorb and be leached beyond $z_p = 0.2 \text{ m}$, where sorption may occur. This gives rise to a new P-front moving into the subsoil, that has a steadily decreasing maximum concentration. At some time this maximum concentration will reach the phreatic water level at $z=L$. If we aim at preventing P-leaching losses to the groundwater, that in due time might cause a eutrophication hazard in the surface water, we might require that the concentration at $z=L$ never exceeds \tilde{c} . When at large redistribution times $c=3 \text{ mmol.m}^{-3}$ at the phreatic water level, and $c=0$ at the surface we may approximate the concentration distribution with

Table 3: Statistics of logtransformed soil properties ($Y=\exp(X)$) and normality of distributions.

Y	FIELD				WATERSHED			
	m_X	s_X	CV(X)	normal	m_X	s_X	CV(X)	normal
M	4.383	0.151	0.034	**	4.164	0.390	0.094	*
F_0	3.082	0.331	0.107	**	2.389	0.878	0.368	*
α_0	-1.301	0.325	-0.250	**	-1.775	0.668	-0.376	**
α_{10}	-0.843	0.188	-0.223	*	-1.006	0.240	-0.239	**
P_W^U	-0.836	0.574	-0.687	*	-1.443	0.681	-0.472	**
P_W^S	1.515	0.168	0.111	**	1.223	0.268	0.219	**
P_i^U	1.184	0.436	0.368	**	0.545	0.765	1.404	**
P_i^S	2.376	0.138	0.058	**	2.159	0.309	0.143	**
β_m	-2.003	0.189	-0.094	**	-2.005	0.190	-0.095	**
K	2.683	0.469	0.17	**	3.063	0.618	0.20	**

*: 0.01 significance; **: 0.05 significance

depth as increasing linearly with increasing z as is shown in Chapter 10. Because of the almost linear adsorption isotherm at such low concentrations we may then assume that on average $\tilde{c} \approx 2 \text{ mmol.m}^{-3}$ in the subsoil. The desorbed amount in the topsoil is then equal to

$$q_1 = \rho z_p (Q_m - \tilde{Q}) \quad (16)$$

where \tilde{Q} is the adsorbed amount at concentration \tilde{c} (equation 2). This amount should be balanced by the amount that can be stored in the subsoil, at $c = \tilde{c}$ if no concentrations exceeding \tilde{c} are allowed to pass the depth $z = L$.

Let us assume that the metal content M in the subsoil is different from the metal content in the topsoil, and that the total sorption in the subsoil is always equal to a few (γ) times the adsorbed amount (e.g. $\gamma = 3$, as $\alpha_{10} = 3 \beta_m$, see also Van Der Zee and Van Riemsdijk [1988], Van Der Zee et al. [1987a]). thus we choose

$$\gamma = \alpha_m / \beta_m \quad (17)$$

$$\epsilon = Q_m^2 / Q_m^1 \quad (18)$$

$$\tilde{Q}^2 = \epsilon \tilde{Q}^1 \quad (19)$$

where α_m is the degree of P-saturation as defined by Van Der Zee and Van Riemsdijk [1988], Q_m^2 is the subsoil adsorption maximum, and \tilde{Q}^2 is the adsorbed amount at $c = \tilde{c}$ in the subsoil. The superscript 1 refers to the topsoil. Hence, at an average concentration of \tilde{c} in the subsoil the storage equals

$$q_2 = \gamma \rho (L - z_p) \epsilon \tilde{Q} \quad (20)$$

where the relatively small storage in the liquid phase is neglected. If we equate q_1 and q_2 (eqs. 16, 20) we find the value z_p may have, such that the concentration at the phreatic water level becomes at maximum 3 mmol.m^{-3} after some long redistribution time. This constraint for z_p is

$$z_p = \gamma \epsilon L \tilde{Q} / [Q_m + \tilde{Q} (\gamma \epsilon - 1)] \quad (21)$$

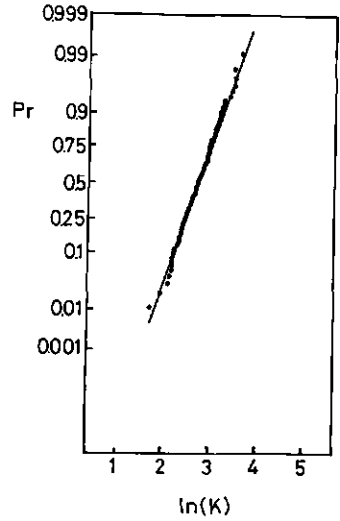
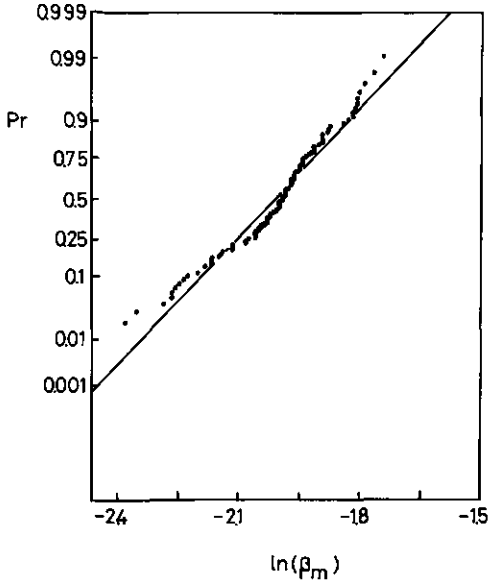
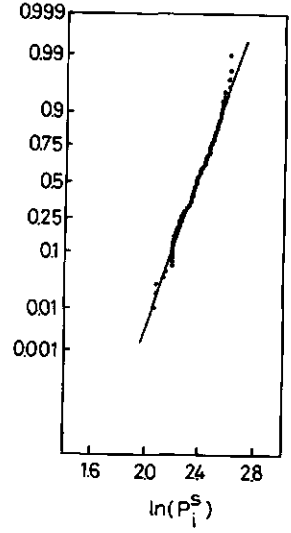
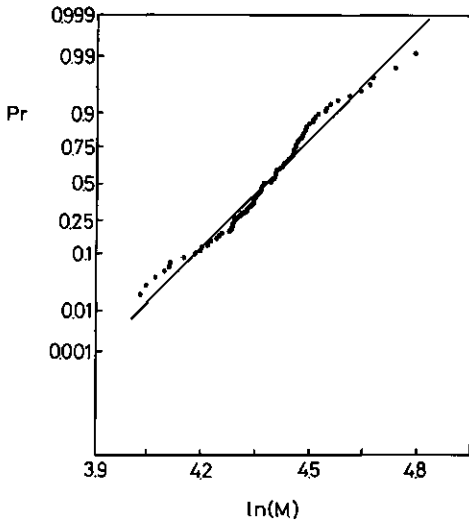


Figure 3: Cumulative probability plots for M (Fig.3a), P_1^B (Fig.3b), β_m (Fig.3c), and K (Fig.3d).

After insertion of equation (2) for \tilde{Q} this yields

$$z_p = LK\tilde{c}\gamma\epsilon / [1 + K\tilde{c}\gamma\epsilon] \quad (22)$$

For a soil column with M , Q_m , etc. uniform with depth (i.e., $\epsilon = 1$) and K equal to $45 \text{ m}^3 \cdot \text{mol}^{-1}$, we find that $\tilde{Q} = 0.08 Q_m$. Hence, equation (21) results in $z_p = 0.08\gamma L / (0.92 + 0.08\gamma) = 0.21 L$ or 21 cm if $L = 1 \text{ m}$, and $\gamma = 3$. Therefore if z_p is smaller than 20 cm the concentration at the phreatic level at 1 m depth will never exceed $2-3 \text{ mmol} \cdot \text{m}^{-3}$. However, we have seen that K may differ with place as it is a spatially variable property. Therefore, at another location in a field K may be e.g. $15 \text{ m}^3 \cdot \text{mol}^{-1}$. As in that case \tilde{Q} is equal to $0.03 Q_m$ we have $z_p = 0.08L$ (eq.21). Due to this variability in K , concentrations exceeding $2-3 \text{ mmol} \cdot \text{m}^{-3}$ may pass the phreatic water level, even if $0.08L < z_p < 0.2L$. At concentrations smaller than $2-3 \text{ mmol} \cdot \text{m}^{-3}$ where we have almost linear adsorption, i.e., $K\tilde{c}\gamma\epsilon < 1$ and with $\gamma < 3$, the dependency of the constraint of z_p on K may be derived from a simplified form of equation (22)

$$z_p \approx \gamma\epsilon K\tilde{c}L \quad (23)$$

which is a manageable expression to evaluate the tolerable saturation of a soil column (z_p) if the eutrophication hazard by P-leaching has to be negligible.

As equations (22) and (23) show, the value of Q_m is not important as Q_m was eliminated from these equations. This surprising result does not mean, however, that in practical situations the assessment of an average of Q_m value for a field will lead to satisfying results. In many cases the metal content M and therefore the adsorption maximum change as a function of depth (Van Der Zee and Van Riemsdijk, 1986c), due to pedogenesis. Such changes are reflected in values of ϵ differing from unity. Clearly such differences have a similar effect on the tolerable value of z_p as the effect of K . In Chapter 10 it is shown, that due to ϵ -values different from unity the rate of the redistribution process may be accelerated or decelerated significantly. Moreover, for a field the metal content and the adsorption maximum of the topsoil may, or may not, be correlated with

M and Q_m of the subsoil. Qualitatively one can imagine that it makes much difference (for a uniform z_p -value throughout the field) whether a topsoil with large Q_m is underlain by a subsoil with low Q_m , or a subsoil with equal or even larger Q_m (eq. 23: the value of ϵ is smaller, equal, or larger than unity, respectively). To assess the heterogeneity in Q_m for different soil layers and the correlation structure between different layers obviously requires a large number of samples. The methods proposed in this paper to assess K in a routine fashion and to assess Q_m directly, or indirectly from M using equation (11), may therefore be useful to evaluate P-redistribution and the hazard of P-leaching past the phreatic water level.

7.5 Conclusions

1. Variability in soil parameters is larger for the watershed than for the field.
2. More P desorbs with the use of the ironoxide impregnated paper (P_i) desorption method than with the conventional (P_w) dilution method. The correlation between the amounts desorbed with these two methods is good.
3. The amount desorbed with the P_i method is proportional to M for the P-saturated samples. The average proportionality factor β_m in $P_i^S = \beta_m M$ equals 0.134 ± 0.023 for the field and 0.135 ± 0.034 for the watershed samples. Assuming that P_i^S represents a fair estimation of Q_m this relation can be used to estimate Q_m from the routinely measurable value of M.
4. The value of the adsorption constant, K, was $K=16.3 \pm 8.6 \text{ m}^3 \cdot \text{mol}^{-1}$ for the field and $K=24.8 \pm 12.6 \text{ m}^3 \cdot \text{mol}^{-1}$ for the watershed.
5. All parameters considered were distributed normally as well as lognormally at the 1% significance level and most parameters also at the 5% significance level. In view of analytical accuracy, variability should at least partly be attributed to the variability of the soil.
6. For long distribution times P initially present in the topsoil may be leached past the phreatic water level. The concentrations that will pass this level depend strongly on the value of K and the

value of Q_m as a function of depth. The approach to assess the values of Q_m and K makes it possible to find the distributions of these parameters for large numbers of samples. This facilitates a risk analysis of P-leaching taking spatial variability of P-adsorption into account.

7.6 Notation

c	concentration in solution ($\text{mol}\cdot\text{m}^{-3}$)
\tilde{c}	eutrophication threshold concentration ($\text{mol}\cdot\text{m}^{-3}$)
CV	coefficient of variation
f	frequency distribution
F	sorbed amount of P, adsorption plus precipitation ($\text{mmol}\cdot\text{kg}^{-1}$) F_0 : sorbed amount for soil as sampled
i	number of occurrence in sorted, monotonically increasing series
K	adsorption constant ($\text{m}^3\cdot\text{mol}^{-1}$)
k_a	adsorption rate constant ($\text{m}^3\cdot\text{mol}^{-1}\cdot\text{h}^{-1}$)
k_d	desorption rate constant (h^{-1})
L	column length; depth phreatic water level (m)
\bar{m}	arithmetic mean
M	oxalate extractable metals (Fe + Al)
N	number of samples
P_i	desorbed phosphate using infinite sink ($\text{mmol}\cdot\text{kg}^{-1}$)
P_w	desorbed phosphate in water ($\text{mmol}\cdot\text{kg}^{-1}$)
Pr	probability
q_i	Amount of phosphate in layer i ($i=1$: topsoil, $i=2$: subsoil) ($\text{mmol}\cdot\text{m}^{-2}$)
Q	adsorbed amount ($\text{mmol}\cdot\text{kg}^{-1}$)
Q_m	adsorption maximum ($\text{mmol}\cdot\text{kg}^{-1}$)
Q^*, Q_0	desorbed and initially adsorbed amount ($\text{mmol}\cdot\text{kg}^{-1}$)
\tilde{Q}	adsorbed amount at $c=\tilde{c}$ ($\text{mmol}\cdot\text{kg}^{-1}$)
r	correlation coefficient
R	solid:solution ratio ($\text{kg}\cdot\text{L}^{-1}$), $R^*=0.001R$, in ($\text{kg}\cdot\text{m}^{-3}$)
s	standard deviation
t	time (hour)
X, Y	generic notations normally and lognormally distributed

variable.

- z_p thickness of P-saturated topsoil layer (m)
 α ratio of sorbed P over M
 α_0, α_{10} ratio α for soil as sampled and after 10 days reaction time at $c \approx 3 \text{ mol.m}^{-3}$
 β_m maximum ratio of adsorbed P over M
 γ ratio of total sorption over reversible adsorption
 ϵ ratio of subsoil adsorption maximum over topsoil adsorption maximum

7.7 References

- Barrow, N.J. The description of desorption of phosphate from soil. *J. Soil Sci.* 30: 259-270, 1979.
- Barrow, N.J. A mechanistic model for describing the sorption and desorption of phosphate by soil. *J. Soil Sci.*, 34: 733-750, 1983.
- Barrow, N.J., L. Madrid, and A.M. Posner. A partial model of adsorption and desorption of phosphate by Goethite. *J. Soil Sci.* 32: 399-407, 1981.
- Beek, J. Phosphate retention by soil in relation to waste disposal. Ph.D. thesis, Agricultural University Wageningen, 1979.
- Beek, J., and W.H. van Riemsdijk. Interactions of orthophosphate ions with soil. In: G.H. Bolt (Editor) *Soil Chemistry B. Physico-Chemical Models*. Elsevier, Amsterdam: 285-348, 1982.
- Bowden, J.W., A.M. Posner, and J.P. Quirk. Ionic adsorption on variable charge mineral surfaces. Theoretical charge development and titration curves. *Aust. J. Soil Res.*, 15: 121-136, 1972.
- Bolt, G.H., and W.H. van Riemsdijk. Ion adsorption on inorganic variable charge constituents. In: G.H. Bolt (Editor) *Soil Chemistry B. Physico-Chemical Models*. Elsevier, Amsterdam, 1982.
- De Haan, F.A.M., S.E.A.T.M. van der Zee, and W.H. van Riemsdijk. The role of soil chemistry and soil physics in soil protection research. *Neth. J. Agric. Sci.* (in press), 1987.
- Enfield, C.G., T. Phan, D.M. Walters, and R. Ellis, Jr. Kinetic model for phosphate transport and transformation in calcareous soils I. *Soil Sci. Soc. Am. J.*, 45: 1059-1064, 1981a.

- Enfield, C.G., T. Phan, D.M. Walters, and R. Ellis, Jr. Kinetic model for phosphate transport and transformation in calcareous soils II. Soil Sci. Soc. Am. J. 45: 1064-1070, 1981b.
- Goldberg, S., and G. Sposito. A chemical model of phosphate adsorption by soils: I Reference oxide minerals. Soil Sci. Soc. Am. J. 48: 772-778, 1984a.
- Goldberg, S., and G. Sposito. A chemical model of phosphate adsorption by soils: II Noncalcareous soils. Soil Sci. Soc. Am. J. 48: 779-783, 1984b.
- Munns, D.N., and R.L. Fox. The slow reaction which continues after phosphate sorption: kinetics and equilibrium in some tropical soils. Soil Sci. Soc. Am. Proc., 40: 46-51, 1976.
- Owen, D.B. Handbook of statistical tables. Addison Wesley Publ. Co., London, 1962.
- Rubinstein, R.Y. Simulation and the Monte Carlo method. Wiley, New York, 1981.
- Sigg, L., and W. Stumm. The interaction of anions and weak acids with the hydrous goethite (α -FeOOH) surface. Colloids Surfaces, 2: 101-117, 1981.
- Simmons, C.S. A stochastic-convective transport representation of dispersion in one dimensional porous media systems. Water Resour. Res. 18 (4), 1193-1214, 1981.
- Sissingh, H.A. Analytical procedure of the P_w -method, used for the assessment of the phosphate status of arable soils in the Netherlands. Plant and Soil, 34: 483-486, 1971.
- Van Der Zee, S.E.A.T.M., and W.H. van Riemsdijk. Sorption kinetics and transport of phosphate in sandy soil. Geoderma 38: 293-309, 1986a.
- Van Der Zee, S.E.A.T.M., and W.H. van Riemsdijk. Model for the reaction kinetics of phosphate with oxides and soil. Proceedings Conf. 'Interactions at the soil-colloid soil solution interface', August 24-29, 1986, Ghent Belgium (in press), 1986b.
- Van Der Zee, S.E.A.T.M., and W.H. van Riemsdijk. Transport of phosphate in a heterogeneous field. Transp. Porous Media. 1: 339-359, 1986c.
- Van Der Zee, S.E.A.T.M. and W.H. van Riemsdijk. Transport of reactive solute in spatially variable soil systems. Water Resour. Res. (in press), 1987.

- Van Der Zee, S.E.A.T.M., L.G.J. Fokkink, and W.H. van Riemsdijk. A new technique for assessment of reversibly adsorbed phosphate. *Soil Sci. Soc. Am. J.* 51: 599-604, 1987a.
- Van Der Zee, S.E.A.T.M., and W.H. van Riemsdijk. Model for long term phosphate reaction kinetics in soils. *J. Environm. Qual.*, 1988.
- Van der Zee, S.E.A.T.M., W.H. van Riemsdijk, Th.M. Lexmond and F.A.M. de Haan, Vulnerability in relation to physico-chemical compound behaviour, and spatially variable soil properties. In: *Vulnerability of soil and groundwater to pollutants*, (W. van Duyvenboden and H.G. van Wageningen, eds.), TNO Committee on Hydrological research, 11, Proceedings and Information, no 38:515-526, 1987b.
- Van Riemsdijk, W.H. Reaction mechanisms of phosphate with $Al(OH)_3$ and a sandy soil. Ph.D. thesis, Agricultural University Wageningen, 1979.
- Van Riemsdijk, W.H., and J. Lyklema. Reaction of phosphate with gibbsite, $Al(OH)_3$, beyond the adsorption maximum. *J. Colloid Interf. Sci.* 76: 55-66, 1980.
- Van Riemsdijk, W.H., L.J.M. Boumans, and F.A.M. de Haan. Phosphate sorption by soils. I. A diffusion-precipitation model for the reaction of phosphate with metal oxides in soil. *Soil Sci. Soc. Am. J.* 48: 541-544, 1984.

8. TRANSPORT OF PHOSPHATE IN A HETEROGENEOUS FIELD

Abstract

A model for the transport of P in an ensemble of vertical homogeneous columns is given. For a single column the dimensionless concentration of P sorbed to the solid phase, Γ , as a function of dimensionless depth, is approximated with a piston profile. The velocity of the P-front within a column depends on the application rate of P and the retention capacity of the soil. For a field, represented by an ensemble of columns differing with respect to P applied (A_T) and retention capacity (F_T), the field average dimensionless concentration $\langle \Gamma \rangle$, at fixed depth and time, is related to A_T and F_T using probability theory. F_T and A_T are expressed in terms of easily measured variables: oxalate extractable P and Fe+Al. With the probability density functions of these random variables the field-averaged profile is calculated. Experimental and computed profiles are reasonably in agreement and differences can be explained by assuming correlation of F_T and A_T . A sensitivity analysis shows the increase in field-scale dispersion if the coefficients of variation of the random variables are increased. Negative correlation of A_T and F_T or a positive correlation of successive applications A_i cause an increase in field-scale dispersion. Trends observed for A_T and F_T must be taken into consideration if the model is used for predictive purposes.

8.1 Introduction

In areas with intensive animal husbandry the animal slurries derived from this activity are generally disposed of by application onto land in agricultural use. Thus large quantities of phosphate (P) present in the slurries are applied to the soil system. The excess with respect to crop uptake is subject to accumulation in the soil due to the reaction with the soil matrix, and to displacement in the soil solution towards the groundwater. In The Netherlands, the intensive

animal husbandry is mainly found in regions with sandy soils. Transport of P towards the surface water may eventually create a eutrophication problem. As P mobility in soils is mainly controlled by the interaction with the soil matrix, the reaction of P with soil and soil minerals has received much attention [for a review see Beek and Van Riemsdijk, 1982]. In non-calcareous sandy soils the reaction of P involves predominantly the amorphous fraction of the oxides of aluminum (Al) and iron (Fe) [Beek, 1979]. This reaction is generally a non-equilibrium and only partially reversible process that depends, amongst others, on the concentrations of P in solution and in the solid phase, and the pH [Raats et al., 1982; Barrow, 1983; Van Riemsdijk et al., 1984]. Recently the (overall) reaction was described by Enfield et al. [1981], Barrow [1983] and Van der Zee and Van Riemsdijk [1986] with two processes, i.e. adsorption and a diffusion-type process. The chemical model was combined with a transport model by Van der Zee et al. [1986], Enfield et al. [1981] and Gerritse et al. [1982] to predict the transport of P in columns. The results show that these nonequilibrium sorption models combined with transport yield acceptable results.

In general, however, the transport of P in the field is of prime interest. To account for the increased heterogeneity found in undisturbed soil columns, the dispersivity is often given a larger value, [e.g. Gerritse et al., 1982; Beek, 1979]. Whereas the transport in an undisturbed column in the field may be described accurately assuming deterministic values for the parameters, this is not always the case if the average process in a field is considered. It was shown by e.g. Biggar and Nielsen [1976] that soil hydraulic properties vary in space. Due to the random nature of the variation of the soil hydraulic variables in three-dimensional space, an accurate deterministic assessment of these variables and the deterministic modelling of transport are impractical, if at all possible. However, if the average behaviour in the flow domain is of interest then the description may be based on probability theory.

For a conservative solute, taking into account the stochastic nature of the variables, the transport was described by e.g. Bresler and Dagan [1979; 1981; 1983], Dagan and Bresler [1979], Amoozegar-Fard et al. [1982]. The stochastic nature is reflected by the use of probability density functions for the random variables.

For the pore water velocity a lognormal distribution was found by e.g. Nielsen et al. [1973], Biggar and Nielsen [1976] and Peck [1977]. Using the lognormal distribution Dagan and Bresler [1979] and Bresler and Dagan [1979] evaluated the probability that the field averaged concentration at a specified depth and time does not exceed a certain value assuming that the unsaturated flow was steady state and neglecting pore scale dispersion. With this probability they calculated the field averaged profile of solute, and showed the non-Fickian behaviour of the field dispersion process. In their later papers Bresler and Dagan [1981, 1983] included pore scale dispersion and transient water flow. Another approach was given by Jury [1982] and tested in the field by Jury et al. [1982]. Assuming the transport to a specified depth to be a random function of the cumulative infiltration, a travel time probability function results. This function was fitted for a particular depth and subsequently used for predictive purposes. Although the model was derived for a single column it may also be used for situations as considered by Bresler and Dagan [1979].

So far the stochastic modelling was mainly limited to non-reacting solutes. However, most potentially hazardous contaminants are in fact moderately to highly reactive. Jury [1983] illustrated the large effect of the coefficient of correlation between the random retardation factor and the random water velocity on transport.

The scope of this study is to describe a model for the field averaged displacement of orthophosphate (P). The sorption chemistry and transport are described in a simplified manner for a single column. This leads to a piston-shaped profile of sorbed P. The profile is then expressed in terms of variables, that can be measured in the laboratory in a routine fashion. The field is assumed to consist of an ensemble of columns that do not interact. Considering the retention capacity and the input of P as random variables an expression for the field averaged profile of sorbed P is given. With experimental data, the statistics of the random variables are estimated and the profile computed with these statistics is compared with the experimentally assessed profile. To our knowledge a comparison of a stochastic transport model for a reactive contaminant with field data has not been done previously. Finally the effects of the different statistics

on the computed profile are shown and the validity of some of the assumptions is discussed.

8.2 Transport at the column scale

Solute transport in porous media may occur by convection and by dispersion. Neglecting production terms and if only vertical transport occurs then the convection dispersion equation may be written as:

$$\frac{\partial}{\partial t} [\rho_s F + \theta c] = \frac{\partial}{\partial z} \left[D \frac{\partial c}{\partial z} \right] - \frac{\partial}{\partial z} [\theta v c] \quad (1)$$

(for symbols: see 8.11). The dispersion coefficient, D , incorporates both molecular diffusion and mechanical dispersion. The local concentration of solute in the solid phase, F , is the sum of the adsorption, Q , which is described with the Langmuir isotherm [Enfield et al., 1981; Barrow, 1983; Van der Zee et al., 1986] and the precipitated amount, S , which is described according to Van Riemsdijk et al. [1984] and Van der Zee and Van Riemsdijk, [1986]. Whereas Q is an equilibrium process at water velocities realistic in the field, S may be a non-equilibrium process.

It is assumed that the column is physically and chemically homogeneous and that water flow is steady state. The function F was shown to be highly nonlinear in both c (for the input concentration considered here) and time [Enfield et al., 1981; Van der Zee et al., 1986]. As the sorption is of the high affinity type, the effects of sorption and dispersion counter each other [Bolt, 1982]. Thus for a homogeneous column a relatively sharp front will develop if a constant concentration at the column entrance is imposed. This sharp front will be propagated through the column with a velocity controlled mainly by the retardation factor (belonging to the concentration-increment imposed) and by the water velocity. As the thickness of the front is relatively small with respect to the column length [Beek, 1979], it is not unreasonable to neglect dispersion altogether. Then equation (1) simplifies to

$$\rho_s \frac{\partial F}{\partial t} + \theta \frac{\partial c}{\partial t} = -\theta v \frac{\partial c}{\partial z} \quad (2)$$

With regard to the water velocities occurring in the field situation, the approximation of local sorption equilibrium is made [De Willigen et al., 1982]. Furthermore the initial concentration in the column is taken zero. In real situations the concentration of P at the surface will be controlled by the dissolution of solid P present in the slurries. De Haan and Van Riemsdijk [1985] showed that this concentration is buffered at the value $c_0 \approx 3000 \text{ mmol/m}^3$. After all the solid P is dissolved (time t^*) the concentration will decrease and this leads to the boundary condition (t_1 is the period of time of one sorption-desorption cycle)

$$0 < t < t_1 \quad z = 0 \quad c = c_0 H(t^* - t) \quad (3)$$

with the Heaviside step function $H(\epsilon) = 0$ for $\epsilon < 0$ and $H(\epsilon) = 1$ for $\epsilon > 0$. Note that t^* depends on the water velocity i.e. the percolated volume of water. It is assumed that the plateau of the isotherm is reached for c values much smaller than c_0 . Moreover since the isotherm is of the high affinity type, during desorption for $t^* < t < t_1$, c is buffered at values much smaller than c_0 [Van der Zee and Van Riemsdijk, 1986].

Whereas c will thus vary in time throughout the entire column ($z > 0$), for F this is only the case at the front. Solving equation (2) for $0 < t < t_1$ yields

$$F = F(c_0) H\left(\frac{vt}{R} - z\right) \quad (4)$$

where the retardation factor R is given by

$$R = 1 + \rho_s F(c_0)/\theta c_0 \quad (5)$$

For a total time τ equal to Mt_1 the front will be propagated in pulses with a mean velocity \tilde{v} (i.e. averaged over τ) given by

$$\tilde{v} = \frac{v \sum_{i=1}^M t_i^*}{R \tau} \quad (6)$$

Thus the front of P in the solid phase at an arbitrary time t may be approximated with

$$F = F(c_0) H\left(\frac{v}{R} \sum_{i=1}^M t_i^* - z\right) \quad (7)$$

The determination of the sorption capacity $F(c_0)$ is difficult because, on time scales practical in the laboratory the sorption S is non-equilibrium. Long term batch experiments or transport experiments at values of v occurring in the field should be dismissed for routine analysis because of the long duration of the experiments. For routine purposes it is preferable to estimate $F(c_0)$ using relationships with soil properties, that may be measured simply and for large numbers of samples. Such soil properties are the contents of the amorphous oxides of aluminum (Al) and iron (Fe) [Beek, 1979]. These contents may be assessed by extracting soil with acid ammonia oxalate [Schwertmann, 1964]. With this extraction almost all soil-P is extracted for sandy soils. Denoting the oxalate extractable amounts (mmol/kg) by the subscript 'ox' the ratio α is defined as

$$\alpha = P_{ox} / (Fe + Al)_{ox} \quad (8)$$

In soils that received large quantities of animal slurries maximum values of α are approximately 0.5-0.6 (Chapter 6, Lexmond et al., 1982). Lexmond et al. [1982] performed long term (250 days) batch experiments and also sorption measurements at constant concentration as described by Van Riemsdijk and Van der Linden [1984], and found that the amount of P adsorbed in the batch experiments is estimated well by extrapolation of the short term sorption experiments. The extrapolation is done on a logarithmic time scale [Van Riemsdijk and De Haan, 1981]:

$$F \sim \ln(t) \quad (9)$$

The results obtained by De Willigen et al. [1982] support the time of 250 days as the contact time where a pseudo sorption maximum is reached. Denoting the sorption calculated by extrapolation of short

term sorption by P_R , then the maximal value, α_m , is calculated with

$$\alpha_m = P_m / (Fe + Al)_{OX} \quad (10)$$

where $P_m = P_{OX} + P_R$ and sorption is measured at $c = 3000 \text{ mmol P/m}^3$. Due to experimental and model error a range of α_m -values is found. The sorption capacity estimated with the mean, $\bar{\alpha}_m$, is denoted with F_m (i.e., $F(c_0)$ is estimated by $F_m = \bar{\alpha}_m (Fe + Al)_{OX}$).

As mentioned, the value of R is generally high. Consequently the travel times of a phosphate front through initially phosphate free soil will be controlled largely by R and thus, in the case of steady state water flow by F_m . The physical distance is not the best space variable to use in the transport equation as $(Fe + Al)_{OX}$ will generally vary with depth. It is convenient to define a transformed dimensionless space variable weighted to the content $(Fe + Al)_{OX}^z$ (where the superscript z denotes variation in z). First the average content over the total depth L considered of $(Fe + Al)_{OX}^z$ is given by

$$(Fe + Al)_{OX} = \int_0^L \rho_s(z) (Fe + Al)_{OX}^z dz / \int_0^L \rho_s(z) dz \quad (11)$$

Then the transformed space variable, ζ , is defined as:

$$\zeta = \int_0^z \rho_s(z) (Fe + Al)_{OX}^z dz / (Fe + Al)_{OX} \int_0^L \rho_s(z) dz \quad (12)$$

The average value of P_{OX} is given by

$$P_{OX} = \int_0^L \rho_s(z) P_{OX}^z dz / \int_0^L \rho_s(z) dz \quad (13)$$

The total P-fixation capacity of the column, F_T , per unit area and assuming ρ_s constant is:

$$F_T = L \rho_s \bar{\alpha}_m (Fe + Al)_{OX} \quad (14)$$

and the total amount of P applied, A_T , may be expressed as

$$A_T = L \rho_s P_{OX} \quad (15)$$

and also as

$$A_T = v \theta c_0 \sum_{i=1}^M t_i^* \quad (16)$$

Combination of (15) and (16) and rearrangement leads to the relation $P_{ox} = \theta c_0 \sum t_i^* / (L \rho_s)$. Approximating $R \sim \rho_s F_m / \theta c_0$, which is acceptable for large R, equation (7) is rewritten in terms of an equivalent, homogeneous soil column with the dimensionless depth coordinate ζ :

$$F = F_m H\left(\frac{A_T}{F_T} - \zeta\right) \quad (17)$$

With equation (17) the transport in one column is expressed in terms of variables that may be assessed in the laboratory (see equations 14 and 15). Due to differences in $(Fe + Al)_{ox}$ for different columns it is convenient to consider the dimensionless concentration of P in the solid phase, $\Gamma = F/F_m$. The profile in terms of Γ

$$\Gamma = H\left(\frac{A_T}{F_T} - \zeta\right) \quad (18)$$

gives an impression of the saturation of the soil column with P.

One of the assumptions made concerns the time-dependent boundary condition at $z = 0$ (eq. 3), which is different from the conditions used by Dagan and Bresler [1979]. As desorption is small for the case of a high affinity isotherm c will fluctuate much in time for small depths whereas Γ does not, once the front has passed these depths. The fluctuation in c implies a time lag between the moment of application and the arrival of solute at the solid phase concentration front. Consequently the additional assumption was made that the development of the Γ -profile, which occurs in discrete time steps, is evaluated after the annually applied amount has reached the front and reacted with the soil.

8.3 Transport at field scale

In recent studies concerning solute transport on the field scale, the soil hydraulic properties were assumed to be random variables

[e.g. Bresler and Dagan, 1983; 1979; Dagan and Bresler, 1979]. In general all soil properties may be considered random variables, characterized by a probability distribution instead of a single value. For an ensemble of vertical, homogeneous columns the random variable X has an expectation at every point $\xi = (x,y)$ in space

$$E \{X(\xi)\} = m(\xi) \quad (19)$$

and a variance defined as

$$\text{VAR} \{X(\xi)\} = E \{[X(\xi) - m(\xi)]^2\} \quad (20)$$

The covariance for two points ξ_1 and ξ_2 is given by

$$C \{X(\xi_1), X(\xi_2)\} = \{[X(\xi_1) - m(\xi_1)][X(\xi_2) - m(\xi_2)]\} \quad (21)$$

As for each point ξ only one realization is measured, these three moments cannot be estimated due to lack of information. To overcome this problem the hypothesis of ergodicity [Papoulis, 1965] is used. Hence, the moments found for the one realization obtained in the field are equivalent to the moments at each location ξ , i.e., spatial and ensemble averaging are assumed equivalent. Furthermore the hypothesis of statistical homogeneity is used [Gutjahr, 1985]. Then the expectation does not depend on ξ and the covariance depends only on the separation vector $h = \xi_1 - \xi_2$ and the probability density function (PDF) is the same for all locations.

In this study only the two prominent variables A_T and F_T are assumed to be random, leaving e.g. v and α_m to future work (see Chapter 9). Of prime interest is the dimensionless solid phase concentration (Γ) as a function of depth and time. Since Γ is a function of the random variables A_T and F_T , it will be random too. Denoting the PDF for fixed ζ and τ by $f_\Gamma(\zeta, \tau; \Gamma)$ then the distribution function is:

$$\text{Pr}(\zeta, \tau; \Gamma^*) = \int_0^{\Gamma^*} f_\Gamma(\zeta, \tau; \Gamma) d\Gamma \quad (22)$$

which represents the probability that $\Gamma < \Gamma^*$ at the specified ζ and

τ . Note that due to the transformation to ζ , the plane in x and y at a specified ζ is physically not a horizontal plane, as in the case of Bresler and Dagan [1981].

The field average of Γ at depth ζ and time τ is given by the first moment [Bresler and Dagan, 1981]:

$$\langle \Gamma(\zeta, \tau) \rangle = \int_0^1 \Gamma f_{\Gamma}(\zeta, \tau; \Gamma) d\Gamma \quad (23)$$

Equation (23) may be rewritten as

$$\langle \Gamma(\zeta, \tau) \rangle = 1 - \int_0^1 \text{Pr}(\zeta, \tau; \Gamma) d\Gamma \quad (24)$$

and equals the fractional area where the piston profile has passed the depth ζ at time τ . Additional moments are given by Skopp [1984]. As $\Gamma(\zeta, \tau)$ depends on A_T and F_T , in general

$$f_{\Gamma} d\Gamma = f_{A_T, F_T} dA_T dF_T \quad (25)$$

where f_{A_T, F_T} is the joint PDF of A_T and F_T .

Assuming independence of A_T and F_T , as no a priori reasons for a physical dependency between these two variables exist, then f_{A_T, F_T} is equal to $f_{A_T} f_{F_T}$. Hence, equation (22) may be rewritten as

$$\text{Pr}(\zeta, \tau; \Gamma^*) = \int_{[\Gamma^*]} f_{A_T} f_{F_T} dA_T dF_T \quad (26)$$

The domain of integration (Γ^*) covers the domain in A_T and F_T that results in $\Gamma(\zeta, \tau) < \Gamma^*$.

8.4 Materials and methods

Soil was sampled from a field shortly after the harvesting of the crop (corn) just before application of slurries at 67 locations along two transects (see Figure 1). Along transect D soil at 51 locations (every 6 m) was sampled from depths 0-0.2 m, and then with increments of 0.1 m to 1 m depth or until freatic water level. Along transect E soil at 16 locations (every 16 m) was sampled to 1 m depth or until

freatic water level with increments of 0.2 m . At each location soil samples obtained from 4 positions in a square (0.4 m x 0.4 m) were mixed.

In the laboratory air dried subsamples were extracted using acid ammonia oxalate [Schwertmann, 1964] and P_{OX} , Fe_{OX} and Al_{OX} were determined as described by Novozamsky et al., [1986]. On different subsamples at a concentration of 3 mol KH_2PO_4/m^3 with a background electrolyte of 1.5 mol $CaCl_2/m^3$ and 2 mol KCl/m^3 the residual sorption capacity was determined. During 24 hours, 5 g soil was shaken end-over-end in 60 ml electrolyte and c was measured afterwards with the molybdenum-blue method of Murphy and Riley [1962]. Extrapolation on a logarithmic time scale yields P_R .

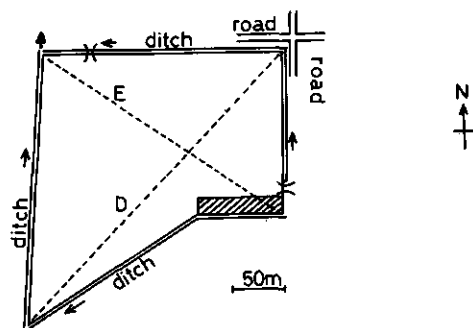


Figure 1: Schematic representation of the field studied

8.5 Calculations

The numerical calculations were done by Monte Carlo simulation, i.e. the result of the transport process for a column is calculated a large number of times, each time using different realizations of the random parameters. These results are used to calculate the sample moments of the transport process in the field (m , σ). Samples of random numbers with a standard normal distribution, required for input, were generated with a manufacturer supplied subroutine package. The distributions were tested using the Kolmogorov-Smirnov test statistic [Rubinstein, 1981], given by the maximal value of $|Pr-\tilde{Pr}|$ in

the sample. Here P_r is the computed cumulative probability of the sorted (monotonically increasing series) sample, i.e., $n/N+1$, where n is the number of appearance in the sorted series and N the maximal number of appearance, the sample size. \tilde{P}_r is the theoretical cumulative probability. The sample was only used if K was less than 1.63, see e.g. Persaud et al., [1985]. With the appropriate values of the statistics the distributions were generated used in the model.

8.6 Results

In Table 1 the statistics m and σ of several variables are given for the depths indicated. Due to the large variation of the groundwater level only results till 0.6 m depth are used. The assumption of homogeneity in depth is clearly not valid. Hence, the transformation of z into ζ in order to construct an equivalent homogeneous column is indeed required.

Table 1: Field averages and standard deviations of variables for three layers. ($N = 67$).

average (mmol/kg)								
z (m)	Fe_{ox}^z	Al_{ox}^z	$(Fe+Al)_{ox}^z$	P_{ox}^z	P_R^z	P_m^z	α_m^z	
0 -0.2	22.5	58.0	80.5	21.6	20.6	42.2	0.53	
0.2-0.4	15.2	61.0	76.2	12.5	22.4	34.9	0.46	
0.4-0.6	4.2	40.6	44.8	1.6	20.8	22.4	0.50	
standard deviation [mmol/kg]								
0 -0.2	7.2	8.8	12.4	5.6	5.0	5.5	0.07	
0.2-0.4	6.9	15.6	17.7	5.0	6.7	9.1	0.07	
0.4-0.6	3.2	20.2	20.2	1.3	10.7	11.5	0.13	

The coefficients of variation ($CV = \sigma/m$) increase with increasing depth. This trend reflects possibly a larger variability at larger depths. However, measurement errors may also be the cause of larger

values of CV, notably for Fe_{Ox} and P_{Ox} with very low mean values. The dispersed profile of P_{Ox} may in part be attributed to agricultural activities (ploughing, mixing up to 0.2-0.3 m depth by heavy machinery, etc.) and to uncertainty due to the sampling layer thickness.

The statistics of some depth-averaged variables are given in Table 2. The coefficient of correlation $\rho(3)$ is only 0.82 and it was noted that the main scatter is due to 5 topsoil samples. The scatter diagram (Figure 2) indicates that most locations conform well to the simplified model. In the following the average value of 0.5 is used for α_m .

For the depth-averaged variables P_{Ox} and $(Fe + Al)_{Ox}$ (used to estimate A_T and F_T), histograms are shown in Figure 3. Also shown are the fitted normal probability density functions (f) given by:

$$f_X = \frac{1}{\sigma_X \sqrt{2\pi}} \exp \left[-\left(\frac{X - \bar{m}_X}{\sigma_X \sqrt{2}} \right)^2 \right] \quad (27)$$

In Figure 4 the field average profile of P is shown in terms of the dimensionless concentration as a function of dimensionless depth. Two experimental profiles are shown, one based on P_m and one based on F_m . Denoting the relative thickness of the P -saturated layer by ζ_p , then

$$\zeta_{p1} = \frac{\int_0^L P_{Ox}^2 dz}{\int_0^L P_m^2 dz} = P_{Ox}/P_m \quad (28)$$

The value of ζ_{p1} is distributed and the probability that $\zeta_{p1} < \zeta^*$ is given by

$$\Pr[\zeta_{p1} < \zeta^*] = \int_0^{\zeta^*} f_{\zeta_{p1}} d\zeta \quad (29)$$

For the piston flow model this expression is equivalent to $\Pr(\zeta, \tau; \Gamma^*)$. Hence, the experimental profile is:

$$\langle \Gamma(\zeta, \tau) \rangle = 1 - \Pr[\zeta_{p1} < \zeta] \quad (30)$$

Likewise the experimental profile based on $\zeta_{p2} = P_{Ox}/F_m$ is obtained. Both profiles are shown in Figure 4 and appear to be slightly different in shape. The mean values of ζ_{p1} and ζ_{p2} are equal (0.36)

and the standard deviations are 0.08 and 0.09, respectively.

Table 2: Field averages and standard deviations of variables averaged with depth (0-0.6 m). Also given the correlation coefficient $\rho(i)$ with $(\text{Fe+Al})_{\text{OX}}$.

i	name	mean (m)	standard deviation (σ)	$\rho(i)$
1	P_{OX}	11.9	3.37	0.59
2	P_{R}	21.3	5.40	0.73
3	P_{m}	33.2	7.22	0.82
4	$(\text{Fe+Al})_{\text{OX}}$	67.2	12.95	
5	α_{m}	0.5	0.07	-0.18

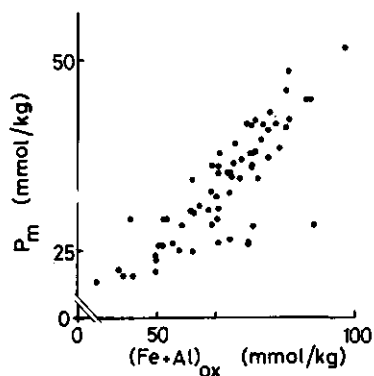


Figure 2: Scatter diagram of P_{m} versus $(\text{Fe+Al})_{\text{OX}}$.

With the statistics of P_{OX} and F_{m} given in Table 2 the field averaged profile may be calculated assuming independent P_{OX} and F_{m} . The results are shown in Figure 4, assuming a normal PDF for F_{m} and P_{OX} . The experimental profiles are steeper than the calculated profiles.

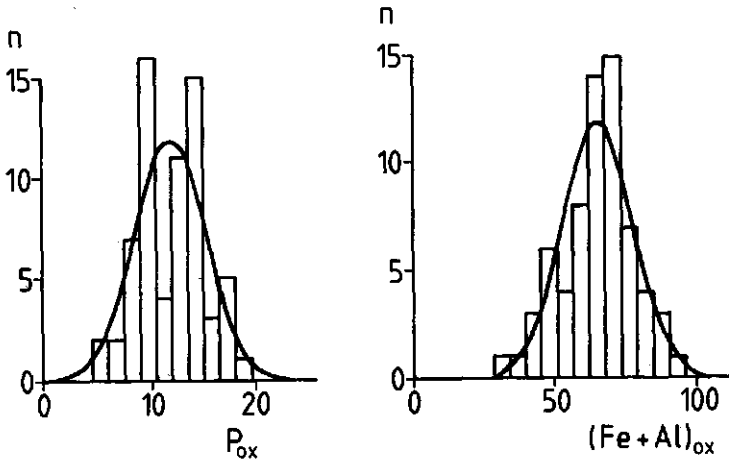


Figure 3: Histograms and fitted probability density functions of the variables P_{ox} and $(Fe+Al)_{ox}$.

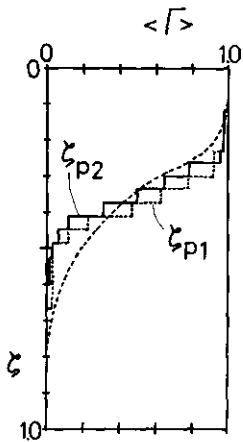


Figure 4: Averaged dimensionless concentration in the solid phase $\langle \Gamma \rangle$ as a function of dimensionless depth ζ . Experimentally found denoted ζ_{p1} and ζ_{p2} (see text), computed: dashed line (reference case).

8.7 Parameter analysis

The statistics of Table 2 used to compute the profiles of Figure 4 are estimated from data of 67 sample locations. It is assumed that these 67 locations are representative for the whole field. This and other assumptions may, however, not be valid. Hence, the estimated values of the statistics may be systematically too high or too low. In order to assess the nature and the sensitivity of a change in the profile due to a change in the model parameters, these parameters were varied.

The resulting profiles for different values of the statistics of F_T are shown in Figure 5a and for different values of the statistics of A_T in Figure 5b. Obviously the mean depth of penetration of the profile is proportional to m_A (the subscript T is omitted when writing m and σ) and inversely proportional to m_F . An increase in one of the standard deviations causes a more dispersed profile. Apparently the field-scale dispersion increases with an increase in the heterogeneity of both F_T and A_T . This is illustrated for the case where F_T is considered not random but constant (at m_F). Then equation (26) is integrated only once over A_T , which yields:

$$\langle \Gamma(\zeta, \tau) \rangle = 0.5 \left\{ 1 - \operatorname{erf} \left[\frac{\zeta m_F - m_A}{\sigma_A \sqrt{2}} \right] \right\} \quad (31)$$

Thus if σ_A increases also the field scale dispersion increases as the error functions decays slower with ζ . If $CV(A_T)$ is large the value of $\langle \Gamma(0, \tau) \rangle$ may be less than unity as in that case the second term in equation (31) is already significant at $\zeta = 0$. This is due to the physically unrealistic probability $\Pr(A_T < 0)$, which is finite for the case of a normal PDF. This is considered later in this study. It is noted that a result similar to equation (31) may be obtained if A_T is constant and F_T is the only random variable.

Since the statistics used to compute the profiles of Figure 4 were derived from the same data set from which the experimental profiles were constructed, the fit of calculated and experimental results can not be considered an independent test of the model. From the differences in Figure 4, a complication not accounted for in the calculations becomes manifest.

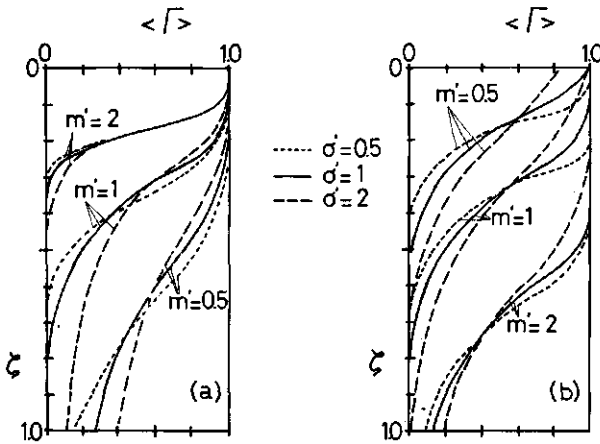


Figure 5: Averaged dimensionless concentration in the solid phase $\langle \Gamma \rangle$ as a function of dimensionless depth ζ . Variation of statistics of F_T (5a) and A_T (5b).

This is the significant degree of correlation between A_T and F_T (Table 2: $\rho(1) = 0.59$). Therefore calculations were done for three values of $\rho(1)$, using the means and standard deviations of Table 2. As expected the effect of the value of $\rho(1)$ on the shape of the profile is large (Figure 6). Thus if relatively large applications of P occur often on locations with a small retention capacity, then the front of P will move much faster in those locations than in the field on average. This is the case for curve 3, which shows a large field-scale dispersion.

In the opposite situation an almost piston-shaped field average profile is found (curve 1). If the random nature of A_T and F_T were neglected just like pore scale dispersion, then a piston shaped profile would be predicted. The front of P would then be situated at $\zeta = 0.36$. Since the experimental curves fall in between the curves 1 and 2 of Figure 6 the description is probably good if the coefficient of correlation $\rho(1) = 0.59$ is taken into account.

8.8 Profile development in time

The calculations done so far are for the reference situation, i.e., the situation at the moment of sampling. To show the development

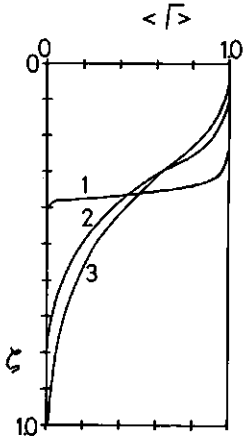


Figure 6: Average dimensionless concentration in the solid phase $\langle T \rangle$ as a function of dimensionless depth ζ . Statistics of reference case. Effect of correlation coefficient, $\rho(1)$.
Curve 1: $\rho = 0.999$; curve 2: $\rho = 0.06$; curve 3: $\rho = -0.998$.

in time, it is assumed that no trends occur in the application rate (for each individual application A_i the statistics m and σ are the same). To estimate the statistics of A_i , it is necessary to know how many applications resulted in the present situation (A_T). Information concerning this field suggests that $M = 10$ annual applications is reasonable. Then it is necessary to know whether and to what degree, individual applications are correlated. For illustration two possibilities are considered. In the first case the individual applications are independent and the statistics for A_i are estimated with

$$m_{A_T} = m_{A_i} M \quad (32)$$

$$\sigma_{A_T} = \sigma_{A_i} \sqrt{M} \quad (33)$$

In the second case where different A_i are completely dependent (a particular location receives the same amount of P at each application), equation (32) does not change but equation (33) becomes:

$$\sigma_{A_T} = \sigma_{A_i} M \quad (34)$$

Hence, for independent applications $CV(A_T)$ decreases with \sqrt{M} whereas

for dependent applications $CV(A_T)$ remains constant. Therefore, the field-scale dispersion will, in general, be larger in the case of dependent applications than in the case of independent applications. In the simplified case of equation (31) a symmetric sigmoid profile results (as is also the case for non-random A_T and random F_T). Then the growth in time of the field scale dispersivity (λ_D^f) can be made explicit. This is done by considering solute transport assuming constant input, $c(0,t) = c_0$, and a linear adsorption isotherm. The well known solution of equation (1) is given (for $t \gg D^*/v^*$) by:

$$c/c_0 = 0.5 \left\{ 1 - \operatorname{erf} \left[\frac{z - v^* t}{2\sqrt{D^* t}} \right] \right\} \quad (35)$$

where $D^* = D/R$ and $v^* = v/R$. Neglecting molecular diffusion the dispersivity is $\lambda_D = D^*/v^*$. Similarly a field scale dispersivity for the profile in the solid phase may be defined. Rewriting (31) in terms of $z (= \zeta L)$ it may be shown, that:

$$\lambda_D^f = \frac{\sigma_{A_T}^2}{2 \rho_s \frac{m_F}{m} \frac{m}{A_T}} \quad (36)$$

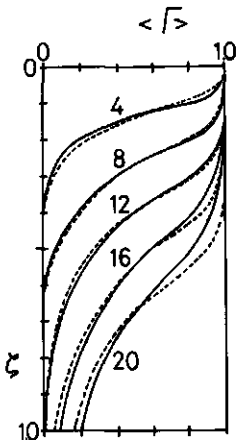


Figure 7: Average dimensionless concentration in the solid phase $\langle T \rangle$ as a function of dimensionless depth ζ . Effect of correlation coefficient for successive applications. Dashed line: $\rho = 0$; solid line: $\rho = 1$. Times (M) indicated in figure.

Clearly, by inserting equation (32) and equation (33) or (34) in (36), the field scale dispersivity is constant for independent applications but proportional to M for completely correlated applications. In the latter case we find that $\lambda_D^f = m \sigma_{A_1}^2 / (2\rho_s m_F m_{A_T})$.

For the field situation considered here where m and σ of A_T are given for $M = 10$ annual applications, clearly the value of σ_{A_T} estimated with equation (33) will be smaller than σ_{A_T} estimated with equation (34) for times shorter than 10 years. For larger times, the opposite will occur. This is shown in Figure 7 where the profiles are shown at different times (M) for the case of dependent and the case of independent A_1 .

It was already noted that if σ_{A_T} is calculated for times shorter than at the reference situation using equation (33), the value of $CV(A_T)$ becomes larger than at the reference case. Then a significant $Pr[A_T < 0]$ may be found. However, even if at the reference situation A_T (or P_{OX}) is approximately distributed normally this does not have to be the case for A_1 . Thus if A_1 is a random variable with a continuous distribution then the sum A_T will become distributed normally if a sufficient number of independent individual applications A_1 are summed. This is expressed in the central limit theorem [Papoulis, 1965]. Hence, for this field also, A_1 may well be distributed e.g. lognormally in which case A_1 can only be positive. (Appendix C; Chapter 9).

8.9 Discussion

It was noted above that P_{OX} and $(Fe + Al)_{OX}$ are correlated. Since physically no relation is expected between these variables the presence of trends should be investigated as these would invalidate the assumptions of stationarity and ergodicity. An indication of a trend in the random variable $X(\xi)$ may be obtained e.g. with the semivariogram $\gamma(h)$ defined by

$$\gamma(h) = \frac{1}{2} E \left\{ [X(\xi + h) - X(\xi)]^2 \right\} \quad (37)$$

which for an intrinsic random function of order zero depends only on h

[Gutjahr, 1985]. If the semivariogram reaches a maximum ('sill') at separation distances h^* exceeding a certain value ('range'), then

$$\gamma(h^*) = \text{var} \{X(\xi)\} = C(0) \quad (38)$$

and the random function is second order stationary for the domain $\{\xi\}$ considered. In Figure 8 the semivariograms for the D-transect of P_{OX} and $(Fe+Al)_{OX}$ are shown. In both cases no sill is reached, suggesting a trend.

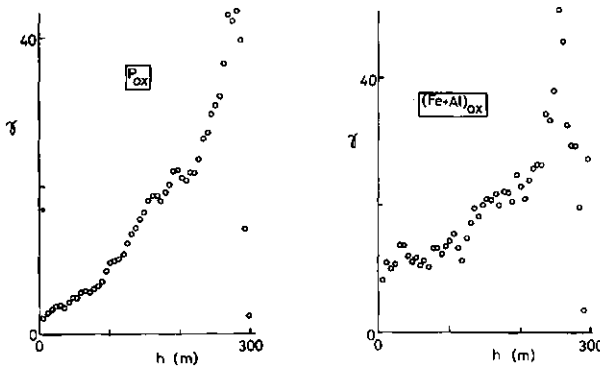


Figure 8: Semivariograms for a: P_{OX} and b: $(Fe+Al)_{OX}$, for D-transect, with 51 sample locations and 50 lag-classes.

The trends are shown in Figure 9 by giving the values of the variables P_{OX} and $(Fe+Al)_{OX}$ as a function of ξ along the transect. Clearly the mean values of both variables decrease as ξ increases.

It appears that the trends are in the same direction, which causes the positive value of $\rho(1)$, and that they almost compensate as no significant trend is observed for ζ_p (in this case ζ_{p2}). It may be noted also that the 'bimodal' shape of the histogram of P_{OX} in Figure 3 reflects the almost step wise change in $P_{OX}(\xi)$.

Since the mean values of both P_{ox} and $(Fe + Al)_{ox}$ depend on the coordinate ξ the assumptions made with respect to statistical homogeneity and ergodicity are not valid for the field studied. However, this does not invalidate the analysis presented. As was shown above, the description of the reference situation is probably accurate if the value of $\rho(1) = 0.59$ is taken into account. The rest of the parameter analysis also holds, if only for a similar field showing no trends and with independent A_T and F_T .

However, whereas the simple model given here is accurate to describe a particular situation, in order to apply it for predictive purposes we must know the spatial nature of the random variables. This is necessary as $\rho(1)$ may well vary in time (i.e., change with each application). Besides the recognition of spatial trends, also the nature of the distribution of an individual application, A_1 , is very important. The assumed shape of the PDF and the estimated statistics of A_1 influence both the PDF shape and the statistics of A_T . Since generally the number of applications can only be estimated, the predictive capabilities of this model are limited mainly by the uncertainties in A_1 .

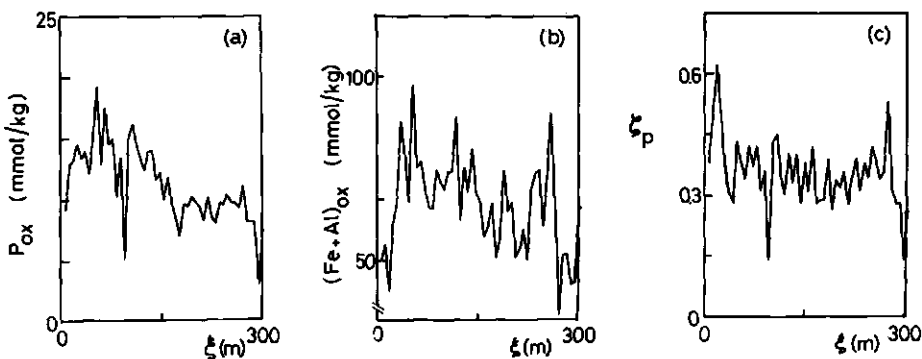


Figure 9: Values of random variables P_{ox} (a), $(Fe+Al)_{ox}$ (b), and ζ_p (c) as a function of location ξ .

The dispersion for the field-average transport may be larger than accounted for by simulation of the transport of P in a homogeneous

column, using realistic values of the physical parameters. For P transport, Beek [1979] was unable to simulate the average P profile in a field, receiving untreated sewage water, by one-dimensional transport simulations using independently evaluated parameter values. It is likely that this was at least partly due to neglecting the random nature of the retention capacity in the field. Surface-water eutrophication occurs already at solution concentrations of P a thousand fold smaller than found in top soils saturated with P derived from animal manure slurries disposal. Therefore we are interested in predicting the breakthrough at the groundwater level for a very small fraction of the total area. Whenever this is the case the heterogeneity of the retention capacity and the variability in the application should be taken into account.

8.10 Conclusions

1. The description of the field-average transport of P neglecting pore scale dispersion but taking into account the random nature of the applied quantity and retention capacity yields satisfactory results.
2. Field-scale dispersion increases with increasing coefficients of variation of applied quantity and of retention capacity.
3. A positive correlation of individual applications or a negative correlation of applied quantity and retention capacity also cause an increase in field-scale dispersion.
4. The presence and nature of trends of random variables need to be known in order to use the model for predictive purposes.

ACKNOWLEDGEMENTS

Permission to sample the field given by Mr. Van den Oever, St. Oedenrode, is very much appreciated. E.H. van Loenen was very helpful and conscientious with respect to the laboratory work for which we are grateful. We also thank J.M.P. Martens and O.R. de Ruyter for technical assistance.

8.11 Notation

A_T	Total amount of P applied [mmol/m ²]
A	Annually applied amount of P [mmol/m ²]
C	Covariance
CV	Coefficient of variation
D	Coefficient of molecular diffusion and hydrodynamic dispersion [m ² /yr]
D*	Effective dispersion coefficient for adsorbing solute, D/R [m ² /yr]
E	Expectation
F	Functional relationship of sorption with time and concentration [mmol/kg]
F_m	Maximal sorption based on (Fe+Al) _{ox} [mmol/kg]
F_T	Total sorption capacity for P of soil layer with thickness L [mmol/m ²]
K	Kolmogorov-Smirnov statistic
L	Length of column [m]
M	Number of applications
N	Number of sample locations
P_m	Maximal sorption based on $P_{ox} + P_R$ [mmol/kg]
P_R	Extrapolated measured sorption [mmol/kg]
Q	Adsorbed amount [mmol/kg]
R	Retardation factor
S	Precipitated amount [mmol/kg]
VAR	Variance
X	Generic notation of a random variable
c	Concentration of P in solution [mmol/m ³]
c_0	Feed solution concentration of P [mmol/m ³]
f	Probability density function
h	Separation vector
λ_D^f	Field scale dispersivity [m]
m	Mean
m'	Ratio of means, m/m_R with m_R for reference situation
t	Time [yr]
t_1	Period in time between successive applications [yr]

t^*	Time required to dissolve solid P [yr]
v	Interstitial water velocity [m/yr]
v^*	Effective interstitial water velocity for adsorbing solute, v/R [m/yr]
\bar{v}	Time averaged propagation velocity of front [m/yr]
x, y, z	Coordinates [m]
α	Ratio between P_m and $(Fe+Al)_{ox}$
γ	Semivariogram
Γ	Dimensionless concentration of P in the solid phase
ϵ	Variable
ρ	Coefficient of correlation
ρ_s	Soil bulk density [kg/m^3]
σ	Standard deviation, $(VAR)^{1/2}$
σ'	Ratio of standard deviations, σ/σ_R with σ_R for reference situation
τ	Total time [yr]
θ	Volumetric water content
ξ	Coordinate [m]
ζ	Dimensionless depth
ζ_p	Dimensionless front penetration depth

8.12 References

- Amoozegar-Fard, A., D.R. Nielsen, and A.W. Warrick. Soil solute concentration distributions for spatially varying pore water velocities and apparent diffusion coefficients. Soil Sci. Soc. of Am. Journal 46: 3-9, 1982.
- Barrow, N.J. A mechanistic model for describing the sorption and desorption of phosphate by soil. J. Soil Sci. 34: 733-750, 1983.
- Beek, J. Phosphate retention by soil in relation to waste disposal. PhD thesis, Agricultural University, Wageningen, 1979.
- Beek, J., and W.H. van Riemsdijk. Interactions of orthophosphate ions with soil. In: Soil Chemistry B, Physico-Chemical Models (Ed. G.H. Bolt). Elsevier Sci. Publ. Co., Amsterdam, pp. 259-284, 1982.
- Biggar, J.W. and D.R. Nielsen. Spatial variability of leaching characteristics of a field soil. Water Resources Research 12 (1):

78-84, 1982.

- Bolt, G.H. Movement of solutes in soil: Principles of adsorption/exchange chromatography. In: Soil Chemistry B, Physico-Chemical Models (Ed. G.H. Bolt). Elsevier Sci. Publ. Co., Amsterdam, pp. 285-348, 1982.
- Bresler, E., and G. Dagan. Solute dispersion in unsaturated heterogeneous soil at field scale: II. Applications. Soil Sci. Soc. Am. Journal 43: 467-472, 1979.
- Bresler, E., and G. Dagan. Convective and pore scale dispersive solute transport in unsaturated heterogeneous fields. Water Resour. Res. 17 (6): 1685-1693, 1981.
- Bresler, E., and G. Dagan. Unsaturated flow in spatially variable fields 3. Solute transport models and their application to two fields. Water Resources Research 19 (2): 429-435, 1983.
- Dagan, G., and E. Bresler. Solute dispersion in unsaturated heterogeneous soil at field scale: I Theory. Soil Sc. Soc. of Am. Journal 43: 461-467, 1979.
- De Haan, F.A.M. and W.H. van Riemsdijk. Behaviour of inorganic contaminants in Soil. In: Contaminated Soil (J.W. Assink and W.J. van den Brink, eds.) Martinus Nijhoff Publ., Dordrecht, pp 19-32, 1986.
- De Willigen, P., P.A.C. Raats and R.G. Gerritse. Transport and fixation of phosphate in acid, homogeneous soils, II Computer simulation. Agriculture and Environment, 7: 161-174, 1982.
- Enfield, C.G., T. Phan, D.M. Wolters and R. Ellis, Jr. Kinetic model for phosphate transport and transformation in calcareous soils, I and II. Soil Sci. Soc. Am. Journal 45: 1059-1064; 1064-1070, 1981.
- Gerritse, R.G., P. de Willigen and P.A.C. Raats. Transport and fixation of phosphate in acid, homogeneous soils, III Experimental case study of acid sandy soil columns heavily treated with pig slurry. Agric. and Environment 7: 175-185, 1982.
- Gutjahr, A.L. Spatial variability: geostatistical methods. In: Soil Spatial Variability (eds.: D.R. Nielsen and J. Bouma), Pudoc, Wageningen, pp. 9-28, 1985.
- Jury, W.A. Simulation of solute transport using a transfer function model. Water Resour. Res. 18: 363-368, 1982.

- Jury, W.A. Chemical transport modelling: current approaches and unresolved problems. In: Chemical mobility and reactivity in soil systems. ASA, SSSA, Madison, Wisconsin, 1983.
- Jury, W.A., L.H. Stolzy, and P. Shouse. A field test of the transfer function model for predicting solute transport. *Water Resour. Res.* 18 (2): 369-375, 1982.
- Lexmond, Th.M., W.H. van Riemsdijk, and P.A.M. de Haan. Onderzoek naar fosfaat en koper in de bodem in het bijzonder in gebieden met intensieve veehouderij. Serie Bodembescherming 9, Staatsuitgeverij, Den Haag, 1982.
- Murphy, J., and J.P. Riley. A modified single solution method for the determination of phosphate in natural waters. *Analytica Chimica Acta*, 27: 31-36, 1962.
- Nielsen, D.R., J.W. Biggar and K.T. Erk. Spatial variability of field measured soil-water properties. *Hilgardia* 42: 215-221, 1973.
- Novozamsky, I., R. van Eck, V.J.G. Houba, and J.J. van der Lee. Use of ICP atomic emission spectrometry for determination of iron, aluminum and phosphorus in Tamm's soil extracts. Accepted for *Publ. Neth. J. Agric. Sci*, 34, 185-191, 1986.
- Papoulis, A. *Probability, Random Variables and Stochastic Processes*. McGraw-Hill Kogakusha Ltd., Tokyo, pp. 327-332, 1965.
- Peck, A.J. Field variability of soil physical properties. *Advan. Irrigation*, 2: 189-221, 1983.
- Persaud, N., J.V. Giraldez, and A.C. Chang. Monte-Carlo simulation of noninteracting solute transport in a spatially heterogeneous soil. *Soil Sci. Soc. Am. Journal*, 49: 562-568, 1985.
- Raats, P.A.C., P. de Willigen, and R.G. Gerritse. Transport and fixation of phosphate in acid, homogeneous soils, I Physico-mathematical model. *Agric. and Environment* 7: 149-160, 1982.
- Rubinstein, R.Y. *Simulation and the Monte Carlo method*. John Wiley & Sons Inc., New York, 1981.
- Schwertmann, U. Differenzierung der Eisenoxiden des Bodens durch Extraction mit Ammoniumoxalaat Lösung. *Zeitschrift für Pflanzenernährung, Düngung und Bodenkunde*, 105: 194-202, 1964.
- Skopp, J. Analysis of solute movement in structured soils. In: *Proceedings ISSS symposium on water and solute movement in heavy clay soils*, 1984, Wageningen, pp. 220-228, 1984.

- Van Riemsdijk, W.H., L.J.M. Boumans and F.A.M. de Haan. Phosphate sorption by soils, I A diffusion-precipitation model for the reaction of phosphate with metal oxides in soil. *Soil Sci. Soc. Am. Journal* 48: 541-544, 1984.
- Van Riemsdijk, W.H., and F.A.M. de Haan, 1981. Sorption kinetics of phosphate with an acid sandy soil, using the phosphatostat method. *Soil Sci. Soc. Am. Journal*, 45: 261-266, 1981.
- Van Riemsdijk, W.H., and A.M.A. van der Linden. Phosphate sorption by soils, II Sorption measurement Technique. *Soil Sci. Soc. Am. Journal*, 48: 541-545, 1984.
- Van der Zee, S.E.A.T.M. and W.H. van Riemsdijk. Sorption kinetics and transport of phosphate in sandy soil. *Geoderma* no. 38, 293-309, 1986.
- Van der Zee, S.E.A.T.M., W.H. van Riemsdijk, and F.A.M. de Haan. Reaction kinetics and transport of phosphate: parameter assessment and modelling. *Nijhoff Publ.*, Dordrecht, pp 157-160, 1985.
- Van der Zee, S.E.A.T.M., L.G.J. Fokkink, and W.H. van Riemsdijk. A new technique for assessment of reversibly adsorbed phosphate. *Soil Sci. Soc. Am. J.*, 51, 599-604, 1987.
- Warrick, A.W., G.J. Mullen, and D.R. Nielsen. Scaling field-measured soil hydraulic properties using a similar media concept. *Water Resour. Res.* 13 (2): 355-362, 1977.

9. TRANSPORT OF REACTIVE SOLUTE IN SPATIALLY VARIABLE SOIL SYSTEMS

Abstract

Transport is studied for reactive solutes and one dimensional fluid flow with sorption described by the Freundlich equation ($Q = kc^n$). For a physically and chemically homogeneous soil column and if the constant feed concentration is larger than the initial concentration the transport occurs in a travelling wave type displacement, with a constant shape of the solute concentration front and constant front propagation velocity, provided $0 < n < 1$. For a negligible initial concentration it is shown that a shock front may be assumed if n is small enough. Field scale transport is described as an ensemble of shock fronts in parallel columns with different flow velocities (v), retardation factors (r) and times of solute input (t_c). These stochastic variables are characterized by probability density functions (PDF). If we assume lognormal distributions, a simple expression for the field averaged profile of dimensionless sorbed solute $\langle \Gamma \rangle$ at a particular time is derived. If t_c is not a distributed variable, but equal to the total time τ , the profile $\langle \Gamma \rangle$ coincides with the field averaged dimensionless concentration profile. It is shown how scaling theory, leading to the PDF of the fluid velocity, may be incorporated in the model. For reasonable parameter values and statistics of the stochastic variables the $\langle \Gamma \rangle$ -profiles are calculated. Notably the effect of a stochastic retardation factor, with statistics derived from the distributions of pH and oc (organic carbon content) found for 84 soils, appears to be profound. The field average displacement calculated is non-sigmoid for the PDF's of oc, pH and t_c chosen. This phenomenon is amplified if v and r are assumed negatively correlated. From the results it is clear that modelling of horizontally large soil systems with averaged properties will in general lead to an underestimation of the moment of first breakthrough at a particular reference level, such as the phreatic water level.

9.1 Introduction

The description of solute transport through soil is of interest in order to quantify salt displacement in salt-affected soils, pollutant mobility (heavy metals, excess fertilizer, pesticides, radionuclides) and the mobility of plant nutrients. Reviews of work done on transport in macroscopically homogeneous columns were given by Bolt [1982] and Cleary and Van Genuchten [1982]. Often, however, soil may not be considered as a homogeneous flow domain due to the presence of structure (macropores, aggregates, and cracks). This structure may cause preferential flow channels that may result in bypass of part of the soil matrix. Then two or more subdomains need to be distinguished and transfer between these domains may be described empirically with a first-order rate expression [Deans, 1963; Skopp and Warrick, 1974; Van Genuchten and Wierenga, 1976; 1977]. In some cases where geometry of the subdomains is known the transfer may be described by modelling the subdomains deterministically. This was done by Rasmuson and Neretnieks [1980] for spherical particles, Tang et al. [1981] and Rasmuson and Neretnieks [1981] for fractured rock, Addiscott [1974] for cubic soil peds, Van Genuchten et al. [1984] and De Willigen [1985] for root channels, and by Valocchi [1985], Parker and Valocchi [1985] and Van Genuchten and Dalton [1986] for several geometries.

Vertical transport through flow domains of large horizontal extent is influenced also by variability of soil properties in the horizontal plane. Spatial variability of soil hydraulic properties was investigated by Nielsen et al. [1973], Biggar and Nielsen [1976], Warrick et al. [1977], and Russo and Bresler [1981]. The variability of hydraulic properties in similar media may be handled using scaling theory (e.g. Peck, 1979). Warrick et al. [1977] showed that a dimensionless scaling factor may be defined that relates the hydraulic conductivity at a particular location in a field to a field-averaged hydraulic conductivity. This scaling factor was found to be lognormally distributed.

The effect of spatially variable hydraulic properties on solute transport was studied by Dagan and Bresler [1979], Bresler and Dagan [1979, 1981, 1983], Amoozegar-Fard et al. [1981] and Persaud et al. [1985]. Using stochastic theory Dagan and Bresler [1979] and Bresler

and Dagan [1979] analytically evaluated the field averaged concentration as a function of depth and time for a non-reacting solute. They neglected pore scale dispersion and assumed that the scaling factor and the steady infiltration rate were stochastic variables. In subsequent papers (1981, 1983) they incorporated transient flow and pore scale dispersion. They showed that non-Fickian behaviour may occur and estimated that the concentration profile may satisfy a diffusion-type equation only after transport distances of 10 to 100 meters. If pore scale dispersion is taken into account with a dispersion coefficient reflecting soil profile heterogeneity this has only a small effect on the concentration profile and spatial variability is dominant. Amoozegar-Fard et al. [1981] who used Monte Carlo techniques, reach the same conclusion. Persaud et al. [1985], also using Monte Carlo techniques, concluded that the correlation between the pore scale dispersion coefficient and the velocity hardly affects the concentration profile.

A somewhat different approach was given by Jury [1982] who described transport in a spatially variable field assuming a distribution of travel times. His transfer function model (TFM) was successfully applied for a field by Jury et al. [1982] and for undisturbed columns and a field site by White et al. [1986]. Using the TFM approach Jury [1983] found a prominent effect of correlation between the retardation factor and the travel time of a non-reacting solute, assuming both are distributed. Sposito et al. [1986] showed that the fraction of immobile water in their two component convection dispersion equation controlled the shape of the travel time distribution.

Field-averaged transport was studied recently for a reacting solute (phosphate) by Van Der Zee and Van Riemsdijk [1986]. They assumed high affinity sorption and equilibrium at time scales relevant in the field. Neglecting pore scale dispersion and desorption, a piston shaped profile results for sorbed P. The dimensionless penetration depth of the sorbed P front was expressed in terms of P applied (A_T) and the sorption capacity (F_T). The variables A_T and F_T appeared to be random variables for a field and consequently the dimensionless penetration depth (equal to the fractional saturation of a column) is also random. The field averaged profile of dimensionless

sorbed P was calculated with Monte Carlo simulations, using the experimental probability density functions (PDF) of A_T and F_T . The description of the experimental profile appeared good and differences could be understood if the trends in the field were taken into account. Sensitivity analyses showed the large effect of the correlation between A_T and F_T .

In this contribution we describe transport of solute adsorbing according to a Freundlich isotherm. In the case of continuous solute input a travelling wave occurs that may be approximated with a piston profile by neglecting pore scale dispersion. Neglecting desorption we approximate the profile of sorbed solute by a piston shape. The penetration depth for a homogeneous column is controlled by the velocity (v), the cumulative time of solute input (t_M) and the retardation factor (r). For a field envisioned as an ensemble of non-interacting columns the variables v , t_M and r may be considered random. We show that by assuming a piston profile at the column scale, a simple expression for the field averaged profile of dimensionless sorbed solute is found if the stochastic variables are lognormally distributed. We illustrate that, assuming lognormal distributions, the incorporation of other stochastic variables may be very simple.

9.2 Theory

9.2.1 Column scale transport

Solute transport in one dimension in the absence of sinks and for steady state flow is described by

$$\frac{\partial}{\partial t} [\rho Q + \theta c] = \theta D \frac{\partial^2 c}{\partial z^2} - \theta v \frac{\partial c}{\partial z} \quad (1)$$

where ρ = dry bulk density (kg m^{-3}), θ = volumetric water content, D = coefficient of hydrodynamic dispersion ($\text{m}^2 \text{y}^{-1}$), v = pore water velocity (m y^{-1}), z = depth (m), t = time (y), c = concentration (mol m^{-3}), Q = sorption (mol kg^{-1}). Equilibrium sorption is given by the Freundlich isotherm:

$$Q = k c^n \quad (2)$$

where k and n are constants. Other isotherms such as the Langmuir isotherm are equally feasible. For a homogeneous column with initial concentration smaller than the input concentration, displacement occurs as a travelling wave provided $0 < n < 1$. Such a travelling wave is characterized by a solute front shape that does not vary in time and that moves through the column with a constant velocity. Travelling wave solutions were given by Reiniger and Bolt [1972] for favourable exchange and Van Duijn and De Graaf [1984] for Freundlich adsorption. Equations (1) and (2) are solved for the conditions

$$c(z, 0) = c_0 \quad z < 0 \quad (3a)$$

$$c(z, 0) = 0 \quad z > 0 \quad (3b)$$

$$c(-\infty, t) = c_0 \quad \frac{\partial c}{\partial z} = 0 \quad t > 0 \quad (4a)$$

$$c(+\infty, t) = 0 \quad \frac{\partial c}{\partial z} = 0 \quad t > 0 \quad (4b)$$

Defining the new variable $\eta = z - at$, where a is the wave velocity [Bolt, 1982], and setting $c(\eta) = c(z, t)$ yields

$$-a \left\{ 1 + \frac{\rho}{\theta} \frac{dQ(c)}{dc} \right\} \frac{dc}{d\eta} = D \frac{d^2 c}{d\eta^2} - v \frac{dc}{d\eta} \quad (5)$$

and

$$c = c_0 \quad \frac{\partial c}{\partial \eta} = 0 \quad \eta \rightarrow -\infty \quad (6a)$$

$$c = 0 \quad \frac{\partial c}{\partial \eta} = 0 \quad \eta \rightarrow \infty \quad (6b)$$

After integration of equation (5) assuming $\frac{dc}{d\eta} \rightarrow 0$ for $\eta \rightarrow \pm \infty$ the wave velocity (a) is found

$$a = v c_0 / (c_0 + \frac{\rho}{\theta} Q(c_0)) = v/r \quad (7a)$$

The retardation factor, r , in case of the Freundlich isotherm is

$$r = 1 + \frac{\rho}{\theta} k \left(\frac{c_0^n - c_1^n}{c_0 - c_1} \right) \quad (7b)$$

for the concentration increment $c_0 - c_1$. Since we have chosen an initial concentration $c_1=0$ we henceforth use the notation $\Delta Q = k c_0^n$. The implicit solution of equation (5) is

$$\frac{\rho a}{\theta D} \int_{\eta_R}^{\eta} d\eta = \int_{c(\eta_R)}^{c(\eta)} \frac{dc}{\left\{ \frac{\Delta Q}{c_0} - \frac{Q(c)}{c} \right\} c} \quad (8)$$

where η_R is an arbitrary reference [Bolt, 1982]. For the Freundlich isotherm this leads to

$$\frac{\rho k a}{\theta D} \int_{\eta_R}^{\eta} d\eta = \int_{c(\eta_R)}^{c(\eta)} \frac{dc}{\frac{\Delta Q}{k c_0} c - c^n} \quad (9)$$

If we set $g = c^{1-n}$ equation (9) may be integrated and this yields after rearrangement and substitution again of c

$$c(\eta - \eta^*) = \left\{ \frac{k c_0}{\Delta Q} \left[1 - \exp \left(\frac{\rho a \Delta Q (1-n)}{\theta D c_0} (\eta - \eta^*) \right) \right] \right\}^{1/1-n} \quad (10a)$$

In equation (10a) η^* is the coordinate with $c = 0$ for $\eta > \eta^*$ and which is given by:

$$\eta^* = - \frac{c_0 \theta D}{\Delta Q \rho a} \left(\frac{1}{1-n} \right) \ln \left[1 - \frac{\Delta Q}{k c_0} \left(\frac{c_0}{2} \right)^{1-n} \right] \quad (10b)$$

We have chosen $c(\eta_R) = c(0) = \frac{1}{2} c_0$.

We will show in a later section that a relatively sharp c-front develops for realistically chosen parameter values if the front is described by equation (10). Due to the non-linear sorption isotherm the effect of dispersion does not lead to continued profile spreading with increasing time but results in the development of a steady state front travelling through the medium with velocity a . Then we may make the approximation of a shock front by neglecting hydrodynamic dispersion. We consider a soil containing initially no solute and with the boundary condition

$$c(0, t) = H(t_c - t) \quad 0 < t < t_1 \quad (11)$$

where t_1 is the length of a time increment considered and where the

Heaviside step function is given by $H(\epsilon)=0$ for $\epsilon < 0$ and $H(\epsilon)=1$ for $\epsilon > 0$. Thus solute enters the column during $0 < t < t_1$ with a concentration of c_0 , followed by a time span equal to $t_1 - t_c$ when a solute-free solution enters. If we consider a number M of such sorption-desorption cycles, which are each of duration t_1 then we may make the following assumption. For a steep isotherm (small n) concentration buffering by desorption is negligible until small values of c are reached [Cleary and Van Genuchten, 1982, p. 357]. At low c the rate of mass displacement is small and therefore little solute redistribution occurs for $t_c < t < t_1$. During successive cycles first the top layer, where desorption occurred, will be filled up with solute. This is followed by a further displacement of the downstream front. Therefore we may assume a pulse-wise propagation of the downstream front of adsorbed solute provided the retardation factor is large. Neglecting the small oscillations in time of the adsorbed amount close to the inlet boundary ($z=0$) we can give a simple expression for the dimensionless front of adsorbed solute, $\gamma=Q/Q(c_0)$. This approximation is better as the number (M) of sorption-desorption cycles considered is larger and is given by

$$\gamma = H\left(\frac{vt_M}{r} - z\right) \quad (12)$$

where t_M is the cumulative time of solute input ($= \sum_{i=1}^M t_{c,i}$) and τ is the total time ($\tau = \sum t_1$).

In the next section we consider an ensemble of parallel, vertical columns. In practice the contents of organic carbon, clay, oxides, etc. are different for different horizons and layers, and this is reflected in $Q(c_0)$ and r . Therefore it is convenient to introduce a dimensionless coordinate, ζ [Van der Zee and Van Riemsdijk, 1986]. Defining $\bar{Q}(c_0)$ as the depth averaged value of $Q(c_0)$ for a column of length L then

$$\zeta = \int_0^z Q(c_0) dz / \bar{Q}(c_0)L \quad (13)$$

Here L may be conveniently chosen e.g. the depth of the water table, and may differ for different columns. Combination of equations (12) and (13) yields the expression for the dimensionless sorption profile

(i.e., the dimensionless amount as a function of depth γ and time τ), which is given by

$$\gamma(\zeta, \tau) = H \left(\frac{vt}{rL} - \zeta \right) \quad (14)$$

Note that $\gamma(\zeta, \tau)$ represents the fractional saturation of a column of length L at the time $\tau = Mt_1$. This fractional saturation is the amount of solute present in the column, divided by the amount present if the concentration equals c_0 in the whole column.

9.2.2 Field scale transport

A field or watershed may be assumed to consist of an ensemble of parallel, vertical columns. The columns differ with respect to the variables X_i , where $i = 1, \dots, N$. The average behaviour of such a flow domain may be described using stochastic theory (Dagan and Bresler, 1979; Van der Zee and Van Riemsdijk, 1986). Then the variables X_i are not given fixed values but are represented by probability density functions (PDF). We assume that each variable X_i has an expectation and a variance and that the assumptions of ergodicity and stationarity are valid (Papoulis, 1965; Russo and Bresler, 1981). The dimensionless concentration in the solid phase is a function of the stochastic variables and thus it is also random. Denoting random variables by capitals then

$$f_{\Gamma}(\zeta, \tau; \Gamma) d\Gamma = f_X(\zeta, \tau; X_1, \dots, X_N) dX_1 \dots dX_N \quad (15)$$

where f_{Γ} is the PDF for Γ (random dimensionless sorption) and f_X is the joint PDF of X_i , $i = 1, \dots, N$. Integration of f_{Γ} yields the distribution function $F_{\Gamma}(\zeta, \tau; \Gamma)$ and inserting Γ^* into F_{Γ} gives the probability

$$\text{Pr} [\zeta, \tau; \Gamma^*] = \int_{-\infty}^{\Gamma^*} f_{\Gamma}(\zeta, \tau; \Gamma) d\Gamma \quad (16)$$

i.e. the probability that Γ is less than or equal to Γ^* at given time and depth. Equations (15) and (16) are combined to

$$\Pr [\zeta, \tau; \Gamma^*] = \iint \dots \int_{[\Gamma^*]} f_X(\zeta, \tau; X_1, X_2, \dots, X_N) dX_1 dX_2 \dots dX_N \quad (17)$$

with $[\Gamma^*]$ the N-dimensional integration domain of combinations of X_1, \dots, X_N that result in $\Gamma < \Gamma^*$. The expectation of Γ at specified ζ and τ is given by the first moment

$$\langle \Gamma(\zeta, \tau) \rangle = \int_0^1 \Gamma f_{\Gamma}(\zeta, \tau; \Gamma) d\Gamma \quad (18)$$

which may be rewritten as

$$\langle \Gamma(\zeta, \tau) \rangle = 1 - \int_0^1 \Pr [\zeta, \tau; \Gamma] d\Gamma . \quad (19)$$

We note that, for the piston flow model adopted here, $\langle \Gamma(\zeta, \tau) \rangle$ is equal to the fraction of the area in the (horizontal) xy-plane where $\Gamma = 1$ with respect to the total area.

The profile $\langle \Gamma(\zeta, \tau) \rangle$ at specified τ may be calculated if f_X is given. We assume that v , t_M , and r are random (notation V , T , and R , respectively) and lognormally distributed. A lognormal PDF for V is in agreement with scaling theory (Peck, 1983) and findings from Biggar and Nielsen [1976], Warrick et al [1977], and Bresler and Dagan [1979]. For a small coefficient of variation (CV defined as the ratio standard deviation/mean) the lognormal PDF has an almost Gaussian shape [Simmons, 1981] Therefore the normal distributions observed by Van der Zee and Van Riemsdijk [1986] for the variables corresponding to T and R could be replaced by lognormal distributions (Appendix C). A lognormally distributed variable is defined in $\langle 0, \infty \rangle$ and a normal distributed variable in $\langle -\infty, \infty \rangle$. Hence the lognormal PDF is physically more appropriate for V , T , and R . It is given by

$$f_X = \frac{1}{\bar{X} \underline{s}_X \sqrt{2\pi}} \exp\left[-\frac{1}{2} \left(\frac{\underline{X} - m_X}{\underline{s}_X}\right)^2\right] \quad (20)$$

where lognormally transformed variables are underscored (i.e.,

$\underline{X} = \ln X$) and

$$\begin{aligned} X &= \text{lognormally distributed variable, } X = A \left(m_X, s_X^2 \right) \\ \underline{X} &= \ln(X), \text{ normally distributed variable, } \underline{X} = N \left(m_X, s_X^2 \right) \end{aligned}$$

\underline{m}_X = mean of X
 \underline{s}_X = standard deviation of X

Two situations may arise, i.e., the stochastic variables may be independent or dependent. Consider a random variable Y , which is a function of independent lognormally distributed X_i ($i = 1, \dots, N_1$) and Z_j ($j = 1, \dots, N_2$), i.e.,

$$Y = \prod_{i=1}^{N_1} X_i / \prod_{j=1}^{N_2} Z_j \quad (21)$$

Then also Y is lognormally distributed with statistics following from the properties of this distribution. Thus for $\underline{Y} = \ln Y$:

$$\underline{m}_Y = \sum_{i=1}^{N_1} \underline{m}_{X_i} - \sum_{j=1}^{N_2} \underline{m}_{Z_j} \quad (22a)$$

and

$$\underline{s}_Y^2 = \sum_{i=1}^{N_1} \underline{s}_{X_i}^2 + \sum_{j=1}^{N_2} \underline{s}_{Z_j}^2 \quad (22b)$$

For independent V , T , and R the statistics of the logarithm of the dimensionless penetration depth ($\underline{Y} = \ln(\frac{VT}{RL})$) are then

$$\underline{m}_Y = \underline{m}_V + \underline{m}_T - \underline{m}_R - \ln(L) \quad (23a)$$

and

$$\underline{s}_Y^2 = \underline{s}_V^2 + \underline{s}_T^2 + \underline{s}_R^2 \quad (23b)$$

The PDF of Y is characterized by equations (20) and (23). We note that

$$\Pr [Y < \zeta^*] = \int_0^{\zeta^*} f_Y dY \quad (24)$$

and that for local piston flow this is equivalent to

$$\Pr [Y < \zeta^*] = \int_0^1 \Pr[\zeta, \tau; \Gamma] d\Gamma \quad (25)$$

A simple expression for $\langle \Gamma(\zeta, \tau) \rangle$ results by combination of equations (19), (20), (24) and (25) and integration. Thus the field averaged profile of adsorbed solute is given by

$$\langle \Gamma(\zeta, \tau) \rangle = \frac{1}{2} \left\{ 1 - \operatorname{erf} \left[\frac{\zeta - m_Y}{s_Y \sqrt{2}} \right] \right\} \quad (26)$$

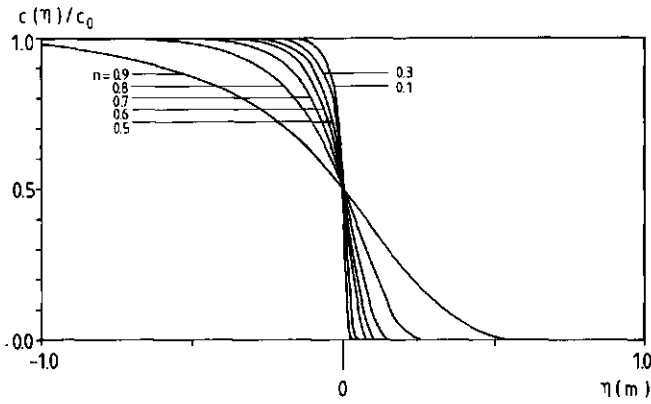
where $\operatorname{erf}(x) = \frac{2}{\sqrt{\pi}} \int_0^x \exp(-x^2) dx$ and ζ is the lognormally transformed dimensionless depth (equation 13). Equation (26) gives the profile as a function of the parameters m_Y and s_Y .

9.3 Discussion

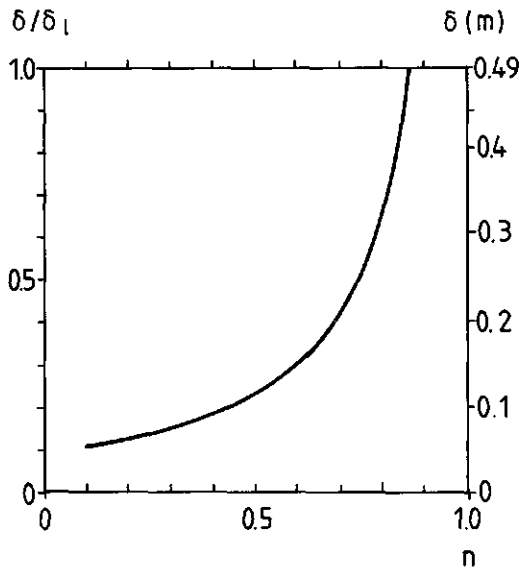
In this section first the approximation of a shock front within a column is justified. This is done by comparing the column scale profile of a solute adsorbing according to a linear isotherm with the travelling wave solution. Then the field scale profile ($\langle \Gamma(\zeta, \tau) \rangle$) is studied. As the field scale profile is determined by f_Y (i.e., m_Y and s_Y^2) we show how f_Y depends on the other variables, that may change in time (T) or that may be correlated (e.g. \underline{V} and \underline{R}). Usually the variability in \underline{V} and in \underline{R} is expressed in terms of the variability of other parameters such as the scaling factor (α) or the distribution coefficient (k). We show how such parameters are incorporated in the description. Besides a sensitivity analysis to show general effects, the profiles $\langle \Gamma(\zeta, \tau) \rangle$ for realistic parameters values and distributions are shown. By considering also transport of a linearly adsorbing solute in an equivalent homogeneous medium the effects of pore scale dispersion and field scale variability are compared.

9.3.1 Column scale profile

The profile giving c as a function of η (equation 10) is shown in Figure 1a, using the parameter values of Table 1. Since our interest is the applicability of the shock front assumption in one column, we evaluate the front thickness (δ) defined as:



(a)



(b)

Figure 1: Concentration front according to the travelling wave solution (equation 10). 1a: Relative concentration as a function of coordinate η . 1b: Front thickness relative to the thickness in case of a linear isotherm (δ/δ_1 , left vertical axis) and front thickness (δ , right vertical axis) as a function of Freundlich power parameter (n). Parameter values of Table 1.

$$\delta = \eta(c = 0.16 c_0) - \eta(c = 0.84 c_0) \quad (27)$$

with $c_1 = 0$. Similarly a front thickness (δ_1) is defined for the case of a linear isotherm. The thickness δ_1 follows from the solution

$$c(z,t) = \frac{1}{2} c_0 \left\{ 1 - \operatorname{erf} \left[\frac{z - at}{2 \sqrt{Dt/r}} \right] \right\} \quad (28)$$

which is valid sufficiently far from the inlet at $z=0$. It is simple to see that

$$\delta_1 = 2 \sqrt{(2DL/v)} \quad (29)$$

Table 1: Parameter values used for calculating the travelling wave for heavy metals (Cu and Cd).

$\theta = 0.3$	$c_1 = 0$
$\rho = 1400 \text{ kg.m}^{-3}$	$c_0 = 0.5 * 10^{-4} \text{ mol.m}^{-3}$
$v = 1 \text{ m.y}^{-1}$	$\text{pH} = 5$
$D = 0.03 \text{ m}^2.\text{y}^{-1}$	$oc = 2 \text{ g/g} \times 100\%$
$k = 0.03$	$k_{\text{Cu}} = 0.04; k_{\text{Cd}} = 0.02$
$n = 0.1 - 0.9$	$n_{\text{Cu}} = 0.45; n_{\text{Cd}} = 0.85$

where L is the depth where the average front is found ($L=at$). Setting $L=1 \text{ m}$ we find $\delta_1 = 0.49 \text{ m}$. In Figure 1b the effect of n on the ratio δ/δ_1 is shown. Clearly an increase in n results in a larger ratio. As $n \rightarrow 1$ an increasingly widening profile results. For $n=1$ equation (10) is not valid, as no travelling wave develops. Since the profile given by equation (10) is a limiting profile ($t \rightarrow \infty$) the value of δ/δ_1 may become larger than unity as δ_1 was evaluated for a particular depth, L . Thus if δ/δ_1 is large whereas interest is mainly to short travel distances, then the assumption of a steeper front than calculated with equation (28) may not be warranted. The k and n values given in Table 1 are appropriate for cadmium [Chardon, 1984] and copper [Lexmond, 1980]. Distinct travelling wave type displacement is not expected for cadmium for travel distances of approximately 1 meter. For copper a travelling wave is expected because the small value of n leads to small values of δ/δ_1 . Hence for Cu the approximation of a shock front may be acceptable. From Chardon's [1984] data it becomes clear that if

an excess of other heavy metals is present (such as Cu, Pb, Zn) competition effects may cause a decrease in n . In such cases Cd may also displace in a sharp front.

9.3.2 Statistics of \underline{Y}

The profile shape is controlled by the statistics of \underline{Y} (equation 26) which in turn depend on the statistics of V , T , R or variables of which these are composed such as the scaling factor, bulk density, adsorption parameters etc. The relationships between \underline{Y} and several variables are discussed here.

9.3.2.1 Time dependence for discontinuous input

Whereas f_V and f_R may be assumed time invariant, this is of course not the case for f_T because t_M increases as τ increases. In the case of discontinuous solute input, i.e., $t_M < \tau$ we may characterize the stochastic variable T with a lognormal PDF. However, since in that case T is defined in $\langle 0, \infty \rangle$ the probability that $T > \tau$ is finite, which is physically unrealistic. Although the situation where one part of the area has $t_M = \tau$ whereas for the other part t_M is smaller than τ may occur, we will not consider this complication here. Instead we assume that approximately $t_M < \tau$ for the whole area which is valid if $\text{Pr}[T > \tau]$ is negligibly small. If we consider $\text{Pr}[T > \tau] < \epsilon$ acceptable, where ϵ is a chosen constant smaller than one, then this leads to a constraint for the combination of m_T and s_T . For m_T of the order of magnitude of $\ln(\tau)$ (i.e., significant average solute input) we find the constraint that after a few years

$$\text{CV}(\underline{T}) < (\ln \tau - m_T) / ((m_T / \sqrt{2}) \text{inverf}(1 - 2\epsilon)) \quad (30)$$

where inverf is the inverse of the error function and $\text{CV}(\underline{T})$ is the coefficient of variation of \underline{T} . Thus as m_T becomes closer to $\ln \tau$ (approaching continuous solute input) the relative spread of \underline{T} must decrease rapidly. In the case of continuous input, the time of input

is no longer a stochastic variable. For illustration, the constraint for

$m_{\underline{T}}/\ln(\tau)$ is shown as a function of $CV(\underline{T})$ in Figure 2 for different values of the constant ϵ . For a combination of $m_{\underline{T}c}$ and $s_{\underline{T}c}^2$, where the subscript c denotes a single (annual) application that satisfies equation (28), we may consider the development in time of these statistics. To do so we assume that successive applications are perfectly correlated, i.e., for a column, t_c is the same for each cycle. This is a reasonable assumption if major trends occur in the application on the field scale, such that part of the field consistently receives more solute than another part. Such a trend was observed by Van Der Zee and Van Riemsdijk [1986] for phosphate applied to a field of 6 ha area in the form of animal manure slurries. Also if a larger scale flow domain is studied such as a watershed that consists partly of differently treated fields, and partly of farmyards and woodlands a perfect correlation may be realistic.

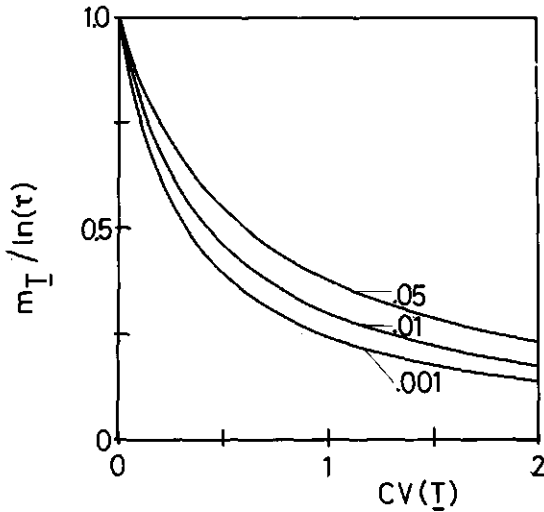


Figure 2: Constraint to the combination of $m_{\underline{T}}$ and $s_{\underline{T}}$ for different values of the probability (ϵ) that total time of solute input (\underline{T}) exceeds total time (τ).

The statistics of \underline{T} after M application cycles are then given by

$$m_{\underline{T}} = m_{\underline{T}_c} + \ln(M) \quad (31a)$$

$$s_{\underline{T}}^2 = s_{\underline{T}_c}^2 \quad (31b)$$

It is noted that if \underline{T}_c is distributed $N(m_{\underline{T}_c}, s_{\underline{T}_c}^2)$ so that it satisfies equation (28), then also \underline{T} found with equation (29) will satisfy this constraint.

9.3.2.2 Limiting case of continuous input

In part of the area, solute may continuously enter at the soil surface ($t_M = \tau$). Also for some situations (sewage farms, fertigation, atmospheric deposition) this may be approximately the case for the whole flow domain studied. Then the time of input is no longer a stochastic variable ($s_{\underline{T}}^2 = 0$) and $m_{\underline{T}}$ in equation (23a) is replaced by $\ln(\tau)$. Due to the larger time of input, the profile will be situated deeper (larger ζ) than in the case of $t_M < \tau$. Denoting the median penetration depths where $\langle \Gamma \rangle = \frac{1}{2}$ by $\zeta_{\frac{1}{2}}$ for the case of discontinuous input, and by $\tilde{\zeta}_{\frac{1}{2}}$ for continuous input then

$$\zeta_{\frac{1}{2}} = \tilde{\zeta}_{\frac{1}{2}} \exp(m_{\underline{T}})/\tau \quad (32)$$

If $t_M = \tau$ no desorption occurs and the profiles in solution and in the solid phase coincide for the piston flow model used. A related problem was considered by Dagan and Bresler [1979] for a non reacting solute. They directed their attention to the description of variability in water flow and the resulting field scale dispersion. Both the hydraulic properties and the recharge were random in their situation and the concentration at the soil surface was constant. This resulted in two different situations in the field as both unsaturated flow and saturated flow with ponding occurred. Total solute input depended on the recharge as is also the case in this study for $t_M = \tau$. If $t_M < \tau$ the total solute deposited at the soil surface ($v t_M \theta c_0$) controls the input. The situation studied by Dagan and Bresler [1979] may be extended to a reacting solute with a linear isotherm with a single valued retardation factor. However, to take into account a stochastic

retardation factor in their model is likely to lead to considerable complications. Therefore their analysis with emphasis on the hydraulic aspects of the problem may be preferred for a non-reacting solute, or in case of a linear isotherm if little variation in the retardation occurs. If the retardation shows much variability in the flow domain or if waterflow is not limiting with respect to input, the description given here may be preferred.

9.3.2.3 Unsaturated flow

Dagan and Bresler [1979] characterized variability of flow using scaling theory. If the PDF of the scaling factor is known it can be readily incorporated in the description given here. Referring for details to their work we adopt their $K(\theta)$ -relationship

$$\frac{K(\theta)}{K_s} = \left[\frac{\theta - \theta_{ir}}{\theta_s - \theta_{ir}} \right]^{1/\beta} \quad (33)$$

where

- K_s = saturated hydraulic conductivity
- θ_{ir} = irreducible volumetric moisture content
- θ_s = saturated volumetric moisture content
- β = a parameter

The stochastic K_s is scaled according to

$$\frac{K_s}{K_s^*} = \alpha^2 \quad (34)$$

where K_s^* is a weighted average given by $K_s^* = m_K \exp(-2m_\alpha - 2s_\alpha^2)$ [Bresler and Dagan, 1979]. The scaling factor α is lognormally distributed. Setting for simplicity $\theta_{ir} = 0$ and assuming no ponding occurs, i.e. unsaturated flow as $v \theta_s > w$ [Bresler and Dagan, 1981]:

$$v = w / \left\{ (w/K_s^*)^\beta \theta_s \exp(-2\beta \ln \alpha) \right\} \quad (35)$$

where w is the water recharge. Defining $\Xi = (K_s^*)^{-\beta} \theta_s$ then $v = w^{1-\beta} \alpha^{-2\beta} \Xi^{-1}$ where w may be assumed either distributed or non-random. In the latter case:

$$m_V = \ln (w^{1-\beta} \underline{s}^{-1}) - 2\beta m_{\underline{\alpha}} \quad (36a)$$

$$s_V^2 = (2\beta s_{\underline{\alpha}})^2 \quad (36b)$$

Since the lognormally distributed V is defined in $\langle 0, \infty \rangle$ it is clear that ponding occurs for those realizations where $v\theta_g < w$. Generally for temperate regions the year-averaged natural recharge, w , will be much smaller than the flow velocities near saturation and the probability

$\Pr [V < w/\theta_g]$ is small enough to neglect ponding in the long term. The recharge is an important variable because it may control solute input. Except for well defined conditions, the distributed recharge will be hard to assess. Sometimes the distribution of the amount of solute deposited on the soil surface is known. Then we may replace the term vt_M , or wv for continuous input, by the rate of solute deposition. This was done by Van der Zee and Van Riemsdijk [1986] for phosphate transport in a heterogeneous field.

9.3.2.4 Distribution of the retardation factor

The variation in the retardation factor which is given by equation (7b), depends (for particular c_0 and c_1) on the variations in the adsorption parameters (k and n) and the bulk density (ρ). The variation in the adsorption parameters depends on variations in the nature and contents of reactive soil components such as clay minerals, metal oxides, organic carbon as well as the solution composition (pH, ionic strength, etc.). Spatial variability of the distribution coefficient (k) of the pesticide Napropamide was studied by Elabd et al. [1986]. Describing sorption with equation (2) it appeared that k was normally distributed with a coefficient of variation of 0.3. The exponent, n , was approximately unity. For adsorption of Cd and Cu it was shown by Lexmond [1980], Christensen [1981], and Chardon [1984] that n is relatively constant over a wide range of experimental conditions. Lexmond [1980] found for a sandy soil that $n \approx 0.5$ for Cu-sorption and Chardon [1984] found $n \approx 0.85$ for Cd-sorption. The Freundlich- k parameter was highly dependent on the composition of soil

matrix and solution. From the data of Lexmond[1980] and Chardon [1984] for Cu and Cd, respectively, the following isotherm can be found:

$$Q = k^* oc (H^+)^{-\frac{1}{2}} c^n \quad (37)$$

where oc = organic carbon content (g/g*100%)
(H⁺) = hydrogen ion activity
k* = Freundlich k with dependencies on oc and (H⁺)
eliminated

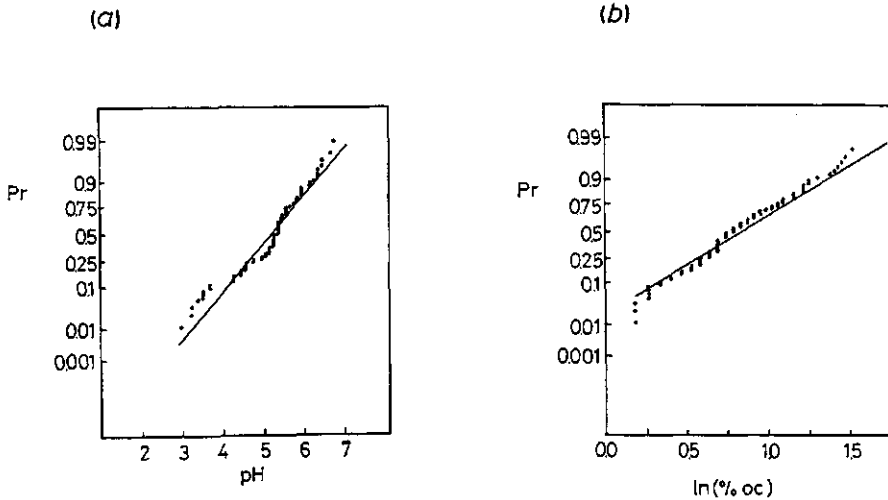


Figure 3: Cumulative probability plots for pH (a) and oc (b), assuming pH is normally distributed $N(5.25, 0.74)$ and oc is lognormally distributed, $\Lambda(0.84, 0.18)$.

Using the data of Chardon [1984] for Cd-sorption we estimated $k^* \approx 2.37 \times 10^{-5}$ for six different soils, with oc ranging from 0.8 to 4.0 wgt-% and pH ranging from 3.4 to 6.4 (with Q in mol kg⁻¹ and c in mol m⁻³).

No data are available for the variability of k^* for Cd or Cu sorption. Hence we assume k^* to be non-random. The distributions for oc and pH are assessed for the 84 Dutch topsoils studied by Van Der Zee and Van Riemsdijk (1986). With 99% significance according to the Kolmogorov-Smirnov test statistic (Birnbaum, 1952) OC was found lognormally distributed with $m_{OC} = 0.84$ and $s_{OC} = 0.42$ whereas pH was normally distributed with $m_{pH} = 5.25$ and $s_{pH} = 0.86$. In Figure 3a and b the probability plots are given for these two variables. With these results and assuming $\rho = 1400 \text{ kg.m}^{-3}$ we can calculate the retardation

$$r \approx \rho \text{ oc } (H^+)^{-\frac{1}{2}} [k^* c_0^{n-1} / \theta] \quad (38)$$

Since the coefficient of variation of ρ is small for the soils studied we neglect the random nature of ρ .

Using the statistics of oc and pH given above the statistics of R are found ($\ln (H^+)^{-\frac{1}{2}} = -\frac{1}{2} \times 2.3 \log (H^+) = \frac{2.3}{2} \text{ pH}$):

$$m_R = m_{OC} + 1.15 m_{pH} + \ln [\rho k^* c_0^{n-1} / \theta] \quad (39a)$$

$$s_R^2 = s_{OC}^2 + (1.15)^2 s_{pH}^2 \quad (39b)$$

These statistics are given in Table 2.

Table 2: Parameter values and distributions used for stochastic transport calculations.

Hydraulic parameters		Chemical parameters	
θ_{ir}	= 0	ρ	= 1400 kg.m ⁻³
θ_s	= 0.4	c_0	= 5 * 10 ⁻⁵ mol.m ⁻³
β	= (7.2) ⁻¹	θ	= 0.2 (eq. 39)
m_K	= 350 m.y ⁻¹	k^*	= 2.4 * 10 ⁻⁵
PDF(α)	= Λ (0, 0.25)	PDF(pH)	= N(5.25, 0.86 ²)
w	= 0.3 m.y ⁻¹	PDF(oc)	= Λ (0.84, 0.42 ²)
PDF(V)	= Λ (0.611, 0.0193)	PDF(R)	= Λ (5.87, 1.16)
PDF(T _c)	= Λ (ln(0.25), 0.317)		

9.3.2.5 Correlated velocity and retardation factor

In the description given so far the stochastic variables were assumed independent. The coefficients of correlation between the travel time of a non-reacting solute and R [Jury, 1983] and between input and retention capacity [Van Der Zee and Van Remsdijk, 1986] had a pronounced effect on the profile shape. Therefore we consider the effect of concentration between V and R. A perfect correlation results if a functional relationship between V and R is given, similar to Jury [1983]:

$$R = \exp(m_R) [\exp(m_V) / V]^\kappa \quad (40)$$

where κ is a parameter. Using this expression the random shock front velocity A is given by $A = V/R = V^{\kappa+1} \exp(-m_R) \exp(-\kappa m_V)$. For correlated V and R we find $m_A = m_V - m_R$ and $s_A^2 = (\kappa + 1)^2 s_V^2$. The value of κ is found from the case of independent V and R where the variance is given by $s_A^2 = (1 + \kappa^2) s_V^2$. Due to the perfect negative correlation between V and R the variance of A increases with respect to the uncorrelated case. Note that as κ becomes large this effect becomes small due to the dominance of f_R on transport.

9.3.3 Profile of sorbed solute

The profile of sorbed solute, $\langle \Gamma(\zeta, \tau) \rangle$, is characterized by the two parameters m_Y and s_Y^2 (i.e., f_Y). In the previous sections the dependency of f_Y on the distributions of V , R , and T was shown and the randomness of Y and R was considered in more detail. In this section we first show how f_Y affects the profile.

The frequency function of the dimensionless penetration depth (f_Y) becomes more symmetrical (Gaussian shaped) as $CV(Y)$ becomes smaller [Simmons, 1981]. Since $CV(Y)$ is given by

$$CV(Y) = [\exp(s_Y^2) - 1]^{\frac{1}{2}} \quad (41)$$

this implies that f_Y becomes more symmetrical as s_Y^2 decreases or as $CV(Y) \rightarrow 0$. A general idea of the profile shape for different

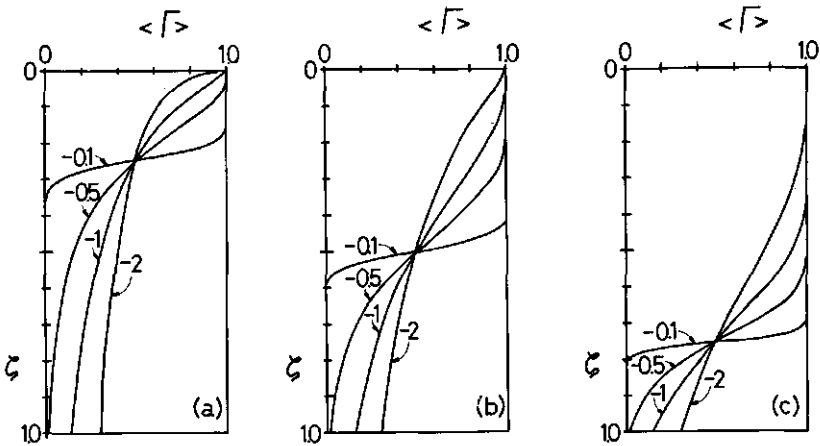


Figure 4: Profiles of field averaged dimensionless sorbed solute, $\langle \Gamma \rangle$.
 a: median penetration depth (Y) is 0.25; b: $Y = 0.50$; c: $Y = 0.75$. Value indicated on the curves is the coefficient of variation of $\ln(Y)$.

\bar{m}_Y and \bar{s}_Y may be obtained from Figures 4a-c. Clearly a Fickian type profile of sorbed solute results when $CV(\underline{Y}) \rightarrow 0$, i.e. small \bar{s}_Y . Comparing Figures 4a-c it may be noted that the value $\langle \Gamma(1, \tau) \rangle$ depends only on $CV(\underline{Y})$, in agreement to equation (26). Therefore it is interesting to show how $CV(\underline{Y})$ depends on the probability density functions of \underline{Y} , \underline{R} , and \underline{T} . Since $CV(\underline{Y})$ is defined as

$$CV(\underline{Y}) = (s_V^2 + s_T^2 + s_R^2)^{1/2} / (\bar{m}_V + \bar{m}_T - \bar{m}_R) \quad (42)$$

it will be affected in a similar fashion by f_V and f_T . Thus only the effects of f_V and f_R on $CV(\underline{Y})$ are shown in Figure 5a and b.

Because the CV -value represents the variability normalized with respect to the mean value of a parameter (which is larger for \underline{R} than for \underline{Y}) the effect of $CV(\underline{R})$ on $CV(\underline{Y})$ is larger than the effect of $CV(\underline{Y})$ on $CV(\underline{Y})$. This may be clearly seen in both Figure 5a and 5b. Using such figures for experimentally evaluated values of $CV(\underline{R})$, $CV(\underline{Y})$ etc., it is

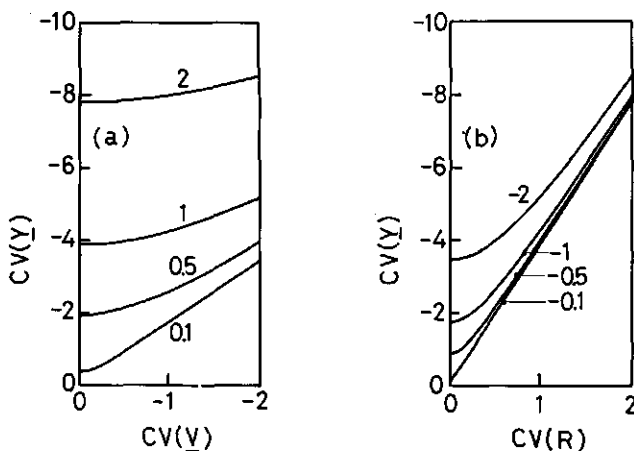


Figure 5: Dependency of $CV(\underline{Y})$ on $CV(\underline{R})$, and on $CV(\underline{Y})$. a: $CV(\underline{Y})$ versus $CV(\underline{Y})$ for designated values of $CV(\underline{R})$ shown on the curves. b: $CV(\underline{Y})$ versus $CV(\underline{R})$ for designated values of $CV(\underline{Y})$ shown on the curves. Parameter values: $\bar{m}_V = -1.2$; $\bar{m}_R = 2.7$; continuous solute input; $\bar{m}_Y = 0.5$ (see Figure 4b).

possible to establish whether one of the stochastic variables controls the value of $CV(Y)$. Thus, in the present case, for $CV(X) > 1$ and $-1 < CV(Y) < 0$ only a small error would result from assuming the pore water velocity to be non-random. In other words: the soil chemistry and the variability of sorption parameters dominates the field scale dispersion for the case given here.

To further illustrate the effect of spatial variability on the profile shape, calculations were done with realistic parameter values for cadmium as given in Table 2. The profiles of Figure 6 are calculated assuming that only V is random (curve 1), that both V and T are random (curve 2), and that V and R are random, respectively. The statistics of V follow from the distribution taken for the scaling factor (α), i.e., $\Lambda(0, 0.25)$. The statistics are in the range reported by Warrick et al. [1977], and Ten Berge [1986]. The single valued annual infiltration rate ($w = 0.3 \text{ m y}^{-1}$) and the saturated volumetric water content ($\theta_s = 0.4$) were given values that are reasonable for Dutch conditions and sandy soil types. The values of m_{K_s} (350 m.y^{-1})

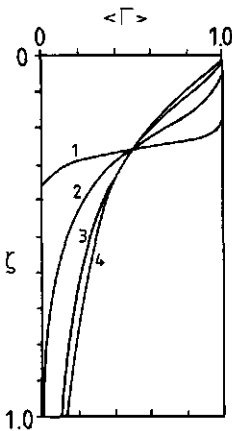


Figure 6: Profiles of field averaged dimensionless sorbed solute ($\langle \Gamma \rangle$) as a function of dimensionless depth, ζ . Curve 1: $s_R^2 = s_{Tc}^2 = 0$, curve 2: $s_R^2 = 0$ and $\tau = 200y$, curve 3: $s_T^2 = 0$, curve 4: $s_{Tc}^2 = 0$, V and R perfectly correlated. Unless indicated differently parameter values as in Table 2. Curves 1, 3 and 4: $\tau = 50y$.

[Stroosnijder, 1976] and $\beta^{-1} = 7.2$ [Bresler and Dagan, 1979] were assumed. These parameter values result in $m_Y = 0.611$ and $s_Y = 0.139$. For the PDF of the input time (T_c) a distribution was assumed for which ϵ (equation 28) equals 0.05, i.e. $T_c:A (\ln(0.25), 0.317)$. With the parameter values and PDF's for oc and pH in Table 2, the distribution of R becomes $R:A (5.87, 1.16)$. This yields a variance for $A (= V/R)$ equal to $s_A^2 = 1.18$ in the case where V and R are uncorrelated. If V and R have a perfect negative correlation s_A^2 becomes 1.48.

The variability in V is relatively small and consequently its effect on the field averaged profile $\langle T(\zeta, \tau) \rangle$ is small (Figure 6; curve 1). Only a little 'field-scale' dispersion occurs and a sigmoid curve is found. The dispersion for this case may be compared to the profile spreading obtained if the field were simulated with an equivalent, homogeneous column with average (i.e. no stochastic) properties. For such an equivalent medium setting $n=1$ the solution of equation (1) is

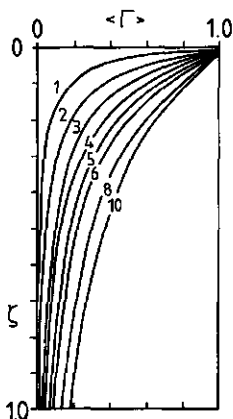


Figure 7: Profile development in time for parameter values of Table 2.

Total time τ is number on the curves multiplied by 25 years.

given by Van Genuchten and Alves [1982] (their case B6), and for the parameter values of Table 2 a front thickness (δ) is found of approximately 0.25 m (mean penetration depth of 0.26 m). Hence, this equivalent front is more dispersed than was calculated for stochastic V. If $n = 0.5$, and assuming the travelling wave is fully developed for a mean penetration depth of 0.26 m, a front thickness of 0.12 m is found. Therefore, for the parameters of Table 2 and continuous solute input, the profiles calculated deterministically for an equivalent medium yield a reasonable prediction of the field averaged profile in the case of insignificant variability in R or if a non-reacting solute is considered.

If the duration of solute input (t_c) is also spatially variable (Figure 6, curve 2), two changes occur with respect to curve 1. First the total time required to find a median penetration depth of 0.26 m becomes larger (four times as large for the present case), and second the profile spreading is significantly enhanced. For the assumed PDF of T_c , (perfect correlation of successive applications) even breakthrough at $z = L$ occurs as $\langle \Gamma(1,200) \rangle = 0.01$.

Assuming continuous input and a distributed retardation factor (R), the 'field scale' dispersion is significantly enhanced. Due to the large value of m_R with respect to m_V the variability in R dominates the shape of the field averaged profile, $\langle \Gamma \rangle$. As $CV(R)$ and $CV(V)$ are approximately the same, this domination of R is in agreement with the discussion given with respect to Figure 5. The profile (curve 3) is clearly non-sigmoid and quite different from the profiles one finds using field-averaged parameters. For the calculation of curve 4 a perfect negative correlation of V and R was assumed. Due to the amplifying effects of variability in V and R on $\langle \Gamma(\zeta, \tau) \rangle$, the 'field scale' dispersion is larger than in curve 3.

In order to calculate the profiles of Figure 6, assumptions were made with respect to the PDF's of V, T_c and R. Where the PDF for V applies to variations found in a single field, the PDF of R reflects variations of different soil types and 84 fields, woodlands, etc. The assumption of perfectly (positively) correlated individual applications may be more valid for an ensemble of different fields, than for an ensemble of columns in one field (see also Van der Zee and Van Riemsdijk, 1986). As no PDF of V for an ensemble of different

fields was available, we have used the distribution given in Table 2. If, however, s_V^2 increases, the effect will be similar to the effect of R, as $A = V/R$ rather than V is the important variable. Consequently, for the ensembles where the PDF's of R and T_c are appropriate, the effect of variability in V may well be significant, and cause a more dispersed profile than curve 1 (Figure 6).

To give an impression of the profile development in time, in the case where V, R and T_c are stochastic variables, profiles were calculated for total times τ ranging from 25 y to 250 y (Figure 7). No Fickian type of displacement occurs if individual applications of solute (Cd) are perfectly correlated. Also in the case of continuous input (where s_Y^2 is also constant and equal to $s_Y^2 = s_R^2 + s_V^2$) no sigmoid profile will occur for large times using the parameter values of Table 2. Hence, in such cases it is in general not warranted to describe field averaged displacement with an equivalent, homogeneous flow domain and reasonable (a priori assessed) parameter values of the transport equation.

9.4 Conclusions

In this contribution we studied transport of reacting solutes in heterogeneous soil systems, using parameter values that are reasonable for cadmium and copper. These solutes sorb according to the Freundlich equation. To evaluate transport in homogeneous columns subjected to an inflowing concentration that is constant and larger than the initial resident concentration, a travelling wave solution of the transport equation is given. If all coefficients in this solution are set equal to unity the equation obtained by Van Duijn and De Graaff [1984] is found. Using realistic parameter values for Cu and Cd, we showed that the travelling concentration wave, has a front thickness that is significantly smaller than would be obtained for a solute with a linear sorption equation. Moreover, once the wave has developed the front thickness and shape do not change with time (or travel distance). This finding validates the approximation to describe the displacement of Cu and Cd with a shock front.

Assuming displacement in a column occurs as a shock front, a

simple expression was developed for the field averaged profile of sorbed solute, using stochastic theory. In this description, a field (or other flow domain with significant heterogeneity in the horizontal plane) is considered to consist of an ensemble of parallel, homogeneous columns that differ with respect to flow velocity, sorption parameter values, and solute input. The variables that differ for each column are considered to be independent, lognormally distributed stochastic variables. The assumption of a lognormal PDF for flow velocity and retardation factor, respectively, and the shape of the distributions as well as how they can be derived from experimental or literature data, were discussed.

The effect of spatial variability on the shape of the field averaged solute profile appeared to be large for the retardation factor and the cumulative duration of solute input. For the stochastic flow velocity this effect was minor for the PDF of V used, and might be discarded if V and R are uncorrelated. If, however, V and R are correlated, or if the variance of V increases by considering variability in the flow velocity for the more diverse ensemble for which the PDF of R applies, then the variability in V may be significant. To show how to evaluate the significance of spatial variation of a variable on the shape of the field averaged solute profile, a relation was given between the coefficient of variation of the penetration depth and the coefficient of variation of the stochastic variables V , T and R .

In general the profile obtained taking spatial variability into account differs from the profile calculated with realistic, field-averaged parameter values. Only in particular cases deterministically and stochastically found profiles yield comparable results.

If solute continuously enters at the soil surface and either little variation in the retardation factor occurs or a non-interacting solute is considered, the description given here reduces to a simplified version of the models given by Bresler and Dagan [1979; 1981; 1983] and Dagan and Bresler [1979]. If spatial variation in V and R is prominent and solute continuously enters at the soil surface the propagation of concentrations in the low concentration range may be considerably faster than found with average parameter values. This particular case is of interest in agricultural land in the Netherlands

due to the continuous, atmospheric deposition of these metals as well as due to the presence of the metals in fertilizers [Van der Zee et al., 1987].

In order to understand the concentrations in groundwater of these metals, as well as other compounds whose displacement may be dominated by spatial variability of the retardation factor, such as pesticides [Elabd et al., 1986] and phosphate [Van der Zee and Van Riemsdijk, 1986], the stochastic nature of transport may be of importance.

9.5 Notation

a	travelling wave velocity, ($m \cdot y^{-1}$) $a = v/r$
c	concentration in solution, ($mol \cdot m^{-3}$)
c_1, c_0	initial (resident) and feed solution concentration ($mol \cdot m^{-3}$)
CV	coefficient of variation (= s/m)
D	hydrodynamic dispersion coefficient (m^2, y^{-1})
f	probability density (frequency) function
F	distribution function, $F = \int f_x dx$
g	transformed concentration, $g = c^{1-n}$
k	Freundlich sorption coefficient ($mol^{1-n} m^{-3n} kg^{-1}$)
k^*	reduced sorption coefficient ($mol^{1-n} m^{-3n} kg^{-1}$)
K	hydraulic conductivity ($m \cdot y^{-1}$), K_s is saturated hydraulic conductivity, reference K_s^* is $m_K \exp(-2m \frac{\alpha}{\alpha} - 2s \frac{\alpha}{\alpha})$
L	reference depth level, column length (m)
m	arithmetic average or expectation value
M	number of yearly sorption-desorption cycles, or years
n	Freundlich power parameter
oc	organic carbon content (wgt-%)
Pr	probability
Q	amount sorbed ($mol \cdot kg^{-1}$)
ΔQ	amount sorbed at c_0 minus amount initially sorbed at c_1 ($mol \cdot kg^{-1}$)
r	retardation factor
s	standard deviation
t	time (y)
t_1, t_c, t_M	time of one sorption-desorption cycle, of solute input (one

	cycle), and total time of solute input in M cycles (y)
v	interstitial fluid velocity ($m \cdot y^{-1}$)
w	fluid recharge rate ($m \cdot y^{-1}$)
X, Y, Z	generic notation random variables
Y	dimensionless penetration depth
z	depth
α	scaling length parameter
β	parameter
γ	dimensionless sorbed amount, $\gamma = Q/Q(c_0)$
Γ	dimensionless random sorbed amount
Γ^*	particular value of Γ
δ	front thickness in one column
δ_1	front thickness for linear isotherm
ϵ	1. heaviside step function argument. 2. probability $Pr [T_M > \tau]$
κ	parameter
η	moving coordinate (m)
η_R, η^*	reference η -value with $c = \frac{1}{2}c_0$, and η -value with $c = 0$ (m)
ρ	dry bulk density ($kg \cdot m^{-3}$)
τ	total time (y)
θ	volumetric moisture content
θ_{ir}, θ_s	irreducible and saturated moisture content
E	parameter
ζ	dimensionless depth
$\zeta_{\frac{1}{2}}, \tilde{\zeta}_{\frac{1}{2}}$	median penetration depths for discontinuous and continuous solute input

9.6 References

- Amoozegar - Fard, A., D.R. Nielsen, and A.W. Warrick. Soil solute concentration distributions for spatially varying pore water velocities and apparent diffusion coefficients, Soil Sci. Soc. Am. J. 46, 3-9, 1982.
- Biggar, J.W., and D.R. Nielsen. Spatial variability of leaching characteristics of a field soil, Water Resour. Res. 12, 78-84, 1976.

- Birnbaum, Z.W. Numerical tabulation of the distribution of Kolmogorov's statistic for finite sample size. *Am. Stat. Ass. J.*, 425-441, 1952.
- Bolt, G.H. Movement of solutes in soil: Principles of adsorption/exchange chromatography, in: G.H. Bolt (ed.) *Soil Chemistry B, Physico-Chemical models*, Elsevier, Amsterdam, 285-348, 1982.
- Bresler, E., and G. Dagan. Solute dispersion in unsaturated heterogeneous soil at field scale: II Applications. *Soil Sci. Soc. Am. J.* 43: 467-472, 1979.
- Bresler, E., and G. Dagan. Convective and pore scale dispersive solute transport in unsaturated heterogeneous fields, *Water Resour. Res.* 17, 1685-1693, 1981.
- Bresler, E., and G. Dagan. Unsaturated flow in spatially variable fields. 3. Solute transport models and their application to two fields, *Water Resour. Res.* 19, 429-435, 1983.
- Chardon, W.J. Mobiliteit van cadmium in de bodem. Ph.D.-thesis, Agricultural University Wageningen, 1984.
- Christensen, T.H. Cadmium sorption onto two mineral soils, Dept. San. Eng., Techn. Univ. Denmark, Lyngby, Denmark, 1980.
- Cleary, R.W., and M.Th. van Genuchten. Movement of solutes in soil: computer simulated and laboratory results, in: G.H. Bolt (ed), *Soil Chemistry B, Physico-chemical models*, Elsevier, Amsterdam, 349-386, 1982.
- Dagan, G., and E. Bresler. Solute dispersion in unsaturated heterogeneous soil at field scale: I. Theory, *Soil Sci. Soc. Am. J.* 43:461-467, 1979.
- Deans, H.H. A mathematical model for dispersion in the direction of flow in porous media. *Soc. Pet. Eng. J.*, 3(1), 49-52, 1963.
- De Willigen, P. Some theoretical aspects of the influence of soil-root contact on uptake and transport of nutrients and water. *Proc. ISSS symposium Water and solute movement in heavy clay soils* (Ed. J. Bouma and P.A.C. Raats). ILRI publ. 37, 268-275, 1985.
- Elabd, H., W.A. Jury, and M.M. Clith. Spatial variability of pesticide adsorption parameters. *Env. Sci. Technol.* 20, 256-260, 1986.

- Jury, W.A. Simulation of solute transport using a transfer function model, *Water Resour. Res.* 18, 363-368, 1982.
- Jury, W.A. Chemical transport modelling: current approaches and unresolved problems, in: *Chemical Mobility and Reactivity in Soil Systems*, ASA, SSSA, Madison, Wisconsin, 1983.
- Jury, W.A., L.H. Stolzy, and P. Shouse. A field test of the transfer function model for predicting solute transport. *Water Resour. Res.* 18(2): 369-375, 1982.
- Lexmond, Th.M. The effect of soil pH on copper toxicity to forage maize grown under field conditions. *Neth. J. Agric. Sci.*, 28, 164-183, 1980.
- Nielsen, D.R., J.W. Biggar, and K.T. Erh. Spatial variability of field measured soil-water properties, *Hilgardia* 42, 215-221, 1973.
- Papoulis, A. *Probability, Random Variables and Stochastic Processes*, McGraw-Hill, Koga Kusha, Tokyo, 327-332, 1965.
- Parker, J.C., and A.J. Valocchi. Constraints on the validity of equilibrium and first-order kinetic transport models in structured soils. *Water Resour. Res.* 22(3): 399-408, 1986.
- Peck, A.J., 1983. Field variability of soil physical properties. *Adv. Irrigation*, 2, 189-221, 1983.
- Persaud, N., J.V. Giraldez, and A.C. Chang. Monte-Carlo simulation of non-interacting solute transport in a spatially heterogeneous soil. *Soil Sci. Soc. Am. J.* 49, 562-568, 1985.
- Rasmuson, A., and I. Neretnieks. Exact solution of a model for diffusion in particles and longitudinal dispersion in packed beds. *Am.Inst.Chem.Eng.J.* 26, 686, 1980.
- Rasmuson, A. and I Neretnieks. Migration of radionuclides in fissured rock: The influence of micropore diffusion and longitudinal dispersion. *J. Geophys. Res.* 86, 3749, 1981.
- Reiniger, P. and G.H. Bolt. Theory of chromatography and its application to cation exchange in soils. *Neth. J. Agric. Sci.*, 20, 301-313, 1972.
- Russo, D. and E. Bresler. Soil hydraulic properties as stochastic processes. I. An analysis of the field spatial variability. *Soil Sci. Soc. Am. J.* 45, 682-697, 1981.
- Simmons, C.S. A stochastic-convective transport representation of dispersion in one dimensional porous media systems. *Water Resour.*

- Res. 18(4), 1193-1214, 1981.
- Skopp, J., and A.W. Warrick. A two-phase model for the miscible displacement of reactive solutes in soils. *Soil Sci. Soc. Am. Proc.*, 38, 545-555, 1974.
- Sposito, G., R.E. White, P.R. Darrah, and W.A. Jury. A transfer function model of solute transport through soil. 3. The convection dispersion equation. *Water Resour. Res.* 22(2), 255-262, 1986.
- Stroosnijder, L. Infiltratie en herverdeling van water in grond. Ph.D. thesis, Agric. Univ. Wageningen. Pudoc, Wageningen, 1976.
- Tang, D.H., E.O. Frind, and E.A. Sudicky. Contaminant transport in fractured porous media: Analytical solution for a single fracture. *Water Resour. Res.* 17(3), 555-564, 1981.
- Ten Berge, H.F.M. Heat and mass transfer at the bare soil surface Ph.D. thesis, Agric. Univ. Wageningen. Wageningen, 1986.
- Valocchi, A.J. Validity of the local equilibrium assumption for modelling sorbing solute transport through homogeneous soils. *Water Resour. Res.* 21, 808-820, 1985.
- Van Genuchten, M.Th., and P.J. Wierenga. Mass transfer studies in sorbing porous media, I. Analytical solutions. *Soil Sci. Soc. Am. J.* 40, 473-480, 1976.
- Van Genuchten, M.Th., and P.J. Wierenga. Mass transfer studies in sorbing porous media, II. Experimental evaluation with tritium ($^3\text{H}_2\text{O}$). *Soil Sci. Soc. Am. J.* 41, 272-278, 1976.
- Van Genuchten, M.Th., and W.J. Alves. Analytical solutions of the one-dimensional convective-dispersive solute transport equation. *USDA Techn. Bull.* no. 1661, 151 p, 1982.
- Van Genuchten, M.Th., D.H. Tang, and R. Guennelon. Some exact and approximate solutions for solute transport through large cylindrical macropores. *Water Resour. Res.* 20, 335-346, 1984.
- Van Genuchten, M.Th., and F.N. Dalton. Models for simulating salt movement in aggregated field soils. *Geoderma* 38, 165-183, 1986.
- Warrick, A.W., G.J. Mullen, and D.R. Nielsen. Scaling field measured soil hydraulic properties using a similar media concept. *Water Resour. Res.* 13(2), 355-362, 1977.
- Van Duijn, C.J., and J.M. de Graaf. Limiting profiles in contaminant transport through porous media. Delft Univ. Techn., Rep. Dept.

Math. and Informatics 84-31 pp 32, 1984.

Van der Zee, S.E.A.T.M. and W.H. van Riemsdijk. Transport of phosphate in a heterogeneous field. Transport in Porous Media 1, 339-359, 1986.

White, R.E., J.S. Dyson, R.A. Haigh, W.A. Jury, and G. Sposito.

A transfer function model of solute transport through soil, 2: illustrative applications. Water Resour. Res. 22(2): 284-254, 1986.

Van der Zee, S.E.A.T.M., W.H. van Riemsdijk, Th.M. Lexmond, and

F.A.M. de Haan. Vulnerability in relation to physico-chemical compound behaviour, and spatially variable soil properties. Proc. Int.'l Conf. 'Vulnerability of soil and groundwater to pollutants', National Institute of Public Health and Environmental Hygiene (in press) 1987 Noordwijk aan Zee, March 30-April 3, 1987.

10. ANALYSIS OF PHOSPHATE LEACHING FROM A HETEROGENEOUS FIELD

Abstract

Disposal of phosphate (P) containing animal manure in quantities far exceeding crop requirements has resulted in P-accumulation in Dutch topsoil. Even if excessive disposal is stopped, accumulated P may desorb and be leached into the groundwater in concentrations, that are environmentally hazardous. The redistribution of P initially present in topsoil is simulated assuming that P-sorption occurs according to the Langmuir isotherm. The effects of the adsorption constant (K), the adsorption maximum (Q_m), and the thickness (L_s) of the initially P-saturated topsoil layer, on the numerically calculated concentration distribution in a soil column, and on the transport rate of the front developing in the subsoil, are in agreement with trends predicted with an approximate analytical solution. Concentrations at the phreatic water level (L) increase faster when K or Q_m are decreased, when L_s is increased, or when the subsoil has a smaller adsorption maximum than the topsoil. Taking spatial (horizontal) variability of Q_m and/or L_s into account results in earlier breakthrough of environmentally undesirable P-concentrations at $z=L$. Due to the buffering of concentrations caused by adsorption/desorption, the quality of groundwater recharge will improve very slowly, once it has been affected adversely. Based on simplifications, that are justified in view of the simulation results, a simple approach is given to identify in a routine fashion field sites, that are suspected of endangering groundwater quality in future. Whereas probabilistic criteria are feasible, it is shown that the evaluation of future groundwater recharge quality in many cases may be done using mean values of stochastic variables.

10.1 Introduction

Animal manure disposal on land in agricultural use has caused a significant phosphate (P) accumulation in soil in some Dutch regions.

Recent government regulations prohibiting future manure disposal on fields that are considered P-saturated, are aimed at preventing the leaching of large amounts of P to ground and surface water, that may cause surface water eutrophication. However, part of the already accumulated P in soil may desorb. Hence, in order for the regulations to be effective it is necessary to also prevent future leaching of large amounts of desorbable P, after disposal is stopped. Therefore the evaluation which field should be considered P-saturated should take the redistribution of reversibly sorbed P into account. A field should then be considered P-saturated if the sorption capacity of the subsoil is too small to prevent future leaching of high P-concentrations due to desorption in the topsoil.

Transport of P in homogeneous columns was studied by Gupta and Greenkorn [1974], Enfield and co-workers [1975, 1981, 1984], Beek [1979], and Van Der Zee and Van Riemsdijk [1986a]. As the experimental conditions for these studies differed also different results were obtained. In the high P-concentration range ($0.2-20 \text{ mol m}^{-3}$) Gupta and Greenkorn [1974] studied transport in washed sand and kaolin clay mixtures, in order to assess the dispersion coefficient and the adsorption constant. They found that a linear isotherm described the data well, except at high clay contents or small concentrations.

Enfield and Shew [1975], Enfield et al. [1981] and Stuanes and Enfield [1984] studied P-displacement at smaller concentrations from the scope of waste water disposal. Enfield and Shew [1975] found a reasonable to good prediction of P-breakthrough for different column lengths if the sorption parameters were estimated using batch experiments. Best results were obtained if they described sorption kinetics with the equation $dS/dt = a c^b S^d$, that was proposed by Enfield [1974]. In later work Enfield et al. [1981] described the overall sorption with a fast, reversible adsorption (Langmuir isotherm) in combination with slower, reversible, first order kinetics precipitation reactions. The reaction in their soil occurs predominantly with calcium compounds in the solid phase. Good agreement was obtained between predicted and experimental breakthrough curves. Stuanes and Enfield [1984] were able to fit breakthrough curves well with an analytical solution for transport with linear adsorption and a first order, irreversible precipitation, in acidic soils.

In the same concentration range as Enfield and co-workers (c up to 0.1 mol.m^{-3}) Beek [1979] described P-sorption with two adsorption processes and one irreversible second order kinetics reaction. Although breakthrough was predicted well for small columns, Beek [1979] was not able to predict the field averaged P-profile for a field of a disposal farm, if he used sorption and dispersion parameters assessed independently with laboratory experiments. For concentrations up to 3 mol.m^{-3} the prediction of breakthrough in small soil columns found by Van Der Zee and Van Riemsdijk [1986a,b] was in good agreement with experimental results. The reaction model used, consisted of a non-equilibrium, reversible adsorption, with equilibrium given by the Langmuir isotherm, and a non-equilibrium irreversible precipitation reaction. The precipitation reaction was described with a semi-empirical equation derived from the unreacted shrinking core model known from chemical engineering literature [Wen, 1968; Van Der Zee and Van Riemsdijk, 1986b].

Whereas P-displacement can be accurately described for small soil columns, the transport in the field usually poses additional problems. Due to differences in the horizontal and the vertical direction of the contents of reactive soil constituents (e.g. Ca, Fe, and Al), the transport velocity of P differs for different soil horizons and different locations in the field. If we envision a field as an ensemble of vertical columns, that have different P-sorption capacities, also the P-displacement rate differs for each column. To take such heterogeneity into account Van Der Zee and Van Riemsdijk [1986c] did not use mean sorption parameters, but characterized both P-input (A_T) and the reaction capacity of the soil till groundwater (F_T) with probability density functions (PDF). Neglecting pore scale dispersion the field averaged profile of sorbed solute was described with stochastic theory. It was found that the spatial variability of A_T and F_T has a large effect on the field averaged profile. In a subsequent paper an analytical expression was derived for the field averaged profile for the case where the flow velocity (v), the retardation factor (R), and the time of solute input (t_m), were lognormally distributed variables [Van Der Zee and Van Riemsdijk, 1987].

In this work the redistribution of P already present in soil is considered. Because of the large time scale involved, experimental evaluation is not well possible, and a modelling approach is necessary. Numerical calculations are done for a soil that is P-saturated in the topsoil layer of thickness L_g , and has a low initial P-content in the subsoil between $z=L_g$ and $z=L$. Only the dissolved and the reversibly adsorbed fractions of topsoil-P are redistributed. The precipitation process, that may occur in the subsoil, is not taken into account. The effects of the adsorption maximum (Q_m), the adsorption constant (K) and the thickness of the initially P-saturated top layer (L_g) on the redistribution process are evaluated for one soil column. The effect of horizontal soil heterogeneity on the field averaged redistribution process is studied by simulating an ensemble of columns where L_g and Q_m are stochastic variables.

10.2 Theory

To describe the redistribution of phosphate (P) in a soil column it is necessary to distinguish different reaction processes. In agreement to earlier work [Van Der Zee and Van Riemsdijk, 1986a,b] the over all reaction is described with a reversible adsorption in combination with an irreversible precipitation. The adsorption process may be described with the Langmuir equation

$$Q = \frac{KQ_m c}{1 + Kc} \quad (1)$$

where Q is the adsorbed amount, mol.kg^{-1} , c is the concentration, mol.m^{-3} , K is the adsorption constant, $\text{m}^3.\text{mol}^{-1}$, Q_m is the adsorption maximum, mol.kg^{-1} . By using equation (1) instead of the rate expression used by Van Der Zee et al., (1986a) the assumption of equilibrium is made. For most practical situations in the field this assumption is valid, in view of the values given for the adsorption and desorption rate constants by Van Der Zee et al. [1986a].

The values of K and Q_m may differ for different soil types and parent materials. For soil developed in sandy parent material it was found that K is $10\text{-}50 \text{ m}^3.\text{mol}^{-1}$, whereas the adsorption maximum Q_m was

found to depend on the amount of oxalate extractable iron and aluminium [Van Der Zee and Van Riemsdijk, 1988, Chapter 7]. This reactive metal content is denoted by M, and the adsorption maximum Q_m equalled approximately 0.135 M. Because M differs from place to place, we may expect that this is also the case for Q_m .

The precipitation reaction is not taken into account. For the topsoil, which we will assume initially P-saturated, neglect of the precipitation process will not affect the results, because this process is supposed to be irreversible [Van Der Zee and Van Riemsdijk, 1986a, Chapter 7]. In the subsoil precipitation may in principle occur. Therefore the P-displacement in the subsoil will be estimated too high if we disregard P-precipitation.

The mathematical formulation of P-transport is based on the convection dispersion equation, and is given for adsorption according to equation (1) by

$$\frac{\partial}{\partial t} [\rho Q + \theta c] = \theta D \frac{\partial^2 c}{\partial z^2} - \theta v \frac{\partial c}{\partial z} \quad (2)$$

where ρ is the dry bulk density, $\text{kg}\cdot\text{m}^{-3}$, θ is the volumetric water fraction, v is the interstitial flow velocity, $\text{m}\cdot\text{y}^{-1}$, D , is the apparent dispersion coefficient, $\text{m}^2\cdot\text{y}^{-1}$. The initial and boundary conditions for the P-redistribution process are chosen as

$$t=0 \quad c=c_i \quad Q=0.99Q_m \quad 0 < z < L_s \quad (3a)$$

$$t=0 \quad c=c_j \quad Q=0.05Q_m \quad L_s < z < L \quad (3b)$$

$$t > 0 \quad (vc - D \frac{\partial c}{\partial z}) = 0 \quad z=0 \quad (4a)$$

$$t > 0 \quad \frac{\partial c}{\partial z} = \text{finite} \quad z=L \quad (4b)$$

The dispersion coefficient, D , in equation (2) is the sum of the molecular diffusion coefficient, D_m (equal to the diffusion coefficient in a clear solution and corrected for the soil tortuosity and volumetric water fraction) and the hydrodynamic dispersion coefficient, D_h . It is assumed that D_h is the result of dispersion as well as stagnant water effects [Raats, 1981; De Smedt et al., 1981; Bolt, 1982] and may be described for large enough displacement times by

$$D_h = v \lambda_d \quad (5)$$

where λ_d is the medium dispersivity at the average water content. In the numerical approximations the suitable corrections for numerical error [Van Genuchten and Wierenga, 1974; Herzer and Kinzelbach, 1987] were taken into account.

A usefull expression for understanding the trends observed numerically for the concentration in the column, may be obtained if dispersion phenomena are neglected in equation (2). First set

$$y = vt \quad (6)$$

$$g = c + \rho Q(c)/\theta \quad (7)$$

Then equation (2) becomes

$$\frac{\partial g}{\partial y} + \frac{\partial c}{\partial z} = 0 \quad (8)$$

Combination of equation (8) with (1) yields

$$\frac{\partial u}{\partial z} + \left[1 + \frac{q}{(1+u)^2} \right] \frac{\partial u}{\partial y} = 0 \quad (9)$$

where

$$q = \rho K Q_m / \theta \quad (10a)$$

$$u = K c \quad (10b)$$

Equation (9) is solved for the conditions

$$u(0, y) = u_0 \quad 0 < y < \gamma \quad (11a)$$

$$u(0, y) = 0 \quad y > \gamma \quad (11b)$$

$$u(z, 0) = 0 \quad g(z, 0) = 0 \quad (12)$$

Thus γ may be considered the time required to saturate a column till a depth of $z=L_g$, if v is constant. If equations (9), (11), and (12) are solved, a shock front is found for $0 < y < \gamma$, that moves along the characteristic

$$y = z \left(1 + \frac{q}{(1+u_0)^2} \right) \quad (13)$$

Below this shock front u equals zero, and above it is u_0 . As at $y=\gamma$ the front reaches $z=L_s$, the concentration at $z=0$ drops to zero and all concentrations between $u=0$ and $u=u_0$ are present in the column. The characteristics for each concentration are different as the retardation factor, $R(u)$, is given by

$$R(u) = 1 + q/(1 + u)^2 \quad (14)$$

which is smaller as u is larger. Hence the characteristics diverge according to

$$y - \gamma - z R(u) = 0 \quad 0 < u < u_0 \quad (15)$$

The characteristic for $u=u_0$ intersects the characteristic for the shock front given by equation (13) at the point (z_0, y_0)

$$z_0 = \gamma (1 + u_0)^2 / qu_0; \quad y_0 = \gamma(1 + u_0)(1 + u_0 + q) / (qu_0) \quad (16)$$

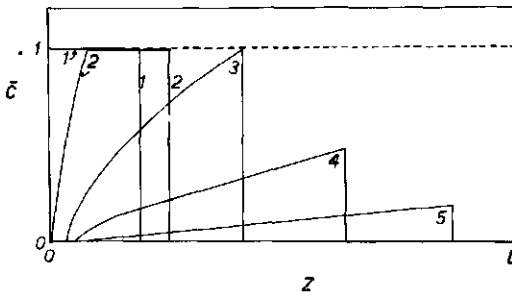


Figure 1: Schematic representation of redistribution according to equations (21) and (22).

Beyond this intersection point a shock is found with diminishing height (the maximum of u decreases as $y-\gamma$ increases). The different stages of the redistribution process are shown in Figure 1. The position of this shock is found by first rearranging equation (15)

$$q (y - \gamma - z) / z = q^2 / (1 + u)^2 \quad (17)$$

Then we write for the retardation factor of the shock front

$$R_f = dy/dz = 1 + q/(1 + u). \quad (18)$$

Hence

$$\frac{dy}{dz} - 1 = q/(1 + u) = \frac{d}{dz}(y - \gamma - z) \quad (19)$$

Combination with equation (17) yields

$$\frac{d}{dz} (y - \gamma - z) = \sqrt{[q(y - \gamma - z)/z]} \quad (20)$$

This equation may be integrated and, after substitution of (16) for the point where the shock begins, this yields (Aris and Amundson, 1973)

$$(y - \gamma - z)^{\frac{3}{2}} = (q z)^{\frac{3}{2}} - (\gamma u_0)^{\frac{3}{2}} \quad (21)$$

The concentration till the penetration depth given by (21) is found from equation (15) after rearrangement

$$u = \sqrt{zq[(y-\gamma) - z]^{-1}} \quad (22)$$

Whereas for understanding the transport in one column is of interest, in practice one is mainly interested in the leaching of P into the phreatic water for a field. This transport process is significantly affected by the heterogeneity of the field with respect to important variables, such as the reaction capacity, the P-amount applied, or the application rate, the flow velocity, etc. Then the field may be considered to be an ensemble of columns, with different parameter values for each column. By solving numerically the transport equations for each column i ($i=1, \dots, N$) the concentration distribution in depth and the distribution of the adsorbed amount in depth may be obtained. After normalization by division with the maximum values (c_0, Q_m) the degree of P-saturation in solution and solid phase, respectively, are found: \bar{c} and \bar{Q} . These properties are distributed and their mean values are given by the first moment. Thus for e.g. \bar{c} at

depth z and time t the mean $\langle \bar{c} \rangle$ is given by

$$\langle \bar{c}(z,t) \rangle = \int_0^1 \bar{c} f_{-}(z,t;\bar{c}) d\bar{c} \quad (23)$$

which we calculate with the arithmetic average of $\bar{c}(z,t)$. In case of an assumed non-random v , we may write for the average amount leached from the field past the phreatic water level at $z=L$

$$J_P = A v \theta c_0 \langle \bar{c}(L,t) \rangle \quad (24)$$

where A is the field surface area. It was found by De Haan and Van Riemsdijk [1986] that in P-saturated topsoils the concentration is buffered at a value of approximately 3 mol P m^{-3} . This value is a thousand fold of the concentrations that may cause in surface water eutrophication. Therefore by comparing $\langle \bar{c}(L,t) \rangle$ with the value

$\langle \bar{c} \rangle = 0.001$ we have an impression of the eutrophication hazard when the leached water enters the surface water.

10.3 Results and discussion

10.3.1 Effect of adsorption constant (K)

In Chapter 7 the numerical values of the adsorption constant ($K=10$ to $50 \text{ m}^3 \cdot \text{mol}^{-1}$) and adsorption maximum ($Q_m \approx 0.135 \text{ M}$) were obtained. For other soil types developed in sandy parent material a larger range in K -values ($K=10-90 \text{ m}^3 \cdot \text{mol}^{-1}$) was found by Van Der Zee and Van Riemsdijk [1986a]. The K -value affects the steepness of the isotherm (equation 1). For the range of the K -values given the adsorption maximum is reached at concentrations of a few $\text{mol} \cdot \text{m}^{-3}$. Hence the differential adsorption capacity, defined as

$$Q'(c) = KQ_m / (1 + Kc)^2 \quad (23)$$

is small for c close to c_0 , or \bar{c} close to unity. This implies that little concentration buffering occurs by desorption at such high concentrations, for all expected K -values. Only when the concentration

has dropped to values of the order $K^{-1} \text{ mol.m}^{-3}$ buffering will be significant. Therefore, when an initially saturated topsoil is leached with water that contains no P, in the first stage \bar{c} decreases rapidly, whereas \bar{Q} remains almost constant at its initial value of unity. Next, as \bar{c} becomes of the order of magnitude of $(c_0K)^{-1}$ the decrease of \bar{c} becomes slow due to desorption, and \bar{Q} begins to decrease significantly.

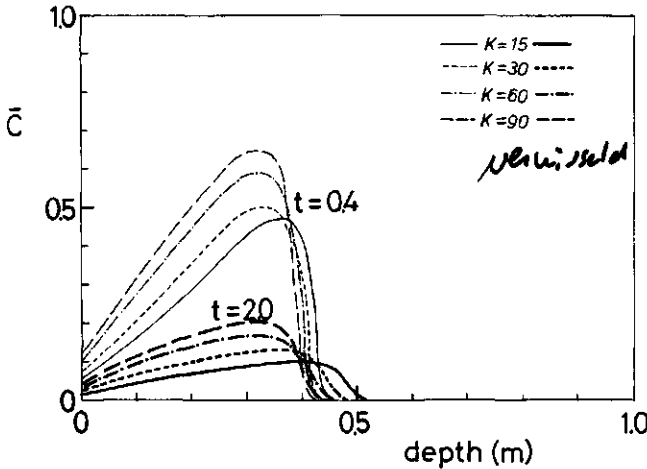


Figure 2: Dimensionless concentration (\bar{c}) as a function of depth (z) for different times (in years) indicated in the figure.

In Figure 2 the dimensionless concentration (\bar{c}) is given as a function of depth (z), for different K-values and times and other parameters as given in Appendix 1. Because the value $(c_0K)^{-1}$ decreases for increasing K, significant buffering occurs at smaller \bar{c} as K is increased. Indeed the initial decrease in \bar{c} is larger as K is larger. On the long term, however, the buffering at small \bar{c} ($\approx (c_0K)^{-1}$) is larger for higher K, as follows from equation (23). Hence, on the long term \bar{c} in the topsoil and passing $z = L_s$ will be higher as K is higher. The K-value also has implications for transport in the subsoil ($z > L_s$). The phosphate leached into the subsoil will partly be adsorbed below $z=L_s$. The adsorbed part will be larger when the product Kc is higher (equations 1 and 23). As was just shown, on the long term this product is higher for water percolating past $z = L_s$ for high K-

values. Hence, at large times the retardation factor of the P-concentration front in the subsoil (equation 18) is highest for high K-values, and the front moves slower. The net effect of parameters on the transport velocity of the subsoil front has compensating factors. As was shown a higher K-value leads to larger values of c passing $z = L_g$. The higher c in the subsoil is, the smaller retardation factor would be expected at first glance (eq. 18; u increases). However, also in the subsoil K is larger, which tends to increase R_f as the fraction of P adsorbed at a particular depth increases. To see which tendency dominates we write equation (22) in the original variables:

$$c = \frac{1}{K} \left\{ \left[\frac{\rho z K Q_m / \theta}{v(t-t_0) - z} \right]^{\frac{1}{2}} - 1 \right\} \quad \text{to be used instead of eq. 22} \quad (24)$$

and insert expression (24) into R_f (equation 18), which in terms of the original variables is given by

$$R_f = 1 + \frac{\rho}{\theta} \frac{K Q_m}{(1 + Kc)} \quad (25)$$

For the depth (z) we insert the value L_g . This implies that we assume that for large times the concentration at $z=L_g$ is a good indication (i.e. almost the same value) of the maximum concentration in the soil column, close to the P-front. It can be seen from Figure 2 and other figures not yet discussed, that this is a justified assumption.

Working this out yields for R_f (which for $y > \gamma$ becomes time dependent)

$$R_f = 1 + \left\{ \frac{\rho K Q_m [v(t-t_0) - L_g]}{L_g \theta} \right\}^{\frac{1}{2}} \quad (26)$$

As we can see from approximation (26), the velocity (v/R_f) of the subsoil front will on the long term (when $c(L_g)$ gives a good impression of R_f) decrease with increasing K and Q_m . Due to the decrease in $c(L_g)$ with increasing time, the front retardation factor increases with time.

Although the effect of K on the redistribution process is shown to be significant (Figure 2), preliminary simulations showed that the sensitivity to L_g and Q_m is much larger. Therefore the other calculations are performed with a K -value of $45 \text{ m}^3 \text{ mol}^{-1}$, which is intermediate in the expected K -range.

10.3.2 Effect of P-saturated layer thickness (L_s)

The dissolved and adsorbed amount of phosphate initially present in the soil equals $(\rho L_s Q_m + \theta L_s c)$. Because the first term predominates, L_s and Q_m in fact represent the amount of P that may be redistributed. In combination with the subsoil thickness and subsoil adsorption maximum, L_s and Q_m control how fast the P-front will move through the subsoil (equation 21). For different values of L_s the concentration profile, $\bar{c}(z)$, was calculated and the result is shown in Figure 3.

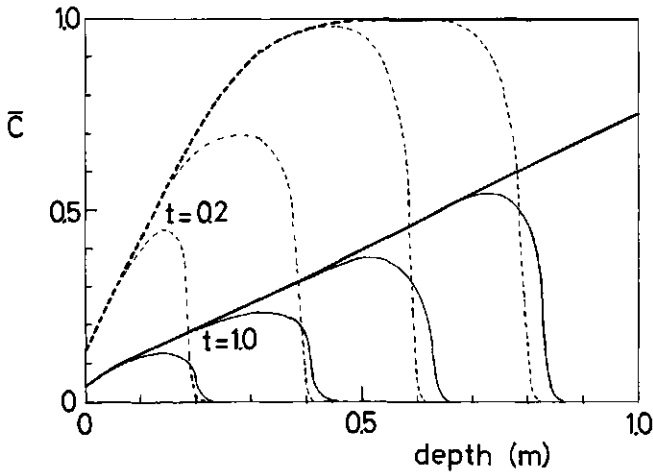


Figure 3: Dimensionless concentration (\bar{c}) as a function of depth (z) for different times and thickness of the initially P-saturated layer (L_s).

At small depths ($z < L_s$) these profiles coincide at a given time, in agreement to approximation (22). The analytical approximation of equations (21) and (22) is not shown in the figure. Because pore scale dispersion was neglected in the analytical solution, the maximum concentration in the column and the penetration depth are not predicted well [Bolt, 1982]. However, to understand the main trends, as in Figure 3, the approximation is helpful. Thus, equation (22) predicts that as γ is larger the concentration at a fixed depth ($z > z_0$) is larger than for smaller γ ($t > \gamma/v$). Indeed, as Figure 3 shows, when L_s is increased the period that high concentrations are leached into

the subsoil increases. This may be made more explicit using equation (24). A dimensionless time is defined as

$$\tau = t/t_s \quad (27)$$

where t_s is the time required to replace one pore volume of the topsoil layer with $0 < z < L_s$. Thus $t_s = L_s/v$, and time is expressed as the number of time units of duration t_s (e.g. $t_0 = \gamma/v = R_f t_s$). Inserted in equation (24) this yields

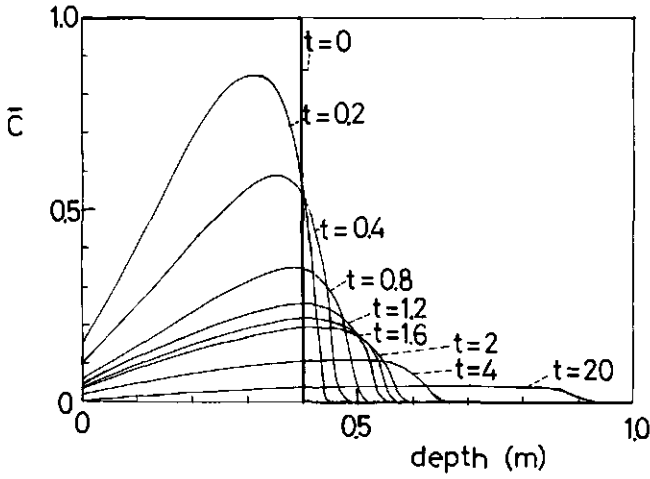
$$c(L_s, t) = K^{-1} \left\{ \left[\frac{\rho K Q_m}{\theta(\tau - R_f - 1)} \right]^{\frac{1}{2}} - 1 \right\} \quad (28)$$

It may be seen immediately from equation (28) that if $\tau - R_f$ is the same for two columns with different values of L_s , the same concentration at the interface at $z=L_s$ is found. In other words: the interface concentration at $z=L_s$ is the same for columns with different values of L_s , if the number of topsoil pore volumes leached is the same. If instead the concentration $c(L_s, t)$ is compared at the same time t , τ will be smallest for the column with largest L_s and largest t_s . The value of

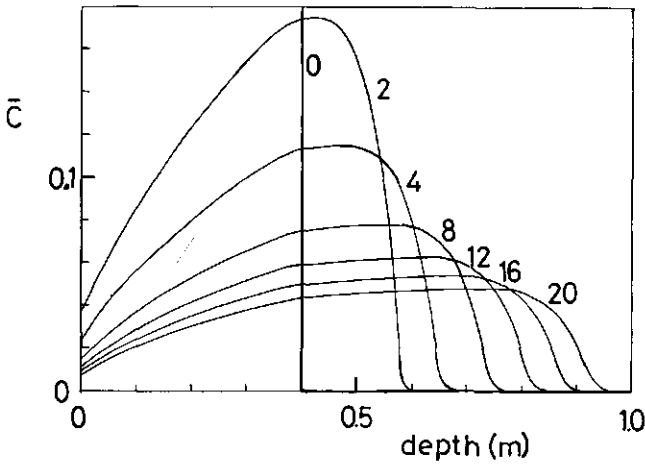
R_f is the same for both columns and equals the retardation factor, for $c=c_0$. Because $\tau - R_f - 1$ is smallest for the column with larger value of L_s , $c(L_s, t)$ is also larger. Working out this result for R_f , similar to equation (26), shows that in a dimensionless τ coordinate system, relative to L_s , both columns behave the same. In the z -coordinate system, however, the subsoil front moves fastest towards the phreatic water level for the column with larger L_s . Moreover, because the amount of reversibly adsorbed P that can be stored in the subsoil, above a fixed phreatic level (taken here at $z=lm$), decreases when L_s increases, the hazard that high concentrations reach the phreatic level increases.

10.3.3 Effect of adsorption maximum (Q_m)

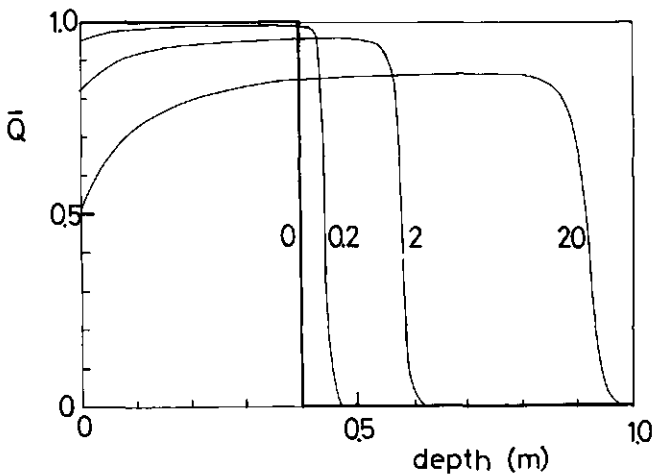
For homogenous columns it was suggested (Chapter 7), that the value of Q_m and the variability in this value do not significantly



(a)



(b)



(c)

Figure 4:
concentration (\bar{c}) as a function of depth (z) for different times, in case of different adsorption maximum of the top soil ($Q_m = 12 \text{ mmol.kg}^{-1}$) and the sub soil ($Q_m = 3 \text{ mmol.kg}^{-1}$).
Figure 4a: short term.
Figure 4b: long term.
Figure 4c: dimension less adsorbed amount (\bar{Q}) as a function of depth.

influence the long term concentrations at the phreatic level when $L_s \ll L$. However, the effect of Q_m is not absent. From equation (26) we can see that R_f increases proportionally with $\sqrt{Q_m}$. Hence, besides some effects on the shape of the concentration distribution, the displacement rate of the front in homogeneous columns is affected by Q_m . Since in Chapter 7 we did not take the rate of displacement into account, but compared different (limiting) situations at large times, this effect of Q_m was not made explicit. Different than might be concluded from that work homogeneous columns with different values of Q_m do not behave the same.

More pronounced effects are seen if Q_m varies with depth. This situation resembles the case of varied L_s -values, because in both cases the storage capacity in the subsoil is varied, relative to the stored P-quantity in the topsoil. For simplicity variations in depth, of Q_m , are accounted for by distinguishing two layers only, where the topsoil again is P-saturated.

In Figure 4a and 4b the concentration profiles are shown for small and large times, respectively, if the subsoil has a much smaller adsorption maximum ($Q_m = 3 \text{ mmol.kg}^{-1}$) than the topsoil (Appendix 1). Whereas this does not very much affect the concentration distribution for $0 < z < L_s$, the front velocity in the subsoil becomes larger, than in the reference case. For a column with two distinct layers with different values of Q_m , the retardation factor R_f in the subsoil becomes proportional to $Q_{m,s}$ of the subsoil, whereas we observed that for a homogeneous column R_f was proportional to $\sqrt{Q_m}$ (equation 26). The front retardation factor is given by

$$R_f = 1 + Q_{m,s} \left\{ \frac{\rho K [v(t-t_0) - L_s]}{L_s \theta Q_{m,t}} \right\}^{\frac{1}{2}} \quad (29)$$

where $Q_{m,s}$ and $Q_{m,t}$ refer to the adsorption maximum in the subsoil and topsoil, respectively. Considering the corresponding \bar{Q} -profiles (Figure 4c) it is clear that a relatively steep P-front is found.

Soil profiles with a high sesquioxide content in the topsoil, where the ploughing layer consists of A and B horizon material, and a low sesquioxide content in the subsoil, are frequently found in Dutch sandy areas [Van Der Zee and Van Riemsdijk, 1986c; 1988]. In these areas the intensive animal husbandry is concentrated that causes the

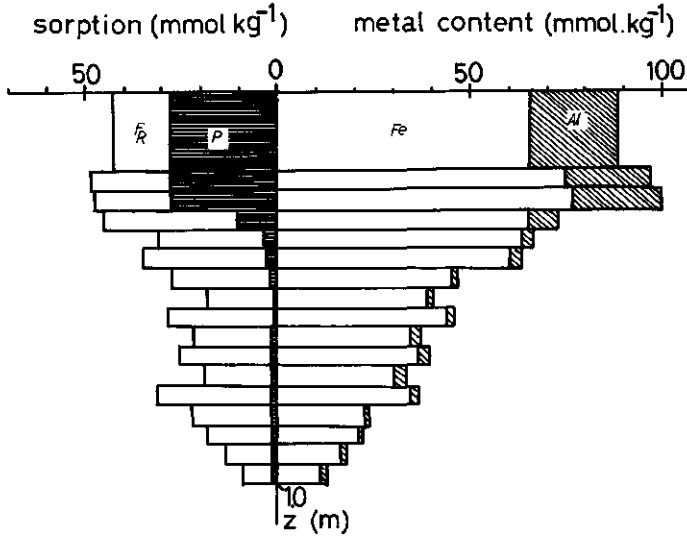


Figure 5: Oxalate extractable amounts of P, Fe, and Al, and the pseudo sorption maximum (F_m), attained at $c = 3 \text{ mmol.m}^{-3}$ and 1-2 years reaction time, as a function of depth (z).

large P input in soil. Generally the decrease of the sesquioxide content (and of Q_m) is more gradual with depth. For illustration the profiles of oxalate extractable Fe, Al and P are shown in Figure 5 for a location in the field studied by Van der Zee and Van Riemsdijk [1986c]. The gradual decrease of the reactive metal content, M, defined by Van der Zee and Van Riemsdijk [1988] from topsoil values of approximately 90 mmol.kg^{-1} to subsoil values of 20 mmol.kg^{-1} is clearly visible. This induces approximately a five fold decrease in the total sorption capacity assessed according to Van der Zee and Van Riemsdijk [1988]. A rather sharp P front is also observed, that shows small P-losses from the ploughing layer ($z < 0.4$) that is not yet P-saturated, to the subsoil. In some situations also the reverse case is found where Q_m increases with increasing depth. Clearly then the subsoil represents a barrier with respect to P-leaching and high concentrations do not reach the phreatic ground water quickly.

10.3.4 Spatial variability of Q_m and L_s

In view of the results given so far the parameters L_s and Q_m can be considered to dominate the P-redistribution process. As was shown by Van Der Zee and Van Riemsdijk [1986c] the amount of P applied to soil, the oxalate extractable sesquioxide content (M) and thus Q_m vary in the horizontal plane. To give an impression of this variation the oxalate extractable Fe, Al, and P are shown in Figure 6 for three layers and for 51 locations on a transect in the field studied by Van Der Zee and Van Riemsdijk [1986c].

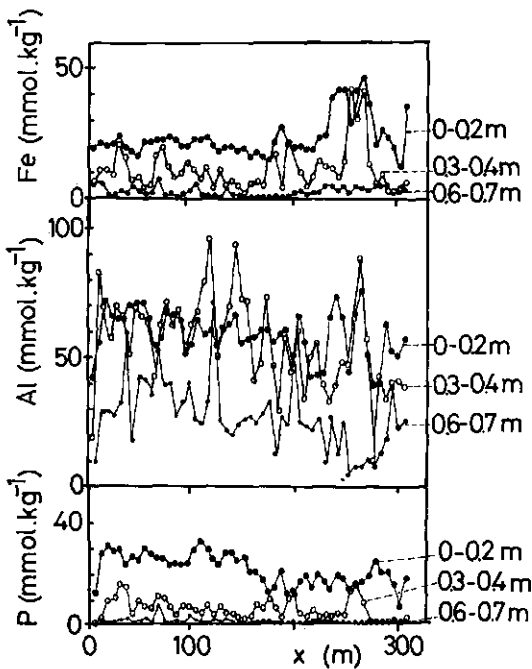


Figure 6: Oxalate extractable amounts of P, Fe, and Al in three layers for 51 locations on a transect.

Besides the profound decrease with increasing depth we see a large random variation around a mean value. Moreover trends occur in the mean value for Al_{ox} , in the layers 0-0.2 m depth and 0.6-0.7 m depth, and P_{ox} in the layer 0-0.2 m depth. These differences correspond with

differences in P sorption capacity and in P applied to the field. Because this spatial variability was shown to have a large effect on the field averaged P-displacement [Van Der Zee and Van Riemsdijk, 1986c] the same may be expected for the redistribution of P, averaged for a field.

Using Monte Carlo simulations the effect of spatial variability of Q_m and L_s on the redistribution of P was studied. In order to understand the results of such simulations it is best not to vary too many parameters at the same time. Therefore other variables, known to be random (e.g. v , θ , K) are kept single-valued. The results apply to independent stochastic variables. Two situations are considered. The first is a field consisting of a number of homogeneous columns (with respect to v , K , Q_m etc.) . For this case the results of a 'field-equivalent' column and a field with random Q_m , L_s , or both, are compared. The second case is a schematization of the field studied by Van Der Zee and Van Riemsdijk [1986c]. Parameter values for both situations are given in Table 1, with other parameters (than Q_m and L_s) given in Appendix 1.

Table 1: Statistics of the adsorption maximum (Q_m) and the thickness of the initially P-saturated topsoil layer (L_s) used for Monte Carlo simulations, assuming normal distributions $N(m; s^2)$, with m = expectation, s^2 = variance.

	Fig. 7	Fig.8	Fig.8	Fig.9
$Q_m(\text{topsoil})$	$N(11;4)$	$N(11;4)$	$11(\text{NR})^1$	$N(11;4)$
$Q_m(\text{subsoil})$	$N(11;4)$	$N(6;9)$	$6(\text{NR})^1$	$N(6;9)$
L_s	$N(0.4;0.01)$	$0.4 (\text{NR})^1$	$N(0.4;0.01)$	$N(0.4;0.01)$

1) (NR) means non random.

In Figure 7 the concentration front is shown for a single column with average properties. We observe at the long term a gradual (almost linear) increase in \bar{c} with increasing z , and a well defined front in the subsoil at $z = 0.7$ m. Taking instead the average concentration calculated for $L_s = 0.4$ and Q_m random (with statistics realistic for the topsoil of the field studied by Van Der Zee and Van Riemsdijk

[1986c]) only small changes occur. The main effect is a more dispersed subsoil front. That only small changes occur is mainly due to the small coefficient of variation ($CV = s/m$) of Q_m .

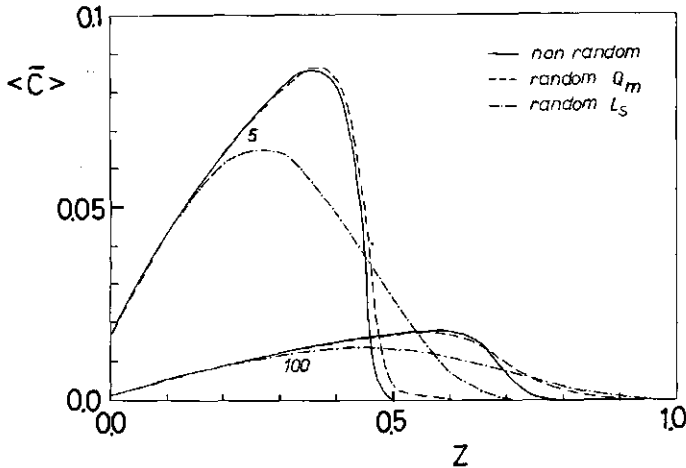


Figure 7: Average dimensionless concentration ($\langle \bar{c} \rangle$) as a function of depth (z) for a field that is homogeneous with depth, when Q_m and L_s are not random, if Q_m is random and L_s is single-valued, and if L_s is random and Q_m is single valued. Time in years indicated in the figure.

A much larger effect is seen if Q_m is single valued and equal to 11 mmol.kg^{-1} , and L_s is taken random. The maximum concentration, $\langle \bar{c} \rangle$, is now located at shallower depth than for the other situations in Figure 7, and no well defined subsoil front is observed, as it is 'smeared out' considerably. That, for the statistics chosen for Q_m and L_s , the sensitivity of the simulation results is largest for the variation of L_s became clear when both L_s and Q_m were taken random. The resulting $\langle \bar{c} \rangle$ -profiles showed minor differences with respect to the case where only L_s is random (and are therefore not shown in Figure 7).

The case of Figure 7 applies to a field with vertical differences only in the initial P contents. For the field studied by Van Der Zee and Van Riemsdijk [1986c] different contents of P_{ox} , Al_{ox} , and Fe_{ox} , were found for different depths (Figure 6). Using the statistics of M

in the topsoil and the subsoil, as well as the statistics of the value of L_s given by Van Der Zee and Van Riemsdijk [1986c] (their variables $(\text{Fe+Al})_{\text{ox}}$ and ζ_p , respectively) P-redistribution in this field is studied. The value of Q_m is found from M by setting $Q_m = 0.135 M$. Parameters not specified in Table 1 are found in Appendix 1.

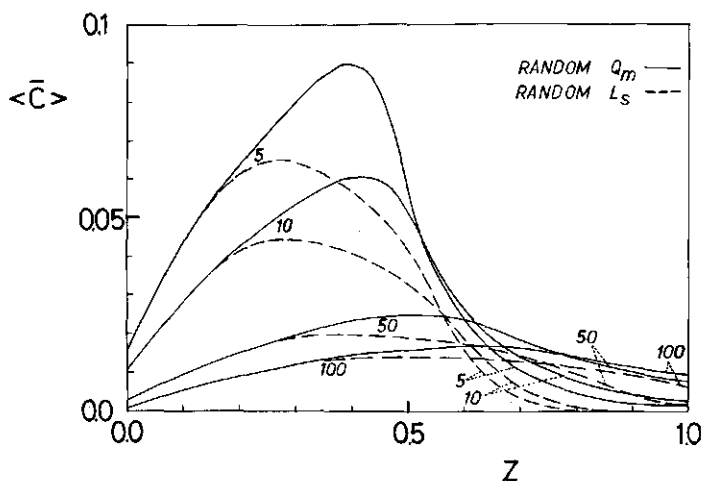


Figure 8: Average dimensionless concentration ($\langle \bar{c} \rangle$) as a function of depth (z) assuming Q_m is random and L_s single-valued and assuming L_s random and Q_m single-valued. Time in years indicated in the figure.

In Figure 8 the field averaged concentration profiles are shown when only Q_m is considered random (and Q_m in topsoil and subsoil are not correlated) or when only L_s is random. In both cases the $\langle \bar{c} \rangle$ -profiles are quite different from the \bar{c} -profiles in Figure 4. If only Q_m is random the profile in the topsoil ($z < 0.4$) is comparable to the top sections of the profiles in Figures 4 and 7. In the subsoil, however, no well-defined front is seen. We see a gradual decrease in $\langle \bar{c} \rangle$ (in the subsoil) with increasing depth, caused by the differences in the ensemble of fronts that each have a different penetration depth. The result differs from Figure 7, because very different combinations of $Q_{m,s}$ and $Q_{m,t}$ lead to very different rates of front movement in the subsoil (eq.29). Another cause is, of course, the relatively large coefficient of variation of $Q_{m,s}$ i.e., $CV = 0.50$. This

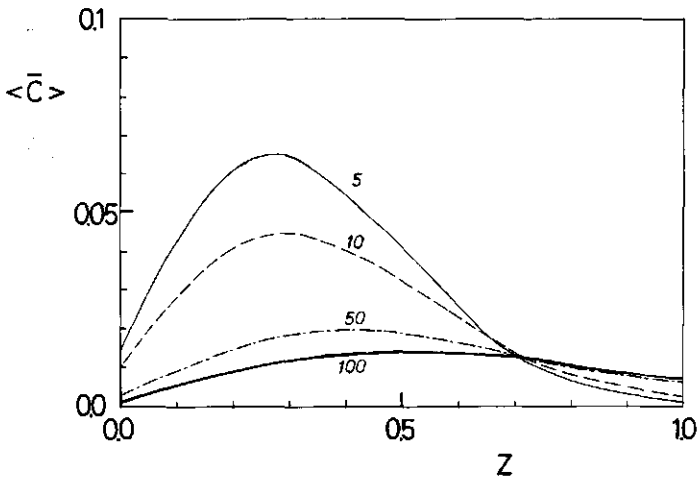


Figure 9: Average dimensionless concentration ($\langle \bar{c} \rangle$) as a function of depth (z) assuming both Q_m and L_s are random. Time in years indicated in the figure.

value was experimentally found by Van Der Zee and Van Riemsdijk [1986c]. Also shown is the situation where Q_m is single valued, though different in topsoil and subsoil, and where L_s is random. The effect of taking only L_s is prominent as the $\langle \bar{c} \rangle$ -profiles are dispersed even more, than if only Q_m is random. Due to the small value of $Q_{m,s}$ the concentrations at the phreatic level increase faster in Figure 8 than in case of Figure 7. When both Q_m and L_s are random (Figure 9) and uncorrelated, a situation is found intermediate to those of Figure 8, but most resembling the case where Q_m is single valued and L_s is random.

10.5 Environmental implications

When the phosphate concentrations in surface waters is the limiting factor for algae growth, which is often the case in the Netherlands, then excessive algae growth may occur at concentrations exceeding a few mmol P m^{-3} . To avoid surface water eutrophication, the P-load supplied by e.g. sewage effluent, diffuse agricultural sources, domestic waste water, etc., should not give rise to concentrations of

1-5 mmol P.m⁻³. Insofar as most surface water recharge originates from groundwater, it is therefore undesirable that concentrations larger than a few mmol m⁻³ are leached into the groundwater. This is a demanding constraint as De Haan and Van Riemsdijk [1986] showed, that the animal manure/topsoil mixture buffers the concentration in P-saturated topsoils at a thousand fold higher value (approximately 3 mol.m⁻³). Hence, it is undesirable that \bar{c} becomes larger than say 10⁻³.

Reviewing the calculation results with this constraint in mind, we can estimate that for a uniform soil column \bar{c} might exceed 10⁻³ at the phreatic groundwater level, if $L_g/L < 0.4$. For a non-uniform soil column, with a subsoil that has an adsorption maximum smaller than the (P-saturated) topsoil adsorption maximum (e.g. as in Figure 4) such concentrations will already leach into groundwater after a few decades. If we furthermore take spatial variability of Q_m and L_g , into account concentrations of the order of magnitude of $\bar{c} \approx 0.01$ may be leached already after five years for the field on average! As may be seen in e.g. Figure 8 and 9, on the long term the concentration does not change (decrease) quickly anymore due to the buffering caused by desorption. Therefore we may conclude that if \bar{c} becomes say 0.01 after five to ten years, it may take (many) decades before it has decreased again to below 10⁻³. In short this means that if the quality of groundwater recharge has at some time become environmentally hazardous, it will not quickly become acceptable again.

It should be noted here that in practice other complications, not considered here, may soften these conclusions. Due to the presence of the precipitation process the P-transport in the subsoil may occur slower. In view of other aspects, however, such as the temporal variations of the phreatic water level, the stochastic nature of the flow velocity, etc., it may not be justified to consider the approach as a worst case risk analysis.

The results indicate how to deal with the identification of those fields that are suspected of being P-saturated (see introduction). Such identification should be feasible on a routine basis, because the total Dutch agricultural area where large excesses of animal manure are produced is large. A simple approach is based on the almost uniform concentration (or \bar{c}) profiles found in one column (e.g. Figure

4), and the small value of \bar{c} that is permitted to be leached. This basis allows us to assume, that at the moment that the maximum concentration that is allowed to leach reaches the phreatic level, and this acceptable maximum concentration is approximately 3 mmol m^{-3} , the concentration throughout the column is on average say $\tilde{c} = 2 \text{ mmol.m}^{-3}$.

Since K^{-1} is larger than 0.001, we may assume a practically linear adsorption isotherm for $\bar{c} < 0.002$. We can now calculate how much P has desorbed in the originally P-saturated topsoil when \bar{c} has decreased from unity to 6.6×10^{-4} ($c=2 \text{ mmol.m}^{-3}$). This amount is

$$q_1 = \rho L_s (Q_{m,t} - \tilde{Q}_t) \quad (30)$$

where \tilde{Q}_t is adsorbed at $\bar{c} = 6.6 \times 10^{-4}$, and the storage in solution is neglected. The amount q_1 should be balanced by the amount (q_2) that may be adsorbed at $\tilde{c} = 2 \text{ mmol.m}^{-3}$ in the subsoil. If we assume that the subsoil has an adsorption maximum ($Q_{m,s}$) different from $Q_{m,t}$ in the topsoil, such that $Q_{m,s} = \epsilon Q_{m,t}$ (and thus $\tilde{Q}_s = \epsilon \tilde{Q}_t$), then q_2 equals

$$q_2 = \rho (L - L_s) \epsilon \tilde{Q} \quad (31)$$

Equating (30) and (31) and insertion of the Langmuir equation for \tilde{Q} yields a constraint for L_s [Chapter 7, $\gamma = 1$]

$$L_s = L K \tilde{c} \epsilon / [1 + K \tilde{c} \epsilon] \quad (32)$$

Equation (32) gives the acceptable value of L_s that leads on the long term to an average concentration of approximately \bar{c} throughout the column. Since for the acceptable range of \bar{c} we have $K\tilde{c}\epsilon \ll 1$ we may simplify (32) to

$$L_s \approx \epsilon K \tilde{c} L \quad (33a)$$

or

$$\tilde{c} = L_s (\epsilon K L)^{-1} \quad (33b)$$

Because we considered only the concentration profile when the subsoil front has reached $z=L_s$, and not at what time this depth is reached, the absolute value of $Q_{m,t}$ could be eliminated in equations (32) and (33). Due to the slow decrease in the concentration at longer times the differences in front arrival times at $z=L_s$ for different columns will hardly result in a significant relaxation of the constraints (32) and (33). Of more importance are the value of \tilde{c} considered acceptable and the random nature of L, K , and ϵ . On the basis of e.g. equation (33a) we may now evaluate for any field, whether future leaching of concentrations larger than $2-3 \text{ mmol m}^{-3}$ will occur, on average. Inserting a mean K -value ($K=45 \text{ m}^3 \text{ mol}^{-1}$), $\epsilon \approx 0.5$, and $\tilde{c} = 2 \text{ mmol.m}^{-3}$, we have $L_s/L = 0.05$, which is much smaller than the mean value (0.36) found by Van Der Zee and Van Riemsdijk [1986c] for the field considered here.

For situations where the measured L_s is not significantly larger than its acceptable value it may be necessary to take the randomness of e.g. K and L_s into account. This may be done using equation (33b). When K and L_s are assumed independently lognormally distributed and denoting the statistics of their logarithmic transforms by m and s^2 , we have [Van Der Zee and Van Riemsdijk, 1987]

$$m_{\ln \tilde{c}} = m_{\ln L_s} - m_{\ln K} - \ln(\epsilon L) \quad (34a)$$

$$s_{\ln \tilde{c}}^2 = s_{\ln L_s}^2 + s_{\ln K}^2 \quad (34b)$$

where \tilde{c} is also lognormally distributed. After specification of the tolerated probability (Pr^*), that \tilde{c} exceeds a values of \tilde{c}^*

$$\begin{aligned} \text{Pr}[\tilde{c} > \tilde{c}^*] &= \int_{\tilde{c}^*}^{\infty} [c/(2\pi)s_{\ln \tilde{c}}]^{-1} \exp\{-\frac{1}{2} [(\ln \tilde{c} - m_{\ln \tilde{c}}) / s_{\ln \tilde{c}}]^2\} d\tilde{c} \\ &= \frac{1}{2} \left\{ 1 - \text{erf} \left[\frac{\ln(\tilde{c}^*) - m_{\ln \tilde{c}}}{s_{\ln \tilde{c}} \sqrt{2}} \right] \right\} < \text{Pr}^* \end{aligned} \quad (35)$$

we find whether unacceptable P-leaching losses will occur. It may be noted that if K or L_s are lognormally distributed with a small coefficient of variation (s/m), they are also reasonably well normally

distributed [Simmons, 1981]. When this is the case [Van Der Zee et al., 1988] and constraint (33b) is met for the mean values of K and L_g , it is reasonable to assume that the field average concentration, $\langle \tilde{c} \rangle$, does not exceed $2\bar{c}$. Then the stochastic approach leading to equation (35) is not necessary, and we may just evaluate the field with field averaged values. In Appendix D of this thesis some attention is given to this situation.

10.6 Conclusions

In this paper the redistribution of P initially present sorbed and in solution in the topsoil is studied. The redistribution of soil-P is of interest to assess the hazard of eutrophication of surface water due to leaching of P already present in soil. Because only the fractions dissolved and reversibly adsorbed P are assumed to be redistributed in the soil profile the precipitation reaction was not taken into account. This implies that the transport velocity of the P-front, that is formed in the initially P-unsaturated subsoil, is overestimated.

The adsorption of P with soil is described with the Langmuir isotherm. Transport was calculated using parameter values for the adsorption constant (K) and the adsorption maximum (Q_m) in the ranges found in Chapter 7. Due to the high value of K and c_0 , the concentration buffering by desorption in the topsoil when a solution without P is percolated, is initially very small. Therefore the concentration decreases fast in the topsoil, until the steep part of the Langmuir isotherm is reached, at $c \approx K^{-1} \text{ mol.m}^{-3}$. Then significant desorption occurs and c becomes almost constant with increasing time. The concentration passing the depth $z \approx L_g$ affects the P-front retardation factor in the subsoil. By evaluation of an approximate analytical solution for P-redistribution if pore scale dispersion is neglected the effects of different parameters on the transport velocity of the P-front in the subsoil can be understood. The moving velocity of the front depends significantly on the amount of P stored in the topsoil and the storage capacity in the subsoil. Thus an increase of the thickness of the initially P-saturated layer or of the

topsoil adsorption maximum causes an increase in the displacement rate of the subsoil front. A decrease in the subsoil adsorption maximum also favours a high subsoil front velocity.

If spatial variability of the P-saturated topsoil thickness and the adsorption maximum is taken into account no well defined subsoil front is found, for the field on average. Instead, a gradual decrease in the field-averaged dimensionless concentration is observed. The trend found if heterogeneity is considered, is a more rapid breakthrough of potentially hazardous concentrations for the field on average at the phreatic groundwater level. Due to concentration buffering by desorption it will take large leaching times before the P-concentration in the groundwater recharge improves to acceptable values again, once it has become too high.

Because the acceptable concentration level is small with respect to the value of K^{-1} , simple criteria may be developed for the assessment whether groundwater recharge quality will in future become unacceptable. The calculations were performed for phosphate. It may be expected, though, that for other contaminants with a highly non-linear adsorption, and relatively small acceptable concentrations in groundwater, the trends observed for P, will also be applicable.

Acknowledgement: Part of the calculations were performed by Maarten Saaltink, whose assistance was appreciated.

10.7 Appendix 1: Parameter values used in the simulations

$$\theta = 0.3$$

$$D_m = 0.00236 \text{ m}^2 \cdot \text{y}^{-1}$$

$$l_d = 0.04 \text{ m}$$

$$v = 1 \text{ m} \cdot \text{y}^{-1}$$

$$\rho = 1400 \text{ kg} \cdot \text{m}^{-3}$$

$$L_S = 0.4 \text{ m (ref.case)}$$

$$Q_m = 12 \text{ mmol} \cdot \text{kg}^{-1} \text{ (ref.case)}, 3 \text{ mmol} \cdot \text{kg}^{-1}$$

$$c_i = c_0 = 3 \text{ mol} \cdot \text{m}^{-3} \text{ (ref.case)}$$

$$K = 45 \text{ m}^3 \cdot \text{mol}^{-1} = 0.045 \text{ m}^3 \cdot \text{mmol}^{-1} \text{ (ref.case)}$$

Ref. case = reference case.

10.8 Notation

A	field surface area (m^2)
c	concentration in solution ($mol.m^{-3}$)
c_0	initial concentration in topsoil ($mol.m^{-3}$)
\bar{c}	dimensionless concentration ($=c/c_0$)
\tilde{c}	average concentration in column at large times ($mol.m^{-3}$)
$\langle \bar{c} \rangle$	horizontally averaged dimensionless concentration
CV	coefficient of variation ($=s/m$)
D	apparent dispersion coefficient ($m^2.y^{-1}$)
$D_m; D_h$	coefficient of molecular diffusion, and hydrodynamic dispersion ($m^2.y^{-1}$)
erf(x)	errorfunction ($= \frac{2}{\sqrt{\pi}} \int_0^x \exp(-x^2) dx$)
f	probability density function
g	total volumetric solute content
J_P	field average leaching rate ($mol.y^{-1}$)
K	adsorption constant ($m^3.mol^{-1}$)
L	column length, phreatic groundwater level (m)
L_s	thickness P-saturated topsoil (m)
l_d	dispersivity (m)
M	oxalate extractable (Fe + Al) ($mmol.kg^{-1}$)
m	arithmetic mean
q	parameter
$q_1; q_2$	desorbed P in topsoil, adsorbed P in subsoil (mmol)
Q	adsorbed amount ($mmol.kg^{-1}$)
\bar{Q}	dimensionless adsorbed amount
\tilde{Q}	adsorbed amount at $c=\tilde{c}$ ($mmol.kg^{-1}$)
$\langle \bar{Q} \rangle$	horizontally averaged dimensionless adsorbed amount
Q_m	adsorption maximum, subscript t: topsoil; s: subsoil. ($mmol.kg^{-1}$)
R(u)	retardation factor at relative concentration u
R_f	front retardation factor
$s; s^2$	standard deviation; variance
t	time (y)
t_s	time to leach one topsoil pore volume (y)

t_0	time to saturate a layer of thickness L_g with phosphate (y)
$u; u_0$	relative concentration ($=Kc$); $u=u_0$ at $c = c_0$
v	pore flow velocity ($m\ y^{-1}$)
y	transformed time (m)
z	depth (m)
ϵ	ratio of subsoil adsorption maximum/topsoil adsorption maximum
γ	transformed saturation time (m)
ρ	dry bulk density ($kg\cdot m^{-3}$)
θ	volumetric water fraction
τ	dimensionless time

10.9 References

- Aris, R, and N.R. Amundson, *Mathematical methods in Chemical engineering volume 2, First order partial differential equations with applications*, Prentice-Hall, Inc., Englewood Cliffs, New Jersey, 1973, 182-221.
- Beek, J., *Phosphate retention by soil in relation to waste disposal*, Ph D-thesis, Agricultural University, Wageningen, 1979.
- Bolt, G.H., *Movement of solutes in soil: Principles of adsorption/exchange chromatography*, in *Soil Chemistry B, Physico-Chemical Models*, edited by G.H. Bolt, pp 285-348, Elsevier, Amsterdam, 1982.
- De Haan, F.A.M., and W.H. van Riemsdijk, *Behaviour of inorganic contaminants in soil*, in *Contaminated soil*, edited by J.W. Assink and W.J. van den Brink, pp. 19-32, Martinus Nijhoff, Dordrecht, 1986.
- De Smedt, F., P.J. Wierenga, and A. van der Beken, *Theoretical and experimental study of solute movement through porous media with mobile and immobile water*. Vrije Universiteit Brussel, 1981.
- Enfield, C.G. and D.C. Shaw, *Comparison of two predictive nonequilibrium one dimensional models for phosphorus sorption and movement through homogeneous soils*. *J. Environm.Qual.* 4: 198-202, 1975.
- Enfield, C.G., T. Phan, D.M. Walters, and R. Ellis, Jr., *Kinetic model for phosphate transport and transformation in calcareous soils, I*,

- Soil Sci. Soc. Am.J. 45: 1059-1064, 1981.
- Gupta, S.P., and R.A. Greenkorn, Determination of dispersion and non-linear adsorption parameters for flow in porous media, Water Resour. Res. 10 (4) pp 839-846, 1974.
- Raats, P.A.C. Transport in structured porous media, in Flow and Transport in Porous Media, edited by A. Verruijt and F.B.J. Barends, pp 221-226, Balkema, Rotterdam 1981.
- Simmons, C.S., A stochastic-convective transport representation of dispersion in one dimensional porous media systems, Water Resour Res. 18 (4) pp. 1193-1214, 1981.
- Stuanes, A.O., and C.G. Enfield, Prediction of phosphate movement through some selected soils, J. Environ.Qual. 13 (2) pp. 317-320, 1984.
- Van Genuchten, M Th., and P.J. Wierenga, Simulation of one-dimensional solute transfer in porous media, Agric. Exp. Station, Bull.628,40 pp.
- Van Der Zee, S.E.A.T.M. and W.H. van Riemsdijk, Sorption kinetics and transport of phosphate in sandy soil, Geoderma 38, pp 293-309, 1986a.
- Van Der Zee, S.E.A.T.M., and W.H. van Riemsdijk, Model for the reaction kinetics of phosphate with oxides and soil, Proc. Conf.Interactions at the Soil Colloid - Soil Solution Interface, August 24-29, Ghent, Belgium, 1986b, (in press).
- Van Der Zee, S.E.A.T.M., and W.H. van Riemsdijk, Transport of phosphate in a heterogeneous field, Transport in Porous Media 1, pp 339-359, 1986c.
- Van Der Zee, S.E.A.T.M., and W.H. van Riemsdijk, Transport of reactive solute in spatially variable soil systems, Water Resour. Res. (in press) 1987.
- Van Der Zee, S.E.A.T.M., L.G.J. Fokking, and W.H. van Riemsdijk, A new technique for assessment of reversibly adsorbed phosphate, Soil Sci. Soc. Am. J. 51, pp 599-604, 1987.
- Van Der Zee, S.E.A.T.M. and W.H. van Riemsdijk, Model for long term phosphate reaction kinetics in soils, J.Environ Qual. (in press), 1988.
- Wen, C.Y., Non-catalytic heterogeneous solid fluid reaction models Ind. Eng.Chem. 60 (9), pp 34-54, 1968.

11. SOLUTE TRANSPORT PARALLEL TO AN INTERFACE SEPARATING TWO DIFFERENT POROUS MATERIALS

Abstract

The transport of solute is studied for a flow domain consisting of two regions that are separated by a sharp interface parallel to the direction of water flow. The two regions have different flow velocities, linear adsorption coefficients and porosities. An approximate analytical solution is given for the depletion of solute in the most permeable region caused by transfer of solute into the less permeable region. To take into account the boundary conditions at the interface, an approximate expression is derived for the concentration at the interface. In the derivations the longitudinal dispersion coefficient is assumed to be zero, and the transversal dispersion coefficient is taken finite. For comparison to numerical results, an expression for the concentration averaged over the height in the permeable region, at given distance and time, is presented. The agreement of numerically obtained breakthrough curves and interface concentrations with the analytical results is shown. Due to the zero longitudinal dispersion coefficient in the analytical approach, differences occur at initial breakthrough. Agreement between numerical and analytical results is good after initial breakthrough provided the assumption of two infinitely thick regions is valid. Lower bound constraints for the thickness of the two regions are given. The assumption made often, of infinite transversal dispersion leads to significant differences compared to numerical results in the case of a large retardation factor, R_2 , in the region with the smallest transport velocity.

11.1 Introduction

The transport of solute in groundwater is the result of convection, diffusion, dispersion and of retarding mechanisms such as adsorption. The mathematical formulation of miscible displacement in

porous media is given by the convection-dispersion equation [Bear, 1979]. Often a major factor that limits the predictive capability of this equation is the heterogeneity of porous media. This problem has motivated a number of studies dealing with the effect of heterogeneity on transport. Since it is recognized that the size of the flow domain is of importance [Fried, 1975] the effect of heterogeneity has been studied on several scales.

Solute transport through structured media received attention from Deans [1963], Skopp and Warrick [1974], Van Genuchten and Wierenga [1976], Raats [1981] and Van Genuchten and Cleary [1982], among others. These studies considered a macroscopically homogeneous soil that is assumed to have both mobile and stagnant water. The transfer of solute between the two phases is controlled by a diffusion type process. Both Deans [1963] and Van Genuchten and co-workers described this transfer with a first-order mass transfer equation. Van Genuchten and Wierenga [1976] gave explicit solutions for the concentrations in the mobile and immobile phases assuming linear adsorption. A review and parameter sensitivity analysis is given by Van Genuchten and Cleary [1982], who also considered non-linear and non-equilibrium adsorption behaviour. Skopp and Warrick [1974] and Raats [1981] described the transfer process by solving a diffusion equation for the stagnant zone. Raats showed that this results in additional large scale dispersion that can be accounted for by an extra term in the transport equation.

A different approach applicable to transport through fractured rock was mentioned by Freeze and Cherry [1979] and further elaborated upon by Neretnieks [1980], Tang et al. [1981], Grisak and Pickens [1980], Rasmuson and Neretnieks [1980, 1981], Rasmuson [1981] and Van Genuchten et al. [1984]. The single fracture model with zero longitudinal dispersion coefficient and infinite transversal dispersion coefficient in the fracture presented by Neretnieks [1980] was extended by Tang et al. [1981], who gave an analytical expression for the convective-dispersive transport in the fracture with simultaneous diffusion of solute into the surrounding rock. Using a numerical model Grisak and Pickens [1980] calculated the concentration distributions in both the fracture and the rock-matrix and obtained good agreement with experimental results. Following earlier work,

Rasmuson and Neretnieks [1980] described the transport of solute through a bed of adsorbing spherical particles with diffusive transport into the particles and one-dimensional convective-dispersive transport in the mobile region. Rasmuson [1981] extended this analysis to two dimensions including dispersion transversal to the macroscopic flow direction. Van Genuchten et al. [1984] used a fracture model for a cylindrical macropore system and gave analytical solutions of this problem.

A fracture model was used by Chen [1985] to describe the radial dispersion in an aquifer with simultaneous diffusive loss in confining layers. Because of the assumption of an infinite transversal dispersion coefficient the concentration in a cross section of the aquifer was constant (Chen, 1985, eq. 2). Solutions were given for the concentration in the aquifer and in the impermeable layers. Dispersion in a perfectly stratified aquifer was studied with the method of moments by Güven et al. [1984], who took both longitudinal and transversal pore scale dispersion into account. Analytical solutions were developed for e.g. the macroscopic longitudinal dispersivity and the concentration perpendicular to the direction of stratification for particular profiles of the flow velocity. Of direct interest to this contribution is their case of a step function velocity profile.

Of importance to this paper is also the work by Verruijt [1971], who studied the steady state dispersion across an interface separating two fluids that move with different velocities. One of the fluids contains a conservative tracer. However, at the interface a condition for the transfer of solute is assumed that does not follow from a natural condition of continuity. A similar problem was addressed by Shamir and Harleman [1967] who investigated the transversal dispersion for two layers 1 and 2 with different flow velocities ($v_1 > v_2$) and solute input in layer 1. They derived a steady state solution for the concentration in a cross section which was verified experimentally. Since both Verruijt [1971] and Shamir and Harleman [1967] gave steady state solutions for the concentration distribution the effect of adsorption could not be studied from their results.

The problem considered in this paper resembles the two-fluid system of Verruijt [1971], except that here the flow domain consists of two regions with different porous materials. These regions are

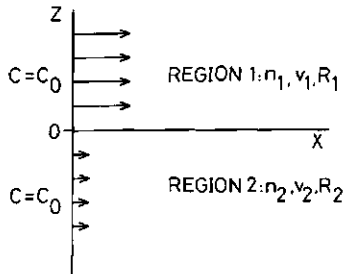


Figure 1: Schematization of the flow domain.

separated by a distinct sharp boundary (figure 1) and each has its own hydraulic and chemical properties which do not vary throughout that region. The porosities (n) and retardation factors (R) are n_1 , and R_1 for region 1 and n_2 and R_2 for region 2. The interstitial flow velocity (v) parallel to the interface is v_1 for region 1 and v_2 for region 2. Solute transport in the direction of waterflow is assumed to be purely convective.

After giving the mathematical formulation of the problem an approximate expression is derived for the concentration at the interface. Using this expression approximate analytical solutions will be derived for the transfer rate of solute from the more permeable region into the less permeable region, and for the breakthrough curves. Special attention is given to the correct formulation of the boundary conditions governing dispersive transfer between the two regions. This is a refinement over the studies by Tang et al. [1981] and Van Genuchten et al [1984] who assumed an infinite transversal dispersion which results in a constant concentration in a cross section of the fractures or pores. Since in this study the transversal dispersion is finite, the concentration perpendicular to the interface will not be constant. Numerical results obtained with a finite difference program are used to assess the applicability of the analytical results.

11.2 Mathematical formulation

The transport of solute through a saturated medium assuming linear adsorption may be described by the convection-dispersion equation as given by Bear [1972]:

$$\frac{\partial}{\partial t} (n R c) = \text{div}(n \underline{D} \text{grad} (c)) - \text{div} (n \underline{v} c). \quad (1)$$

where n is the porosity, R is the retardation factor, c is the concentration, \underline{D} is the tensor of hydrodynamic dispersion, \underline{v} is the vector of the interstitial flow velocity and t is time.

The initial and boundary conditions for eq. (1) are (Figure 1):

$$c(x, z, t) = 0 \quad t < 0 \quad -\infty < z < \infty \quad 0 < x < \infty \quad (2)$$

$$c(0, z, t) = c_0 \quad t > 0 \quad -\infty < z < \infty \quad (3)$$

It is assumed throughout that water flows parallel to the interface in the positive x -direction and that transport in the x -direction is purely convective, i.e. no hydrodynamic dispersion occurs in the direction of x . Then the transport equation (1) reduces for region 1 to:

$$R_1 \frac{\partial c}{\partial t} = D_{1z} \frac{\partial^2 c}{\partial z^2} - v_1 \frac{\partial c}{\partial x} \quad x > 0, \quad z > 0 \quad (4)$$

where $D_{1z} = \alpha_T v_1 + D^*$, with α_T the transversal dispersivity and D^* the coefficient of molecular diffusion.

Similarly for region 2:

$$R_2 \frac{\partial c}{\partial t} = D_{2z} \frac{\partial^2 c}{\partial z^2} - v_2 \frac{\partial c}{\partial x} \quad x > 0, \quad z < 0 \quad (5)$$

where $D_{2z} = \alpha_T v_2 + D^*$.

Equations (4) and (5) are solved simultaneously subject to the conditions (2) and (3) and the continuity conditions at the interface:

$$\lim_{z \rightarrow 0} c(x, z, t) = \lim_{z \rightarrow 0} c(x, z, t) \quad (6)$$

and

$$\lim_{z \rightarrow 0} n_1 D_{1z} \frac{\partial c}{\partial z} (x, z, t) = \lim_{z \rightarrow 0} n_2 D_{2z} \frac{\partial c}{\partial z} (x, z, t) \quad (7)$$

for $x > 0$ and $t > 0$. Without loss of generality we assume throughout this paper that $c_0 = 1$ (arbitrary units) and that $v_2/R_2 < v_1/R_1$.

11.3 Analytical approximation

Since solute transport in the positive x -direction is only due to convection, the solution of equation (4) for $z > 0$ and equation (5) for $z < 0$ must be of the form (Figure 2)

$$c(x, z, t) = 1 \quad x < \frac{v_2}{R_2} t \quad (8a)$$

$$c(x, z, t) = g(x, z, t) \quad \frac{v_2}{R_2} t < x < \frac{v_1}{R_1} t \quad (8b)$$

$$c(x, z, t) = 0 \quad x > \frac{v_1}{R_1} t \quad (8c)$$

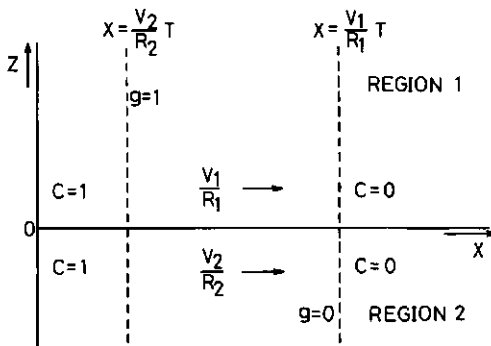


Figure 2: Schematization of the analytical solution eq. (8).

for all $t > 0$ and $-\infty < z < \infty$.

Note that eq. (8) satisfies initial condition (2) and boundary condition (3). The function g describes the transverse dispersion process between the two materials when the solute front in region 1 is moving faster than the solute front in region 2. Thus, $g(x, z, t)$ is

composed of solutions of equations (4) and (5) for $z > 0$ and for $z < 0$, respectively, which are matched at $z = 0$ such that the continuity conditions (6) and (7) are satisfied. The function g is chosen to satisfy the moving boundary conditions

$$g(x,z,t) = 1 \quad \text{for } x = \frac{v_2}{R_2} t, \quad z > 0, \quad t > 0 \quad (9)$$

$$g(x,z,t) = 0 \quad \text{for } x = \frac{v_1}{R_1} t, \quad z < 0, \quad t > 0 \quad (10)$$

The following method is used to obtain g . Let $c_b(x,t)$ be the (unknown) concentration at the contact interface $z = 0$. Then

$$c(x,0,t) = c_b(x,t) \quad \text{for } x > 0 \text{ and } t > 0 \quad (11)$$

and hence at the interface:

$$g(x,0,t) = c_b(x,t) \quad \text{for } \frac{v_2}{R_2} t < x < \frac{v_1}{R_1} t \text{ and } t > 0. \quad (12)$$

Then, to find g in region 1, the following problem has to be solved.

$$R_1 \frac{\partial c}{\partial t} = D_{1z} \frac{\partial^2 c}{\partial z^2} - v_1 \frac{\partial c}{\partial x}$$

$$\text{in } \frac{v_2}{R_2} t < x < \frac{v_1}{R_1} t, \quad z > 0, \quad t > 0 \quad (13a)$$

$$c\left(\frac{v_2}{R_2} t, z, t\right) = 1 \quad \text{on } z > 0, \quad t > 0, \quad (13b)$$

$$c(x,0,t) = c_b(x,t) \quad \text{on } \frac{v_2}{R_2} t < x < \frac{v_1}{R_1} t, \quad t > 0. \quad (13c)$$

The objective is now to first solve eq. (13) in terms of the concentration c_b . In doing this, it is convenient to make use of the following coordinate transformation. First, let $v_s = \frac{v_1}{R_1} - \frac{v_2}{R_2}$. Then set

$$\xi = x - \frac{v_2}{R_2} t, \quad (14a)$$

$$\zeta = z, \quad (14b)$$

$$\tau = t - \frac{x - \frac{v_2}{R_2} t}{v_s} = \frac{1}{v_s} \left(\frac{v_1}{k_1} t - x \right) \quad (14c)$$

and finally set $u(\xi, \zeta, \tau) = c(x, z, t)$. This leads to the following transformed problem

$$\frac{\partial u}{\partial \xi} = k^+ \frac{\partial^2 u}{\partial \zeta^2} \quad \text{in } \xi > 0, \zeta > 0, \tau > 0 \quad (15a)$$

$$u(0, \zeta, \tau) = 1 \quad \text{on } \zeta > 0, \tau > 0 \quad (15b)$$

$$u(\xi, 0, \tau) = c_b(\xi, \tau) \quad \text{on } \xi > 0, \tau > 0 \quad (15c)$$

where k^+ is a constant given by

$$k^+ = \frac{D_1 z}{R_1 v_s} \quad (16)$$

The solution method for eq. (15) is standard (e.g. Carslaw and Jaeger, 1959, p. 29-32). Denoting the solution of eq. (15) by u^+ , one finds for this function in terms of c_b :

$$u^+(\xi, \zeta, \tau) = \operatorname{erf}\left(\frac{\zeta}{2\sqrt{(k^+\xi)}}\right) + \frac{2}{\sqrt{\pi}} \int_{\zeta/2\sqrt{(k^+\xi)}}^{\infty} c_b\left(\xi - \frac{\zeta^2}{4k^+y}, \tau\right) e^{-y^2} dy \quad (17)$$

where $\operatorname{erf}(x) = \frac{2}{\sqrt{\pi}} \int_0^x e^{-y^2} dy$.

In view of eq. (7), it is necessary to find an expression for the derivative with respect to ζ of u^+ at $\zeta=0^+$. To do this straightforward from eq. (17) appears difficult. A derivation of which the details are omitted shows that ($\mu = y \frac{2}{\zeta} \sqrt{(k^+\xi)}$)

$$\begin{aligned} \frac{\partial u^+}{\partial \zeta}(\xi, 0^+, \tau) &= \frac{1}{\sqrt{(\pi k^+\xi)}} [1 - c_b(\xi, \tau)] \\ &+ \int_1^{\infty} \left\{ c_b\left(\xi - \frac{\xi}{\mu^2}, \tau\right) - c_b(\xi, \tau) \right\} d\mu \end{aligned} \quad (18)$$

To find the function g in region 2, consider the problem

$$R_2 \frac{\partial c}{\partial t} = D_{2z} \frac{\partial^2 c}{\partial z^2} - v_2 \frac{\partial c}{\partial x}$$

$$\text{in } \frac{v_2}{R_2} t < x < \frac{v_1}{R_1} t, \quad z < 0, \quad t > 0, \quad (19a)$$

$$c\left(\frac{v_1}{R_1} t, z, t\right) = 0 \quad \text{on } z < 0, \quad t > 0, \quad (19b)$$

$$c(x, 0, t) = c_b(x, t) \quad \text{on } \frac{v_2}{R_2} t < x < \frac{v_1}{R_1} t, \quad t > 0. \quad (19c)$$

As in the previous case, this problem can be transformed using eq. (14):

$$\frac{\partial u}{\partial \tau} = k^- \frac{\partial^2 u}{\partial \zeta^2} \quad \xi > 0, \quad \zeta < 0, \quad \tau > 0 \quad (20a)$$

$$u(\xi, \zeta, 0) = 0 \quad \xi > 0, \quad \zeta < 0 \quad (20b)$$

$$u(\xi, 0, \tau) = c_b(\xi, \tau) \quad \xi > 0, \quad \tau > 0 \quad (20c)$$

where $k^- = D_{2z}/R_2$.

The solution of eq. (20) is

$$u^-(\xi, \zeta, \tau) = \frac{2}{\sqrt{\pi}} \int_{-\zeta/2\sqrt{k^- \tau}}^{\infty} c_b\left(\xi, \tau - \frac{\zeta^2}{4k^- y^2}\right) e^{-y^2} dy. \quad (21)$$

Similar to the previous case, the derivative of u^- with respect to ζ at $\zeta=0^-$ is given by

$$\frac{\partial u^-}{\partial \zeta}(\xi, 0^-, \tau) = \frac{1}{\sqrt{\pi k^- \tau}} \left[c_b(\xi, \tau) - \int_1^{\infty} \left\{ c_b\left(\xi, \tau - \frac{\tau}{\mu^2}\right) - c_b(\xi, \tau) \right\} d\mu \right] \quad (22)$$

The continuity condition (7) in terms of the new variables becomes

$$n_1 D_{1z} \frac{\partial u^+}{\partial \xi} (\xi, 0^+, \tau) = n_2 D_{2z} \frac{\partial u^-}{\partial \xi} (\xi, 0^-, \tau) . \quad (23)$$

Inserting (8) and (22) into this expression gives the following integral equation for the unknown function c_b :

$$\begin{aligned} A \sqrt{\left(\frac{\xi}{\tau}\right)} [c_b(\xi, \tau) - \int_1^{\infty} \{c_b(\xi, \tau - \frac{\tau}{\mu^2}) - c_b(\xi, \tau)\} d\mu] \\ = 1 - c_b(\xi, \tau) + \int_1^{\infty} \{c_b(\xi - \frac{\xi}{\mu^2}, \tau) - c_b(\xi, \tau)\} d\mu , \quad (24) \end{aligned}$$

where the constant A is given by

$$A = \frac{n_2}{n_1} \frac{D_{2z}}{D_{1z}} \sqrt{\left(\frac{k^+}{k^-}\right)} = \frac{n_2}{n_1} \sqrt{\left(\frac{D_{2z} R_2}{D_{1z} R_1} \frac{1}{v_s}\right)} \quad (25)$$

In view of the boundary conditions (9) and (10), a solution of eq. (24) has to satisfy

$$c_b(0, \tau) = 1 \quad \text{for } \tau > 0 \quad (26a)$$

and

$$c_b(\xi, 0) = 0 \quad \text{for } \xi > 0 \quad (26b)$$

To find the general solution described by eq. (8) we have to solve first the interface concentration c_b from eqs. (24) - (26), substitute the result into eqs. (21) and (17) and define the function g according to

$$g(x, z, t) = u^+ \left(x - \frac{v_2}{R_2} t, z, \frac{1}{v_s} \left(\frac{v_1}{R_1} t - x\right)\right), \quad z > 0 \quad (27a)$$

$$g(x, z, t) = u^- \left(x - \frac{v_2}{R_2} t, z, \frac{1}{v_s} \left(\frac{v_1}{R_1} t - x\right)\right), \quad z < 0 \quad (27b)$$

11.3.1 Approximate interface concentration

Attention is now focused on the solution of integral eq. (24). To obtain a solution we apply a Taylor series expansion with respect to ξ and τ to the integrands in (24). A first and simple approximation follows when the first term of the Taylor expansion is used. Then $c_b(\xi, \tau - \frac{\tau}{\mu^2}) \approx c_b(\xi, \tau)$ and $c_b(\xi - \frac{\xi}{\mu^2}, \tau) = c_b(\xi, \tau)$, and eq. (24)

reduces to the algebraic equation

$$A \sqrt{\frac{\xi}{\tau}} c_b = 1 - c_b \tag{28}$$

with the solution

$$c_b^{(1)}(\xi, \tau) = \frac{1}{1 + A \sqrt{\frac{\xi}{\tau}}} \quad \text{for } \xi > 0 \text{ and } \tau > 0 \tag{29}$$

Observe that this approximate solution satisfies eq. (26).

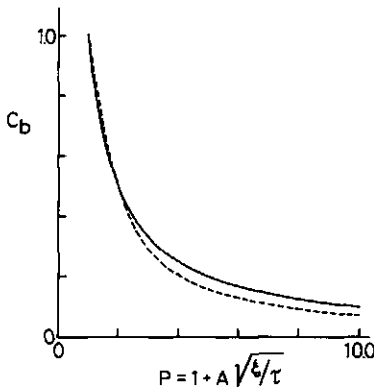


Figure 3: Concentration c_b at the interface as a function of p . Solid line: the approximation of $c_b^{(1)}$ according to (29) and dashed line: approximation $c_b^{(2)}$ according to (37) and (38).

A second and more complicated approximation arises when the first and second terms of the Taylor expansion are used. This leads to

$$c_b(\xi, \tau - \frac{\tau}{\mu^2}) \approx c_b(\xi, \tau) - \frac{\tau}{\mu^2} \frac{\partial c_b}{\partial \tau}(\xi, \tau) \tag{30a}$$

$$c_b \left(\xi - \frac{\xi}{\mu^2}, \tau \right) = c_b(\xi, \tau) - \frac{\xi}{\mu^2} \frac{\partial c_b}{\partial \xi}(\xi, \tau) \quad (30b)$$

Substituting these expressions into eq. (24) gives the differential equation

$$A \sqrt{\left(\frac{\xi}{\tau}\right)} \left\{ c_b + \tau \frac{\partial c_b}{\partial \tau} \right\} = 1 - c_b - \xi \frac{\partial c_b}{\partial \xi} \quad (31)$$

This equation is solved by introducing a similarity transformation. If

$$\eta = \xi/\tau \quad \text{and} \quad f(\eta) = c_b(\xi, \tau), \quad (32)$$

then the function f satisfies the ordinary differential equation

$$A/\eta \left\{ f - \eta \frac{df}{d\eta} \right\} = 1 - f - \eta \frac{df}{d\eta}. \quad (33)$$

To solve this equation it is convenient to set

$$p = 1 + A/\eta \quad \text{and} \quad \bar{f}(p) = f(\eta). \quad (34)$$

Now for f to be a solution of (33), the function \bar{f} should satisfy

$$(p-2)(p-1) \frac{d\bar{f}}{dp} - 2p\bar{f} + 2 = 0. \quad (35)$$

Since $\xi > 0$ and $\tau > 0$ in (24) and (31), eq. (35) must be solved for $p > 1$. Considering eq. (26) and remembering that \bar{f} represents an approximate interface concentration, it is obvious to look for solutions of eq. (35) which satisfy

$$\bar{f}(1) = 1 \quad \text{and} \quad \bar{f}(\infty) = 0. \quad (36)$$

Using the standard method of variation of constants, one can show that the solution of the boundary value problem (35), (36) is given by:

$$\bar{f}(p) = \frac{1}{6} (p^2 - 6p + 11) \quad 1 < p < 2 \quad (37a)$$

$$\bar{f}(p) = \frac{1}{6(p-1)^2} (4p - 5) \quad p > 2 \quad (37b)$$

This function is shown in Fig. 3. In terms of the variables ξ and τ the approximation is

$$c_b^{(2)}(\xi, \tau) = \bar{f}(1 + A \sqrt{(\xi/\tau)}) \quad (38)$$

Figure 3 also shows the function $1/p$ which corresponds to the first approximation $c_b^{(1)}$ in terms of p (Eq. (29) and (34)).

11.3.2 Loss of solute from the permeable zone

The transverse dispersion process between the two regions is now considered using the approximate expressions for the interface concentration c_b derived in the previous subsection. First, let t and x be given such, that $t > 0$ and $\frac{\sqrt{2}}{R_2} t < x < \frac{1}{R_1} t$ and let the dispersive loss of solute from the permeable region into the region with low permeability be denoted by $V(x, t)$. Then:

$$V(x, t) = \int_0^{\infty} \{1 - c(x, z, t)\} dz \quad (39)$$

for a unit surface area of the interface. In terms of the variables ξ , ζ and τ , eq. (39) becomes:

$$\tilde{V}(\xi, \tau) = \int_0^{\infty} \{1 - u^+(\xi, \zeta, \tau)\} d\zeta \quad \text{with } \xi > 0 \text{ and } \tau > 0, \quad (40)$$

where u^+ is the solution of eq. (15). Since u^+ satisfies eq. (15), the function $1 - u^+$ also satisfies that equation i.e.:

$$\frac{\partial}{\partial \xi} (1 - u^+) = k^+ \frac{\partial^2}{\partial \zeta^2} (1 - u^+) \quad (41)$$

Integration with respect to ζ from $\zeta=0$ to $\zeta=\infty$ gives

$$\frac{\partial}{\partial \xi} \tilde{V}(\xi, \tau) = k^+ \frac{\partial u^+}{\partial \zeta}(\xi, 0^+, \tau). \quad (42)$$

This expression is integrated with respect to ξ using the boundary condition $\tilde{V}(0, \tau) = V(\frac{1}{R_1} t, t) = 0$; this yields

$$\tilde{V}(\xi, \tau) = k^+ \int_0^{\xi} \frac{\partial u^+}{\partial \zeta} (s, 0^+, \tau) ds \quad (43)$$

Next, eq. (18) is substituted into eq. (43) to give

$$\begin{aligned} \tilde{V}(\xi, \tau) &= \sqrt{\left(\frac{k^+}{\pi}\right)} \int_0^{\xi} \frac{1}{\sqrt{s}} [1 - c_b(s, \tau)] \\ &+ \int_1^{\infty} \left\{ c_b\left(s - \frac{s}{\mu}, \tau\right) - c_b(s, \tau) \right\} d\mu ds \end{aligned} \quad (44)$$

In order to evaluate this expression, the first and second terms of the Taylor expansion are used in the second integral. In accordance with eq. (31), the approximation

$$\tilde{V}(\xi, \tau) = \sqrt{\left(\frac{k^+}{\pi}\right)} \int_0^{\xi} \frac{1}{\sqrt{s}} [1 - c_b(s, \tau) - s \frac{\partial c_b}{\partial s}(s, \tau)] ds \quad (45)$$

is found. Integration by parts gives:

$$\tilde{V}(\xi, \tau) = \sqrt{\left(\frac{k^+}{\pi}\right)} \int_0^{\xi} \frac{1}{\sqrt{s}} [1 - \frac{1}{2} c_b(s, \tau)] ds - \sqrt{\left(\frac{k^+ \xi}{\pi}\right)} c_b(\xi, \tau) \quad (46)$$

or

$$\tilde{V}(\xi, \tau) = 2\sqrt{\left(\frac{k^+ \xi}{\pi}\right)} [1 - \frac{1}{2} c_b(\xi, \tau)] - \frac{1}{2}\sqrt{\left(\frac{k^+}{\pi}\right)} \int_0^{\xi} \frac{1}{\sqrt{s}} c_b(s, \tau) ds. \quad (47)$$

In this expression, the approximations $c_b^{(1)}$ and $c_b^{(2)}$ from subsection 11.3.1 are substituted, giving (i=1,2)

$$\begin{aligned} \tilde{V}^{(1)}(\xi, \tau) &= 2\sqrt{\left(\frac{k^+ \xi}{\pi}\right)} \left\{ 1 - \frac{1}{2} c_b^{(1)}(\xi, \tau) \right. \\ &\left. - \frac{1}{2} \sqrt{\left(\frac{\tau}{\xi}\right)} \int_0^{\xi} c_b^{(1)}(s, \tau) d\left(\frac{s}{\tau}\right) \right\} \end{aligned} \quad (48)$$

Next, define

$$c_b^{(1)}(\xi, \tau) = \frac{1}{p} = f^{(1)}(p) \text{ and } c_b^{(2)}(\xi, \tau) = \bar{f}(p) = f^{(2)}(p) \quad (49)$$

with p given by eq. (34). Then eq. (48) becomes:

$$\tilde{V}^{(1)}(\xi, \tau) = 2\sqrt{\left(\frac{k^+ \xi}{\pi}\right)} \left\{ 1 - \frac{1}{2} f^{(1)}(p) - \frac{1}{2(p-1)} \int_1^p f^{(1)}(q) dq \right\} \quad (50)$$

For the first approximation, i=1, this yields

$$\tilde{V}^{(1)}(\xi, \tau) = 2 \sqrt{\left(\frac{k^+ \xi}{\pi}\right)} \left\{ 1 - \frac{1}{2p} - \frac{1}{2(p-1)} \ln p \right\} \quad (51)$$

and for the second approximation (i=2)

$$\tilde{V}^{(2)}(\xi, \tau) = 2 \sqrt{\left(\frac{k^+ \xi}{\pi}\right)} \left\{ 1 - \frac{1}{2} \bar{F}(p) - \frac{1}{2(p-1)} \bar{F}(p) \right\}, \quad (52)$$

where the function \bar{F} is given by

$$\bar{F}(p) = \frac{1}{6} \left(\frac{1}{3} p^3 - 3p^2 + 11p \right) - \frac{25}{18} \quad 1 < p < 2 \quad (53a)$$

$$\bar{F}(p) = \frac{1}{6} \left(4 \ln(p-1) + \frac{1}{p-1} \right) + \frac{10}{18} \quad p > 2 \quad (53b)$$

Since transport is often studied by measuring breakthrough curves, we also want to evaluate the average concentration in the permeable region at given x and t . Let H be the height in the permeable region over which the concentration is averaged. Then

$$\bar{c}_H(x, t) = \frac{1}{H} \int_0^H c(x, z, t) dz \quad (54)$$

This expression is rewritten as

$$\bar{c}_H(x, t) = 1 - \frac{1}{H} \int_0^H \{1 - c(x, z, t)\} dz. \quad (55)$$

If the averaging height, H , is chosen large enough such that $c(x, z, t) = 1$ for all $z > H$, then approximately:

$$\bar{c}_H(x, t) = 0 \quad \text{for } t < \frac{R_1}{v_1} x \quad (56a)$$

$$\bar{c}_H(x, t) = 1 - \frac{1}{H} V(x, t) \quad \text{for } \frac{R_1}{v_1} x < t < \frac{R_2}{v_2} x \quad (56b)$$

$$\bar{c}_H(x, t) = 1 \quad \text{for } t > \frac{R_2}{v_2} x \quad (56c)$$

Equations (51) and (52) may be substituted into this expression to give the average concentrations $\bar{c}_H^{(1)}$ and $\bar{c}_H^{(2)}$, respectively.

11.4 Numerical approximation

The analytical solutions were based on several simplifying assumptions. To assess the validity of these assumptions, numerical calculations that do not incorporate the simplifications were done for a few typical cases. For this purpose we used a finite difference program. In this program we first calculated steady-state flow using a direct Gaussian elimination method. The resulting flow velocities were then used to calculate mass transport according to eq. (1). Contrary to the analytical method, the numerical model contains a small hydrodynamic dispersion term in the flow direction. The longitudinal dispersion coefficient is given by $D_x = \alpha_L v + D^*$, where α_L is the longitudinal dispersion and v is the flow velocity (v_1 for region 1 and v_2 region 2).

The equation solved in the numerical model was the finite difference equivalent of (1) on a bounded domain subject to the conditions:

$$c(x,z,t) = 0 \quad t < 0 \quad -B < z < H \quad 0 < x < L \quad (57)$$

$$c(0,z,t) = c_0 \quad t > 0 \quad -B < z < H \quad (58a)$$

$$\frac{\partial c}{\partial z}(x,-B,t) = 0 \quad t > 0 \quad 0 < x < L \quad (58b)$$

$$\frac{\partial c}{\partial z}(x,H,t) = 0 \quad t > 0 \quad 0 < x < L \quad (58c)$$

$$\frac{\partial c}{\partial x}(L,z,t) = 0 \quad t > 0 \quad -B < z < H \quad (58d)$$

Here B is the thickness of region 2 and H the thickness of region 1. The constant L is the length of the system. Because of the small longitudinal dispersion coefficient, steep gradients of the concentration will occur. This may lead to numerical overshoot when using finite difference methods as discussed by Fried [1975] and Gray and Pinder [1976]. This numerical overshoot is avoided if the gradient

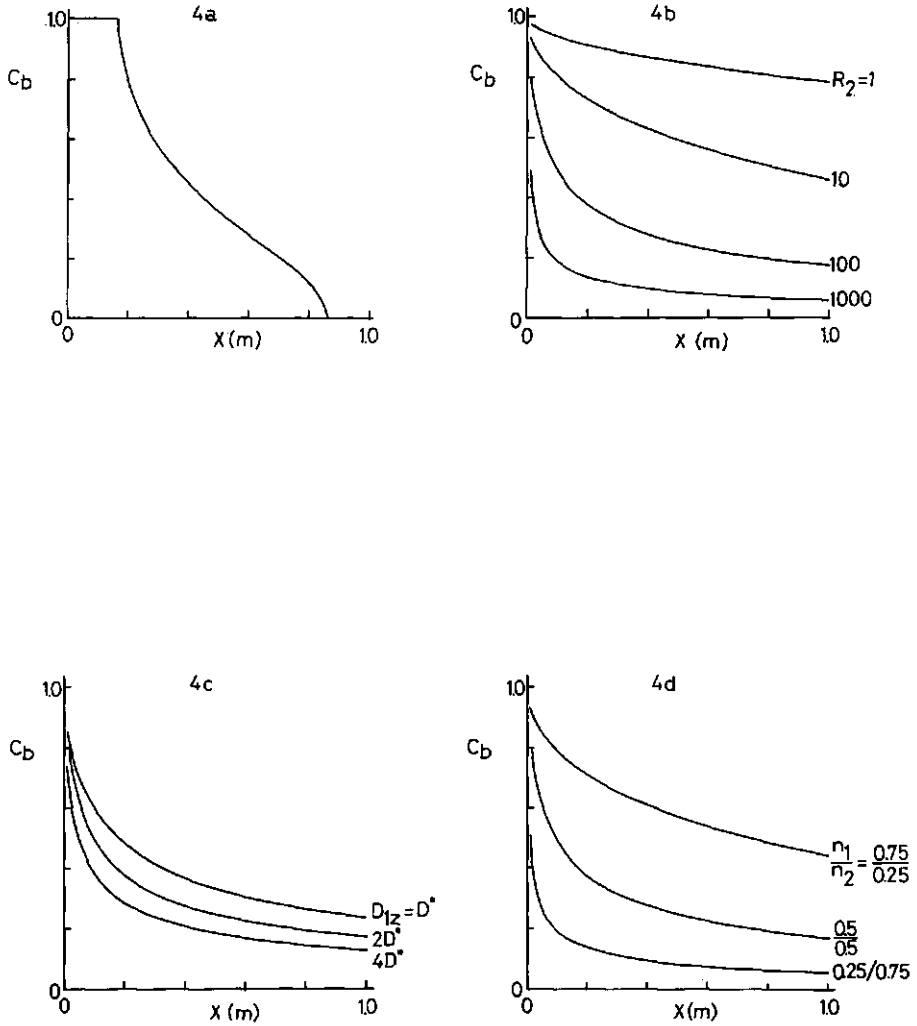


Figure 4: Concentration at the interface $c_b^{(2)}$ as a function of x , at $t=150$ and parameters as in Table 1 unless indicated differently, 4a: $t=29$, $v_2=v_1$ and $R_2=5$, 4b: effect of R_2 , 4c: effect of D_{1z} , 4d: effect of n_1/n_2

is approximated by backward differences, in which case numerical dispersion will be introduced [Lantz, 1971]. The numerical calculations were performed employing central differences with respect to both space and time derivatives. The discretizations were subject to restrictions as reported by Lantz [1971] and Price et al. [1966]. This lead for the discretization in the x-direction to:

$$\Delta x < 2 \alpha_L \quad (59)$$

The scheme used is convergent and unconditionally stable [Smith, 1965]. The equations for mass-transport are solved using an iterative line successive overrelaxation method.

The numerical values of variables used in the calculations are listed in table 1. Inequality (59) is satisfied for the chosen values of Δx and α_L . These values were constant throughout the entire domain. The discretizations with respect to z and t were not constant. Near the interface where the gradients are largest Δz was taken 0.001 (m). Moving further away from the interface, Δz is increased in both directions. The discretization of time was finest ($\frac{1}{2}$ day) until well after breakthrough occurred, with larger timesteps thereafter. The combined discretizations in space and time appeared to be acceptable as a further refinement did not significantly affect the results.

The choice of the parameters was such that no flow of water occurred in the second region ($v_2 = 0$) whereas $v_1 = 12.5$ m/yr. Retardation factors were varied to analyse their effect. In agreement to many natural systems the region with the highest permeability (or velocity v) was given the smallest retardation factor ($R_1=1$). Values used for R_2 were 1, 10, 100 and 1000. The value of the molecular diffusion coefficient $D^*=0.032$ (m^2/yr) is in agreement to values given in literature (Bolt, 1982). The value of D_{1x} was 0.345 and D_{2x} equals D^* . The ratio of α_T/α_L was 0.1 throughout the entire domain and is in the range as reported by Bear [1979], Fried [1975] and De Josselin De Jong [1958] for well-sorted granular materials. The porosities n_1 and n_2 were set equal.

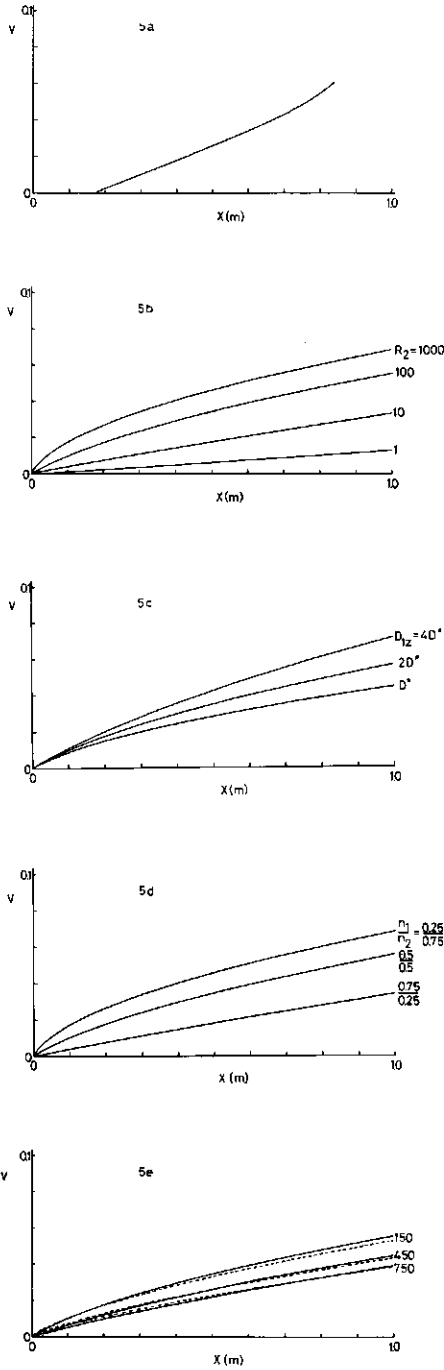


Figure 5: Loss term $v^{(2)}$ as a function of x at $t = 150$. See text Fig. 4a-d for Fig. 5a-d. Figure 5e: Approximation $v^{(1)}$ (dashed line) and $v^{(2)}$ (solid line) for three times.

11.5 Results and discussion

In this section the results of the analytical approximation are given and compared with the numerical calculations for some typical cases. Differences between the numerical and analytical approximations are discussed in more detail later.

Figure 3 shows the concentration c_b at the interface as a function of p . Both the simple approximation $c_b^{(1)} = 1/p$ and the approximation $c_b^{(2)}$ as given by eqs. (37) and (38) are presented. Note that these approximations are only defined for $\xi > 0$. For negative values of ξ , (i.e. $x < v_2 t/R_2$), the concentration c_b is simply set to be $c_b = 1$.

The complete range of c_b is shown in Fig. 4a for the approximation $c_b^{(2)}$. For the more general case with flow in both regions, and for $v_1 t/R_1 < 1.0$ such that no breakthrough occurs at $x = 1.0$ three domains are found: the domain $0 < x < v_2 t/R_2$ where $c_b = 1$, the domain $v_2 t/R_2 < x < v_1 t/R_1$ where c_b is given by the solution of the integral equation (24) and the domain $x > v_1 t/R_1$ where $c_b = 0$. When $v_2 = 0$ and $v_1 t/R_1 > 1$, only one domain is present on the interval $0 < x < 1.0$. This is shown in Fig. 4b-d, where the effects of several parameters upon the distribution of the concentration along the interface are illustrated. Parameter values are those in Table 1 unless indicated differently. For a given time and position, the concentration c_b decreases when R_2 increases (Fig. 4b). Clearly, if R_2 is unity, the storage capacity in region 2 close to the interface will be depleted quickly and the concentration c_b will rise fast. In case of a large R_2 -value, c_b becomes small as the dispersion rate towards and across the interface is small with respect to the storage capacity in region 2. The effect of decreasing D_{1z} likewise results in a smaller c_b . The effect of varying of n_1/n_2 on $c_b^{(2)}$ is presented in Fig. 4d, showing that $c_b^{(2)}$ increases with increasing n_1/n_2 .

The loss term V using the second approximation $v^{(2)}$ as given by eq. (52) is shown as a function of x in Fig. 5a-e. The curve presented in Fig. 5a corresponds to the same situation as Fig. 4a for c_b . Naturally, also $v^{(2)}$ is defined only for $v_2 t/R_2 < x < v_1 t/R_1$. For values of x outside this domain $v^{(2)}$ does not change. Thus $v^{(2)} = 0$ for $x < v_2 t/R_2$, and for $x > v_1 t/R_1$. Again for the case when $v_2 = 0$, effects of several parameters on $v^{(2)}$ are illustrated.

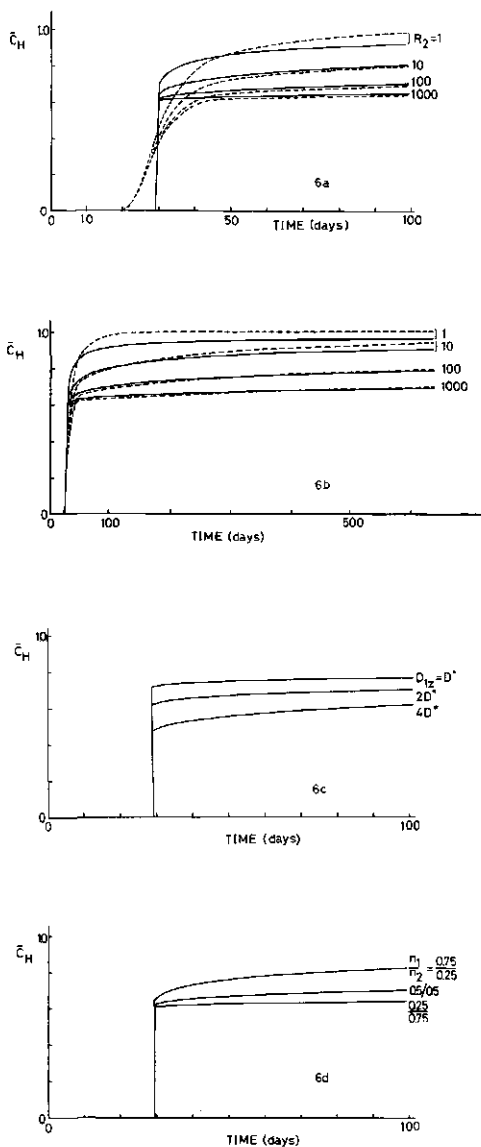


Figure 6: Breakthrough curves at $x = 1$. Analytical approximation (solid line) and numerical approximation (dashed line).
 6a: effect of R_2 , short term breakthrough, 6b: as 6a, long term breakthrough, 6c: effect of D_{12} , 6d: effect of n_1/n_2

The values chosen for the parameters for Fig. 5b-d correspond to the same values used for Fig. 4b-d, respectively. As was shown in Fig. 4b, larger values of R_2 will cause smaller values of c_b , which implies larger concentration gradients in a cross section (see also Fig. 9, to be discussed later). Hence the loss term will increase with increasing R_2 . In the same manner, V also increases with increasing D_{1z} (Fig. 5c). As shown in Fig. 5d the trend for n_1/n_2 is found to be opposite to the trend for R_2 and D_{1zz} . Fig. 5e finally shows a decreasing V with time; for reference also the approximation $V^{(1)}$ is given.

Assuming an averaging height $H = 0.2$ m and $v_2 = 0$ breakthrough curves from region 1 were calculated. Results for $x = 1$ m are presented in Fig. 6 for different values of R_2 , D_{1z} and different ratios n_1/n_2 . The effect of R_2 on the breakthrough curve appears prominent. The significant tailing observed for high values of R_2 is in agreement with results of immobile zone models (e.g. Van Genuchten and Cleary, 1982). In Fig. 6d the effect of the ratio n_1/n_2 is shown, which appears to be large, exhibiting pronounced tailing at small n_1/n_2 .

The analytical and the numerical approaches are compared in Fig. 6a and 6b for the breakthrough curves, and in Fig. 7 and 8 for the concentration at the interface, c_b . In all cases the more accurate approximation using the first two terms of the Taylor expansion (eq. 30) is taken for the analytical approach. Fig. 7 shows c_b as a function of x for three times, with $R_2=100$ and $v_2=0$. The agreement appears good and only for small x and relatively large t minor differences are seen. Differences appear to be somewhat smaller for the larger R_2 -value.

This same effect of R_2 is also noticeable from the breakthrough curves in Fig. 6a and 6b. The effect of hydrodynamic dispersion occurring in the flow direction accounted for in the numerical approach yet absent in the analytical approximation, is prominent in Fig. 6a. After first breakthrough, however, the agreement between the analytical and the numerical results is considered excellent for large R_2 (i.e., 100, 1000). The limiting case where $R_2=1$ shows large differences for all times considered.

The distribution of the concentration in a cross-section of the flow domain is shown in Fig. 9 for the reference case $v_2=0$. Continuity of

the flux across the interface requires that $(\frac{\partial c}{\partial z})_1 / (\frac{\partial c}{\partial z})_2 = D^* / D_{1z}$. This is shown to be indeed the case in Fig. 9 (for $D_{1z} \approx 2D^*$). Note again as in Fig. 4 that the concentration at the interface is smallest for the largest value of R_2 .

11.6 Discussion

In the previous section we showed that the agreement between the numerical and the analytical results is good for large values of R_2 but that the differences become significant for small values of R_2 . The differences are attributed mainly to the different boundary conditions used for the two approaches in the direction of negative z . In the analytical approach the impermeable region is not bounded, whereas in the numerical approach the impermeable region has a finite thickness B , while at $z = -B$ a Neumann boundary condition is used (eq. 58b).

Hence, contrary to the analytical solution, the storage capacity in the impermeable region is finite for the numerical solution. As soon as this storage capacity becomes depleted, the concentrations in both the permeable and the impermeable region will increase faster for the numerical than for the analytical approximation. To estimate the time when this occurs, consider eq. (1) for the domain $-B < z < 0$ and for the case where $v_2 = 0$:

$$R_2 \frac{\partial c}{\partial t} = D^* \frac{\partial^2 c}{\partial z^2} \quad (60)$$

with the conditions:

$$c(z, 0) = 0 \quad (61)$$

$$c(0, t) = 1 \quad t > 0 \quad (62a)$$

$$\frac{\partial c}{\partial z}(-B, t) = 0 \quad t > 0 \quad (62b)$$

The solution may be written as an infinite series of complementary error functions. Maintaining only the first three terms this yields

$$c(z, t) \approx \operatorname{erfc}\left(\frac{-z}{2\sqrt{D^* t/R_2}}\right) - \operatorname{erfc}\left(\frac{2B-z}{2\sqrt{D^* t/R_2}}\right) + \operatorname{erfc}\left(\frac{2B+z}{2\sqrt{D^* t/R_2}}\right) \quad (63)$$

The solute flux at $z=0$ is:

$$D^* \frac{\partial c}{\partial z} (0, t) \sim D^* \left(\frac{R_2}{\pi D^* t} \right)^{1/2} \left\{ 1 - 2e^{-\frac{B^2 R_2^2}{D^* t}} \right\} \quad (64)$$

Note that the second term in the right hand side of eq. (64) represents the influence of the boundary at $z = -B$. This was not taken into account in the previous analytical approximation, where B was assumed to be infinite. Consequently the assumption of an infinite thickness of the impermeable region in the analytical approach is valid if the restriction

$$e^{-\frac{B^2 R_2^2}{D^* t}} \ll 0.5 \quad (65)$$

is satisfied. For the chosen values of B and D^* the deviations will be less than 4% for $t/R_2 < 0.02$. Hence if $R_2=1$ then the influence of the boundary is almost at once noticeable whereas for e.g. $R_2=100$ this will take two years.

In section 11.5 we showed the prominent effects of the retardation factor R_2 in region 2 and of the transversal dispersion coefficient D_{1z} in region 1. Here we discuss the limiting cases where $R_2 \rightarrow \infty$ and $D_{1z} \rightarrow \infty$ in more detail. We give simple analytical expressions for the corresponding concentration distributions and compare the results with the expressions presented in this study.

11.6.1 Limiting case I: $R_2 \rightarrow \infty$

The assumption of infinite R_2 implies that region 2 has an infinite storage capacity. Consequently one expects that the concentration at the interface is zero. This follows directly from the expressions given in section 11.3: $R_2 \rightarrow \infty$, implies $k^- = D_{2z}/R_2 \rightarrow 0$. Consequently the solution of eq. (20) can only be $u^- = 0$. Therefore the continuity condition (6) leads to $c_b = 0$ and the concentration in region 1 is given by:

$$c(x, z, t) = \text{erf}(z/2/(k^+ x)) \quad x < v_1 t / R_1 \quad (66a)$$

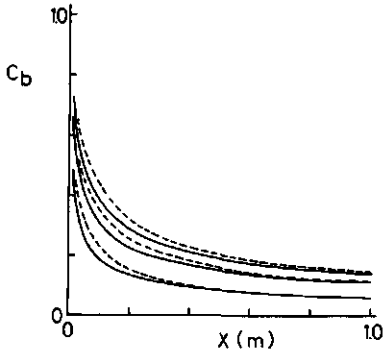


Figure 7:
750 Comparison of analytical (solid line)
450 and numerical (dashed line) solution
150 for c_b as a function of distance for
three times and $R_2 = 100$.

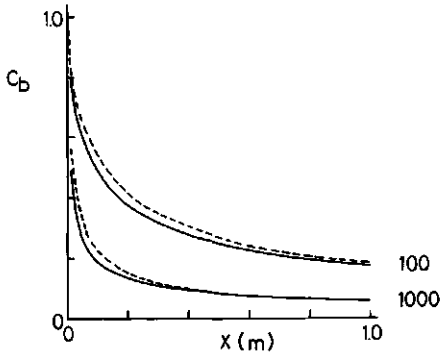


Figure 8:
100 Same as Fig. 7, for $t=750$ and two
1000 values of R_2 .

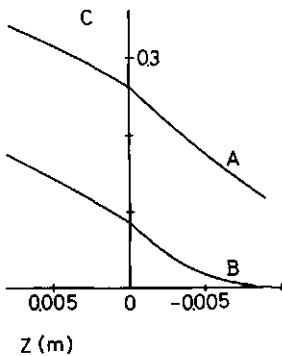


Figure 9:
Concentration distribution in a cross
section at $x=0.525$ m and $t=150$.
Numerical solution for the reference
case $R_2=100$ (A), and for $R_2=1000$ (B).

$$c(x,z,t) = 0 \qquad x > v_1 t / R_1 \qquad (66b)$$

From eq. (66) a simple criterion for the applicability of eq. (56) can be derived. In order to express the average concentration in region 1, $\bar{c}_H(x,t)$, in terms of the solute loss $V(x,t)$ it was assumed that H had been chosen such that $c(x,H,t) \approx 1$. When $c_b > 0$ the concentration in region 1 will be larger than the concentration with $c_b = 0$. Hence, if we choose H in (66) such that $c(x,H,t) \approx 1$ then this value will give a lower bound for the averaging height in the more general case where $c_b > 0$.

Assuming that eq. (56) is applicable when $c(x,H,t) > 0.995$, it follows from the above that $H/2/(k^+x) > 2$. This implies

$$H > 4 \sqrt{[(\alpha_T + D^*) / v_1] x} \qquad (67)$$

Condition (67) is used to calculate the average concentration from eq. (66):

$$\begin{aligned} \bar{c}_H(x,t) &= 1 - \frac{1}{H} \int_0^H [1 - c(x,z,t)] dz \\ &= 1 - \frac{1}{\Delta} \int_0^\Delta \text{erfc}(s) ds \end{aligned} \qquad (68)$$

where $\Delta = H/2/(k^+x)$. Since $\Delta > 2$ we may approximate eq. (68) by

$$\begin{aligned} \bar{c}_H(x,t) &\approx 1 - \frac{1}{\Delta} \int_0^\infty \text{erfc}(s) ds \\ &= 1 - \frac{2}{H} \sqrt{(k^+x/\pi)} \end{aligned} \qquad (69)$$

Therefore

$$\bar{c}_H(x,t) \approx 1 - \frac{2}{H} \sqrt{(k^+x/\pi)} \qquad x < \frac{v_1}{R_1} t \qquad (70a)$$

$$\bar{c}_H(x,t) = 0 \qquad x > \frac{v_1}{R_1} t \qquad (70b)$$

This expression also follows from section 3 : when $R_2 \rightarrow \infty$, then $A \rightarrow \infty$ (eq. 25) and $p \rightarrow \infty$ (eq. 34). Thus the solute loss becomes $V = 2\sqrt{(k^+x/\pi)}$ in both eq. (51) and eq. (52). Substitution into

eq. (56) gives eq. (70). The value of \bar{c}_H given by eq. (70) equals the value of \bar{c}_H at first breakthrough in Figure 6.

11.6.2 Limiting case II: $D_{1z} \rightarrow \infty$

This implies an infinite transversal dispersivity for the more permeable region and complete mixing in a cross section of this region. This assumption is frequently made in the literature [e.g. Grisak and Pickens, 1980; Tang et al., 1981; Van Genuchten et al., 1984]. For the permeable region, the transport equation is given by (again setting $D = D_{1z}$ and $v = v_1$)

$$\frac{\partial c}{\partial t} + v \frac{\partial c}{\partial x} = D \frac{\partial^2 c}{\partial z^2} \quad x > 0, z > 0, t > 0 \quad (71)$$

and the average concentration is defined by eq. (54). Inserting (54) in (71) yields

$$\frac{\partial}{\partial t} \left(\frac{1}{H} \int_0^H c(x, z, t) dz \right) + v \frac{\partial}{\partial x} \left(\frac{1}{H} \int_0^H c(x, z, t) dz \right) = \frac{D}{H} \frac{\partial c}{\partial z} \Big|_0^H \quad (72)$$

If we assume that H is large enough, such that $\frac{\partial c}{\partial z}(x, H, t) \approx 0$, then (72) may be rewritten as

$$\frac{\partial \bar{c}}{\partial t} + v \frac{\partial \bar{c}}{\partial x} = - \frac{D}{H} \frac{\partial c}{\partial z} \Big|_{z=0^+} \quad (73)$$

where we write \bar{c} instead of \bar{c}_H .

At the interface $z=0$, continuity of flux requires

$$n_1 D_1 \frac{\partial c}{\partial z} \Big|_{0^+} = n_2 D^* \frac{\partial c}{\partial z} \Big|_{0^-} \quad (74)$$

where it is assumed that $v_2 = 0$ and thus $D_{2z} = D^*$. Combining (73) with (74) gives

$$\frac{\partial \bar{c}}{\partial t} + v \frac{\partial \bar{c}}{\partial x} = - \frac{D}{H} \frac{n_2}{n_1} \frac{\partial c}{\partial z} \Big|_{0^-} \quad (75)$$

In eq. (75) the concentration c follows from the transport equation for the impermeable region:

$$R_2 \frac{\partial c}{\partial t} = D^* \frac{\partial^2 c}{\partial z^2} \quad z < 0, t > 0 \quad (76)$$

Eq. (75) and (76) may be solved if the additional assumption is made that

$$\bar{c}(x,t) = c(x,0,t) \quad (77)$$

Both (75) and (76) hold under general conditions whereas (77) holds only when the concentration in the permeable region 1 deviates little from its average value $\bar{c}(x,t)$. This will be the case when $D_{1z} \rightarrow \infty$. The solution is then [Carslaw and Jaeger, 1959, p. 396]:

$$\bar{c}(x,t) = \text{erfc} \left[\frac{n_2}{n_1} \frac{x}{2vH} \sqrt{(D^* R_2 \frac{1}{t-x/v})} \right], \quad t > x/v \quad (78a)$$

$$\bar{c}(x,t) = 0, \quad t < x/v \quad (78b)$$

This solution may be compared to the analytical and numerical results obtained with a finite transversal dispersivity. Numerical calculations indicated that for $R_2=1$ concentrations in a cross section of region 1 are relatively constant; hence differences involved in choosing a finite or an infinite transversal dispersivity will be small in that case. For larger R_2 -values the concentration in a cross section of region 1 is not constant at all (Fig. 9). Then large differences between the solutions for finite and infinite transversal dispersivities are expected.

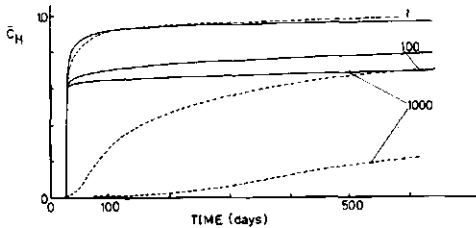


Figure 10:
Calculated breakthrough curves for different values of R_2 . Analytical approximation (solid line); limiting case $D_{1z} \rightarrow \infty$, eq. (77) (dashed line).

Figure 10 shows the breakthrough curves calculated with equation (78) for $R_2=1, 100, \text{ and } 1000$, along with the corresponding analytical curves shown in Fig. 6. The agreement for $R_2=1$ appears to be good. However, for larger values of R_2 , the differences become important and the calculated breakthrough occurs much later than for a finite transversal dispersivity. Hence the assumption of an infinite transversal dispersivity is questionable in situations where the thickness H of the permeable region is relatively large with respect to the value of D_{1z} and where R_2 has high values. The assumption of an infinite D_{1z} is probably justified for many cases encountered in the literature due to the relatively small values of H for the macropore and fracture widths considered [Van Genuchten et al., 1984, Tang et al., 1981]. For a fracture thickness H in the range of 10^{-6} - 10^{-3} m [Neretnieks et al., 1982, Rasmuson et al., 1982] and a diffusion coefficient equal to D^* the characteristic diffusion time $t_c = H^2/D^*$ is a factor 10^4 to 10^8 smaller than for region 1 in this study. Clearly a significant transversal concentration gradient, e.g. as given in Fig. 9, will not develop in such fractures. This was shown also by Carslaw and Jaeger [1959, p. 98]. In their Fig. 10a the concentration gradients disappear as $D t_c / H^2 \rightarrow \infty$. With $H = 10^{-3}$ m and $D = D^*$ gradients would become small within a few hours.

11.7 Summary and conclusions

In this contribution we studied solute transport in a flow domain consisting of two semi-infinite regions with different porous materials. Water flow is parallel to the sharp interface separating the two regions. In the direction of flow only convection occurs whereas dispersion occurs perpendicular to the flow direction. If the transport velocities (v/R) are different for the two regions transversal dispersion will cause solute to be transferred from region 1, with the highest transport velocity, to region 2. Taking into account continuity of concentration and of flux across the interface approximate analytical solutions were derived for the concentration at the interface and the loss of solute in region 1. Using these solutions expressions could be given for the concentration averaged

for a cross section of height H at designated distance x and time t . With these expressions breakthrough curves for the region with largest transport velocity were constructed.

The results obtained with the analytical solution were compared to numerical results. Since in the analytical approach two semi-infinite regions were considered the solutions are only of use if restrictions for the thickness H of the more permeable region and the thickness B of the less permeable layer are met. Lower bound restrictions for H and B are given. If these conditions are met the agreement between analytically and numerically calculated breakthrough is reasonable to good except for first breakthrough. Due to the neglect of longitudinal dispersion in the analytical approach the differences at the moment of first breakthrough for region 1 at designated x are significant.

Hence, due to the restrictions on H and B and the assumption of zero longitudinal dispersion coefficient the applicability of the analytical solution is limited to relatively short travel distances in natural flow domains consisting of different, rather homogeneous layers. Examples are stratified aquifers, aquifers bounded by confining layers as studied by Chen [1985] or laboratory analogons as considered by Shamir and Harleman [1967]. Contrary to the steady state solutions given by Shamir and Harleman [1967] the effect of adsorption on the concentration distribution may be studied with the analytical solution presented in this study. We assumed a finite value for D_{1z} at the expense of ignoring longitudinal dispersion. It was shown that this may lead to smaller differences with the numerical solution than if D_{1z} is assumed infinitely large. Then the analytical solution derived here is preferred over solutions with $D_{1z} \rightarrow \infty$. Although the numerical approach does not have the shortcomings of any of the analytical solutions it is noted that very fine discretizations in the longitudinal and transversal distances and in time were required. For the flow domain considered in this study as well as for more realistic scenarios computing will be very demanding with respect to time and expenses. Thus, a preliminary study for systems resembling the flow domain considered in this study with the analytical solution presented may be worthwhile.

Acknowledgements: Part of this work was carried out while the authors were at Delft Soil Mechanics Laboratory, Delft, The Netherlands. Comments and suggestions of M.Th. van Genuchten, and the reviewers of Water Resources Research helped to improve the manuscript.

Table 1: Parameter values

Parameter	Value for Reference Case	Variations
B	0.05 m	
H	0.20 m	
L	1.0 m	
n_1, n_2	0.5	0.75, 0.25
n_1/n_2	1	3, 1/3
v_1	12.5 m/year	
v_2	0 m/year	12.5
D^*	0.032 m ² /year	
D_{1z}	0.063 m ² /year	D^* , $4D^*$
D_{1x}	0.345 m ² /year (numerical approach)	
R_1	1	
R_2	100	1, 5, 10, 1000
α_L	0.025 m (numerical approach)	
α_T/α_L	0.1 (numerical approach)	

11.8 References

- Abramowitz, M. and I.A. Stegun, Handbook of Mathematical Functions, 1046 pp., Dover Publ., Inc., New York, 1964.
- Bear, J., Dynamics of Fluids in Porous Media, pp. 579-664, American Elsevier, New York, 1972.
- Bolt, G.H., Movement of solutes in soil: Principles of adsorption/exchange chromatography, in Soil Chemistry B. Physico-Chemical Models, edited by G.H. Bolt, pp. 285-348, Elsevier, Amsterdam, 1982.
- Carslaw, H.S., and J.C. Jaeger, Conduction of Heat in Solids, 510 pp., Clarendon Press, Oxford, 1959.

- Chen, C.-S. Analytical and approximate solutions to radial dispersion from an injection well to a geological unit with simultaneous diffusion into adjacent strata. *Water Resour. Res.* 21 (8), 1069-1076, 1985.
- Deans, H.H., A mathematical model for dispersion in the direction of flow in porous media, *Soc. Petrol. Eng. J.* 3 (1), 49-52, 1963.
- De Josselin De Jong, G., Longitudinal and transverse diffusion in granular deposits, *Transactions American Geophysical Union*, 38, 67-74, 1958.
- Freeze, R.A. and J.A. Cherry, *Groundwater*, pp. 408-413, Prentice-Hall, Inc., Englewoods Cliffs, New Jersey, 1979.
- Fried, J.J., *Groundwater Pollution*, pp. 47-48, Elsevier, Amsterdam, 1975.
- Gray, W.G. and G.F. Pinder. An analysis of the numerical solution of the transport equation. *Water Resour. Res.*, 12 (3), 547-555, 1976.
- Grisak, G.E., and J.F. Pickens, Solute transport through fractures media, 1. The effect of matrix diffusion, *Water Resour. Res.*, 16(4), 719-730, 1980.
- Güven, O., F.J. Molz and J.G. Melville. An analysis of dispersion in a stratified aquifer. *Water Resour. Res.* 20(10), 1337-1354, 1984.
- Lantz, R.B. Quantitative evaluation of numerical diffusion (truncation error), *Soc. Petrol. Eng. J.*, 11 (9). 315-320, 1971.
- Neretnieks, I. Diffusion in the rock matrix: an important factor in radionuclide retardation? *J. Geophys. Res.*, 85, 4379-4397, 1980.
- Neretnieks, I., T. Eriksen and P. Tähtinen. Tracer movement in a single fissure in granitic rock: some experimental results and their interpretation. *Water Resour. Res.* 18(4), 849-858, 1982.
- Price, H.A., R.S. Varga and J.E. Warren, Application of oscillation matrices to diffusion convection equations. *J. Math. Phys.*, 45, 301-311, 1966.
- Raats, P.A.C., Transport in structured porous media, in: *Flow and transport in Porous Media*, edited by A. Verruijt and F.B.J. Barends, pp. 221-226, Balkema, Rotterdam, 1981.
- Rasmuson, A., Diffusion and sorption in particles and two-dimensional dispersion in a porous medium, *Water Resour. Res.*, 17 (2), 321-328, 1981.

- Rasmuson, A. and I. Neretnieks, Exact solution of a model for diffusion in particles and longitudinal dispersion in packed beds, *AIChEJ.*, 26, 686, 1980.
- Rasmuson, A., and I. Neretnieks. Migration of radionuclides in fissured rock: the influence of micropore diffusion and longitudinal dispersion, *J. Geophys. Res.*, 86, 3749, 1981.
- Rasmuson, A., T.N. Narasimhan and I. Neretnieks. Chemical transport in a fissured rock: verification of a numerical model. *Water Resour. Res.* 18 (5), 1479-1492, 1982.
- Shamir, U.Y., and D.R.F. Harleman. Dispersion in layered porous media. *Proc. Am. Soc. Civ. Eng., J. Hydr. Div. HY5*, p. 237-260, 1967.
- Skopp, J. and A.W. Warrick, A two-phase model for the miscible displacement of reactive solutes in soils, *Soil Sci. Soc. Am. Proc.*, 38, 545-555, 1974.
- Smith, G.D. *Numerical Solution of Partial Differential Equations: Finite Difference Methods*, Clarendon Press, Oxford, 1978.
- Tang, D.H., E.O. Frind and E.A. Sudicky, Contaminant transport in fractured porous media: Analytical solution for a single fracture, *Water Resour. Res.*, 17 (3), 555-564, 1981.
- Van Genuchten, M.Th. and R.W. Cleary. Movement of solutes in soil: Computer simulated and laboratory results, in *Soil Chemistry B, Physico-Chemical Models*, edited by G.H. Bolt, pp. 349-386, Elsevier, Amsterdam, 1982.
- Van Genuchten, M.Th., D.H. Tang and R. Guennelon. Some exact solutions for solute transport through soils containing large cylindrical macropores. *Water Resources Research*, Vol. 20 no. 3, pp. 335-346, 1984.
- Van Genuchten, M.Th. and P.J. Wierenga. Mass transfer studies in sorbing porous media: I analytical solutions. *Soil Sci. Soc. Am. J.*, 40, 473-480, 1976.
- Verruijt, A. Steady dispersion across an interface in a porous medium, *J. Hydrol.*, 14, 337-347, 1971.

12. GENERAL CONCLUSION

In this thesis a number of problems were studied, that concerned phosphate sorption in soil, and reactive solute transport. In the course of this work a (rapidly increasing) number of assumptions was made. Thus, a microscopic description of P-sorption for oxide particles developed in Chapter 3 was gradually simplified to a step function type of overall sorption under field conditions. One of the recurrent themes, therefore, which was explicitly mentioned in some of the chapters, was that model sophistication should be compatible to the knowledge of the system, and to the primary goals of the study: the answers searched for. To employ microscopic descriptions at e.g. a field scale is unpractical, hardly feasible in many cases due to the limited system knowledge, and often not required for the accuracy wanted. If a microscopic description (e.g. as in Appendix B) is used for a field (a 'field-equivalent column') this may even lead to errors as the controlling phenomena, such as horizontal variability, may not be recognized. The approach that should be followed has therefore 'fractal' characteristics. Different questions are asked at different scales of interest, and different questions require generally that emphasis is given to different problem controlling phenomena. In cases where measurement at the scale of interest is not (directly) possible, such as for P-displacement in fields, microscopic considerations may become very important. Understanding of allowable simplifications and of methods to generate the model input for evaluation at the macroscopical scale may be obtained from microscopic, mechanistic considerations.

SUMMARY

When the solute inflow rate into the soil system exceeds the accumulation rate, this implies for a non-decaying solute that outflow occurs at the system boundaries. One of the pathways by which solute may leave the soil system is by leaching to the ground water. In case of leaching of unacceptable concentrations, one of the consequences may be ground water and surface water quality deterioration. For The Netherlands this situation may occur for phosphate, which is applied to soil in e.g. animal manure disposed of in the intensive animal husbandry, and for some heavy metals, due to e.g. the enhanced (atmospheric) deposition. To evaluate how the leached concentrations of these contaminants change in time, the interaction with the soil and the transport process must be quantified. The scope of this thesis was to describe the sorption (rate) of phosphate in soil, as a function of some dominant soil parameters and concentration, and to describe the effects of heterogeneity of the soil system on transport. Emphasis was given to sorption and transport of phosphate due to disposal of animal manure.

One of the methods frequently employed in this thesis, to quantify P-adsorption and desorption, was a new desorption technique described in Chapter 2. In this batch desorption technique, iron oxide impregnated filterpaper is used as an infinite sink for soil phosphate. With this method the desorption kinetics were studied for nine sandy soils, which yielded desorption rate constants, that were in agreement with values reported in the literature. It was shown that the method may also be used to evaluate the content of desorbable P for quite different soils on a routine basis. It is also useful at low P-contents, where conventional dilution methods fail.

In Chapter 3 an approximate sorption kinetics model was developed. The reactions occurring at the microscopic scale were described as a relatively fast, reversible adsorption onto the surfaces of reactive iron and aluminium compounds, and an irreversible diffusion-precipitation process, that involves the bulk of these compounds, and approaches equilibrium very slowly. The net adsorption rate was described by Langmuir kinetics. The diffusion-precipitation process was described with a relation, derived from the formulation of

the unreacted shrinking core model known from chemical engineering. This relation involves a composite, dimensionless exposure variable equal to the time integrated phosphate concentration in solution. The diffusion precipitation model is applicable, when diffusion type resistances are conversion rate limiting, or in case of a first order reaction rate. As was shown for three different cases in Chapter 4, then time may be scaled with the diffusing reactant concentration in solution.

Parameter assessment for the sorption model was discussed in Chapter 5. This assessment is complicated by the simultaneous occurrence of the adsorption and the diffusion-precipitation processes. Due to the assumed irreversibility of the latter process, desorption studies (in batch and column leaching experiments) yielded the adsorption/desorption parameters. Once these were known, the amount of P adsorbed could be calculated for sorption experiments, and the difference between calculated adsorption and measured total sorption was set equal to precipitated P. The diffusion-precipitation model parameters were then obtained by simultaneously fitting precipitated P as a function of exposure, for all concentrations. Validation of the sorption model was done by comparing measured P-concentration breakthrough curves for small columns with numerical predictions based on the independently assessed sorption parameter values. Agreement appeared to be reasonable to good for the data given in Chapter 5.

The procedures described in Chapters 2 and 5 were considered too involved for evaluating P-sorption for many different soils and for large reaction times, in a routine fashion. Therefore in Chapter 6 a simplified sorption model was developed that did not have this shortcoming. The kinetics of total P-sorption appeared to conform well to the description of diffusion-precipitation given in Chapter 3. The sorption rate constant (k) for total sorption, was assessed for a large number of different soils, with different initial P-contents, for four reaction periods. Also the dependency of the pseudo sorption maximum for total sorption, on the amount (M) of metals (Fe, Al) extractable with acid ammonia oxalate was assessed. An accurate description was obtained if total sorption is expressed as the product of the sorption rate constant (k), the metal content (M), and the

logarithm of the exposure variable, as defined in Chapter 3.

When, besides total sorption, also the reversibly sorbed amount of phosphate is important, a routine method for evaluating the adsorption parameters is also of interest. In Chapter 7, a procedure was described to find the adsorption constant (K) from the amounts desorbed with a conventional dilution method, and with the procedure discussed in Chapter 2, respectively. With the last method also the adsorption maximum may be measured for P-saturated soil samples. The adsorption maximum appeared to be proportional to the oxalate extractable metal content (M), just as the pseudo maximum for total sorption. The adsorption parameters, the metal content (M), and the amounts desorbed with the two techniques were shown to be lognormally as well as normally distributed. The effect of the uncertainty, due to the distributed nature of parameters and variables, on environmental constraints with respect to P-leaching was discussed for illustration.

More emphasis to the effect of heterogeneity, expressed in such distributions, on transport, was given in Chapters 8, 9, and 10. In Chapter 8 the spatial variability of the excess amount of P applied to a field, and of the total sorption capacity were assessed. Assuming purely convective transport, the effect of such variability on P-transport was numerically studied for the field on average. This effect appeared to be so profound that it is in general not justified to use field average values of parameters and variables, to study phosphate displacement in a field. Experimental data of the field were in good agreement with theoretical results, in view of the correlation structure observed in the field.

In Chapter 9 a similar problem as in Chapter 8 was studied, for displacement of heavy metals (Cu, Cd) in a field with spatially variable flow velocity, (Freundlich) adsorption coefficient, and metal input. In this theoretical study an analytical solution was given for the field-averaged transport, assuming lognormal distributions of spatial variates, and assuming purely convective transport. Illustrations were given how variability in soil properties, and scaling theory for flow in similar media may be incorporated in the model.

In Chapter 10 redistribution of reversibly adsorbed P already present in the topsoil was studied. First some trends were made

explicit for a single column, if disposal of P is stopped. The effects were shown of the thickness of the P -saturated topsoil layer, the adsorption constant, and the adsorption maximum, on the concentration distribution in a soil column as a function of time, taking pore scale dispersion into account, but neglecting the diffusion-precipitation in the subsoil. The redistribution process was studied numerically for a field exhibiting pronounced spatial variability with respect to the amount of P initially present, and with respect to the adsorption maximum. This stochastic approach showed large differences with results obtained for the 'field equivalent column' with average parameter values, in agreement to the conclusions of Chapters 8 and 9.

In Chapter 11 transport was studied for a hypothetical flow domain consisting of two different porous materials. These two regions are separated by a sharp interface parallel to the direction of flow, and have different porosities, flow velocities, and retardation factors. The importance of transversal dispersion on transport was shown. Due to transfer of solute from the region one, with high transport velocity, into the region two, with small transport velocity, resulted in a non-symmetrical breakthrough curve for region one. The numerically evaluated results were in good agreement with an analytical solution. A constraint was given for using an infinite transversal dispersion coefficient in region one. This assumption is commonly made in the literature.

In the appendices several additional results were given attention, that were not yet addressed in the main text. In Appendix A the travelling wave solution was given for transport in the case of adsorption according to the Langmuir isotherm. In Appendix B the transport in a column at field conditions was described. It appeared that the shock front assumption in many cases may be acceptable, and that omission of the diffusion-precipitation process, as was done in Chapter 10 may not be warranted. In Appendix C some background information was given on the distributions used, and in Appendix D on the Protocol Phosphate Saturated Soils.

SAMENVATTING

Indien de snelheid waarmee opgeloste niet-afbreekbare stoffen het bodemsysteem binnen komen groter is dan de snelheid waarmee zulke stoffen in dit systeem worden vastgelegd, dan betekent dit dat een fractie van deze stoffen het bodemsysteem verlaten. Een van de wegen via welke opgeloste stoffen het bodemsysteem kunnen verlaten, is door uitspoeling naar het grondwater. In geval de concentraties die uitspoelen te hoog zijn, kan een van de consequenties de verslechtering van de grond- en oppervlaktewaterkwaliteit zijn. In Nederland kan deze situatie optreden voor fosfaat, dat in de intensieve veehouderij, middels het uitrijden van overmatige hoeveelheden dierlijke mest, op het land wordt gebracht, en voor enkele zware metalen, als gevolg van de vergrote (atmosferische) depositie. Om te kunnen beoordelen hoe de uitgespoelde concentraties van deze verontreinigingen in de tijd veranderen, moeten de interactie met de bodem en het transportproces gekwantificeerd worden. Het doel van deze dissertatie was om een beschrijving te geven van de fosfaat vastlegging, en de snelheid hiervan, in de bodem, in afhankelijkheid van enkele belangrijke bodem parameters en de fosfaat concentratie, en om het effect van bodemheterogeniteit op transport van verontreinigingen te beschrijven. De nadruk is gegeven aan de vastlegging en het transport van fosfaat als gevolg van overmatige mestdoseringen.

Een van de technieken waarvan in het werk voor deze dissertatie geregeld gebruik werd gemaakt, om fosfaat (P) adsorptie en desorptie te kwantificeren, is een nieuwe methode die in Hoofdstuk 2 beschreven staat. In deze desorptie-schud methode, wordt met ijzeroxide geïmpregneerd filterpapier gebruikt als een sorbens met een zeer hoge sorptie affiniteit en capaciteit voor P aanwezig in de bodem. Met deze methode werd de desorptiekinetiek bestudeerd voor negen zandgronden, waarbij desorptie-snelheidsconstanten gevonden werden, die met literatuurwaarden in overeenstemming zijn. Tevens werd getoond, dat de methode ook bruikbaar is om het gehalte van desorbeerbaar P van tamelijk verschillende bodems routinematig vast te stellen. Bij lage P-gehalten, waar conventionele verdunningsmethoden te kort schieten, is deze methode ook bruikbaar.

In Hoofdstuk 3 werd een sorptie kinetiek model ontwikkeld. De reacties die op de microscopische schaal plaats vinden werden beschreven als een relatief snelle, reversibele adsorptie op het oppervlak van reactieve ijzer- en aluminium bestanddelen, en een irreversibel diffusie-precipitatie proces, waarbij ook het interne volume van deeltjes van deze bestanddelen betrokken is, en dat zeer langzaam nadert tot een evenwicht. De netto adsorptie snelheid werd met Langmuir kinetiek beschreven. Het diffusie-precipitatie proces werd beschreven met een relatie, die afgeleid werd van de formulering het niet-omgezette krimpende kern model, bekend van de chemische technologie. Deze relatie maakt gebruik van een samengestelde, dimensieloze blootstellingsvariabele, gelijk aan de over de tijd geïntegreerde fosfaatconcentratie in oplossing. Het diffusie-precipitatie model is bruikbaar wanneer diffusieve weerstanden snelheidsbepkend zijn voor omzetting of in geval van een interne eerste orde reactiesnelheid. Zoals werd getoond voor drie verschillende gevallen in Hoofdstuk 4 kan in dat geval de tijd geschaald worden met behulp van de diffunderende reactantconcentratie in oplossing.

De bepaling van de parameterwaarden van het vastleggingsmodel werd besproken in Hoofdstuk 5. Deze bepaling wordt gecompliceerd door het gelijktijdig optreden van de adsorptie en het diffusie-precipitatie proces. Als gevolg van de veronderstelde irreversibiliteit van het laatste proces, levert onderzoek van desorptie (schud- en kolom-uitspoelexperimenten) de adsorptie/desorptie parameters. Zodra deze bekend waren, kon de hoeveelheid geadsorbeerd P berekend worden voor sorptie-experimenten, waarna het verschil tussen berekend geadsorbeerd P en de gemeten totale vastlegging gelijk gesteld werd aan geprecipiteerd P. De diffusie-precipitatie modelparameters werden toen vastgesteld door, voor alle beschouwde concentraties, de hoeveelheid geprecipiteerd P simultaan te fitten als functie van de blootstelling. Validatie van het sorptiemodel werd uitgevoerd door gemeten P-concentratie doorbraakkrommen voor kleine kolommen te vergelijken met numerieke voorspellingen, waarbij gebruik gemaakt werd van de onafhankelijk vastgestelde sorptieparameter waarden. Voor de data gegeven in Hoofdstuk 5 bleek de overeenkomst redelijk tot goed te

zijn.

De procedures beschreven in de Hoofdstukken 2 en 5 werden als te ingewikkeld beschouwd om P-sorptie routinematig te evalueren voor veel verschillende gronden, en voor grote reactietijden. Daarom werd in Hoofdstuk 6 een vereenvoudigd sorptiekinetiek model ontwikkeld, dat deze tekortkoming niet heeft. De kinetiek van totale P-sorptie bleek goed overeen te komen met de beschrijving van diffusie-precipitatie, die gegeven werd in Hoofdstuk 3. De sorptie snelheidsconstante (k) voor totale sorptie, werd bepaald voor een groot aantal verschillende gronden, met verschillende initiële P-gehalten, voor vier reactieperioden. Ook werd de afhankelijkheid bepaald tussen het pseudo sorptie maximum, en de met zuur ammonium-oxalaat extraheerbare metaal hoeveelheid (M) van de metalen Fe en Al. Een accurate beschrijving werd verkregen indien de totale sorptie wordt uitgedrukt als het product van de sorptie snelheidsconstante (k), het metaalgehalte (M), en de logaritme van de blootstelling, zoals gedefinieerd in Hoofdstuk 3.

Wanneer naast de totale sorptie ook de reversibel vastgelegde hoeveelheid fosfaat van belang is, dan is ook voor de vaststelling van de adsorptieparameters een routinematige methode wenselijk. In Hoofdstuk 7 werd een procedure beschreven om de adsorptieconstante (k) te bepalen met behulp van de hoeveelheden die gedesorbeerd worden met een conventionele verdunningsmethode, en met de methode van Hoofdstuk 2. Voor P-verzadigde grondmonsters leidt de laatstgenoemde methode tot het adsorptiemaximum. Het adsorptiemaximum bleek evenredig te zijn met het oxalaat extraheerbare metaalgehalte (M), evenals het pseudomaximum voor totale vastlegging. De adsorptieparameters, het metaalgehalte (M), en de volgens de twee methoden gedesorbeerde hoeveelheden bleken zowel lognormaal als normaal verdeeld te zijn. Ter illustratie werd het effect besproken van onzekerheid, als gevolg van de verdelingen van parameters en variabelen, op milieuhygenische beperkingen ten aanzien van P-uitspoeling.

In de Hoofdstukken 8, 9, en 10 wordt meer nadruk gelegd op het effect op transport van heterogeniteit, zoals beschreven met genoemde verdelingen. In Hoofdstuk 8 werd vastgesteld wat de ruimtelijke variabiliteit is van de overmatige gedoseerde hoeveelheid P en de totale sorptie capaciteit. In de veronderstelling dat zuiver

convectief transport optreedt, werd numeriek het effect van een dergelijke variabiliteit op het perceelsgemiddelde P-transport bestudeerd. Dit effect bleek dermate groot, dat het in het algemeen niet juist is om perceelsgemiddelde waarden van variabelen en parameters te gebruiken om de verplaatsing van fosfaat in een perceel te bestuderen. Experimentele gegevens van het perceel bleken goed overeen te komen met theoretische resultaten, gezien de correlatiestructuur vastgesteld voor het perceel.

In Hoofdstuk 9 werd een probleem bestudeerd dat vergelijkbaar is met dat van Hoofdstuk 8, voor het transport van zware metalen (Cu, Cd) in een perceel met ruimtelijk variabele stroomsnelheid, (Freundlich) adsorptie coefficient, en metaal invoer. In dit theoretische onderzoek werd een analytische oplossing gegeven voor het perceelsgemiddelde transport, waarbij lognormale verdelingen van ruimtelijke variabelen en zuiver convectief transport werden verondersteld. Geïllustreerd werd hoe variabiliteit in bodemeigenschappen en scaling-theorie voor stroming in gelijkvormige media in het model ingebouwd kunnen worden.

In Hoofdstuk 10 werd de herverdeling van reversibel geadsorbeerd P, dat reeds aanwezig is in de bovengrond, bestudeerd. Eerst werden enkele trends getoond voor een enkele kolom, indien de overmatige dosering van P wordt beëindigd. De effecten werden getoond van de dikte van de met P verzadigde bovenlaag, de adsorptieconstante, (K), en het adsorptie maximum, (Q_m), op de concentratieverdeling in een bodemkolom als functie van de tijd, indien dispersie in rekening wordt gebracht en diffusie-precipitatie in de ondergrond wordt verwaarloosd. Numeriek werd het herverdelingsproces bestudeerd in een perceel met aanzienlijke ruimtelijke variabiliteit ten aanzien van de hoeveelheid P die initieel in de bodem aanwezig is, en ten aanzien van het adsorptie maximum. Deze stochastische benadering laat zien dat grote verschillen optreden tussen de gevonden resultaten en de resultaten voor een 'aan het veld equivalente kolom' met gemiddelde parameterwaarden, in overeenstemming met de Hoofdstukken 8 en 9.

In Hoofdstuk 11 werd transport bestudeerd voor een denkbeeldig medium, dat bestaat uit twee poreuze materialen. Deze twee gebieden worden gescheiden door een scherp grensvlak evenwijdig aan de stromingsrichting, en hebben verschillende porositeiten, snelheden, en redardatie factoren. Door de stofoverdracht van het gebied (regio 1)

met een hoge transport snelheid naar het gebied met een lage transportsnelheid, wordt een asymmetrische doorbraakcurve gevonden voor het eerste gebied. De numeriek gevonden resultaten zijn in goede overeenstemming met een analytische oplossing. Voor de aanname van een perfecte menging in de richting die loodrecht op het grensvlak staat in regio 1 werd aangegeven, wanneer deze veronderstelling geldig is. De genoemde veronderstelling wordt vaak gemaakt in de literatuur.

In de bijlagen worden enkele extra resultaten beschouwd, die niet aan de orde kwamen in de hoofdtekst. In Appendix A werd een lopende golf oplossing gegeven voor het geval van transport met adsorptie volgens de Langmuir isotherm. In Appendix B werd transport onder veldomstandigheden in een kolom beschreven. Het bleek dat de schokfront benadering in veel gevallen acceptabel kan zijn maar dat het verwaarlozen van het diffusie-precipitatie proces, zoals in Hoofdstuk 10, vaak een niet toelaatbare vereenvoudiging is. In Appendix C werd enige achtergrond informatie gegeven over de gebruikte verdelingen en in Appendix D evenzo over het Protokol Fosfaat Verzadigde Gronden.

APPENDICES

APPENDIX A: A TRAVELLING WAVE SOLUTION FOR TRANSPORT OF A SOLUTE REACTING ACCORDING TO THE LANGMUIR ISOTHERM

In this appendix, I present a solution for the shape and width of the front for a solute adsorbing reversibly according to the Langmuir isotherm. Consider the transport equation:

$$\frac{\partial}{\partial t} [\rho Q + \theta c] = \theta D \frac{\partial^2 c}{\partial z^2} - J^v \frac{\partial c}{\partial z} \quad (\text{A-1})$$

Division by θ and setting $v = J^v/\theta$ yields

$$\frac{\partial}{\partial t} \left\{ \frac{\rho Q}{\theta} + c \right\} = D \frac{\partial^2 c}{\partial z^2} - v \frac{\partial c}{\partial z} \quad (\text{A-2})$$

After transformation by setting $\eta = z - at$ ($d\eta = dz = -a dt$) eq. (A-2) becomes:

$$-a \frac{d}{d\eta} \left\{ \frac{\rho Q}{\theta} + c \right\} = D \frac{d^2 c}{d\eta^2} - v \frac{dc}{d\eta} \quad (\text{A-3})$$

This equation may be integrated for the conditions

$$\frac{dc}{d\eta} = 0 \quad \eta \rightarrow \pm \infty$$

$$\lim_{\eta \rightarrow +\infty} c = c_i$$

$$\lim_{\eta \rightarrow -\infty} c = c_f$$

First we write

$$\Delta c = c_f - c_i$$

$$\Delta Q = Q(c_f) - Q(c_i) = Q_f - Q_i$$

The front velocity found by integration of eq. (A-3), is given by

$$a = \frac{\theta \Delta c v}{\rho \Delta Q + \theta \Delta c} \quad (\text{A-4})$$

and is seen to equal $a = v/R$, where R is the front retardation factor. Integrating eq. (A-3) from η is $-\infty$ to η yields:

$$-a \left\{ \frac{\rho}{\theta} (Q - Q_f) + (c - c_f) \right\} = D \frac{dc}{d\eta} - v(c - c_f) \quad (\text{A-5})$$

After rearrangement and insertion of eq. (A-4) the result is given by:

$$\frac{D \theta}{a \rho} \frac{dc}{d\eta} = \frac{\Delta Q}{\Delta c} (c - c_f) + Q_f - Q \quad (\text{A-6})$$

Equation (A-6) corresponds to eq. (9) of Van der Zee and Van Riemsdijk [1987] for $c_i = 0$. The relation between Q and c is given by the Langmuir equation.

$$Q = \frac{Q_m K c}{1 + K c} \quad (\text{A-7})$$

Therefore

$$\frac{\Delta Q}{\Delta c} = \frac{Q_f - Q_i}{c_f - c_i} = \frac{Q_m K}{(1 + K c_f)(1 + K c_i)} \quad (\text{A-8})$$

$$Q_f - Q = \frac{Q_m K (c_f - c)}{(1 + K c_f)(1 + K c)} \quad (\text{A-9})$$

Hence eq. (A-4) may be rewritten as

$$a = \frac{v \theta (1 + K c_f)(1 + K c_i)}{\rho Q_m K + \theta (1 + K c_f)(1 + K c_i)} \quad (\text{A-10})$$

Inserting eqs. (A-8) and (A-9) into eq. (A-6) yields

$$\frac{D \theta}{a \rho} \frac{dc}{d\eta} = \frac{Q_m K^2 (c - c_i) (c - c_f)}{(1 + K c)(1 + K c_i)(1 + K c_f)} \quad (\text{A-11})$$

Equation (A-11) is rearranged as

$$\frac{1 + K c}{(c - c_i)(c - c_f)} dc = \frac{a \rho Q_m K^2}{D \theta (1 + K c_i)(1 + K c_f)} d\eta \quad (\text{A-12})$$

Now eq. (A-12) is integrated from η_R to η where $c_R = \frac{1}{2} (c_f + c_i)$. Before doing so, first multiply with $(c_f - c_i)$.

For the left hand side of eq. (A-12) this yields

$$\begin{aligned}
 & \int_{c_R}^c \frac{(1+K c) (c_f - c_i)}{(c - c_i)(c - c_f)} dc \\
 &= \int_{c_R}^c \left\{ \frac{-(1+K c_f)}{c_f - c} - \frac{(1+K c_i)}{c - c_i} \right\} dc \\
 &= \left[(1+K c_f) \ln(c_f - c) - (1+K c_i) \ln(c - c_i) \right]_{c_R}^c \\
 &= (1+K c_f) \ln\left(\frac{c_f - c}{c_f - c_R}\right) - (1+K c_i) \ln\left(\frac{c - c_i}{c_R - c_i}\right) \tag{A-13}
 \end{aligned}$$

Inserting eq. (A-10) the right hand side becomes

$$\begin{aligned}
 & \frac{a \rho Q_m K^2 (c_f - c_i)}{D \theta (1+K c_i)(1+K c_f)} \int_{\eta_R}^{\eta} d\eta \\
 &= \frac{v \rho Q_m K^2 (c_f - c_i) (\eta - \eta_R)}{D \{ \rho Q_m K + \theta (1+K c_i) (1+K c_f) \}} \tag{A-14}
 \end{aligned}$$

The front shape is therefore given by

$$\frac{\left(\frac{c_f - c}{c_f - c_R}\right)^{1+K c_f}}{\left(\frac{c - c_i}{c_R - c_i}\right)^{1+K c_i}} = \exp \left\{ \frac{v \rho Q_m K^2 (c_f - c_i) (\eta - \eta_R)}{D \{ \rho Q_m K + \theta (1+K c_i) (1+K c_f) \}} \right\} \tag{A-15}$$

Assuming $\eta = \eta_R = 0$ geeft then $\eta = \eta_R = 0$ for $c = c_R = \frac{1}{2}(c_f + c_i)$.
 Defining the front as $\Delta\eta$ belonging to the concentration interval $(1-2\varepsilon)\Delta c$, and setting

$$c_L = c_f + \varepsilon \Delta c \quad (\text{A-16a})$$

$$c_H = c_f - \varepsilon \Delta c \quad (\text{A-16b})$$

$$\eta_L = \eta(c_L) \quad (\text{A-16c})$$

$$\eta_H = \eta(c_H) \quad (\text{A-16d})$$

$$\Delta\eta = \eta_L - \eta_H \quad (\text{A-16e})$$

an expression may be obtained for the front thickness (see Figure A-1 for an illustration).

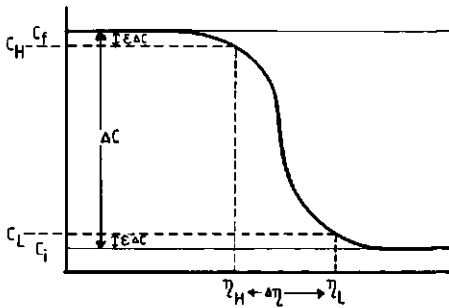


Figure A-1: Schematic representation of the front thickness

Equation (A-15) is given schematically by

$$\frac{A}{B} \frac{a_1}{b_1} = \exp \left\{ \frac{K_1}{K_2} \eta \right\}$$

or also

$$\frac{K_1}{K_2} \eta = a_1 \ln A - b_1 \ln B \quad (\text{A-17})$$

Inserting

$$A = \frac{c_f - c}{c_f - c_R} = \frac{c_f - c}{\Delta c / 2}$$

$$\text{and } B = \frac{c - c_i}{c_R - c_i} = \frac{c - c_i}{\Delta c / 2}$$

this yields

$$\frac{K_1}{K_2} \eta = a_1 \ln(c_f - c) - b_1 \ln(c - c_i) + (b_1 - a_1) \ln\left(\frac{\Delta c}{2}\right)$$

Working this out for c_L and c_H results in

$$\frac{K_1}{K_2} \eta_L = a_1 \ln\{(1-\epsilon)\Delta c\} - b_1 \ln\{\epsilon \Delta c\} + (b_1 - a_1) \ln \frac{\Delta c}{2}$$

$$\frac{K_1}{K_2} \eta_H = a_1 \ln\{\epsilon \Delta c\} - b_1 \ln\{(1-\epsilon)\Delta c\} + (b_1 - a_1) \ln \frac{\Delta c}{2}$$

Subtraction yields $\Delta\eta = \eta_L - \eta_H$:

$$\frac{K_1}{K_2} \Delta\eta = (a_1 + b_1) \ln \frac{1-\epsilon}{\epsilon}$$

Hence

$$\Delta\eta = \frac{K_2}{K_1} (a_1 + b_1) \ln \frac{1-\epsilon}{\epsilon}$$

$$= \frac{D \{ \rho Q_m K + \theta(1+K c_f)(1+K c_i) \} \{ 2+K(c_f+c_i) \}}{v \rho Q_m K^2 (c_f - c_i)} \ln \frac{1-\epsilon}{\epsilon}$$

$$\Delta\eta = \frac{D}{v} \left\{ \frac{1+\theta}{\rho Q_m K} (1+K c_f)(1+K c_i) \right\} \frac{2+K(c_f+c_i)}{K(c_f-c_i)} \ln \frac{1-\epsilon}{\epsilon} \quad (\text{A-18})$$

Acknowledgement : I wish to thank Aukje Gjaltema for discussions and for noticing some sloppiness in the original derivation.

APPENDIX B: VALIDITY OF THE SHOCK FRONT ASSUMPTION FOR PHOSPHATE TRANSPORT AT FIELD CONDITIONS

One of the major assumptions made in Chapter 7 [Van Der Zee and Van Riemsdijk, 1986] was that P displaces in soil as a shock front. The background of this assumption was that in case of high affinity sorption, the effects of dispersion and non-linearity in c of sorption counteract. This leads to a relatively sharp front, that moves through soil with a constant velocity and constant front shape, in case of a uniform soil profile. Examples of such travelling waves were provided (analytically) by Reiniger and Bolt [1972], Bolt [1982], Van Duijn and De Graaf [1984] (see also Van Der Zee and Van Riemsdijk, [1987]), and in Appendix A.

The solutions provided in the referenced literature were based on several assumptions, i.e., uniformity of the soil column, steady state flow, equilibrium sorption, and, in case the feed concentration exceeds the resident concentration:

$$F'(c) > 0 \quad ; \quad F''(c) << 0 \quad (B-1)$$

While constraint (B-1) may be valid for most cases of practical interest for P-displacement, we are also interested in the validity of the shock front approximation in case of soil layering, fluctuations in the feed concentration, and of course non-equilibrium sorption. For those cases analytical solutions are hardly feasible, and numerical approaches must be used.

The aim of this appendix is to briefly indicate that P-transport is sorption controlled, a relatively sharp P-front (sorbed plus dissolved) may be expected also in layered soils, and what the effect is of diffusion-precipitation on results as given in Chapter 10, where only adsorption was taken into account. This will be done for a soil resembling the NKR-1 soil (Chapter 5), a feed concentration of $c_0 = 3 \text{ mol m}^{-3}$ (or zero), and realistic flow and dispersion parameter values as given in e.g. Chapters 9 and 10.

Because exposure (I) may reach much higher values than in experiments as described in Chapter 5 and 6, a sorption function is needed that extrapolates to large I and is in agreement to findings in

Chapter 6. Instead of a polynomial of $\ln(I)$, that results in $S \rightarrow \infty, I \rightarrow \infty$, a function with a distinct sorption maximum was assumed:

$$S = S_m / \{ 1 + B I^{-K} \} \quad (\text{B-2})$$

The value of B equals

$$B = (S_m - a_0) / a_0 \quad (\text{B-3})$$

where a_0 is the first polynomial constant, and K_s follows from the polynomial constants, and S_m . The relation (B-2) is matched with the polynomial at the point $I = 1$ and the point $S = \frac{1}{2} S_m$ (see Figure B-1).

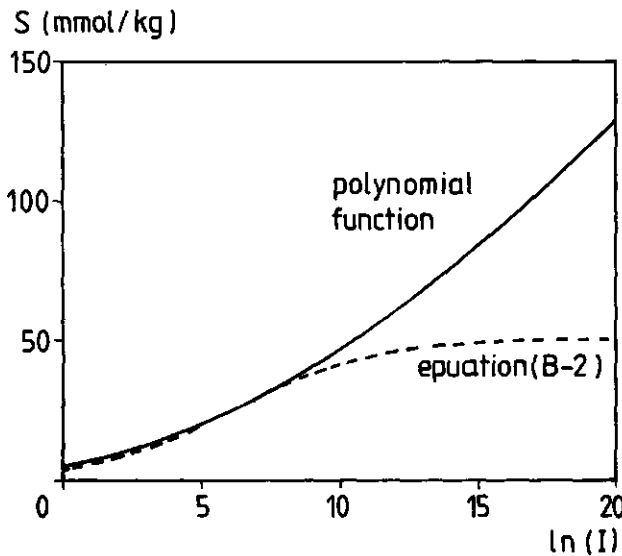


Figure B-1: Exposure-sorption curves: polynomial (solid line) and function (B-1) (dashed line).

As in Figure B-1 time used to calculate I is in minutes, the second point ($\ln(I) < 8$) falls in the experimentally evaluated domain of I . The curve given by (B-2) is shown to approach a maximum value, chosen at $S_m = \frac{1}{2} M - Q_m$ (Chapter 6, 7).

Fronts are shown in Figure (B-2), assuming adsorption (Q) equilibrium, for the dimensionless quantities $\bar{c} = c/c_0$, $\bar{Q} = Q/Q_m$, $\bar{S} = S/S_m$, and $\bar{F} = F/F_m$ (equal to $(Q + S)/Q_m + S_m$). For a reference case with a uniform soil profile, the \bar{c} -front is shown in Figure B-2 for different times. The curves for different times are almost similar, and practically overlap when translated horizontally.

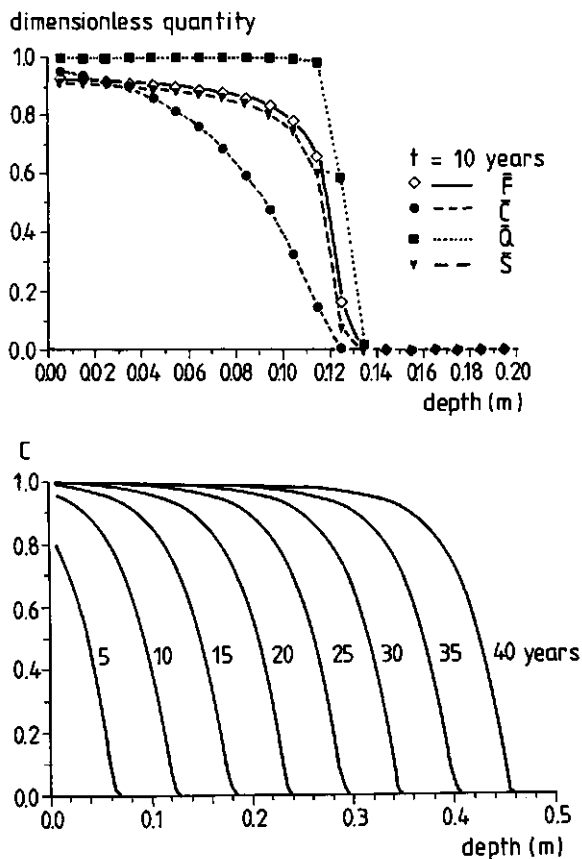


Figure B-2: Fronts for different times, reference case.

This indicates that fixed front shapes, travelling at a constant velocity, are attained already after a few years of continuous P-inflow. These fronts are relatively sharp for \bar{Q} , \bar{S} , and \bar{F} compared to the front obtained with linear (or no) sorption. Due to the kinetic nature of S , \bar{S} and \bar{F} do not become unity, and these fronts exhibit tailing. For the analysis of Van Der Zee and Van Riemsdijk [1986] this

does not in validate their shock front assumption, as this tailing is easily taken into account by adapting their $\alpha_m (= F_m/M)$. The gradual increase in \bar{c} implies that even if the F-shock front arrives at a reference level, the assumption of an instantaneous increase of $\bar{c}= 0$ to $\bar{c}= 1$ is not valid. Variation of flow or dispersion parameters in a realistic range has minor effects of the calculated front shapes, suggesting sorption control of transport.

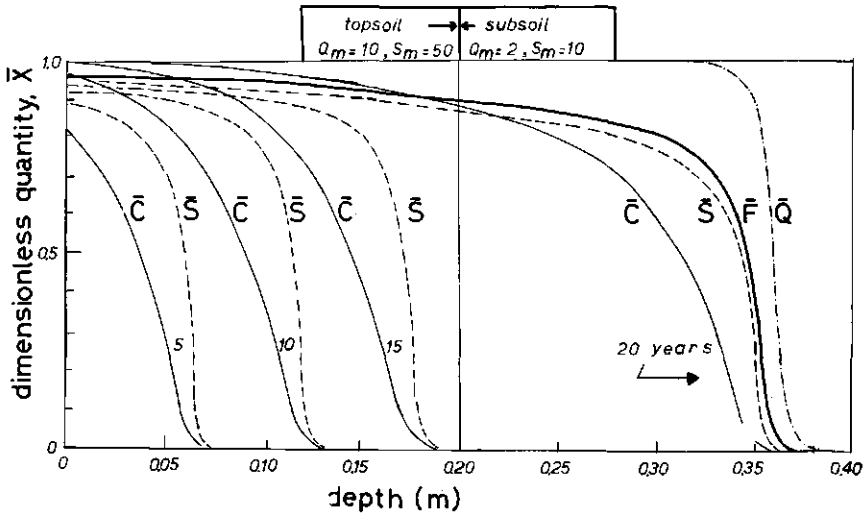


Figure B-3: Fronts if the subsoil has a smaller metal content: subsoil is $0.2 < z < 0.4$, $M(\text{subsoil}) = M(\text{topsoil})/5$.

Somewhat larger effects were found if layers with different values of M (and thus of Q_m, S_m, F_m) were present: Figure B-3. For this situation the kinetics (rate of approach of S to the maximum, S_m) were kept the same for all layers, and only the maximum values differed.

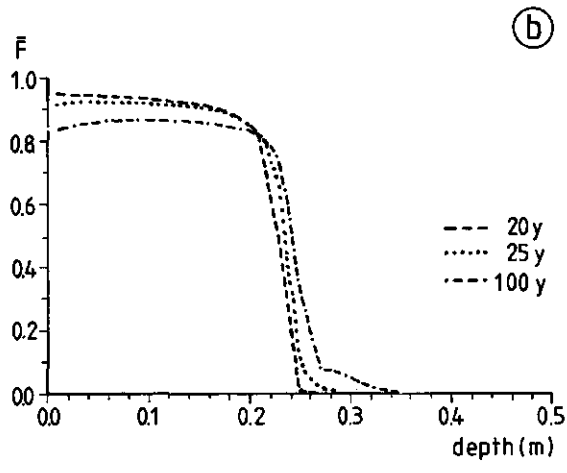
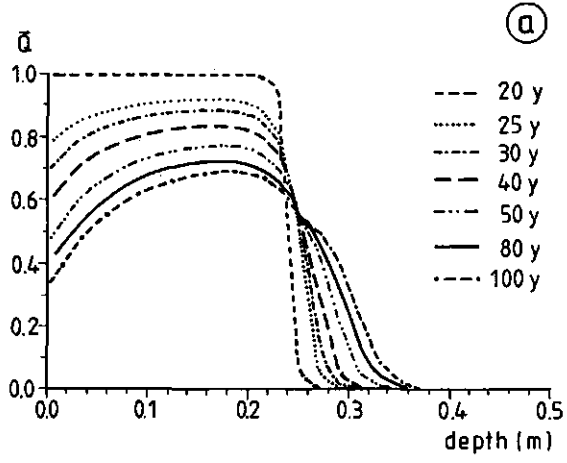


Figure B-4: Fronts at different times if P-inflow stops after 20 years.

Differences can largely be understood from the differences in the distribution ratio ($= \rho \Delta F / \theta \Delta C$) for different layers.

For the soil considered also calculations were done if P-inflow stopped after 20 years. Taking also diffusion-precipitation into account (different from Chapter 10), is shown to affect the P-redistribution process significantly. Even when c decreases rapidly with increasing time, precipitation accounts for a large fraction of sorbed P, in the subsoil that contains little P at $t=20$ years: Figure B-4. Because the concentration becomes already small at small times, the \bar{Q} -profiles are shown. Redistribution is shown for a feed concentration equal to $c_0 = 3 \text{ mol.m}^{-3}$ till $t=20$ years and zero feed concentration afterwards. The upper part of the curves resembles those of Chapter 10. Due to the precipitation, the downstream front moves slower than in Chapter 10. The cross-over point at $z=0.25$ m gives the depth where $c = c_e$ and $Q(c) = Q(c_e)$. At larger depths, $Q(c) < Q(c_e)$ and the retardation is due only to adsorption. Therefore the fronts (of \bar{Q}) move faster below $z=0.25$ m. This is seen from the secondary front that develops below this depth. Inspection of the \bar{S} -fronts (not shown) for the situation of Fig. B-4 showed that \bar{S} is significant at depths larger than the position of the downstream front at $t=20$ years. Hence, front propagation velocities of Chapter 10 (\bar{Q} , \bar{c}) are in error (i.e., too high). This result is of major importance for the protocol P-saturated soils and is currently subject of further study. The results also indicate relatively sharp fronts for \bar{Q} , \bar{S} , and \bar{F} for $t > 20$ y, and also support the approximations made in Chapter 10 with respects to the \bar{Q} -shock front in the subsoil.

REFERENCES

- Bolt, G.H., Movement of solutes in soil: Principles of adsorption/exchange chromatography, in Soil Chemistry B, Physico-Chemical Models, edited by G.H. Bolt, pp 285-348, Elsevier, New York, 1982.
- Reiniger, P., and G.H. Bolt, Theory of chromatography and its application to cation exchange in soils. Neth. J. Agric. Sci, 20: 301-313, 1972.

- Van Der Zee, S.E.A.T.M., and W.H. van Riemsdijk, Transport of reactive solute in spatially variable soil systems, *Water Resour. Res.* 23 (11), 2059-2069, 1987.
- Van Der Zee, S.E.A.T.M., and W.H. van Riemsdijk, Transport of phosphate in a heterogeneous field, *Transport Porous Media*, 1, 339-359, 1986.
- Van Dijn, C.J., and J.M. de Graaf, limiting profiles in contaminant transport through porous media, Rep. 84-31, 32 pp. Dept. Math. & Inform., Delft Univ. Technol., Delft The Netherlands, 1984.

APPENDIX C: SOME PROPERTIES OF THE NORMAL AND LOGNORMAL DISTRIBUTIONS

For easy reference some important properties of the used normal and lognormal distributions are presented.

Consider the normally distributed variate X with probability density function (PDF)

$$f_X = [s_X \sqrt{2\pi}]^{-1} \exp \{-0.5[(X-m_X)/s_X]^2\} \quad (C-1)$$

with $s_X > 0$, and $-\infty < X < \infty$. We denote this distribution by $X = N(m_X, s_X^2)$. The statistics for the distribution are found by moment theory. For the expectation of X^k we write $\mu'_k = E\{X^k\}$, ($k = 0, 1, 2, \dots$) which is the k -th raw moment. The k -th central moment is given by

$$\mu_k = E\{(X - E\{X\})^k\} \quad (C-2)$$

These moments may be evaluated by

$$\mu'_k = \int_{-\infty}^{\infty} X^k f_X dX \quad (C-3a)$$

$$\mu_k = \int_{-\infty}^{\infty} (X - E\{X\})^k f_X dX \quad (C-3b)$$

Now we have $\mu'_0 = 1$ by definition, as f_X is a density function. The expectation value equals μ'_1 , which is m_X for the normal PDF. The variance, given by μ_2 , is easily found to be s_X^2 , and the coefficient of variation is then given by $CV(X) = s_X/m_X$.

The reproductive properties are additive. This means that if

$$X = a + \sum_{i=1}^n b_i X_i \quad b_i \neq 0 \quad (C-4)$$

where $X_i = N(m_{X_i}, s_{X_i}^2)$ and X_i ($i = 1, \dots, n$) are independent, then X is distributed

$$X = N\left(a + \sum b_i m_{X_i}, \sum b_i^2 s_{X_i}^2\right) \quad (C-5)$$

Hence, if a stochastic process X_i is repeated independently M times and summed (e.g. M independent P -applications [Van Der Zee and Van Riemsdijk, 1986]) $X = \sum X_i$ has the distribution

$$X = N\left(\sum_{i=1}^M m_{X_i}, \sum_{i=1}^M s_{X_i}^2\right) = N(M m_{X_1}, M s_{X_1}^2) \quad (C-6)$$

This is so because a_i is zero and b_i equals unity. Note that M independent repetitions of X_1 implies for X that $X = \sum X_i$. In case of M perfectly correlated repetitions we have instead that the process is multiplied by a factor M , i.e., $X = M X_1$ (where i has only one discrete value). Hence, in that case [Van Der Zee and Van Riemsdijk, 1986]

$$X = N(M m_{X_1}, M^2 s_{X_1}^2) \quad (C-7)$$

For the lognormal distribution eq. (1) becomes

$$f_Y = [Y s_X \sqrt{2\pi}]^{-1} \exp \left\{ -0.5 \left[\frac{X - m_X}{s_X} \right]^2 \right\} \quad (C-8)$$

where Y is the exponential transform ($\exp X$), hence $X = \ln Y$.

The lognormal distribution for Y is denoted by $Y = \Lambda(m_X, s_X^2)$, where X is normally distributed. That the distribution of Y is characterized by the statistics of X is easily seen, as

$$f_Y dY \stackrel{\text{def}}{=} f_X dX \quad (C-9)$$

and

$$f_Y dY = \frac{1}{Y} f_X dY = f_X d \ln Y = f_X dX \quad (C-10)$$

If it is not realized that Y is distributed lognormally, one might calculate the statistics of Y (i.e., m_Y and s_Y^2) assuming a normal PDF (eq.1). The statistics found then are related to those of $X (= \ln Y)$ by the expressions given in Table C-1

Table C-1: Equations relating the statistics of Y and of $X (= \ln Y)$, assuming both X and Y normal

$m_Y = \exp \left(m_X + \frac{1}{2} s_X^2 \right)$	$m_X = \ln(m_Y) - \frac{1}{2} s_Y^2$
$s_Y^2 = \exp(2m_X + s_X^2) [\exp(s_X^2) - 1]$	$s_X^2 = \ln(1 + (s_Y^2/m_Y^2))$
median = $\exp(m_X)$	median = m_X
mode = $\exp(m_X - s_X^2)$	mode = m_X

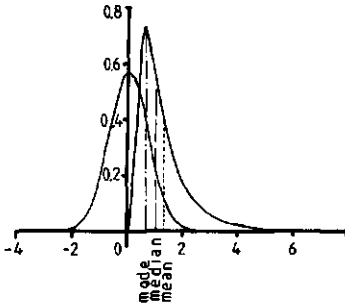


Figure C-1: The normal and lognormal PDF. Symmetric curve: normal PDF, $N(0,0.5)$, asymmetric curve : lognormal PDF, $\Lambda(0,0.5)$.

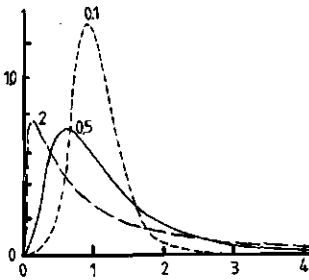


Figure C-2: The lognormal PDF, $\Lambda(0, s_X^2)$ with s_X^2 given at the curves

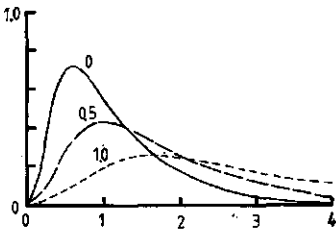


Figure C-3: The lognormal PDF, $\Lambda(m_X, 0.5)$ with m_X given at the curves.

Hence if Y is incorrectly assumed normally distributed, $Y=N(m_Y, s_Y^2)$, the coefficient of variation equals $CV(Y) = \sqrt{[\exp(s_X^2) - 1]}$, while the median, mean, and mode do not coincide. That the normal and lognormal distributions have approximately the same shape for a small coefficient of variation follows from Figures C-1 to C-3, and from Table C-1. Thus when $CV(Y) \rightarrow 0$ this implies that $\exp(s_X^2) \rightarrow 1$, i.e., $s_X^2 \rightarrow 0$.

It is readily seen from Table C-1 that for $s_X^2 \rightarrow 0$ the mean, mode, and median start to coincide, as they should for a normal PDF [Simmons, 1982, Van Der Zee and Van Riemsdijk, 1987].

The reproductive properties of the normal PDF being additive the same properties of the lognormal PDF will be multiplicative.

Indeed if Y is given by

$$Y = r \prod_{i=1}^M Y_i^{p_i} / u \prod_{j=1}^M Y_j^{q_j} \quad (C-11)$$

where Y_i, Y_j are independent variate sequences, that are lognormally distributed $\Lambda(m_{X_{i,j}}, s_{X_{i,j}}^2)$ and $r = \exp(v), u = \exp(w)$ are positive constants, then

$$Y = \Lambda(v - w + \sum p_i m_{X_i} - \sum q_j m_{X_j}, \sum p_i^2 s_{X_i}^2 + \sum q_j^2 s_{X_j}^2) \quad (C-12)$$

The agreement between eqs (5) - (7) and eq (12) is easily seen.

Equation (12) is a somewhat extended version of eq. (22) of Van Der Zee and Van Riemsdijk [1987]. In their case of $v \sim \alpha^{-2}$ (their eqs. 33-35) the variance of v is given by $s_{\ln v}^2 = (2 s_{\ln \alpha})^2$.

Again, as with the discussion of eqs. (6) and (7), it is noted that $Y=Y_1 \cdot Y_1$, is not equivalent to $Y=Y_1^2$, because in the latter case dependence and in the earlier case independence is assumed, implicitly.

REFERENCES

- Simmons, C.S., A Stochastic-convective transport representation of dispersion in one-dimensional porous media systems, *Water Resour.* 18. 1193-1214, 1982
- Van Der Zee, S.E.A.T.M., and W.H. van Riemsdijk, Transport of phosphate in a heterogeneous field, *Transp. Porous Media* 1, 339-359, 1986
- Van Der Zee, S.E.A.T.M., and W.H. van Riemsdijk, Transport of reactive solute in spatially variable soil systems, *Water Resour. Res.* 23, 2059-2069, 1987

APPENDIX D: PROTOCOL PHOSPHATE SATURATED SOILS

The protocol is a prescription on the details of soil sampling, soil sample treatment and laboratory analysis, and data evaluation, to which in principle each field is subjected in a region suspected of harbouring many phosphate saturated soils. To bound such regions the Dutch Soil Survey Institute compares regional P-surplusses and the estimated P-sorption capacity (similar to Chapter 6,8), using the criteria developed in Chapter 7. Since preliminary calculations suggested that the problem areas may be large, the protocol will have to be manageable for a large number of fields.

Based on the findings of Chapter 7 we find an acceptable thickness (L_g) of the P-saturated layer as:

$$L_g \approx \gamma \varepsilon K \tilde{c} L \quad (D-1)$$

In eq. (D-1) L equals l_m or a groundwater level (GG) that on average is exceeded only say 4 out of 12 months (i.e., shallower level), if GG is less than one meter from the soil surface. The depth, L , equals the depth of sampling. Sampling is done from 0-0.2 m and 0.2 m - L . Therefore analysis in the laboratory reveals differences in reactivity between the two sample layers. From Chapter 6 we have that reactivity is proportional to M (oxalate extractable metals, Fe + Al).

Hence ε , which gives an indication of reactivity changes with depth, may be estimated by $\varepsilon = M_2/M_1$, where the subscripts 1 and 2 refer to the 0-0.2 and 0.2- L layers, respectively. The adsorption coefficient, K , was taken equal to those in Chapter 7, and is assumed to be a constant. In the same Chapter 7 the range of values of \tilde{c} , for which eq. (D-1) holds, is given. The value where eutrophication occurs is set at $5 \text{ mmol} \cdot \text{m}^{-3}$, i.e., 0.15 mg P l^{-1} . The parameter γ indicates how important the precipitation process is in the subsoil (below L_g), assuming piston flow occurs also for depths larger than L_g . This last assumption proved to be valid in Chapter 10, where $\gamma = F/Q$ equalled unity. In Appendix B it was indicated that the shock front assumption may be acceptable also if $\gamma > 1$. As to the precise value of γ uncertainty remains. The value of $\gamma = 3$ (i.e., $F \approx F_m$; $Q \approx Q_m$; $\alpha \approx \alpha_m$) may be somewhat optimistic at the long term, but appeared valid for

short times of Appendix B.

Equation (D-1), with the product $\gamma \in K \tilde{c}$ constant may be reformulated as

$$L_g/L = \text{constant} \quad (\text{D-2})$$

Hence, for any soil for which L and ϵ was estimated the allowable value of L_g is known. In practice L follows from groundwater level maps, where 7 level classes are distinguished, and ϵ results from the laboratory work. We denote the acceptable value of L_g/L by Y. This value may be compared to the experimentally found value of L_g/L , denoted by Z. This value follows from the oxalate extractable amounts of the two layers 1 and 2 (with thickness $L_1 = 0.2$ m, $L_2 = L - 0.2$):

$$Z = (L_1 P_{\text{ox}(1)} + L_2 P_{\text{ox}(2)}) / (L_1 M_1 + L_2 M_2) \quad (\text{D-3})$$

Thus we might conclude that a field is P-saturated if $Z > Y$.

A refinement is necessary, in view of the limited number of samples, used for the mixing samples on which P_{ox} and M are assessed. Since P_{ox} and M are extracted with a surplus extractant, some sort of capacity parameter is obtained that is not subject to re-equilibration processes. Hence, an average M-value found for n samples may be expected to equal the M-value found for a mixing sample involving the n original samples. Intuitively, if only one original sample ($n=1$) is used and the variance of M is significant then the average value will not be estimated well. Suppose, we want to set Z such that at 97.5% confidence

$$Z + \Delta Z < Y \quad (\text{D-4})$$

For a variance of Z equal to s^2 and using n samples for the mixing sample this yields [Snedecor and Cochran, 1982]

$$(\Delta Z)^2 > 4 s^2 / n \quad (\text{D-5})$$

The criterion (D-5) follows from the 95% two sided confidence interval for the mean of Z. However, a complication arises when the mean values of the variables M_i , $P_{\text{ox}(i)}$, and Z, ($i=1,2$) are not known, because of

the assumption made with respect to s^2 . For practical reasons, it is impossible to assess the variances of the relevant variables for each field. To avoid this we may therefore assume that either s^2 is the same for all fields, or that the coefficient of variation, $CV (=s/m$, with m the mean value) is the same for all fields. Based on the few data at the field scale, it seemed more appropriate to assume that CV has a fixed value. In that case the uncertainty in the mean affects the value of s^2 . An approximation taking this effect into account is

$$(\Delta Z)^2 > 4 (s^2/n) [1 + t_n/\sqrt{4n}]^2 \quad (D-6)$$

which follows again from the 95% two sided confidence interval of the mean of Z , and where t_n is the appropriate student-t at sample size n . The constraints (D-5) and (D-6) are shown in Figure D-1.

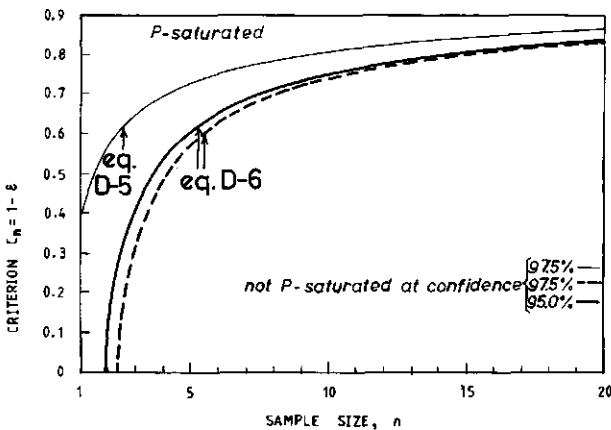


Figure D-1: Constraints for the ratio Z/Y to classify a field as Phosphate saturated or Phosphate unsaturated, where $\Delta Z = \epsilon Y$ and the criterion $C_n = Z/Y < (1 - \epsilon)$. Assumed was that $CV(Y) = 0.3$

At sample sizes of $n=5$ and $n=15$, we find $\Delta Z = 0.42$ and $\Delta Z = 0.20$,

respectively. Hence, for $n=5$ we have $Z < 0.58 Y$, and for $n=15$ we have $Z < 0.8 Y$, in order to decide that a field is not P-saturated.

The criteria based on eq. (D-4) and Figure D-1 imply that animal manure disposal should be discontinued when Z exceeds a prescribed value which is smaller than Y . The constraint becomes more demanding when the uncertainty, caused by a small number of samples, increases. According to this approach disposal is not allowed on a respectable number of fields that would not be considered P-saturated if the number of samples were large. Whereas, from the environmental point of view this is acceptable, it enhances the already existing problems concerning alternative ways to dispose of manure. Because alternatives to on-land disposal have insufficient capacity compared to the manure quantities that may not be disposed on land already, a different criterion may be necessary.

Thus, one may decide to 'fine' (force discontinuation of on-land disposal) only in those cases that with large confidence violate the constraint $Z < Y$. Then disposal on land is allowed provided

$$Z \leq Y + \Delta Z \quad (D-7)$$

at a chosen confidence (e.g. of 97,5%). The corresponding criterium may be easily derived. Only cases that dearly violate the constraint $Z < Y$ are fined. If the second approach is adopted, contra-expertise with the same or with a larger number of samples is likely to bring about the same decision as the original one, for a particular field. In the first approach (D-4) this is not the case.

Which of the two approaches is still subject to discussion. The choice is only partly a technical one, as also considerations of a political and legal nature are involved. In view of the explanatory nature of the technical protocol [Van der Zee et al., 1988] only the environmental consequences of both approaches will be indicated.

REFERENCES

- Snedecor, G.W., and W.G. Cochran, Statistical methods, 7th edition, Iowa State Univ. Press, 1982.
- Van Der Zee, S.E.A.T.M., W.H. van Riemsdijk, and F.A.M. de Haan,

Protokol Fosfaat Verzadigde Gronden, en Toelichting, Agric.Univ.
Wageningen, 1988 (in preparation).

Curriculum vitae

Sjoerd van der Zee werd op 7 maart 1955 geboren te Heerlen. In 1972 behaalde hij het diploma HAVO-B en in 1974 het diploma Atheneum-B, beide aan het Bernardinus College te Heerlen.

In 1974 begon hij met de studie aan de Landbouwhogeschool te Wageningen, in de studierichting Bodemkunde en Bemestingsleer. Na het behalen van het kandidaatsdiploma in 1978 bracht hij van juli tot december 1978 zijn praktijktijd door op het "Department of Agricultural Engineering" van het Technion, Israel Institute of Technology, te Haifa (Israël). In het kader van een doctoraal onderzoek bodemnatuurkunde bracht hij de periode van april tot september 1979 door bij het USDA Sedimentation Laboratory, te Oxford, Mississippi (USA). In 1981 slaagde hij voor het doctoraal examen met als vakken bodemnatuurkunde en bodemscheikunde (verzwaard hoofdvak), kolloïdchemie (bijvak) en geologie (bijvak).

De periode van oktober 1981 tot februari 1984 was hij werkzaam bij de afdeling Fysisch en Chemisch Onderzoek, van het Laboratorium voor Grondmechanica, te Delft, eerst in het kader van vervangende militaire dienst, later in een vast dienstverband.

In februari 1984 keerde hij terug naar de Vakgroep Bodemkunde en Plantevoeding van de Landbouwhogeschool te Wageningen, voor een promotieonderzoek naar het transport van fosfaat in de bodem, hetgeen geleid heeft tot dit proefschrift.

Sinds februari 1987 is het dienstverband tijdelijk verlengd ten behoeve van de ontwikkeling van zg. protocol fosfaat verzadigde gronden voor het ministerie van Volkshuisvesting, Ruimtelijke Ordening en Milieubeheer (VROM), en om het college element "transport van stoffen in de bodem" te bewerken tot een computer ondersteund onderwijselement. Daarnaast is hij plaatsvervangend lid van de Programmerings- en Studiegroep "Water en Bodem" van de RMNO, en lid van de werkgroep "Verspreidingsmodellen" van het ministerie van VROM (DGMH).